

THESIS ON CIVIL ENGINEERING F55

# **Heating System Efficiency Aspects in Low-Energy Residential Buildings**

MIKK MAIVEL

**TUT**  
**PRESS**

TALLINN UNIVERSITY OF TECHNOLOGY  
Faculty of Civil Engineering  
Department of Structural Design

**This dissertation was accepted for the defence of the degree of Doctor of Philosophy in Civil Engineering on May 22, 2015.**

**Supervisor:** Professor Jarek Kurnitski,  
Department of Structural Design, Tallinn University of  
Technology

**Co-supervisor:** Professor Teet-Andrus Kõiv,  
Department of Environmental Engineering, Tallinn  
University of Technology

**Opponents:** Professor Sture Holmberg  
KTH Royal Institute of Technology, Sweden

Dr.-Ing.habil. Joachim Seifert  
Dresden University of Technology, Germany

Defence of the thesis: June 30, 2015

Declaration:

*Hereby I declare that this doctoral thesis, my original investigation and achievement, submitted for the doctoral degree at Tallinn University of Technology, has not been submitted for any academic degree.*

*Mikk Maivel*



European Union  
European Social Fund



Investing in your future

**ARCHIMEDES**



**DoRa**



**Mobilitas**

ESF programm

Copyright: Mikk Maivel, 2015

ISSN 1406-4766

ISBN 978-9949-23-782-1 (publication)

ISBN 978-9949-23-783-8 (PDF)

EHITUS F55

# **Küttesüsteemi efektiivsuse aspektid madalenergia eluhoonetes**

MIKK MAIVEL



## TABLE OF CONTENTS

LIST OF ORIGINAL PUBLICATIONS .....	7
AUTHOR'S CONTRIBUTION.....	8
ABBREVIATIONS.....	9
1 INTRODUCTION.....	10
1.1 Background .....	10
1.1.1 Modeling of heating system losses.....	11
1.1.2 Radiator impact on system's overall efficiency .....	13
1.1.3 Modeling of seasonal performance of a heat pump.....	13
1.2 Aims and content of the study .....	15
1.3 Outline of the thesis.....	16
2 METHODS.....	17
2.1 Calculations of heating system losses .....	17
2.1.1 Losses calculated by the <i>German method</i> .....	17
2.1.2 Emission losses calculated by the <i>French method</i> .....	18
2.2 Detailed simulation model for calculating losses .....	19
2.2.1 Basic overview of the simulation model .....	19
2.2.1 Dynamic component models for heating systems .....	24
2.3 Modeling and analytical calculation for radiators with parallel and serial connected panels.....	26
2.3.1 Radiator configurations .....	26
2.3.2 Heat output and temperature measurements.....	27
2.3.3 Analytical model of the EN 442-2 test room heat transfer .....	27
2.3.4 Case study in a dynamic simulation environment.....	30
2.4 Detailed Heat Pump Model .....	31
2.4.1 Dynamic model of the heat pump heating system.....	31
2.4.2 Connection schemes .....	32
2.4.3 Basic equations.....	34
2.4.4 IDA-ESBO simulation .....	34
2.4.5 Hand calculations with the measured correlation.....	36
3 RESULTS.....	37
3.1 Heating System Losses.....	37

3.1.1	Radiator heating system losses.....	37
3.1.2	Radiator and Floor Heating System Losses.....	42
3.2	Comparison of Radiators.....	51
3.2.1	Laboratory measurements at 50 °C flow temperature .....	51
3.2.2	Laboratory measurements of dynamic performance at 70 °C flow temperature.....	54
3.2.3	Simulation Results.....	56
3.3	Heat Pump .....	58
3.3.1	IDA-ESBO heat pump simulation.....	59
3.3.2	Calculation based on laboratory measurements .....	62
4	DISCUSSION .....	68
4.1	Heating system losses and recommendation for further work .....	68
4.2	Comparison of radiators and recommendations for further work .....	71
4.3	Effect of return temperature on heat pump performance and recommendations for further work.....	71
5	CONCLUSIONS.....	73
	LIST OF REFERENCES .....	77
	ACKNOWLEDGEMENT.....	82
	ABSTRACT .....	83
	KOKKUVÕTE.....	85
	PAPERS PRESENTED BY THE CANDIDATE.....	87
	PUBLICATIONS.....	91
	CURRICULUM VITAE .....	167
	ELULOOKIRJELDUS.....	169

## LIST OF ORIGINAL PUBLICATIONS

The thesis is based on four academic publications in peer-reviewed journals:

- I Maivel, M.; Kurnitski, J. (2014). Low Temperature Radiator Heating Distribution and Emission Efficiency in Residential Buildings. *Energy and Buildings*, 69C, 224 - 236.
- II Maivel, M.; Konzelmann, M.; Kurnitski, J. (2015). Energy performance of radiators with parallel and serial connected panels. *Energy and Buildings*, 86, 745 - 753.
- III Maivel, M.; Kurnitski, J. (2015). Heating System Return Temperature Effect on Heat Pump Performance. *Energy and Buildings*, 94, 71-79.
- IV Maivel, M.; Kurnitski, J. (2015). Radiator and floor heating operative temperature and temperature variation corrections for EN 15316-2 heat emission standard. *Energy and Buildings*, 99, 204 - 213.

And on following conference publications:

- V Maivel, M; Kurnitski, J (2013). Low Temperature Radiator Heating System Detailed Dynamic Simulation - Distribution and Emission Efficiency. CLIMA 2013, 11th REHVA World Congress and the 8th International Conference on Indoor Air Quality, Ventilation and Energy Conservation in Buildings. Prague, Czech Republic, on June 16 – 19, 2013. Elsevier.
- VI Maivel, M.; Kurnitski, J. (2014). Heating System Return Temperature Effect on Heat Pump Performance. In: 11th International Energy Agency Heat Pump Conference 2014 Conference Proceedings: 11th International Energy Agency Heat Pump Conference Montreal, May 12-16, 2014. International Energy Agency.

## **AUTHOR'S CONTRIBUTION**

The author of the thesis is the main author in all the peer-reviewed papers and conference publications. All the simulations presented in papers I-VI were made by the thesis author. Overall methodology was developed in collaboration of the co-author prof. Jarek Kurnitski. Principal hypothesis and the investigation theme were developed mainly by the co-author. Laboratory measurements and analytical comparison of radiators in paper II were made by co-authors. All results in papers I-VI were discussed and conclusions were made by both authors.

## ABBREVIATIONS

CEN	The European Committee for Standardisation
CFD	computational fluid dynamics
COP	coefficient of performance
DIN	Deutsches Institut für Normung (German Institute for Standardization)
EN	European Standard
EPBD	Energy Performance of Buildings Directive
EU	European Union
IDA ICE	IDA Indoor Climate and Energy
IDA-ESBO	IDA Early Stage Building Optimization
IEA HPP	International Energy Agency Heat Pump Programme
ISO	International Organization for Standardization
nZEB	Nearly zero energy building
PPD	predicted percentage dissatisfied
RT	The French regulation
SPF	seasonal performance factor
TRY	Test Reference Year
UK	United Kingdom

# 1 INTRODUCTION

It is generally accepted in the European Union (EU) that buildings account approximately for 40% of the total primary energy use [1]. EU has adopted an ambitious target to improve energy efficiency by 20%. To achieve the goal, the directive on the energy performance of buildings (EPBD) was adopted in 2010 (2010/31/EU [1]). This directive is compulsory for each member state.

In 2010 residential buildings used 26.7% [2] of the total primary energy. The proportion of energy allocated to space heating in buildings is 57% [3]; when averaged through the EU (annual heating energy use has been estimated at 173 kWh/m<sup>2</sup> in apartment buildings and between 150 and 230 kWh/m<sup>2</sup> in residential buildings [4]), respectively in Northern-Europe (Estonia) 62% in apartment buildings [5] and 70% in dwellings [6]. Historically, primary energy use for space heating in the residential sector has been substantially higher compared to buildings with well-insulated and advanced ventilation systems [7].

In nearly zero energy buildings (nZEB), the situation is totally different - the share of energy use for space heating from the total delivered energy (space heating; supply air heating; domestic hot water; cooling; fans and pumps; lighting and appliances) is only 25% in nZEB detached houses and even 12% in apartment buildings in northern climate [8]. This overall situation has created a new challenge for heating systems. An obvious requirement for reduction of the control and system losses is underlined in existing buildings with higher heating energy need.

On the whole, three main possibilities are available to decrease heating energy need and to achieve ambitious EU targets:

- Minimizing heat losses – lowering U-values or tightening the building envelope elements;
- Minimizing heating system distribution and emission losses;
- Producing heat more efficiently.

It is well known that energy consumption for space heating can be significantly reduced. In terms of the current thesis, minimizing heat losses were not topical. It has been reported that insulating the envelope elements are cost optimal and profitable [9] [10].

Today we are facing new challenges like using, producing and distributing heat more efficiently to ensure accurate indoor climate for occupants. The thesis investigates the overall efficiency of heating systems in residential buildings. Although heat production is a wide topic, we will analyze the impact of return temperature on the residential heat pump coefficient of performance (COP) because it is directly influenced by the heat distribution and emitting system. Heat pumps conform to today's understandings and the nZEB concept.

## 1.1 Background

To implement the EU building energy efficiency strategies, European Committee for Standardization (CEN) has worked out more than forty different

relevant standards. Besides the standardization framework, many project reports and studies have been conducted to find solutions for reduction of energy needs for space heating. Besides the energy efficiency, thermal comfort is sometimes more important for occupants. Thus, the future challenge is to produce, distribute and emit heat by low losses, at the same time keeping thermal quality through occupied area.

### 1.1.1 Modeling of heating system losses

Heating need or energy use for heating can be modeled by European Standard (EN) 13790 [11], but it has relevant mistake - it calculates heating need by constant indoor temperature, but actual indoor temperature fluctuates. At real temperatures, heating need obviously decreases due to the control and system losses. An extensive study has shown that heating systems are substantially oversized (e.g., circulation pump for three times), and system optimization will decrease energy needs by 7.3% [12]. Another paper reports that adding a thermostatic valve will decrease energy needs by 2 to 10% [13].

According to the CEN standard EN 15316-1:2007 [14], a heating system can be divided into four main parts: generation, storage, distribution and emission whereas all these parts have losses (Figure 1-1).

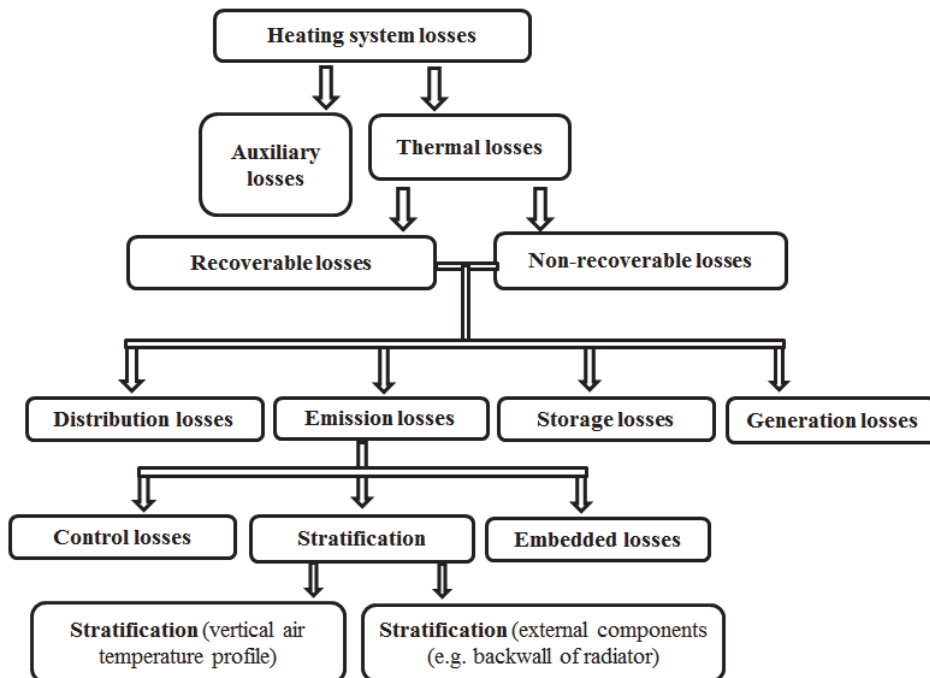


Figure 1-1 Classification of heating system losses according to the EN 15316-1:2007.

In the thesis focus is on the distribution and emission losses, generation and storage losses are excluded. Heat generation losses (i.e. boiler efficiency) have been extensively studied in product development projects as well as in scientific

studies. Some studies have concluded that it is possible to save energy up to 20% by improving boiler control [15] or up to 15% by changing a conventional boiler to a condensing boiler [16]. Studies of different heat distribution systems in an apartment building report that higher efficiency allows apartment based solutions [17]. Generation losses with calculation equations and tabulated values are described in the following CEN standards: 15316-4-1:2007[18]; 15316-4-2:2007 [19]; 15316-4-3:2007[20]; 15316-4-4:2007 [21]; 15316-4-5:2007 [22]; 15316-4-6:2007 [23], and 15316-4-7:2007 [24].

Distribution and emission losses have been studied scarcely. The reference study of EN 15316 [25] reports tabulated values for distribution and emission losses of 15% for heating curves 55/45 °C and 19% for 70/55 °C in a radiator heating system in a residential dwelling in Brussels. No reference could be found for low temperature heating systems. A very early study [26] reports an additional emission loss up to 5% of the heat emission of radiators in old buildings with poor insulation and less than 1% in new buildings with good insulation. The reason of very limited studies might be the complicated dynamic phenomena of distribution and emission losses. Distribution losses contribute as internal heat gains and may not be estimated by theoretical hand calculations because of the utilization process of dynamic heat gain rather than constant flow rates in the pipes. In addition to wall insulation, emission losses depend on the flow temperatures and the heat output of radiators and they need also dynamic treatment. Until now, building energy simulation tools typically have given no support to detailed modeling of the heating system with a pipework, thermostats and radiators all with continuously changing flow rates and temperatures.

In addition, several studies have compared different heat emission systems, especially floor and radiator heating. It has been concluded that a low-temperature heating system improves thermal comfort [27]. CFD based steady state investigations indicate that higher PPD is achieved with floor heating, although low- and medium temperature radiator heating systems reach more steady air speed and temperature level in occupied zones, especially close to the window [28]. It has been shown that low-temperature radiant panels can help to achieve 11-27% of energy compared to conventional heating systems [29]. On the whole, most recent studies concentrate on conventional buildings, but a totally different situation prevails in low-energy buildings where heat losses are minimized.

International Organization for Standardization (ISO) standards 7726 [30] and 7730 [31], which are widely used in thermal comfort calculations and measurements, are based on the use of operative temperature as a perceived temperature determining general thermal comfort of an occupant. Operative temperature is not yet implemented in the new updated prEN 15316-2:2014 methodology that calculates heating system losses from air temperature. The use of operative temperature the occupant is experiencing instead of air temperature will cause a difference in the heat emission losses depending on radiant temperatures in a room. In principle, operative temperature control results in a

thermal state in a room that leads to exactly the same thermal sensation by occupants, independent of the used heat emission system. In the case of conventional air temperature controlled floor and radiator heating systems, the thermal sensation could be slightly different at the same air temperature set point because of a different operative temperature.

### **1.1.2 Radiator impact on system's overall efficiency**

Losses caused by radiators are divided into three main factors: losses due to non-uniform temperature distribution (stratification), losses to the outside from heating devices embedded in the structure and losses due to imperfect control of the indoor temperature. Emission losses standard [32] provides tabulated values for all of these factors as efficiency values, which can be used to calculate the total emission efficiency. In the case of radiators, no embedded components are present. Stratification losses depend on over-temperatures and losses via external components, i.e. location of the radiator. In rooms with mechanical supply air, the temperature gradient is low [33].

Data available on the emission efficiency of radiators allow taking into account the heating curve and the insulation level of a building. To quantify the differences due to radiator configuration, more detailed methods are needed.

Radiators with serial connected panels have been reported to be able to provide 11% of energy saving [34]. However, this has been argued with up to 100% higher radiation heat transfer and also shorter heating up time of radiators.

The limitation of the standard EN15316-2.1:2007 and its new version prEN 15316-2:2014 is that the effect on the operative temperature on heat emissions is not accounted, as the calculation procedure is fully based on air temperature. In reality, different radiators have some effect on the radiant temperature and the operative temperature is the basic parameter of the thermal comfort standard ISO 7730:2005. An operative temperature, the temperature a human being is sensing, is calculated as an average of air and mean radiant temperature. Therefore, to compare the energy efficiency of a heat emitter accurately, it is necessary to conduct measurements and simulations at the same operative temperature that was taken into account in this study.

### **1.1.3 Modeling of seasonal performance of a heat pump**

Heat pump heating systems are popular and widely used for preparing domestic hot water and space heating all over Europe, especially in Nordic countries. Heat pumps are considered as one possible solution to reduce primary energy consumption and have often been proposed as a substitute for conventional systems (electric, gas boilers, oil boilers, etc.) to produce domestic hot water and space heating [35]. Heat pumps have been regarded financially attractive because of reasonably short payback periods, in particular in colder climates or at higher heating needs [36].

As a common solution, a heat pump is connected with a floor heating system where the temperature curve is lower than in a conventional radiator heating system. In this thesis research, special focus was on heat pump performance in a

radiator system where temperature drop is typically higher in sizing and in operation as compared with floor heating; and it ensures lower return water temperature. In sizing, typical temperature drops are 15 to 20 °C in a conventional radiator heating system, 10 to 15 °C in low temperature radiator heating and 5 to 10 °C in an underfloor heating system. Most of existing heat pump models and software do not consider the effect of return water temperature on COP, because that would require dynamic heat output and flow rates calculation in the building that can be done with dynamic simulation tools, and usually a simple condenser model assumption are used. Therefore, models that neglect calculation of the actual return temperature are more suitable for floor heating systems where temperature differences are smaller. All the heat pump models make some assumptions and simplifications. Scarpa has considered three main types of approaches: numerical approximation, general thermodynamic and detailed approach. Most detailed approaches achieve an accuracy of less than 10% [37]. In this thesis, a general thermodynamic approach was used. From literature, many models and calculation approaches of heat pump performance can be found, but most of them are simplified mostly the consumption side [38], i.e. it is complicated to model accurate consumption and inlet-outlet temperatures. Or alternatively, models describe steady state calculations as specified in standards [39].

Heat pump COP is influenced by its working mode, i.e. space heating or domestic hot water preparation. This thesis will concentrate on the space heating mode because energy need for space heating is a dynamic process; energy need for domestic hot water is influenced by a usage profile. Heat pump performance testing is described in EN 14511-2 [40] and ISO 5151:2010 [41]. International Energy Agency Heat Pump Program (IEA HPP) has launched Annex 28 to compare different standards EN [42]. Karlsson's work under IEA HPP Annex 28 includes heat pump tests by both EN standards (14511 and 255). The results show that the former standard EN 255-2 [43] gives higher COP values than EN 14511-2 due to mass-flows not defined in EN 255, which resulted in unrealistically low inlet condensing temperatures in a few testing points. According to EN 14511-2, heat pumps were tested at standard rating conditions of the temperature difference of 5 °C (for outlet temperature up to 45 °C). Karlsson's test results, like earlier studies [44], show that heat pump COP is influenced by the condenser inlet temperature (i.e. lowering return water temperature will increase heat pump performance). Evidently, the temperature difference of 5 °C used in testing of heat pumps underestimates the performance for radiator heating systems quantified in this study. For instance, Nyers' calculations by the steady-state mathematical model show that the condenser performance increases 1.9 times if the inlet water temperature decreases from 50 to 20 °C [45].

## 1.2 Aims and content of the study

This thesis research concentrates on the efficiency of the heating system the quantification and improvements of which were analyzed in low energy buildings with relatively small heating needs. The main focus was on the distribution and emission efficiency, but the generation efficiency was included in the heat pump analyses.

Properly designed heating systems with high efficiency could decrease the energy use without compromising thermal comfort. Considering stringent energy performance requirements on the one hand and ensuring occupants expectations on the high level thermal comfort on the other hand, it is essential to generate, distribute and emit heat more efficiently, which could be based, for instance, on lower temperature levels, more accurate control and other technical solutions. A motivation for the study was a very limited number of scientifically reported studies on the heating system emission and distribution losses.

The main aim of this thesis was to test and develop a calculation methodology for the efficiency of heating system distribution and emission based on a validated and detailed simulation model (I, IV). This approach was compared to the use of existing tabulated values of distribution and emission losses. Because the tabulated values do not exist for well-insulated buildings, the focus was set to the determination of efficiency values of low temperature systems in a low energy building.

The work was carried out for residential low-energy buildings in a cold (Tallinn, Estonia) and Central European (Munich, Germany) climate. Specific objectives were as follows:

- to provide input for updating of 15316-2-1 standard, which is under revision together with other EPBD standards for the preparation of second generation EPBD standards, regarding:
  - include all components of emission losses for radiator and floor heating in residential buildings (I, IV);
  - introduce an operative temperature correction in order to enable fair comparison of the radiator and the floor heating (IV)
- to determine distribution heat losses in heated rooms, which could serve as an input in the future development of 15316-2-3 standard (I);
- to determine the effect of insulating on distribution losses (I);
- to quantify the differences in heat emission efficiency for radiators with parallel and serial connected panels (II);
- to analyze thermal comfort and operative temperature in the EN 422 radiator test room (II);
- to analyze the performance of radiator heating with a heat pump, especially the effect of the return temperature on the seasonal performance of a heat pump (III).
- to test hand calculations of SPF based on hourly heating energy needs and the return temperature of the theoretical heating curve (III)

### 1.3 Outline of the thesis

Introduction gives an overview of the heating system losses and defines the problem statement.

In Paper I, a building with a full heating system (including special circulation pump, pipe, valve, controller and radiator models) was simulated. Distribution and emission losses were quantified by dynamic simulation, including all flow and heat transfer effects. This was arguably the most detailed modeling attempt for a radiator heating system so far done by a building energy simulation tool. A conventional and a low temperature radiator heating system were calculated for a carefully selected detached house and an apartment building. All the calculations were conducted with Tallinn and Munich climate files to make results usable across Europe. As a result, the input for the revision of EN 15316-2-1 standard was provided, consisting of new tabulated values for tabulated values of the emission system of a residential radiator heating system.

Paper II investigates and compares radiators of serial and parallel connected panels. Laboratory measurements for the same size and type of radiators with parallel and serial connected panels were conducted in the EN 442-2:2003 test room at the same conditions to quantify energy savings. Due to small differences, the heat transfer process was analytically modeled in the EN 442-2:2003 test room in order to be able to correct operative temperature levels up to 0.2 °C. This allowed the comparison at exactly the same temperature levels. Additionally, the seasonal energy performance was analyzed by dynamic simulation software, which has limitations for a radiator model, but still allowed modeling of the radiator surface temperatures according to the laboratory measurements. Adequate scientific comparison of serial and parallel radiators was conducted, including energy, heat output and operative temperature effects.

In Paper III the heat pump model was added to the detailed heating system model to analyze the dynamical return temperature effect on the seasonal performance factor (SPF) of the heat pump. Laboratory measurements were performed as well to quantify this effect against the condenser model. Applying the derived condensing temperature correlation equation in the simulations, the effect of large temperature drops in a radiator heating system and the effect of the studied connection schemes were quantified.

Paper IV compared emission losses of a radiator and a floor heating system and simulation results with the revised 15316-2-1 standard tabulated values. Standard methodology uses heating system control by air temperature, but to consider the same thermal sensation for occupants, the operative temperature control was investigated. In addition, a simple one room model with different numbers of external envelope elements was used to analyze operative temperature effects analytically. Operative temperature sensitivity to occupant location in a room was studied with two different locations. The paper compared a radiator and a floor heating system at exactly the same thermal sensation of occupants and proposed operative temperature correction and some floor heating values for the revised 15316-2-1 tabulated values.

## 2 METHODS

### 2.1 Calculations of heating system losses

Some losses are typical of all the main parts of a heating system: generation, storage, distribution, and emission. According to 15316-2-3:2007 [46], distribution losses consist of system thermal losses and auxiliary losses (pumping energy etc.). In autumn 2014, a preliminary version of updated prEN 15316-2:2014 was sent to the public enquiry. The methodology of the updated standard has been partly changed. The current 2007 version describes two possible ways for the calculation of emission losses: one adopted from the German regulation DIN 18599 [47] - energy losses of the heat emission system and the other - adopted from the French regulation RT 2005 [48] - equivalent increase in indoor temperature. The new standard relies on the French method and all tabulated values are described by the increase of the indoor temperature. Emission losses studied consist of the heat loss due to non-uniform temperature distribution, the heat loss due to the heat emitter position, and the heat loss due to control indoor temperature. Classification of heating system losses is shown in (Figure 1-1). Emission losses are described and tabulated values can be found in 15316-2-1:2007 [32].

All thermal losses are divided to recoverable and non-recoverable losses according to 15316-1:2007. The distribution losses caused by pipes in an unheated area are calculated as non-recoverable losses and losses in heated rooms contribute as recoverable losses until the temperature set-point is not exceeded. When the set-point is exceeded, the part of the loss becomes non-recoverable; this part can be quantified based on the comparative calculation with ideal heating and control. Emission losses caused by the heat emitter (radiator) position are the additional back-wall losses through the external wall behind the radiator (compared to the heat loss through the same external wall without a radiator) and the control losses are caused by the thermostatic valve type controller. 15316-2-1:2007 allows use of both calculation methods: *German* and *French*, but the new updated version recommends to use the *French* method.

#### 2.1.1 Losses calculated by the *German method*

The losses by the *German* method [47] are defined as additional losses to space heating energy need in %. The efficiency  $\eta$  is a reciprocal value, i.e. the energy use with losses can be calculated as  $1/\eta$ . All losses in series or parallel can be calculated as additional losses for the system in % or as the total system efficiency. If losses are in series, the subsystem efficiencies may be calculated and the total system efficiency is calculated by Eq. (1).

$$\eta_{tot} = \eta_{emission} \cdot \eta_{distribution} \cdot \eta_{storage} \cdot \eta_{generation} \quad (1)$$

where  $\eta_{emission}$  is the emission efficiency;  $\eta_{distribution}$  is the distribution efficiency;  $\eta_{storage}$  is the storage efficiency and  $\eta_{generation}$  is the heat generation efficiency. Calculation rules can be found in the 15316:2007 standard or sub-standards. For

example, if the heating energy need in a room is 100 kWh, at emission losses 10 kWh and distribution losses 15 kWh,  $\eta_{emission} = 100/110=0.909$  and  $\eta_{distribution} = 110/125=0.88$ . The total efficiency is  $\eta_{tot} = 0.909 \cdot 0.88=0.8$ , which can be calculated also as  $100/125=0.8$ .

Emission efficiency, depending on the parallel components, can be calculated with 15316-2-1:2007 by Eq. (2).

$$\eta_{emission} = \frac{1}{4 - (\eta_{stratification} + \eta_{control} + \eta_{embedded})} \quad (2)$$

Where  $\eta_{control}$  is the part of efficiency level for room temperature control;  $\eta_{embedded}$  is the part of efficiency level for specific losses of the external components (embedded systems) and  $\eta_{stratification}$  is the stratification efficiency, which is the part of efficiency level for a vertical air temperature profile (non-uniform temperature) calculated by Eq. (3).

$$\eta_{stratification} = \frac{\eta_{str1} + \eta_{str2}}{2} \quad (3)$$

Stratification is influenced by:

- over-temperature ( $\eta_{str1}$ ) that is neglected in this study, but analyzed in the discussion;
- specific heat loss via external components ( $\eta_{str2}$ ), (e.g. additional heat loss from a back-wall of radiator), which is considered by the simulation model.

### 2.1.2 Emission losses calculated by the *French method*

The new standard relies on the French method and all the tabulated values are described by the increase of the indoor temperature. In this method, an equivalent temperature considering emission losses is calculated from the tabulated values by Eq. (4).

$$\theta_{int;inc} = \theta_{int;ini} + \Delta\theta_{str} + \Delta\theta_{ctr} + \Delta\theta_{emb} + \Delta\theta_{rad} + \Delta\theta_{im} + \Delta\theta_{hydr} + \Delta\theta_{roomaut} \quad (4)$$

where  $\theta_{int;ini}$  is initial internal temperature (°C);  $\Delta\theta_{str}$  is spatial variation of temperature due to stratification (K) (Eq. (5));  $\Delta\theta_{ctr}$  is control variation (K);  $\theta_{ctr1}$  or  $\Delta\theta_{ctr2}$  where  $\Delta\theta_{ctr1}$  should be used for standard calculation if no information is available and  $\Delta\theta_{ctr2}$  should be used for calculations with certified products. Alternatively, product specific values can be used if proved by certification;  $\Delta\theta_{emb}$  is temperature variation based on an additional heat loss of embedded emitters (K) (Eq. (6));  $\Delta\theta_{rad}$  is temperature variation based on radiation by the type of the emission system (K);  $\Delta\theta_{im}$  is temperature variation based on an intermittent operation and on the type of the emission system (K) (Eq. (7)),  $\Delta\theta_{hydr}$  is temperature variation based on non-balanced hydraulic systems (K);  $\Delta\theta_{roomaut}$  – temperature variation based on a stand alone or networked operation room automation of the system (K);  $\theta_{int;inc}$  is temperature variation based on all losses (K).

$$\Delta\theta_{str} = \frac{\Delta\theta_{str;1} + \Delta\theta_{str;2}}{2} \quad (5)$$

Stratification is influenced by the over-temperature ( $\Delta\theta_{str;1}$ ) and specific heat loss via external components ( $\Delta\theta_{str;2}$ ), (e.g. additional heat loss from the back-wall of a radiator).

$$\Delta\theta_{emb} = \frac{\Delta\theta_{emb;1} + \Delta\theta_{emb;2}}{2} \quad (6)$$

Embedded heat loss is to be formed from the data for the main influence parameters system ( $\Delta\theta_{emb;1}$ ) and specific heat losses via laying surfaces ( $\Delta\theta_{emb;2}$ ).

$$\Delta\theta_{im} = \Delta\theta_{im;emt} + \Delta\theta_{im;ctr} \quad (7)$$

where  $\Delta\theta_{im;emt}$  is temperature variations based on an intermittent operation on the type of the emission system (K);  $\Delta\theta_{im;ctr}$  is temperature variations based on the intermittent operation of control (K).

## 2.2 Detailed simulation model for calculating losses

### 2.2.1 Basic overview of the simulation model

All the calculations were performed by the dynamic simulation software *IDA Indoor Climate and Energy 4.5* [49]. This tool is carefully validated and has advanced features for detailed building energy simulations [50]. IDA-ICE has several features to consider losses described in section 2.1. One limitation has been made for the ( $\eta_{str1}$ ) component. Although the program has two zone modes – climate and energy, where a vertical temperature gradient may be calculated by the climate mode; it is simplified and the program user should define the gradient value or the ventilation displacement degree. Thus, in our approach we used previous lab test results for calculating over-temperature losses. Two test reference years were used for outdoor climate, Estonian TRY [51] and Munich [52]. The detached house analyzed represents a typical recently built detached house (Figure 2-1), which has been used as a reference building in Estonian cost optimal calculations [8]. By small changes, the same house was modified to describe a multi-story apartment building. External wall at one end of the building was made adiabatic, which means that the model unit represents one apartment of a long building. Similarly, the external roof was changed to adiabatic, which means that the building will continue upwards. In the transformation from a detached house to an apartment building, technical space and one small window on the top left were “lost” – to ensure that the apartment building is more compact. All other geometry characteristics of a house unit remained the same in the transformation. Main technical data for both buildings are shown in Table 2-1. External envelopes of the buildings are identical in Tallinn and Munich.

Room set-point temperature of 21 °C was used in all zones/rooms. Heating was controlled with the heating curve compensated by the outdoor air temperature (the supply water temperature increases to the maximum as the outdoor

temperature decreases to the design outdoor temperature) and with individual room control with room thermostats. In a few cases in paper I, a limited heating period was used because numeric problems could not fully close the thermostatic valve. A limited period shows the real conditions. The balance point temperature was used to construct the limited heating period (balance point temperature was the outdoor temperature at which all thermostatic valves were fully closed, indicating no heating need (i.e. internal gains will exceed the heat losses)). The balance point temperature of 11 °C in a detached house and 9 °C in an apartment building were in compliance in both climates.

During the simulations, two different heating curves for radiator heating were used 70/55 °C as a conventional heating system and 45/35 °C as a low temperature heating system; in addition, 35/28 °C was used for an underfloor heating system. Advanced radiator model (with mass) was used. For the room temperature control, most common room controllers were simulated, including on-off and proportional controller (P) without hysteresis, both with proportional/on-off band of 2 K, and proportional-integrated (PI) controller leading to almost ideal room temperature control. Controller models can be found in [50]. Controller sensor is controlled by air or by the operative temperature.

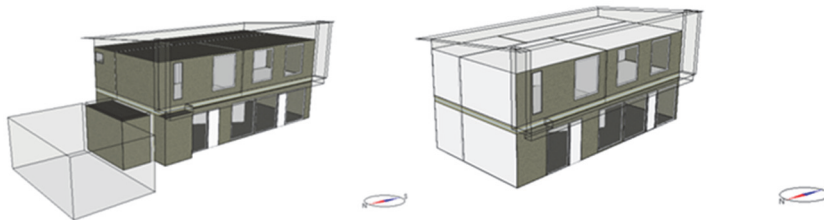


**Figure 0-1 Estonian reference detached house on the left, and the house transferred to describe an apartment building on the right (white envelope elements are adiabatic).**

In the detached house model, no cooling system was used, but in the apartment building model, ideal coolers were used with a cooling set point temperature of 25 °C. Ideal cooler and heater are standard models from the IDA-ICE library and they are imaginary equipment, which describe heating or cooling need without system losses. A mechanical supply and exhaust ventilation system with heat recovery (temperature ratio of 80%; supply air temperature set-point +18°C) was used in both modes. All energy calculation input data follow the Estonian regulation of minimum requirements for energy performance [53][54].

**Table 2-1 Basic data of the house/building**

			Detached house	Apartment building
U-value (W/(m <sup>2</sup> K))	Exterior wall		0.17 (lightweight)	0.17 (heavyweight)
	Roof		0.14 (lightweight)	0.14 (heavyweight)
	Ground floor		0.17	0.17
	Windows (triple pane glazing, g=0.5)		0.8	0.8
	Specific heat loss coefficient H/A <sub>net</sub> (W/(m <sup>2</sup> K))		0.58	0.44
Ventilation	Ventilation (continuous) rate l/(s m <sup>2</sup> )		0.46	0.56
	Leakage rate q <sub>50</sub> . m <sup>3</sup> /(h m <sup>2</sup> )		0.6	0.6
		Usage (max = 1)	W/m <sup>2</sup>	W/m <sup>2</sup>
Internal gains	Occupants	0.6	2	3
	Lighting	0.1	8	8
	Equipment	0.6	2.4	3
			W/m <sup>2</sup>	W/m <sup>2</sup>
Heating power need	Tallinn		Average 29.9 (15.9...49.1)	Average 22 (7.8...31.8)
	Munich		Average 23.9 (11...39.5)	Average 15.4 (6.3...25.9)
			kWh/m <sup>2</sup>	kWh/m <sup>2</sup>
Gross heating energy need	Tallinn	Heat from ventilation heat recovery	55	69
		Heat from internal and solar heat gains	59	70
		Heat from heating system	46	26
	Munich	Heat from ventilation heat recovery	45	57
		Heat from internal and solar heat gains	61	72
		Heat from heating system	31	16

Two pipe radiator heating systems were used. To report heat losses from pipes, we have defined connection and distribution pipes as follows. Distribution pipes are pipes which do not serve the room where they are located (i.e. distribution pipes are not connected with room radiators, Figure 2-2. When the distribution pipe enters the last room, it is transformed to the connection pipe according to this definition. Therefore, the connection pipes are defined as the pipes located in the room where the radiator is (it applies also if the room has two radiators). To analyze the insulation effect, several calculations were performed for pipes not insulated, distribution pipes insulated or all pipes insulated.

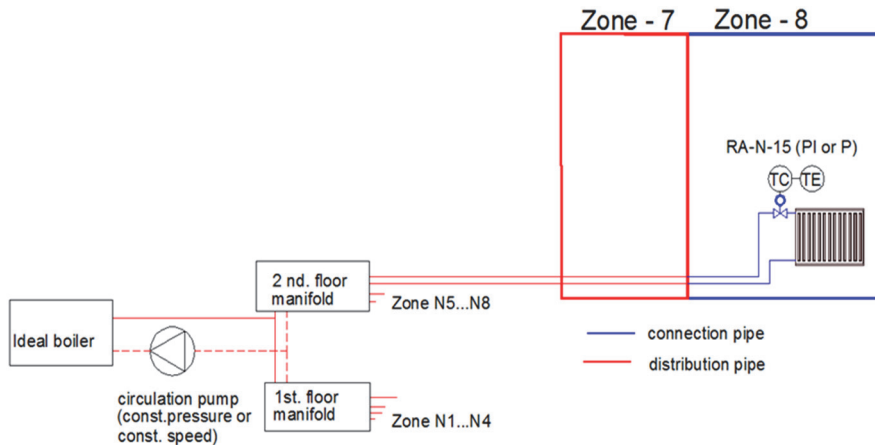


**Figure 2-2 Scheme of the heating system. Two last zones are shown to explain the definition of connection and distribution pipes used in heat loss reporting.**

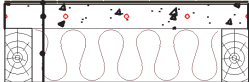
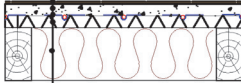
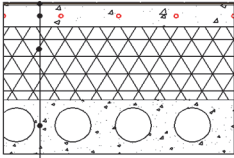
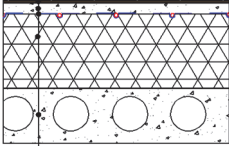
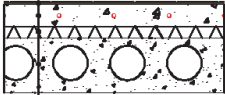
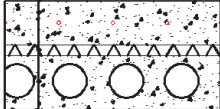
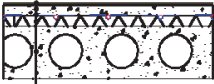
The system has one circulation pump which either has constant pressure control or constant speed control. In the constant speed mode, the system has a small bypass between manifolds (a pipe with a diameter of 0.0001 m and length of 1 m). Bypass was necessary to run simulations for the spring-summer period when radiator thermostatic valves are often closed.

In paper IV, the thermal comfort and emission losses of a floor heating system were studied. The floor heating is influenced substantially by the floor construction (used floor types are shown in Table 2-2).

Slab on the ground structure was the same in the apartment building and the detached house, but mid-floor construction type varied according to lightweight and heavyweight structures.

As different from radiator heating, floor heating has embedded losses caused by a higher share of thermal mass compared to radiator heating.

**Table 2-2 Simulated floor construction type for the apartment building and the detached house**

Detached house			
Mid-floor	<p>Wet system, 1<sup>st</sup> floor</p>  <p>Parquet 8 mm Concrete 65 mm Isolation 100 mm</p>	<p>Dry system, 1<sup>st</sup> floor</p>  <p>Parquet 8 mm Screed 25 mm Aluminium fin 0.5 mm Heavy isolation 25 mm Isolation 100 mm</p>	
	Slab on ground	<p>Wet system, ground floor</p>  <p>Parquet 8 mm Concrete 65 mm Heavy isolation 340 mm Hollow-core slab 265 mm</p>	<p>Dry system, ground floor</p>  <p>Parquet 8 mm Screed 25 mm Aluminium fin 0.5 mm Heavy isolation 340 mm Hollow-core slab 265 mm</p>
Apartment building			
Mid-floor	<p>Wet system (65 mm), 1<sup>st</sup> floor</p>  <p>Parquet 8 mm Concrete 65 mm Heavy isolation 25 mm Hollow-core slab 265 mm</p>	<p>Wet system (100 mm), 1<sup>st</sup> floor</p>  <p>Parquet 8 mm Concrete 100 mm Heavy isolation 25 mm Hollow-core slab 265 mm</p>	<p>Dry system, 1<sup>st</sup> floor</p>  <p>Parquet 8 mm Screed 25 mm Aluminium fin 0.5 mm Heavy isolation 25 mm Hollow-core slab 265 mm</p>

In the case of floor heating, it is necessary to calculate separately losses caused by the ground or mid-floor. The overall calculation scheme is shown in Figure 2-3 for calculating emission losses from mid-floor, in which case the ground floor had an ideal situation, e.g. a heating system based on ideal heaters. With this scheme, additional losses from the slab were eliminated that allowed us to simulate only the mid-floor losses. Afterwards, mid-floor losses were eliminated to calculate emission losses of the ground floor.



**Figure 2-3 Calculation scheme for calculating emission losses for mid-floor (left) and ground floor (right).**

## 2.2.1 Dynamic component models for heating systems

### *Ideal heater*

An ideal heating system was used for the reference simulations without any emission and distribution losses. It consists of ideal heaters (massless) in all rooms which have no defined physical location, but are described with convection and radiation heat output fraction (typically 40% radiation and 60% convective). Power is calculated by the simple Eq. (8).

$$Q = C \cdot Q_{\max} \quad (8)$$

where  $Q$  is the maximum power of the unit (W);  $C$  is the control signal of the unit (controlled by a PI-controller and takes input from zone air temperature). An ideal heater is controlled by a PI controller, where control losses are minimal or de-facto not existing [50].

A dynamic detailed radiator model for a standard radiator of IDA-ICE is connected to the external envelope element and has an additional heat loss from the backside of the radiator, but the radiator has no mass and the flow rate is not calculated [49]. We used a detailed radiator model, which has a thermal mass. Heat balance of the water side is calculated by Eq. (9).

$$P = q_m \cdot C_{liq} \cdot (T_{in} - T_{out}) \quad (9)$$

where  $P$  is a heat flux from the water (W);  $q_m$  is water mass flow (kg/s);  $C_{liq}$  is the specific heat of water (J/kgK);  $T_{in}$  is the water inlet temperature to the radiator (°C);  $T_{out}$  is the water outlet temperature from the radiator (°C).

The total heat generated by the radiator is modeled by Eq. (10).

$$P = K \cdot l \cdot dT^n \quad (10)$$

where  $K$  is the power law coefficient which depends on the width and type of the radiator (W/(mK<sup>n</sup>));  $l$  is the length of the radiator (m);  $dT$  is logarithmic temperature difference between the water and the air (°C);  $n$  is a coefficient describing radiator convective and radiative emission share (typically 1.28).

The total heat balance for the radiator is written by Eq. (11).

$$P = Q_{front} + Q_{conv} + Q_{wall} \quad (11)$$

where  $Q_{front}$  is the heat transfer on the front side of the unit (long wave radiation and convection) (W);  $Q_{conv}$  is an extra convective heat load, e.g. from the back side and possible fins (W);  $Q_{wall}$  is heat transfer between the back side of the unit and the facing zone surface (W).

Heat storage caused by the thermal mass is calculated by Eq. (12).

$$m_{rad} \cdot C_{liq} \cdot \frac{dT_{surf}}{dt} = Q_{liq} - Q_{air} \quad (12)$$

where  $m_{rad}$  is a mass of water inside the radiator (kg);  $C_{liq}$  the specific heat of water (J/kgK);  $dT_{surf}$  radiator surface temperature (°C);  $dt$  is a time (s);  $Q_{liq}$  is heat flux water to surface (W);  $Q_{air}$  is heat flux from the radiator surface to the zone/room (W).

Radiator control loop is a standard model with PI or P control in our simulations. In [50] radiator thermostat (P-controller with hysteresis) was compared with ideal P control and minimal differences were found. Therefore, we neglected the effect of hysteresis in our simulations. Simulated dynamic radiators were equipped with RA-N 15 valve bodies, which all were fully open (i.e. the system was not balanced, but just controlled by P or PI thermostats).

### ***Pipe model***

For detailed calculations, a special pipe model was used (not included in the standard IDA-ICE model library). The pipe model provided a possibility to model a real system where pipes have dimensions (length and diameter and have pressure losses) and to simulate heat emissions of the pipes. All pipes were located in the room air, i.e. surface installation of pipes was considered. It is known that the surface installation has roughly the same heat emissions as an embedded installation in the protective sleeve (not insulated) as a rule of thumb. Heat emissions of pipes were calculated by Eq. (13):

$$Q_{amb} = q \cdot C_{liq} \cdot (t_{in} - t_{out}) \quad (13)$$

where  $Q_{amb}$  is a heat flux from the pipe (W) to the ambient;  $q$  is a mass flow (kg/s);  $C_{liq}$  is the specific heat of water (J/kgK);  $t_{in}$  is the water inlet temperature (K), and  $t_{out}$  is the water outlet temperature (K). Outlet temperature depends on the pipe length, pipe diameter and insulation. Heat flux from pipes can be calculated with a logarithmic temperature difference between the pipe's inner temperature and the ambient temperature by Eq. (14).

$$\Delta t_{log} = \frac{Q_{amb}}{U_{wall} \cdot \pi \cdot d_{in} \cdot l} \quad (14)$$

where  $U_{wall}$  is the total heat transfer coefficient from fluid to ambient air (W/(m<sup>2</sup>K)), for which constant values were used, calculated by the basic heat transfer equation (Eq. (15) for circular pipes where heat transfer coefficients are expanded.

$$\frac{1}{U_{wall}} = R = \frac{1}{2 \cdot \pi \cdot \lambda} \ln \frac{d_{out}}{d_{in}} + \frac{1}{\pi d_{out} \left( 1.21 \left( \frac{\Delta t}{d_{p,i}} \right)^{0.25} + \frac{4\sigma \left( \frac{\Delta t}{2} \right)^3}{1 + \left( \frac{\varepsilon_1 \cdot A_1}{\varepsilon_2 \cdot A_2} \right) (1 - \varepsilon_2)} \right)} \quad (15)$$

where  $\Delta t$  is the temperature difference between mean air and pipe (°C);  $\sigma = 5.67 \cdot 10^{-8}$  W/m<sup>2</sup>K<sup>4</sup> is the radiation heat transfer coefficient;  $\varepsilon_1$  is pipe surface emissivity;  $\varepsilon_2$  is surrounding surface emissivity;  $d_{out}$  is pipe outer diameter mm;  $d_{in}$  pipe inner diameter mm;  $\lambda$  thermal conductivity W/(mK).

In the calculation with pipework, all radiators receive somewhat lower temperature than that from the boiler.

### ***Circulation pump model***

Two types of control - constant pressure and constant speed control of the pump, were used (Figure 2-4). Pipe model calculates pressure drops whereas thermostatic valves also generate pressure drops. Because of single losses (losses caused by branches, valves etc.) of the pipework were neglected (have no effect on simulated heat emissions); 3000 Pa constant pressure head was enough for the system. Hand-made sizing calculation at the design outdoor temperature showed that the pressure head of of a circulation pump of 3000 Pa was sufficient for the system. Constant pressure control is implemented in IDA-ICE as a standard model. To use constant speed control, the pump model with the curve shown in Figure 2-4 was used.

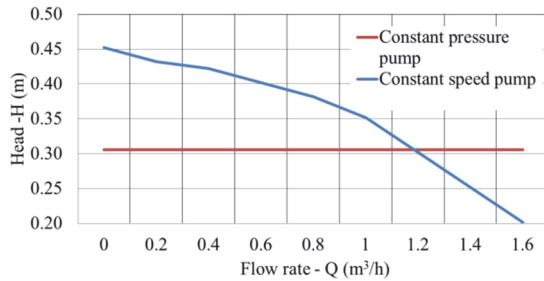


**Figure 2-4 Operation curves of a circulation pump for constant pressure and constant speed control.**

## **2.3 Modeling and analytical calculation for radiators with parallel and serial connected panels**

### **2.3.1 Radiator configurations**

The studied radiator configurations are shown in Figure 2-5. The parallel connected panels are in theory most effective in respect of the heat output, utilizing maximally the flow temperature level. In the case of serial connected panels, hot water flows first through the front (room-side) panel and then to the back (wall side) panel. The cooled water then returns to the heating pipework. The idea of serial connection is to increase the room side surface temperature of the radiator, which will increase radiation heat transfer and the operative temperature.

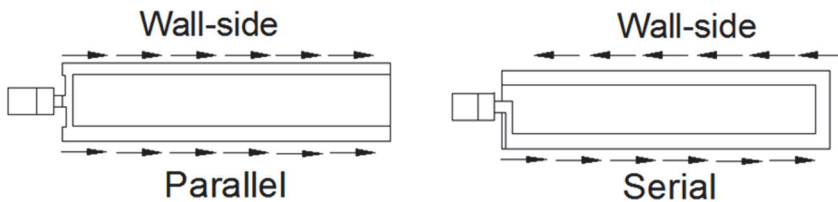


**Figure 2-5 Studied radiator types with parallel and serial connected panels.**

### 2.3.2 Heat output and temperature measurements

Heat emission of two radiators at a given room air temperature was measured in the test chamber conforming to EN 442-2:2003 requirements [55]. Two-panel radiators measured were physically of the same size, 0.6 m height and 1.4 m length, with parallel and serial connected panels and two convection fin plates in between, both type 22. The rated heat output of parallel panels was 2393 W and for serial panels 2332 W at the over-temperature  $\Delta T=50$  °C according to EN 442-2:2003. The air temperature and heat emission of the radiators was controlled with the same proportional thermostat, which was a typical radiator thermostat complying with EN 215:2004 [56] and operating across the proportional band of 2 °C with the set point of 20 °C in all tests.

In addition to the standard heat output measurement arrangements, the radiators and all surfaces were equipped with temperature measurement sensors. The effect of radiant heat transfer was estimated by measuring the 150 mm globe temperature. Figure 2-6 illustrates the measurement arrangement and temperature measurement points.

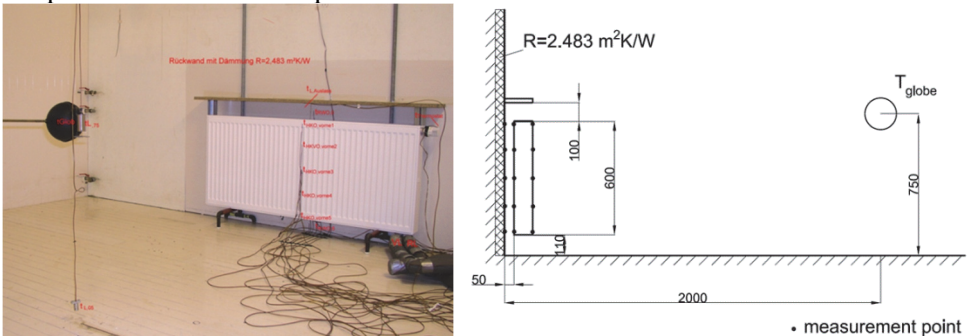


Figure 2-6 Radiator and temperature measurement point locations. The room floor area is 4.0 by 4.0 m and the room height 3.0 m.

### 2.3.3 Analytical model of the EN 442-2 test room heat transfer

In laboratory measurements, the room air temperature set point was 20 °C, but in reality the air temperature varied by 0.1...0.2 K at different test runs. To enable the comparison at exactly the same operative temperature in the room, the correction was applied through the analytical model of the room. In the EN 442-2 test room, the radiator heat emission is controlled by cooling of all room surfaces with a water-based circulation system. Therefore, the radiator heat emission  $q_{tot}$  is controlled with surface temperature  $T_s$ , which is the same for all room surfaces.  $q_{tot}$  was measured from the water flow side (Figure 2-7).

To change the surface temperature  $T_s$  in order to recalculate all consequent heat transfer effects and other temperatures at the same operative temperature, it is necessary to describe and solve the relation between  $q_{tot}$  and  $T_s$ :

$$q_{tot} = f(T_s) \quad (16)$$

Heat flows in the room and symbols used are shown in Figure 2-7. Heat losses consist (unit W) of radiation ( $q_r$ ) and convection ( $q_c$ ) and heat transmission through insulation in the wall where the radiator is mounted ( $q_w$ ) Eq. (17).

$$q_{loss} = q_r + q_c + q_w + q_{bw} \quad (17)$$

where  $q_{bw}$  is the heat conduction through the area behind the radiator. Radiator heat emission is described as Eq. (18).

$$q_{tot} = q_{front} + q_{cr} + q_b \quad (18)$$

where  $q_{front} = q_r + q_{cf}$  consists of radiation ( $q_r$ ) and convection from the front panel ( $q_{cf}$ ),  $q_{cr}$  is convection from convection fins and  $q_b$  is the total heat transfer from the rear panel. Because  $q_{tot}$  and surface temperatures were measured, it is necessary to calculate only  $q_r$ . According to the steady state heat balance,  $q_{tot} = q_{loss}$ .

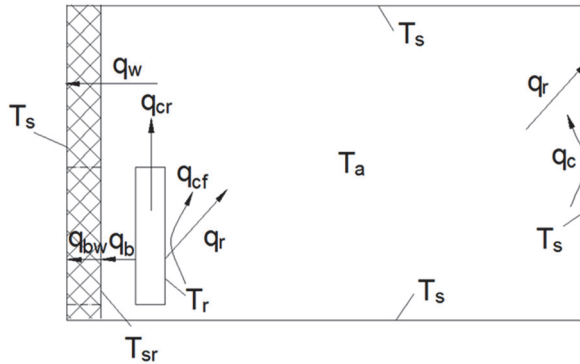


Figure 2-7 Heat balance of the EN 442-2 test room. Heat from cooled surfaces ( $T_s$ ) is removed with a water flow.

Net radiative heat exchange can be calculated from the longwave radiation [30] Eq. (19).

$$q_r = \sigma \cdot A_r \cdot F_{er-s} \cdot (T_r^4 - T_s^4) \quad (19)$$

where  $\sigma = 5.67 \cdot 10^{-8} \text{ W}/(\text{m}^2\text{K}^4)$  is the Stefan-Boltzman constant and  $F_{er-s}$  is the total exchange factor Eq. (20).

$$F_{er-s} = \frac{1}{\frac{1}{F_{r-s}} + \left(\frac{1}{\varepsilon_r} - 1\right) + \frac{A_r}{A_s} \left(\frac{1}{\varepsilon_s} - 1\right)} \quad (20)$$

Because of the view factor  $F_{r-s} = \sum_{i=1}^5 F_i = 1$ , by Eq. (21), the total exchange factor becomes Eq. (21).

$$F_{er-s} = \frac{1}{\frac{1}{1} + \left(\frac{1}{0.95} - 1\right) + \frac{0.84}{68} \left(\frac{1}{0.9} - 1\right)} = 0.899 \quad (21)$$

As the net radiation heat exchange can be calculated by Eq. (19) and  $q_{tot}$  is measured, convection  $q_c$  can be calculated from the heat balance as in Eq. (22).

$$q_c + q_w + q_{bw} = q_{tot} - q_r \quad (22)$$

where heat transmission through insulation on the wall where the radiator is mounted can be calculated from measured air and surface temperatures and thermal resistance of the insulation in the wall area behind the radiator by Eq. (23).

$$q_{bw} = U_{bw} \cdot A_r \cdot (T_{sr} - T_s) \quad (23)$$

where the wall surface temperature  $T_{sr}$  is measured and  $U_{bw}=1/2.483=0.402$  W/(m<sup>2</sup>K). Through the rest of the insulated wall Eq. (24).

$$q_w = U_w \cdot A_w \cdot (T_a - T_s) \quad (24)$$

where a building code default value of the surface heat resistance of 0.13 (m<sup>2</sup>K)/W was used to calculate  $U_w=1/(2.483+0.13)=0.383$  W/(m<sup>2</sup>K). With Eqs. (19), (23) and (24), convection heat transfer rate  $q_c$  can be calculated Eq. (25). From  $q_c$ , the convection heat transfer coefficient  $h_c$  can be calculated Eq. (26).

$$q_c = h_c \cdot A_s \cdot (T_a - T_s) \quad (25)$$

$$h_c = c \cdot (T_a - T_s)^{0.25} \quad (26)$$

where  $c$  is a constant.

This set of equations can be used for small adjustments of the room temperature, which is needed to recalculate the results to the same operative temperature as follows:

- change the measured  $T_{s,1}$  value to  $T_{s,2}$
- calculate new over-temperature (logarithmic temperature difference between the water and the air) for the radiator and newly adjusted heat emission (27).

$$q_{tot,2} = q_{tot,1} \cdot \frac{\Delta T_{ln,2}}{\Delta T_{ln,1}} \quad (27)$$

- calculate the new value of  $q_c$  with Eq. (22) and iterate the new  $T_{a,2}$  so that the constant from Eq. (26) remains the same, i.e.  $c_2 = c_1$ .

This calculation provides a new air temperature  $T_a$  and a new heat emission of the radiator for the given change of the surface temperature value  $T_s$ . The results apply for small changes because the radiator surface temperatures and the wall surface temperatures behind the radiator are not corrected, i.e. secondary effects are not accounted.

From the new  $T_s$  and  $T_a$  values, the operative temperature can be calculated and the procedure is to be repeated until the desired operative temperature is achieved. The operative temperature was calculated with the angle factors and equations of ISO 7726:1998 [30]. For this purpose, we used an angle factor between a small plane element and the surrounding surfaces used to calculate the plane radiant temperature given in Annex C of the standard. The mean radiant temperature was calculated from the plane radiant temperatures in six directions and the projected area factors for a person in the same six directions given in

Annex B of the standard. The operative temperature was calculated as an average of the air and the mean radiant temperature. For the comparison, the mean radiant temperature was calculated also from the measured standard globe temperature with the equation given in the standard.

### 2.3.4 Case study in a dynamic simulation environment

IDA-ICE [57] simulation software with a standard water radiator model was used to model the EN 442-2 test room and a typical residential room (with the same dimensions). In the test room, the radiator was located on the internal wall and on other three walls, floor and ceiling were external at  $-22\text{ }^{\circ}\text{C}$  outdoor temperature (typical of designing outdoor temperature in Estonia, Tallinn), Figure 2-8. In the case of an apartment room, the radiator was located on the external wall with a window and there was another external wall (two external walls and all other surfaces were internal), Figure 2-9. The apartment room had exhaust ventilation without heat recovery.

The IDA-ICE radiator model is a generic radiator model, which calculates heat transfer by convection and radiation from the front panel and the rest of heat emission is an extra convective heat transfer, as described with equations below. The front panel surface temperature depends on the radiator size, flow temperature and water mass flow (the latter is typically set by the return temperature in the model). Compared to the measurements, the same radiator size and flow temperature were used for a parallel radiator. To achieve the same front panel surface temperature as measured, slightly higher return temperature was necessary. In the case of a serial radiator, we increased also the flow temperature so that the front panel temperature was identical to the measured value. Firstly, the simulation was run at  $-22\text{ }^{\circ}\text{C}$  outdoor temperature to compare the differences in heat outputs and secondly, all year round with Estonian TRY [51] for annual heating energy.

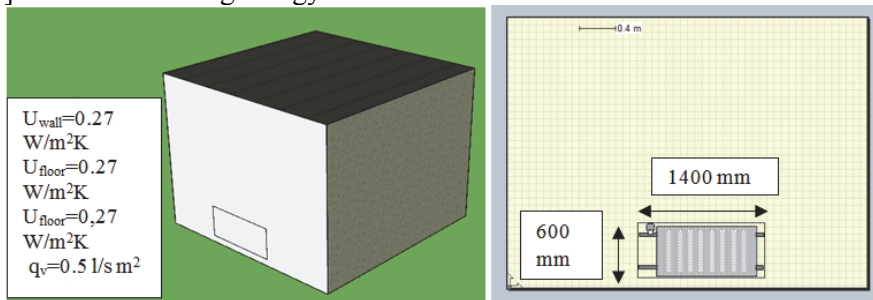


Figure 2-8 Simulated EN 442-2 room and the radiator in IDA-ICE model (white wall is adiabatic)

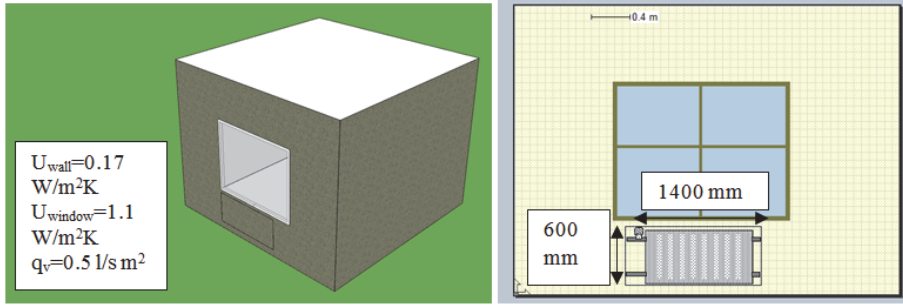


Figure 2-9 Simulated residential room and the radiator in the IDA-ICE model (roof is adiabatic)

In the water radiator model, the leaving water temperature was calculated by Eq. (28).

$$T_{ret} = T_a + (T_{flow} - T_a) \cdot e^{-\frac{T_{flow} - T_{ret}}{\Delta T_{in}}} \quad (28)$$

where  $T_{ret}$  is the return temperature and  $T_{flow}$  is the flow temperature. The radiator model was described in section 2.2.1.

## 2.4 Detailed heat pump model

Heat pump and a low-temperature heating system is a good combination for reaching EU goals. To calculate the efficiency of the heat pump model, in the laboratory measurements, heat pump performance was measured as a function of the return temperature. In modeling, two methods were used to calculate the heat pump performance as a function of heating system flow/return temperatures. In the first step, a dynamic simulation was conducted with an existing heat pump model of IDA-ICE simulation software. In the second step, an improved model based on laboratory measurements and the correlation derived was used to calculate the seasonal performance ratio of the heat pump with actual heating system flow/return temperatures. Four connection schemes of the heat pump were analyzed with dynamic simulations based on these methods.

### 2.4.1 Dynamic model of the heat pump heating system

The heating system described in section 2.2.1 was used in simulating heating system flow and return temperatures.

The standard plant model was replaced to the IDA-ESBO plant model, which includes the heat pump model [58]. IDA-ESBO has more advanced plant models than those of IDA-ICE, including a possibility to model different heat pumps, solar panels, wind turbines, stratification tanks etc. In the current work, the IDA-ESBO plant model was integrated to the IDA-ICE on an advanced level. The heat pump selected is a residential on-off type pump with variable condensing temperature with working fluid R407C. Main parameters of the investigated heat pump used in the mathematical model of calculating the seasonal performance of a heat pump are shown in Table 2-3. In the radiator heating system equipped

with thermostatic valves, much fluctuation of the water flow occurs, resulting in a temperature drop, which is much higher compared to the 5 °C temperature difference in the testing value of the steady-state standard heat pump (Figure 2-10 (left)). Constant pressure circulation pump was used in all simulation cases and annual mass-flow in the space heating circuit is shown in Figure 2-10 (right). Mass-flow and temperature values in Figure 2-10 were computed with IDA-ICE.

**Table 2-3 Basic information about the heat pump**

Heat output	5 kW
$\Delta t_{\log,eva.}$	8 °C
$\Delta t_{\log,cond.}$	8 °C
$t_{brine.in}$	0 °C
$t_{brine.out}$	-3 °C
$t_{water.in}$	30 °C
$t_{water.out}$	35 °C
$COP_{test.conditions}$	4.3

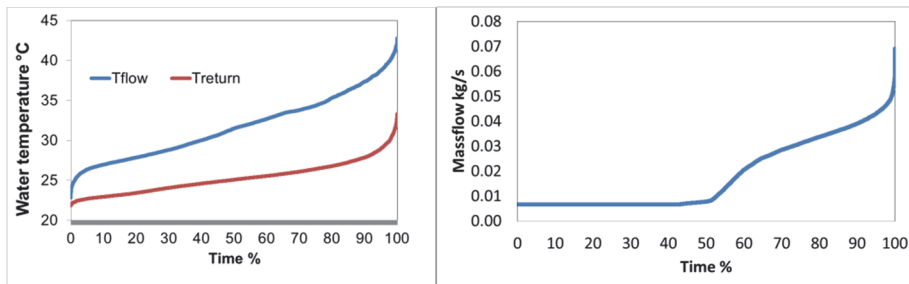


**Figure 2-10 Duration curves of temperature drop (flow and return) in the radiator heating system (left) and the duration curve of annual mass flow in the space heating circuit (right). 100% = 8760 hours.**

## 2.4.2 Connection schemes

Manufacturers recommend a connection scheme depending on the usage profile, consumption and working mode. Four most used types of connection schemes were analyzed. In the first step, connection No 1 (Figure 2-11) where on-off type ground source heat pump with working fluid R407C connected to the heating system through the stratification tank was modeled in IDA-ESBO simulations. This connection has three circulation pumps (between the ground loop and the evaporator; the condenser and the stratification tank and for the space heating system). Stratification tank should have an additional top-up heater because heat pumps often have sized to cover approximately 60% of the heating power at the design outdoor temperature [59], but in this study the heat pump was sized to cover 100% of the building heating need at the design outdoor temperature,

which in Tallinn is  $-22\text{ }^{\circ}\text{C}$  (in simulations an additional top-up heater was neglected).

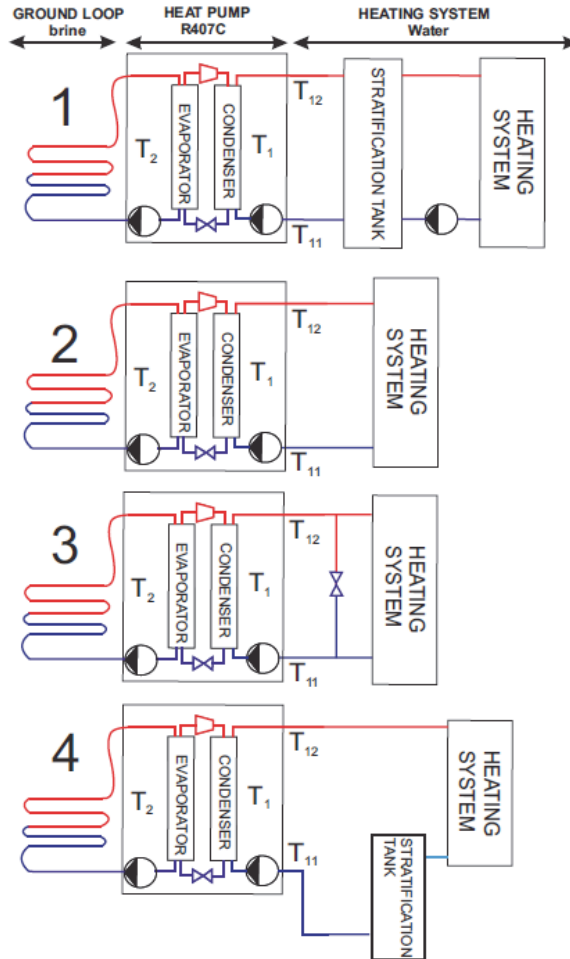


**Figure 2-11 Calculation schemes (E- evaporator; C- condenser; ST – stratification tank; SHS – space heating system).**

Connection No. 2, 3 and 4 are also popular in domestic solutions. Connection No 2 is a direct connection, No 3 has a bypass and No 4 has an additional tank increasing the system water volume, which helps on-off operation of the heat pump. No 1 was both simulated with the IDA-ESBO plant and calculated analytically. Connections 2, 3 and 4 were then analyzed with verified analytical formulas. Hourly flow/return temperatures of the heating system were simulated with the IDA-ICE simulation model with a detailed radiator heating system and the effect of direct calculation from the heating curve was also tested.

### 2.4.3 Basic equations

The efficiency of the heat pump can be expressed with the COP, which is the quotation between the useful heating capacity and the power input Eq. (29). The theoretical upper limit for the COP of a heat pump operating between the condensation and the evaporation temperature is expressed by the Carnot coefficient of performance. The real COP should consider the compressor power factor or exergy efficiency Eq. (30).

$$COP_c = \frac{Q_1}{W} = \frac{T_1}{T_1 - T_2} \quad (29)$$

where  $COP_c$  is the Carnot coefficient of performance;  $Q_1$  is a useful heating capacity (W),  $W$  is a total power (circulation pumps were included) (W);  $T_1$  is a condensing temperature (K);  $T_2$  is an evaporating temperature (K).

$$COP_r = COP_c \cdot \eta \quad (30)$$

where  $COP_r$  is the heat pump coefficient of the performance;  $\eta$  is exergy efficiency, which is in a range of 0.4...0.6 for conventional domestic water/water heat pumps [60] 0.3 to 0.4 for air/water heat pumps and 0.15 to 0.3 for air/air heat pumps [39].

The seasonal performance factor SPF of a heat pump was calculated with Eq. (31).

$$SPF = \frac{\phi}{P} \quad (31)$$

where  $\phi$  is heating and/or cooling energy produced by a heat pump (kWh/a), electrical energy used for producing heating or cooling energy (kWh/a) (circulation pumps were included).

### 2.4.4 IDA-ESBO simulation

In ordinary heat pump selection programs, the condensing temperatures are often calculated from the condenser outlet temperature (heating system flow temperature). The IDA-ESBO heat pump model includes physical models of heat exchangers. Water side heat balance is given by Eq. (32) and the heat exchanger by Eq. (33). These equations allow us to derive the condensing temperature Eq. (34).

$$Q_{evap/cond} = m \cdot C_p \cdot (T_{12} - T_{11}) \quad (32)$$

where  $Q_{evap/cond}$  is the heat flux from the heat exchanger (condenser or evaporator) W;  $m$  is mass flow in the space heating circuit kg/s;  $C_p$  is the specific heat of water (J/kgK);  $T_{11}$  is the return water temperature from the space heating circuit K;  $T_{12}$  is the flow water temperature to the space heating circuit K.

$$Q_{evap/cond} = U \cdot A \cdot \frac{(T_{12} - T_{11})}{\ln\left(\frac{T_1 - T_{11}}{T_1 - T_{12}}\right)} \quad (33)$$

where  $U$  is the condenser heat transfer coefficient  $W/(m^2K)$ ;  $A$  is the condenser area  $m^2$ ;  $T_1$  is the condensing temperature  $K$ .

$$T_1 = T_{11} + \frac{T_{12} - T_{11}}{\left(1 - EXP\left(-\frac{U \cdot A}{m \cdot C_p}\right)\right)} \quad (34)$$

Equation (34) is illustrated in Figure 2-12, showing the dependency between the heating system return ( $T_{11}$ ) and the condensing ( $T_1$ ) temperature at the constant flow temperature of  $50^\circ C$  at constant power (Figure 2-12 (left)) and constant mass-flow (Figure 2-12 (right)).

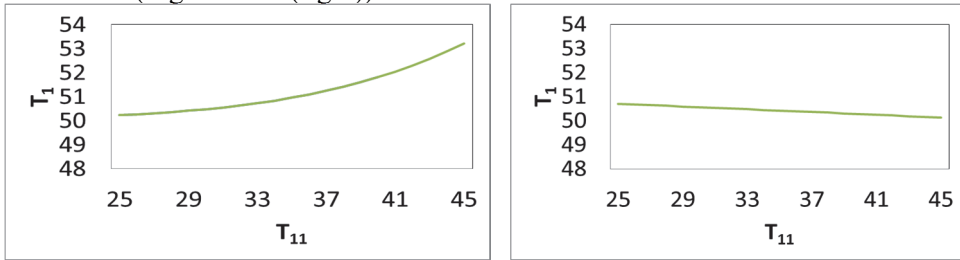


**Figure 2-12 Dependency between the return and the condensing temperature at constant power of 1000 W(left) and constant mass-flow (right) of 0.012 kg/s at constant flow ( $T_{12}$ ) temperature of  $50^\circ C$ .**

$U \cdot A$  characterize the heat exchanger, varying in a time step. IDA-ESBO calculates it on hourly bases with Eq. (35).

$$U \cdot A = \frac{Q_{evap/cond}}{\Delta t_{log.cond.}} = \frac{m \cdot C_p \cdot (T_{12} - T_{11})}{\Delta t_{log.cond.}} \quad (35)$$

Where  $\Delta t_{log.cond.}$  is a condenser logarithmic temperature difference, which characterizes the heat exchanger, usually given as a constant value from the heat pump producer but the IDA-ESBO heat pump model calculates it for every time step. IDA-ESBO calculates the condensing temperature compared to Eq. (34) in a slightly different format, as shown in Eq. (36).

$$\begin{aligned}
T_1 &= T_{11} + \frac{T_{12} - T_{11}}{(1 - EXP(-\frac{U \cdot A}{m \cdot C_p}))} = T_{11} + \frac{T_{12} - T_{11}}{1 - EXP(-\frac{m \cdot C_p \cdot (T_{12} - T_{11})}{m \cdot C_p \cdot \Delta t_{\log,cond}})} = & (36) \\
&= T_{11} + \frac{T_{12} - T_{11}}{1 - EXP(-\frac{T_{12} - T_{11}}{\Delta t_{\log,cond}})}
\end{aligned}$$

#### 2.4.5 Hand calculations with the measured correlation

In the working process of a real heat pump, condensing temperature is not conditionally constant, i.e. heat transfer of the heat exchanger is a dynamic process. A correlation was derived for the condensing temperature as a function of the flow and the return temperature. For that purpose, laboratory measurements were conducted for a domestic on-off type brine to the water heat pump with variable condensing at constant flow temperature and the heating capacity of the heat pump for four different return temperatures. In addition, previous measurements of 28 test results of the IEA Annex [42] were utilized to expand the measured data set.

### 3 RESULTS

#### 3.1 Heating system losses

##### 3.1.1 Radiator heating system losses

###### 3.1.1.1 Results of one basic low temperature calculation case

To show the level of detail of the simulation and the logic of main results, one of the main calculation cases of a detached house Det45-PI (detailed heating system with heating curve 45/35 °C with a PI controller) in Estonian climate is described below. Calculation time step is determined by the tool, based on an hourly output. As simulations in IDA-ICE were made with real calculated room temperatures; effects of poor control or internal gains can be easily seen as elevated room temperatures. Radiator heat emissions fluctuate considerably within a year. While thermostatic valve is closed, heat output is close to 0 W and heat outputs close to designed values can be reached for limited periods when the valves are fully open; the heat output duration curves for all radiators are shown in Figure 3-1.

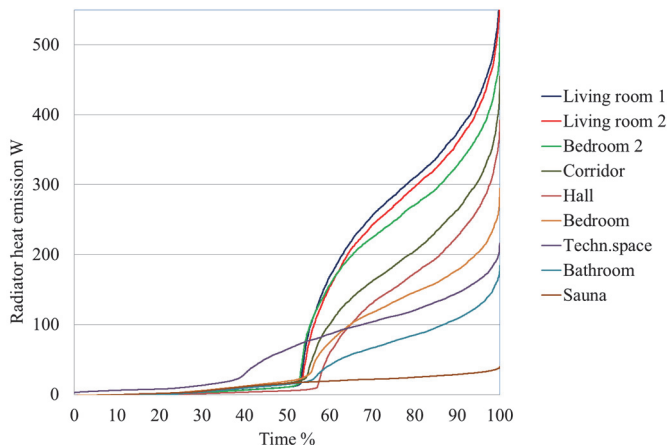


Figure 3-1 Duration curve of D-Det45-PI radiator heat emission in all rooms.

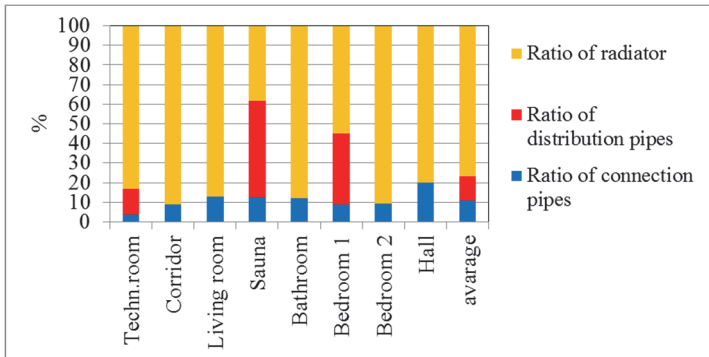


Figure 3-2 Ratio of heat emissions to different zones.

Results show that about 20 % of heat emissions to the room are from pipes in a low-temperature heating system (Figure 3-2).

It can be seen in Figure 3-1 that nearly half a year, almost no heating need is present, corresponding to the balance point temperature of 11 °C in a detached house and 9 °C in an apartment building.

### 3.1.1.2 Non-recoverable emission and distribution losses: control, stratification and back-wall losses

Significant heat losses can be caused by the control of the heat emission system. While energy need is calculated with ideal control (or with constant room temperature according to EN ISO 13790 [11]), the real room temperature will vary according to the control type and variations in the gains, (Figure 3-3). We studied a P-controller with a proportional band of 2 °C, describing a typical radiator thermostat and a PI-controller providing de-facto ideal control. The simplest available PI controllers are battery operated thermostatic valves, i.e. they can be used as common thermostats.

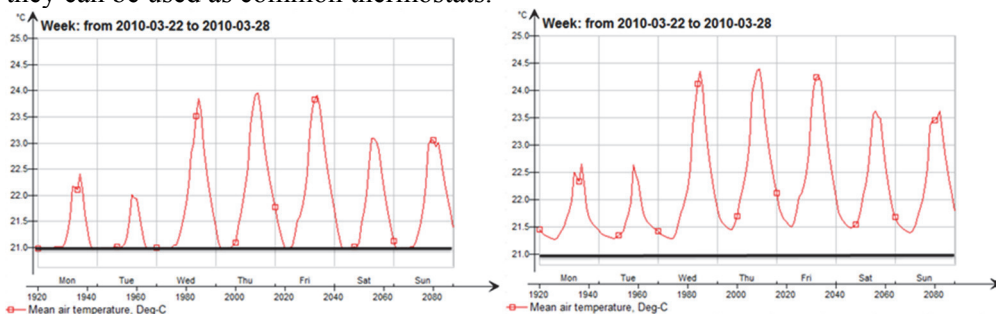
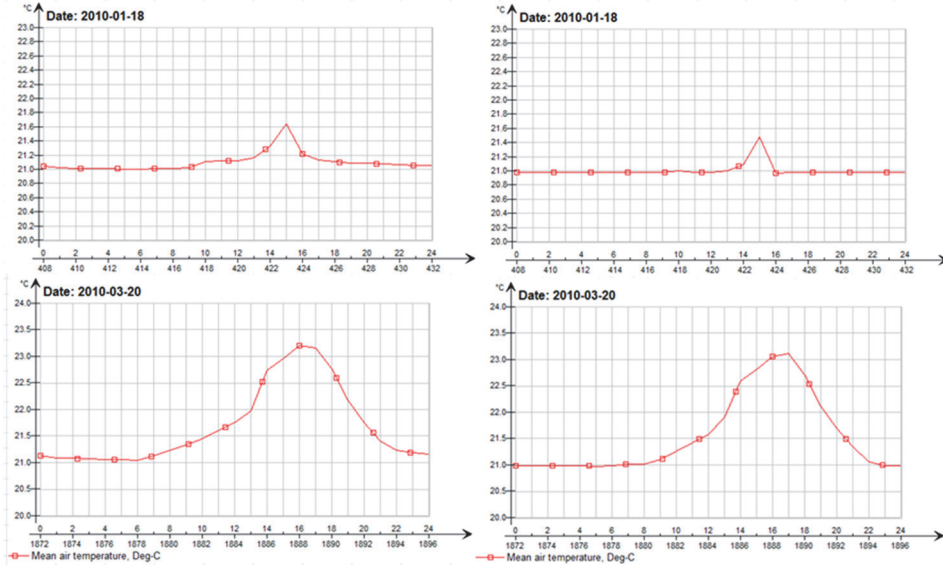


Figure 3-3 Comparison of indoor air temperature by a P- (right) and a PI- (left) controller in one week.

Because of overheating phenomena of the P-controller (caused by the flow rate of 50% at the temperature set point), simulations were made to find out the P-controller's set-point temperature that will give thermal comfort equal to that of the PI-controller. The set-point of the P-controller affected the boiler output. The

results show that the set-point could be dropped with the P-controller to keep the same room temperature as with the PI-controller. The set point of 20.5 °C with the P-controller ensured an air temperature of at least 21 °C during severe winter and in spring conditions, as shown in Figure 3-4. Therefore, realistic control losses were decreased from 13% with the set point of 21 °C to 3.3%. Control losses are summarized in Table 3-1.



**Figure 3-4 Comparison of room mean air temperature by the P-controller (set-point of 20.5 °C (left)) and the PI-controller (with a set-point of 21 °C (right)).**

**Table 3-1 Summary of control losses with the P- and the PI-controller**

Mode	Climate	Simulation case	P-controller (set point 20.5 °C)		P-controller (set point 21 °C)		PI-controller (set point 21 °C)	
			Control losses. %	Control efficiency. $\eta$	Control losses. %	Control efficiency. $\eta$	Control losses. %	Control efficiency. $\eta$
Apartment building	Tallinn	Det-45	3.34	0.97	12.99	0.89	0.00	1.00
		Det-70	3.99	0.96	18.22	0.85	0.00	1.00
	Munich	Det-45	3.72	0.96	15.44	0.87	0.00	1.00
		Det-70	4.40	0.96	16.10	0.86	0.00	1.00
Detached house	Tallinn	Det-45	2.05	0.98	8.61	0.92	0.00	1.00
		Det-70	2.81	0.97	8.70	0.92	0.00	1.00
	Munich	Det-45	5.28	0.95	13.43	0.88	0.00	1.00
		Det-70	6.24	0.94	13.43	0.88	0.00	1.00

Other components in emission losses are caused by stratification (vertical temperature gradient and additional heat loss through the external wall behind the radiator). For the loss due to the vertical temperature profile 15316-2-1:2007,

a tabulated value gives the efficiency of 0.95 (for the heating curve 55/45 °C). However, there is evidence that due to non-uniform temperature, these losses may be neglected in mechanically ventilated low energy buildings because of mixing caused by the supply airflow, which results in a very small vertical temperature gradient. The vertical temperature difference of 0.7 °C in a 2.5 m high room was reported in [33]. We used the data reported to calculate the average room air temperature when the air temperature at 0.6 m height is 21 °C. The data shown in Figure 3-5 [33] resulted in the average room air temperature of 21.05 °C that corresponds to the loss of 0.60% (efficiency of 0.994) according to our calculations.

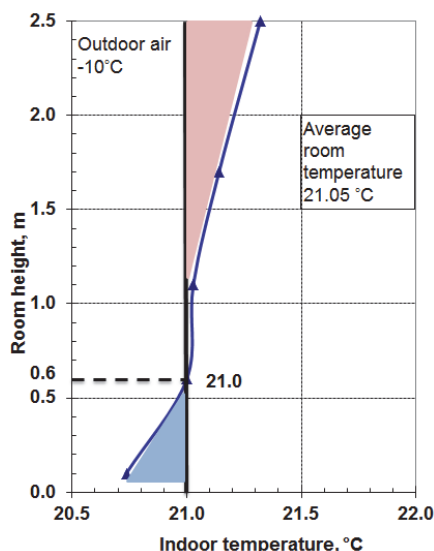


**Figure 3-5 Temperature gradient data reported in [33], resulting in the average room air temperature of 21.05 °C.**

Emission losses due to radiator position were calculated from heat flow density differences from the external wall element behind the radiator (radiators located in the external walls) and the element describing the rest of the external wall. Such calculation was possible, as IDA-ICE generates a special wall element behind the radiator with its dimensions. Temperature level (heating curve) had lower effect on the emission loss than the radiator size, because the loss was slightly smaller with a conventional heating curve because of smaller size of radiators. Additional emission heat losses from the back side of the radiator were between 0.2 and 0.25% with the heating curves studied, which gives an emission efficiency of about 0.998.

Based on the results of control (in Table 3-1) and stratification efficiencies (0.994 and 0.998), total emission efficiency can be calculated by Eqs. (2) and (3). Stratification losses add 0.4% to the control losses and the total emission losses become 0.4% (efficiency of 0.996) with the PI-controller and in between 2.6–6.5% (efficiency 0.975-0.939) with the P-controller.

### 3.1.1.3 Circulation pump control and insulation of the pipes

Three insulation levels of the distribution and connection pipes were analyzed. Cases where only distribution pipes were insulated with an insulation thickness of 40 mm are marked with letter (D) as “distribution”. In another case, with distribution pipes with an insulation thickness of 40 mm and connection pipes with an insulation thickness of 20 mm is marked with (DC). Cases not insulated have no letter in the case code, i.e. Det-45 and Det-70 have no insulation. The results were calculated with constant pressure and constant speed circulation pump control. To show the effect of insulation, Table 3-2 underlines absolute difference relative to fully insulated distribution and connection pipes. This absolute difference provides a better indication of the effect of insulation than absolute values reported in paper I, because simulations in paper I were conducted with not fully closing thermostatic valves, i.e. valves caused some distribution losses during the warm season while there was no practical heating need. In paper IV the results were partly recalculated with fully closed thermostatic valves, but the insulation effect was not analyzed further. The results show that the losses are somewhat reduced with insulated pipes by the heating curve of 70/55 °C. At the heating curve of 45/35 °C, the insulation has no practical effect. To test the model, we ran some simulations also with 100 mm insulation, which provided a better effect, but was still not able to cut distribution losses. Periodic operation, i.e. thermostats closed for a long time in spring and autumn, reduced the expected effect of insulation.

**Table 3-2 Effect of insulation at constant speed and constant pressure pump control on the distribution and emission efficiency in Estonian climate. All cases have a PI-controller.**

Mode	Simulation case	Const. pressure pump		Const. speed pump	
		Distribution and emission losses, %	Distribution and emission efficiency, $\eta$	Distribution and emission losses, %	Distribution and emission efficiency $\eta$
Apartment building	Det.45	0.84	0.99	1.22	0.99
	Det-45-D	0.64	0.99	0.79	0.99
	Det-45-DC	0.00	1.00	0.00	1.00
	Det70	7.63	0.93	9.50	0.91
	Det70-D	3.53	0.97	4.45	0.96
	Det70-DC	0.00	1.00	0.00	1.00
Detached house	Det.45	0.06	1.00	0.22	1.00
	Det-45-D	0.06	1.00	0.00	1.00
	Det-45-DC	0.00	1.00	0.00	1.00
	Det-70	1.01	0.99	0.69	0.99
	Det70-D	0.46	1.00	0.00	1.00
	Det70-DC	0.00	1.00	0.00	1.00

With constant speed circulation pump control, the higher losses occur especially during warmer months, indicating higher heat emissions from the pipes and worse utilization of internal gains, (Table 3-2).

### 3.1.2 Radiator and floor heating system losses

#### 3.1.2.1 Air temperature control

This section compares the tabulated values of the standard with dynamic simulation results when air temperature set points were used for thermostats.

Tabulated temperature variation components according to the prEN 15316-2:2014 and the total temperature variations for the investigated buildings calculated by Eq. (4) are shown in Table 3-3.

**Table 3-3 Temperature variations with the PI-control according to tabulated values of prEN 15316-2**

Temperature variation	Radiator heating 45/35 °C	Radiator heating 70/55 °C	Floor heating wet 35/28 °C (mid-floor)	Floor heating dry 35/28 °C (mid-floor)	Floor heating wet 35/28 °C (slab on ground)
$\Delta\theta_{\text{int;ini}}$	21.00	21.00	21.00	21.00	21.00
$\Delta\theta_{\text{str}}$	0.25	0.25	0.00	0.00	0.00
$\Delta\theta_{\text{ctr}}$	0.70	0.70	0.70	0.70	0.70
$\Delta\theta_{\text{emb}}$	0.00	0.00	0.40	0.25	0.40
$\Delta\theta_{\text{rad}}$	0.00	0.00	0.00	0.00	0.00
$\Delta\theta_{\text{im}}$	0.00	0.00	0.00	0.00	0.00
$\Delta\theta_{\text{hydr}}$	0.00	0.00	0.00	0.00	0.00
$\Delta\theta_{\text{roomaut}}$	-0.50	-0.50	-0.50	-0.50	-0.50
Total:	21.45	21.45	21.60	21.45	21.60

Results in Table 3-3 shows that there was no difference between the apartment building and the detached house, and the temperature variations for floor heating were the same for mid-floor and slab on ground. The standard does not distinguish climatic location and the same tabulated values should be used in all climates.

Temperature variations caused by emission losses are complicated to simulate because of fixed set points. Therefore, emission losses in kWhs were simulated and temperature variations were recalculated from the results simulated with different air temperature set points. This allowed deriving correlations between losses and temperature variations, which depend on the building type and location. These correlation equations describe linear dependence between the emission loss value and the set-point temperature (i.e. the losses were computed at different set-point temperatures with 0.1 °C step, 21.1, 21.2...22 etc.). Two

buildings in two climates resulted in four formulas: for a detached building in Tallinn  $\Theta=0.0846\eta+0.012$ , Munich  $\Theta=0.0616\eta+0.023$  and for an apartment building in Tallinn  $\Theta=0.0564\eta+0.012$  and Munich  $\Theta=0.0436\eta+0.023$  (where  $\Theta$  is temperature variation K and  $\eta$  is heating system emission loss %) (Figure 3-6 and Figure 3-7).

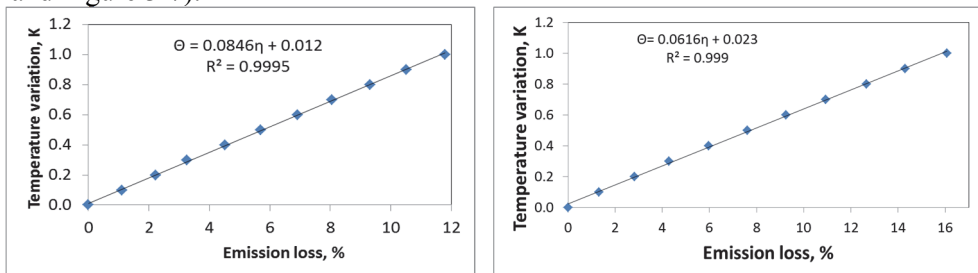


**Figure 3-6 Derived formula for calculating temperature variation from emission losses in a detached house in Tallinn (left) and Munich (right).**

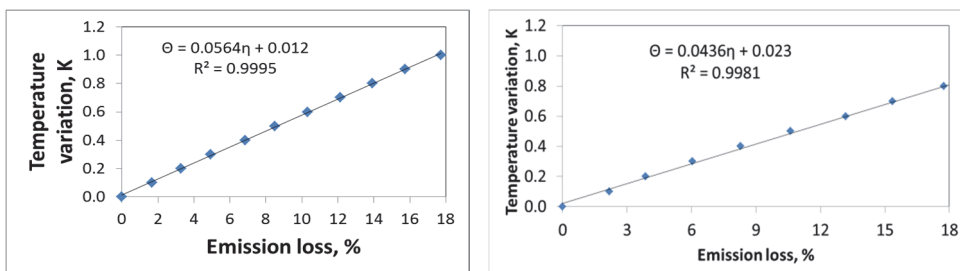


**Figure 3-7 Derived formula for calculating temperature variation from emission losses in an apartment building in Tallinn (left) and Munich (right).**

Radiator heating system emission and distribution losses were comprehensively studied in paper I, therefore based on these results, only the main cases were used in this study. Simulated results for floor and radiator heating systems are shown in Table 3-4 and Figure 3-8.

**Table 3-4 Simulated temperature variations (indoor air set-point temperature 21 °C).**

	Heating system	PI control, K	P (radiator) / on-off (UFH) control, K	Always on – no control, K (heating curve)
Detached house	45 °C/35 °C	0.11	0.29	
	70 °C/55 °C	0.11	0.35	
	Tallinn UFH – 35 °C/28 °C wet c. (mid-floor)	0.57	1.18	0.64 (30 °C/23 °C)
	UFH – 35 °C/28 °C wet c.(slab on ground)	0.78	1.67	1.25 (30 °C/23 °C)
	45 °C/35 °C	0.12	0.45	
	70 °C/55 °C	0.12	0.51	
Munich	UFH – 35 °C/28 °C wet c. (mid-floor)	0.67	1.22	0.95 (30 °C/23 °C)
	UFH – 35 °C/28 °C wet c.(slab on ground)	0.84	1.69	1.50 (30 °C/23 °C)
Apartment building	45 °C/35 °C	0.09	0.28	
	70 °C/55 °C	0.09	0.31	
	Tallinn UFH – 35 °C/28 °C wet c. (mid-floor)	0.16	0.86	0.96 (28 °C/22 °C)
	45 °C/35 °C	0.06	0.22	
	70 °C/55 °C	0.11	0.30	
	Munich UFH – 35 °C/28 °C wet c. (mid-floor)	0.20	0.97	1.40 (28 °C/22 °C)

Table 3-4 compares the PI-control as an advanced control of a heating system and the P-control for radiator heating and on-off for floor heating as conventional systems. In addition, there are always-on results with no control to show the effect of self-control of floor heating without any controller; as there is always flow during the heating season, the heating curve dropped to avoid overheating. Results show that self-control can be even more effective than the P-control in a detached house. In an apartment building, due to a higher share of internal gains, it was impossible to set a correct heating curve that would allow keeping the desired indoor temperature, and the losses were higher. Compared to the PI, temperature variations with conventional control were substantially higher, especially for floor heating. Thus, it is essential to use advanced control systems to decrease energy use.

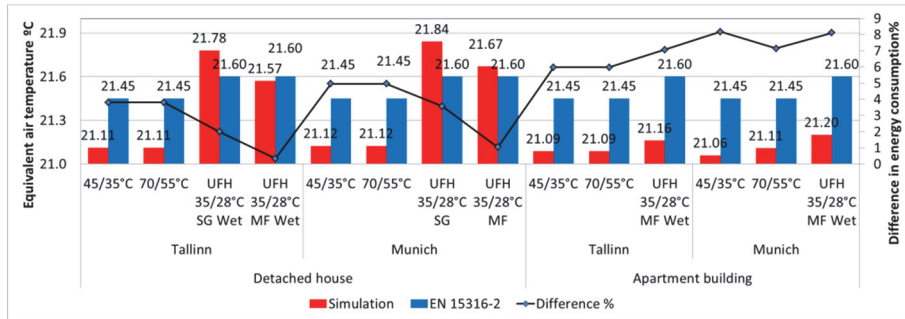


**Figure 3-8 Comparison of air temperature calculated with prEN 15316-2 and simulation with the PI-control (MF – mid-floor; SG – slab on ground).**

Figure 3-8 shows that the difference in energy consumption between the standard calculation and the simulation was up to 8%. For radiator heating, the standard recommends to use slightly higher emission losses than simulated. The overestimation is reasonable, 0.3-0.4 K in equivalent temperature, which is on the safe side. In contrast, in the detached house, the standard tabulated values were too low for the floor heating system and the losses were underestimated, which suggests splitting the tabulated values in the standard according to the thermal mass (lightweight vs. heavyweight) of the building.

Losses in floor heating systems depend also on the floor construction. Table 3-5 shows the results by the building mass and construction type.

**Table 3-5 Variations in floor heating system temperature by emission losses**

Floor type	Construction method	Wall mass	Tallinn		Munich	
			Detached house	Apartment building	Detached house	Apartment building
Slab on ground	Wet	Lightweight	0.78		0.84	
		Heavyweight	0.72			
	Dry	Lightweight	0.88		0.96	
		Heavyweight	0.73			
Mid-floor	Wet	Lightweight	0.57		0.67	
		Heavyweight (65 mm concrete)	0.43	0.16		0.2
	Wet(100mm)	Heavyweight (100 mm concrete)		0.12		0.14
		Dry	Lightweight	0.48		0.6
		Heavyweight	0.3	0.2		0.19

Table 3-5 shows that beside climate, also the floor type and building overall thermal mass affect emission losses. The results are in line with Zhou [61] who has indicated that using different thermal mass in the floor construction has a

substantial effect on indoor climate quality and energy efficiency and that larger thermal mass ensures less temperature variations.

### 3.1.2.2 Operative temperature control and thermal comfort analysis

A single zone test room was used to analyze the effect of different heat emission systems on operative temperature. First, calculations were made for one external wall and the number of external elements was increased up to five, following the external element numbering shown in Figure 3. Two different occupant locations were studied – in the centre of the room like in standard EN 422 [22] and 0.6 m from the wall with the window and the radiator. The latter represents the borderline of the occupied zone, and in some cases this location can be more critical than the centre and therefore it needs to be checked to fulfil the operative temperature requirement within the whole occupied zone. Figure 3-9 and 3.10 summarize the results at -22 °C outdoor temperatures for a low-energy building and a less insulated BAU building.

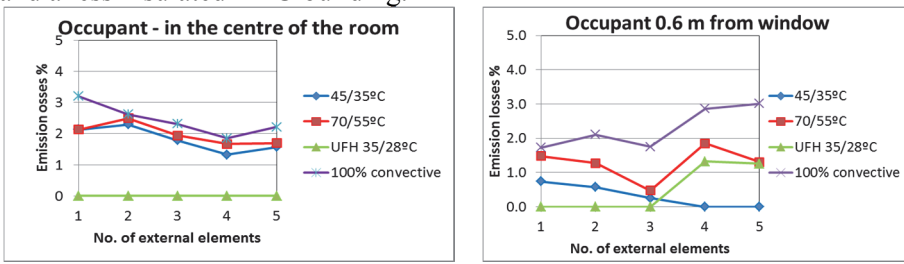


Figure 3-9 Additional heating energy at -22 °C outdoor temperature relative to the case with the lowest energy with insulation level corresponding to a low-energy building.

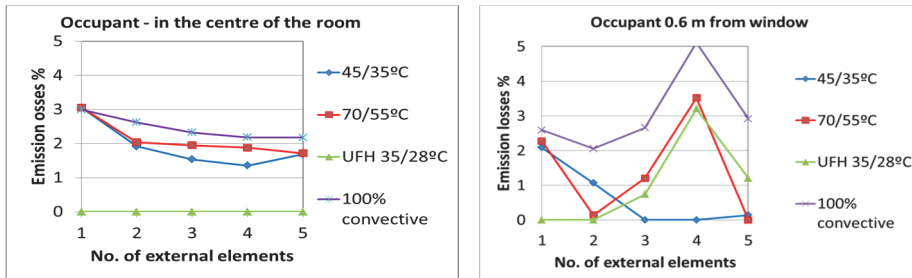
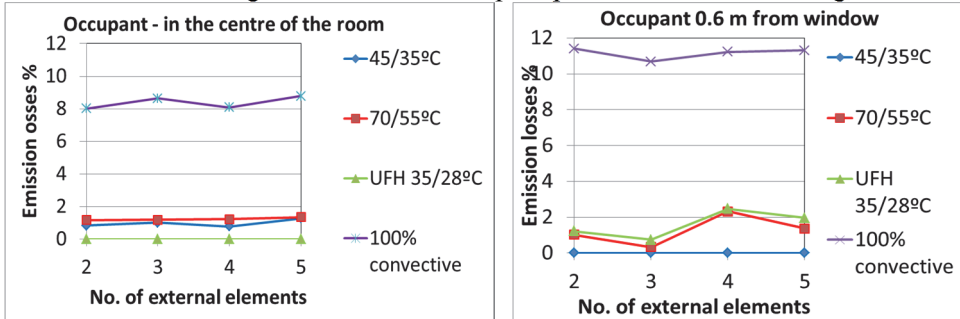


Figure 3-10 Additional heating energy at -22 °C outdoor temperature relative to the case with the lowest energy with insulation level corresponding to a less insulated (BAU) building.

While an occupant was in the middle of room, the emission losses were not so sensitive for an external construction type and the number of external walls. Best results were achieved with floor heating (heat losses of the floor were neglected because of adiabatic floor boundary condition). Moving the occupant close to the radiator and external wall changed the results remarkably and emission losses were more sensitive to the number of external elements – in the case of 3-5 external elements, the low-temperature radiator heating system secured the lowest emission losses.

Previous simulations were made on a steady state situation at constant outdoor temperature (-22 °C). To analyze heating system dynamics, the annual simulations with the PI-control were conducted, which provided smaller differences but stronger effect of the occupant position, as shown in Figure 3-11.



**Figure 3-11 Additional annual heating energy in Tallinn relative to the case with the lowest energy with insulation level corresponding to a low-energy building.**

According to annual energy calculations while the occupant was in the middle of the room, losses were the smallest still with floor heating, but when the occupant was close to the radiator, the lowest losses were reached with a low-temperature radiator heating system, independent of the number of external elements.

Components of operative temperature calculation, mean air temperature and mean radiant temperature were observed for the steady state case in Figure 3-12, showing that the mean air temperature was rising almost linearly while the occupant location was the centre of the room.

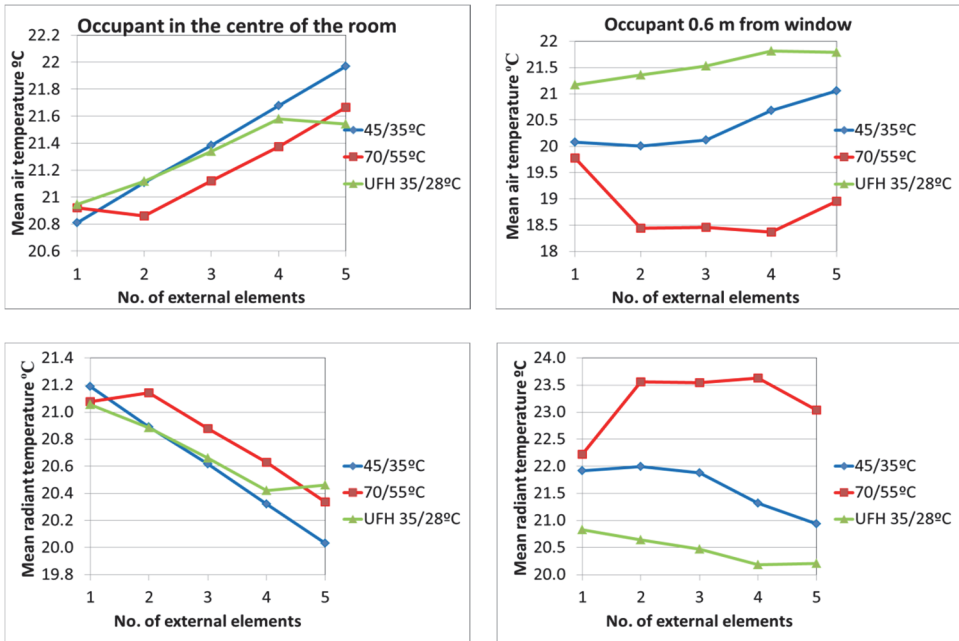


Figure 3-12 Calculated mean air and radiant temperature at -22 °C outdoor temperature with the insulation level corresponding to a low-energy building.

To determine the correction of operative temperature which will ensure proper indoor temperature in the whole occupied zone, both occupant locations were considered. Operative temperature at 0.6 m from the external wall was calculated for the case which had 21 °C operative temperature with the occupant located in the centre of the room and at the centre of the room for the case of 21 °C operative temperature with the occupant 0.6 m from the external wall (Figure 3-13).

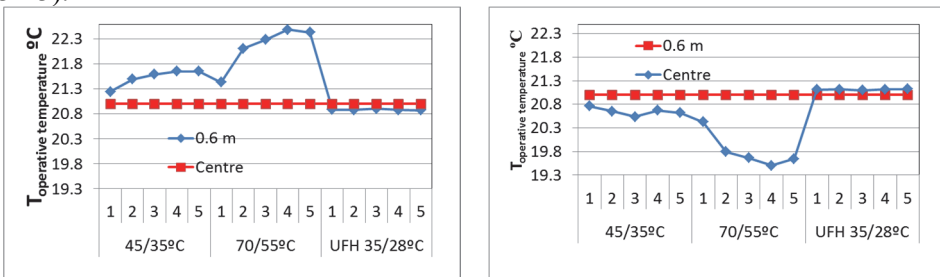
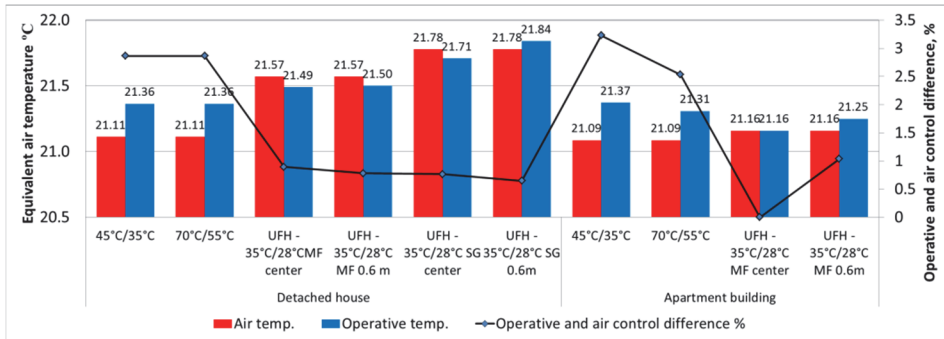


Figure 3-13 Comparison of operative temperatures according to different occupant locations at -22 °C outdoor temperature with the insulation level corresponding to a low-energy building.

Figure 3-13 shows that while keeping the operative temperature +21 °C in the centre of the room, the operative temperature close to the radiator is up to 1.4 °C higher, but in the case of floor heating, the operative temperature is almost on the same level through the occupied zone, however it decreases very slightly 0.6 m from the external wall. These results show that the critical occupant location for the radiator heating is the centre of the room, but 0.6 m from the external wall for the floor heating.

### 3.1.2.3 Heating system emission losses with operative temperature control

The temperature variations were simulated with the PI-control for the cases described in the Methods section with the operative temperature control (Figure 3-14). As described in section 3.2.2, for the floor heating system, the critical occupant’s location of 0.6 m from the external wall was used in addition to the default locations in the centre of the room.



**Figure 3-14 Air temperature and emission losses with operative temperature set point of 21 and PI-control C (UFH – underfloor heating, MF – mid-floor; SG – slab on ground) in Tallinn.**

In addition to the effect of the operative temperature, these results include all other emission losses, as described in the Methods sections. The operative temperature control has increased temperature variations in the case of radiator heating, but in the case of floor heating, changes are in both directions, indicating multiple effects of occupant position and external walls in real buildings. The results of 45/35 °C radiator heating and floor heating (0.6 m occupant location) are illustrated with monthly balance of heating energy need in the apartment and detached building in Tallinn, as shown in Figure 3-15, Figure 3-16 . For the ideal heater without any losses, 40% radiation share was used.

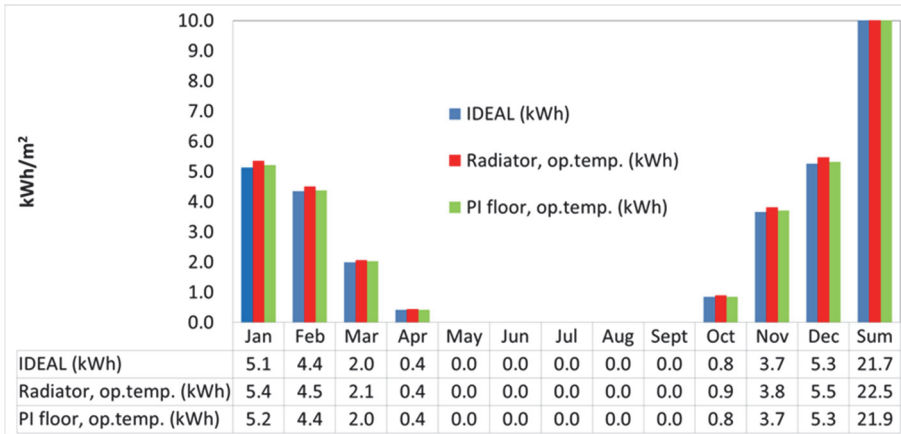


**Figure 3-15 Comparison of heating energy need in the case of low temperature radiator and floor heating systems with the PI-control in the apartment building in Tallinn.**

Figure 3-15 shows that the difference in the annual heating energy need between the floor and the radiator heating is 2.9% (annual energy need for radiator heating was 3855 kWh and for floor heating 3746 kWh, respectively) in the apartment building with heavy-weight structures.

Floor heating resulted in higher energy need in late spring and late autumn that is explained by slower response time on internal and solar gains.

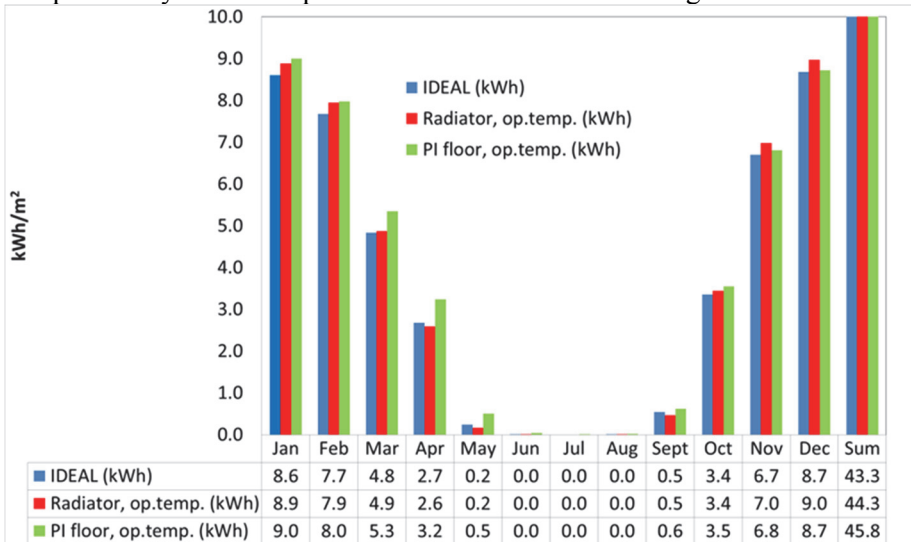


**Figure 3-16 The same results as in Figure 3-15 for the detached house.**

In the detached house with light-weight structures, the situation was vice versa and the low temperature radiator heating showed 3.3 % lower heating energy need than floor heating (annual heating energy need was 7890 kWh for radiator heating and 8155 kWh for floor heating ).

## 3.2 Comparison of radiators

### 3.2.1 Laboratory measurements at 50 °C flow temperature

Two flow temperatures were used, 50 °C and 70 °C. Both measurement cycles were repeated (Test 1, Test 2) in order to control the repeatability. The thermostat with the set point as close as possible to 20 °C in all tests changed the water flow rate with respective changes in the return water temperature according to the heating need. The same thermostat was used in the measurements for both radiators tested. All tests were started with heating up step change, which was about 2-3 °C in the room air temperature; initial room temperature (no water flow in the radiator) was about 18 °C. At the start, the water flow was rapidly raised from zero to the nominal value of 109 kg/h, which was used in all measurements.

After the step change, the flow temperature of 50 °C led to stable operation, where the heat output from the water flow decreased from about 900 W to 800 W levels, corresponding to a situation where internal heat gains are close to 15% of the nominal heat output, Figure 3-17. Water mass flow stabilized to significantly lower level in parallel radiators. Flow and return temperatures in Figure 3-18 show that a parallel radiator is operated at significantly lower return temperature on this temperature level. It was estimated that 3 % higher heat output of a parallel radiator at  $\Delta T$  50 °C increased to about 10% higher heat output at  $\Delta T$  25 °C.

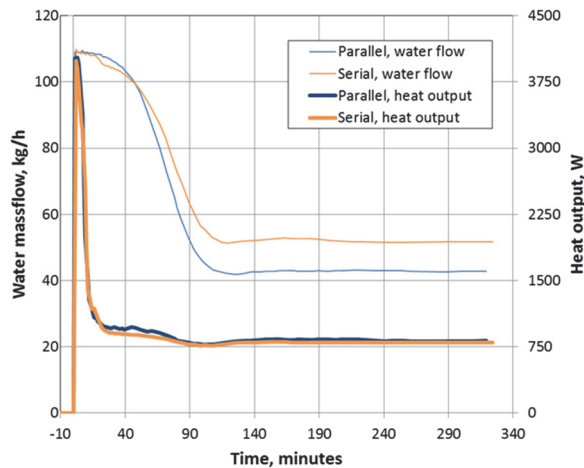
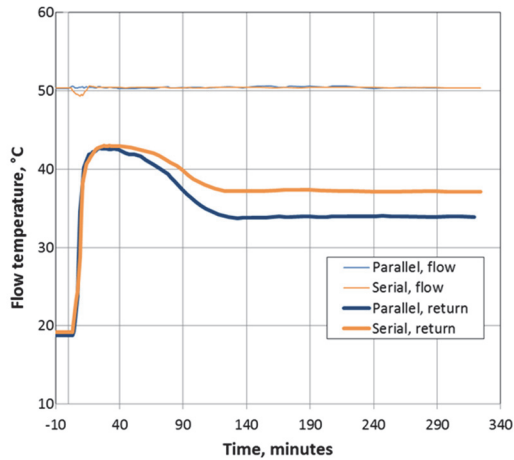
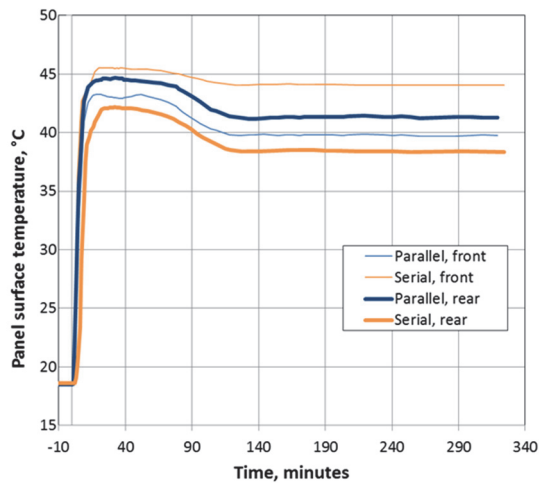


Figure 3-17 Test 1 with 50 °C flow temperature: water mass flows and heat outputs from water side.



**Figure 3-18 Flow and return temperatures at 50 °C in Test 1.**

Average front and rear panel’s surface temperatures (calculated as an average of 5 measurement points) show higher front panel and lower rear panel temperature in the case of a serial radiator, Figure 3-19. Results of room air and room cooled surface temperature showed that it was impossible to keep exactly the same temperatures in both tests (Figure 3-20). Initial temperature ( $t = -10$  min in Figure 3-19) was lower in the case of a parallel radiator, and the cooled surface temperature remained lower during the whole test, resulting also in a lower air temperature.



**Figure 3-19 Front and rear panel surface temperatures at 50 °C in Test 1.**

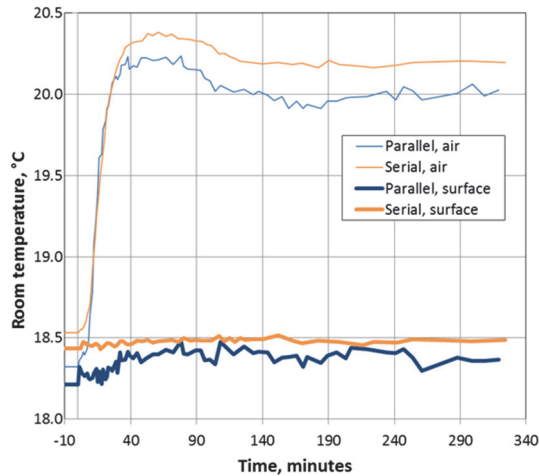


**Figure 3-20 Room air and cooled surface temperatures at 50 °C in Test 1.**

Room temperatures were analyzed for a stabilized period of 130 to 320 minutes for Test 1. For this period, an average air temperature, cooled surface temperature, the mean radiant temperature and operative temperature were calculated, Table 3-6. The operative temperature was calculated as an average of the air and the mean radiant temperature and was also estimated from the globe temperature, as described in section 2.3.3. Results show that cooled surface temperature in the case of parallel radiator was 0.1 °C lower and 0.2 °C lower at air and operative temperatures. Operative temperatures estimated from the globe temperature were about 0.2 °C higher, but the differences between the cases were the same.

**Table 3-6 Room temperatures in 50 and 70 °C tests, all values are in °C. Operative temperatures at 0.6 m height were by 0.02-0.03 °C lower than at 0.75 m height**

	Air, $T_a$	Cooled surfaces, $T_s$	Front panel $T_r$	Mean radiant, $T_{rad,mean}$	Operative , $T_{op,0.75}$ m	Operative from globe $T_{op,globe}$
Parallel 50 °C Test 1	19.98	18.38	39.7	18.79	19.39	19.62
Serial 50 °C Test 1	20.19	18.48	44.0	18.97	19.58	19.82
Parallel 50 °C Test 2	19.88	18.39	38.5	18.78	19.33	19.55
Serial 50 °C Test 2	20.07	18.47	43.1	18.95	19.51	19.74
Parallel 70 °C Test 1	19.69	17.88	40.3	18.31	19.00	19.26
Serial 70 °C Test 1	19.81	17.98	45.6	18.51	19.16	19.43

Because the temperatures were not exactly the same, the cooled room surface temperature was adjusted as described in section 2.3. The adjustment was done in two directions. In the case of a parallel radiator 50 °C Test 1,  $T_s$  was changed so that  $T_{op}$  changed from 19.39 to 19.58 °C. Adjusted parallel was then compared with serial having the same operative temperature of 19.58 °C, Table 3-7. To test

the accuracy of the analytical model, serial 50 °C Test 1 was adjusted in another direction, resulting in operative temperature change from 19.58 to 19.39. Adjusted serial was then compared with parallel having the same operative temperature. The adjustment results in Table 3-7 show the air temperature change of 0.18 °C and cooled surface temperature change of 0.20 °C in both cases. Measured heat output 824.9 W of parallel changed to 815.1 W and correspondingly measured heat output 798.7 W of serial changed to 807.3 W. After the adjustment, at equal operative temperatures, the heat output of the serial radiator was by 2.0 and 2.1 % smaller in these two cases. This 2.0 – 2.1 % is equal to heat emission reduction of a serial radiator. Analytically calculated net radiation from the front panel of radiators was 120 W and 148 W for parallel and serial, corresponding to 15 % and 18 % radiation share, respectively. The same procedure was used for 50 °C Test 2. This resulted in the negative reduction of -4.2 – -4.5%, i.e. the parallel radiator used less energy. Without adjustments to the same operative temperature, the saving of the serial radiator was about 3 % and -3 % in 50 °C Test 1 and Test 2, respectively, showing the effect of adjustments by about 1%.

**Table 3-7 Analytically calculated adjusted values of temperatures and heat outputs of radiators**

	Test 1 $T_{op}$ 19.39 → 19.58	Test 1 $T_{op}$ 19.58 → 19.39	Test 2 $T_{op}$ 19.33 → 19.51	Test 2 $T_{op}$ 19.51 → 19.33
Air, $T_{a, adjusted}$ , °C	20.16	20.00	20.05	19.90
Cooled surf., $T_{s, adjusted}$ , °C	18.58	18.28	18.58	18.29
Parallel 50 °C, heat	815.1	824.9	713.1	722.4
Serial 50 °C, heat output,	798.7	807.3	745.0	752.7
Saving of Serial, %	2.01	2.14	-4.48	-4.20

The difference between the results from Test 1 and 2 was higher than the declared accuracy of the EN 442-2 test room of +/- 1%. The measurement result showed very small but continuous swings in water flow rates and temperatures, which can explain the differences between Test 1 and 2, indicating that during the tests, the steady state conditions were not completely achieved because of the use of a proportional thermostat with limited control accuracy.

### 3.2.2 Laboratory measurements of dynamic performance at 70 °C flow temperature

The tests at 70 °C flow temperature corresponded to oversizing of radiators by about factor 2 (roughly 1600 W vs. 800 W). Initial room temperatures were reasonably close in tests with both radiators, which enabled an exact comparison of dynamic response during the heating up step change of about 3 °C. In the case of a parallel radiator, initial room air and surface temperatures were about 0.1 °C lower, but the parallel radiator reached the same temperature as a serial radiator in 9 minutes. After that the air temperature curves are almost identical with

slightly higher maximum value for the parallel in 43 minutes, Figure 3-21. After the heating up phase, the thermostat valve was not able to keep stable temperature in both cases because of oversized radiators.

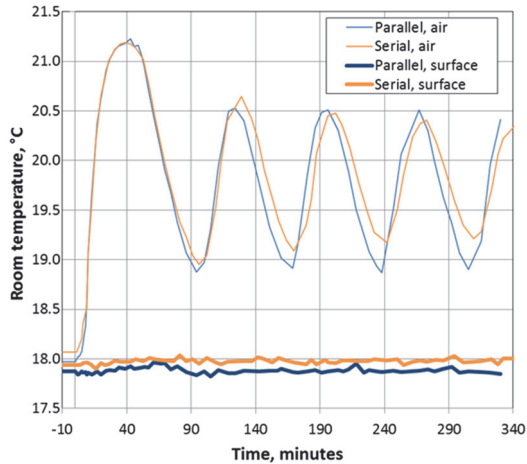


**Figure 3-21 Dynamic step response of the room air temperature at 70 °C in Test 1.**

Water mass flow and heat output of radiators are shown in Figure 3-22. Similar to 50 °C test, the parallel radiator showed slightly higher peak power. Return temperature results in Figure 3-23 show lower performance of the parallel radiator as compared to the 50 °C test where the return temperature of the parallel radiator was significantly lower. Panel surface temperatures showed similar performance as in the 50 °C test, Figure 3-24.

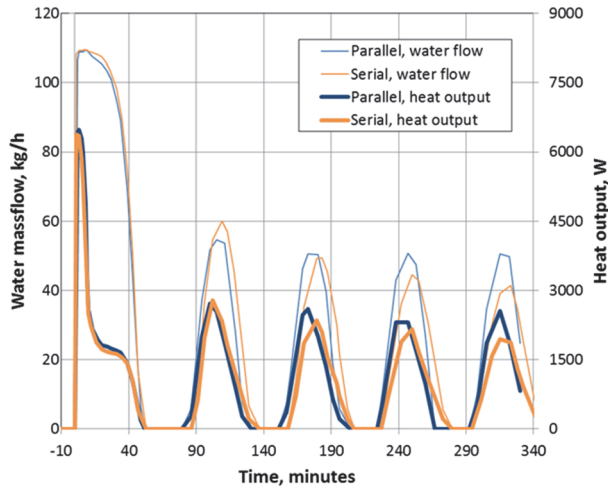


**Figure 3-22 Water mass flows and heat outputs from water side at 70 °C in Test 1.**

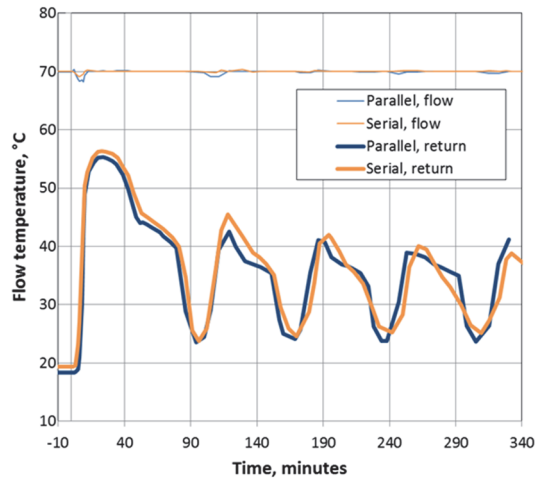


Figure 3-23 Flow and return temperatures at 70 °C in Test 1.

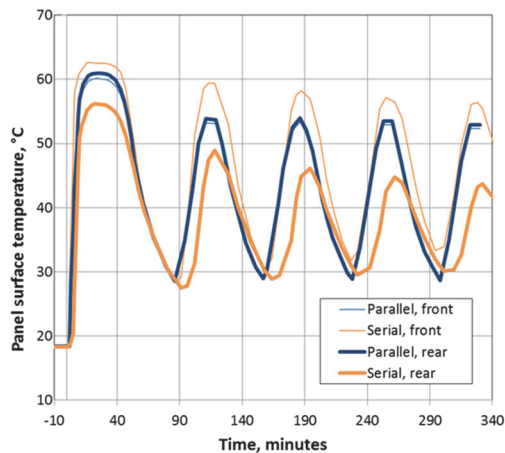


Figure 3-24 Front and rear panel surface temperatures at 70 °C in Test 1.

### 3.2.3 Simulation results

In the simulation of a residential room described in section 2.3.4, a PI-controller was used which kept the operative temperature set point of 19.5 °C with high accuracy. In the case of the EN 442-2 test room, U-values were selected so that heat losses were about 800 W at the outdoor temperature of -22 °C. The IDA-ICE radiator model provided identical front panel surface temperature for the parallel radiator when the return temperature was about 6 °C higher than that in the measurements. To achieve the measured front panel surface temperature of the serial radiator, the flow temperature was increased to 57.6 °C. With these settings, the front panel surface temperatures were the same as in the measurements for both radiators and the simulation resulted in the air

temperatures of 20.69 °C and 20.58 °C for parallel and serial cases, respectively and nearly the same heat emission of radiators, Table 3-8.

**Table 3-8 Simulation results of the EN 442-2 test room described in section 2.3. All values at -22 °C outdoor temperature**

	Parallel	Serial
Flow temperature, °C	50.0	57.6
Return temperature, °C	39.8	43.4
Front panel surface temperature, °C	39.8	44.1
Rear panel surface temperature, °C	39.8	44.1
Air temperature, °C	20.7	20.6
Front panel $q_{\text{front}}$ , W	178.7	227.1
Convection $q_{\text{cr}}$ , W	624.7	576.2
Back side $q_{\text{b}}$ , W	0.0	0.0
Water massflow, kg/h	67.7	48.6
Total heat output $q_{\text{tot}}$ , W	803.4	803.3

In the case of a residential room, the input data used resulted in slightly smaller heat losses, i.e., about 630 W compared to 800 W of the laboratory tests. At the outdoor temperature of -22 °C, the model provided identical front panel surface temperature for the parallel radiator roughly at the same flow temperature of 53 °C (vs. 50.5 °C in the measurements). To achieve the measured front panel surface temperature of the serial radiator, the flow temperature was increased to 58.7 °C. With these settings, the rear panel surface temperatures were not correct, as can be seen from Table 3-9. To achieve measured rear panel temperatures, other simulations were run with corrected flow temperatures and the back side heat transmission from these simulations were used to correct the total heat emission of the radiator (having an effect of 0.2–0.8 W, as can be seen from Table 3-9).

**Table 3-9 Simulation results of a residential room described in section 2.3. All values are at -22 °C outdoor temperature, except the annual energy use**

	Parallel	Serial
Flow temperature, °C	53.0	58.7
Return temperature, °C	38.3	43.1
Front panel surface temperature, °C	39.9	44.1
Rear panel surface temperature, °C	39.9	44.1
Air temperature, °C	19.6	19.5
Flow temperature for back wall correction,	57.7	53
Rear panel surfaces temperature at corrected	41.4	38.4
Front panel $q_{\text{front}}$ , W	179.2	227.7
Convection $q_{\text{cr}}$ , W	446.8	396.8
Back side $q_{\text{b}}$ , W	8.6	9.2
Corrected back side $q_{\text{b, corrected}}$ , W	8.8	8.4
Total heat output $q_{\text{tot}}$ , W	634.6	633.7
Corrected total heat output $q_{\text{tot}}$ , W	634.8	632.9
Water massflow, kg/h	0...36.0	0...32.4
Annual heating energy use, kWh/(m <sup>2</sup> a)	64.9	64.5

Simulated heat outputs show the difference of 1.9 W corresponding to the saving of 0.3 % by a serial radiator. In annual energy simulation, a serial radiator provided heating energy saving of 0.7 % and slightly higher front panel surface temperature, as shown in Figure 3-25. The maximum room air temperature difference appeared at -22 °C outdoor temperature, 19.61 and 19.48 °C in the case of a parallel and a serial radiator, respectively.

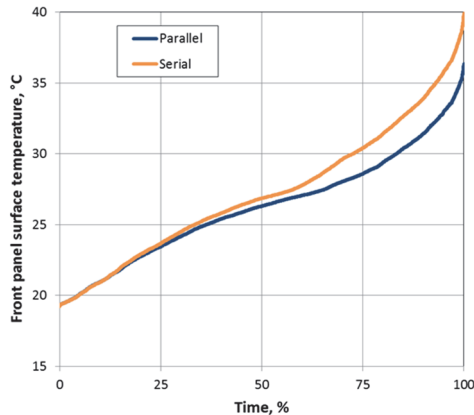


**Figure 3-25 Duration curve of the radiator front panel surface temperatures (100% = 8760 h).**

The difference between the results from the simulated EN 442-2 test room and the residential room (no saving vs. 0.3% saving of Serial) shows the effect of cold surfaces in the room. In the EN 442-2 test room, the radiator faces five cold surfaces, and the higher surface temperature of the serial radiator increased the radiant temperature (the air temperature was lower in the simulation at the fixed operative temperature set point), but this provided no energy saving because of more intensive radiation heat exchange. In the case of the residential room, the radiator on the external wall faces mainly internal walls and floors and the effect of higher radiator front panel and radiant temperatures resulted in a quantifiable energy saving of 0.3 %. These results indicate that in the EN 442-2 test room with cooled surfaces radiator type is neutral, i.e. radiators with higher convection or radiation share will provide similar heat emission at the fixed operative temperature.

### 3.3 Heat pump

Results are presented in two subsections. The first part contains the description of the model and its features, such as comparison of part-load effect and stratification tank. Besides that, this section includes the seasonal coefficient of performance value calculations with the IDA-ESBO dynamic simulation and SPF calculation with simplified formulas (Eqs. 31-38) for connection scheme No 1.

The second part covers the derivation of the equation of variable condensing temperature correlation from the laboratory test measurement and SPF calculation for different connection schemes (Figure 2-11).

### 3.3.1 IDA-ESBO heat pump simulation

The aim of this section is to give an overview of the IDA-ESBO simulation model and its results via connection No 1. A similar approach was used by Salvalai who made parameter estimation of the heat pump model in the IDA ICE environment, but his model based on producers' performance maps is a simplified version, different from the IDA-ESBO current model with more detailed properties [62].

#### *Stratification tank*

IDA-ICE heat pump model was run via a stratification tank (in our case, tank volume was 0.5 m<sup>3</sup>, which is sufficient for a low-energy detached house). The tank model includes the tank with its dimensions and volume. The tank has heat losses and the model has a possibility to set the number of layers and a fill ratio. By default, the fill ratio is 0.2 (i.e. 20% of all water is heated to the highest set-point). The simulated tank stratification with eight layer temperatures is shown in Figure 3-26.

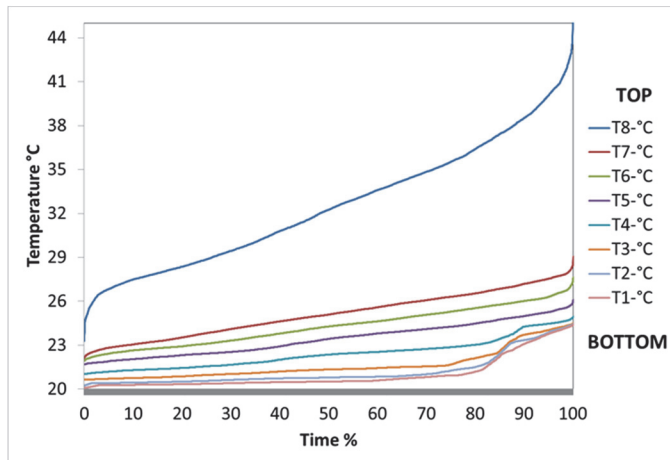


Figure 3-26 Duration curve of stratification tank layer temperatures. 100% = 8760 hours.

Layer 8 is the temperature on the top of the tank and shows the flow temperature to the heating system. The tank is connected only with a space heating system, i.e. domestic hot water heating is neglected in this study.

#### *Part load effect for heat pump performance*

IDA-ESBO library has an on-off type heat pump. However, it may be operated as a capacity controlled heat pump. According to previous studies, a variable speed heat pump can improve the energy performance in the range of 10-25% [16] due to lower condensing temperatures and fewer on/off cycles with

variable-speed pump compared to intermittent control. On the whole, part-load helps to increase the life expectancy of a heat pump and the ability to extend the operating range of the compressor provides an opportunity to reduce the need for supplementary heat in Nordic climates, where supplementary heat is necessary. IDA-ESBO simulation results showed that variable speed control helped to achieve 13% higher SPF than simple on-off control (SPF with on-off control was 3.07 and with variable speed 3.48, respectively). In the part-load working mode, condenser mass flow is lower than in the on-off working mode (Figure 3-27).

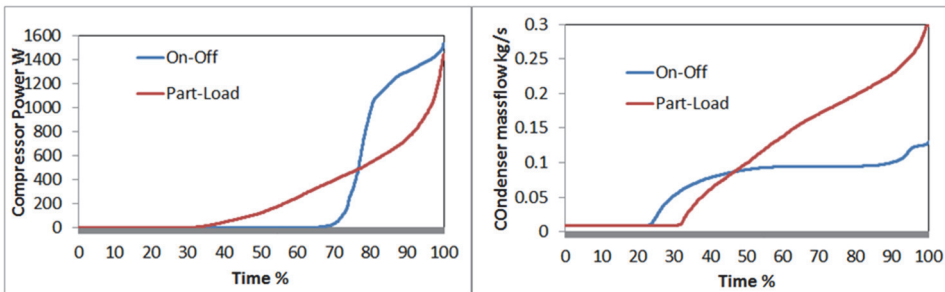


Figure 3-27 Duration curve of compressor power (left) and condenser mass flow (right) in the on-off and the part-load working mode. 100% = 8760 hours.

***Constant refrigerant temperature heat exchanger – calculation with simplified formulas***

To use Eqs. (29) and (30), the annual performance of the heat pump was first calculated with the IDA-ESBO simulation. Hourly exergy efficiency values calculated with the IDA-ICE simulation results and Eq. (30) were in the range of 0.50...0.63 with an average efficiency value of 0.57. Figure 3-28 shows the corresponding hourly COP values of IDA-ESBO simulation; Carnot ideal process with Eq. (29) (evaporating and condensing temperature from IDA-ICE results) and heat pump efficiency of 0.57 hand calculated with Eq. (32).

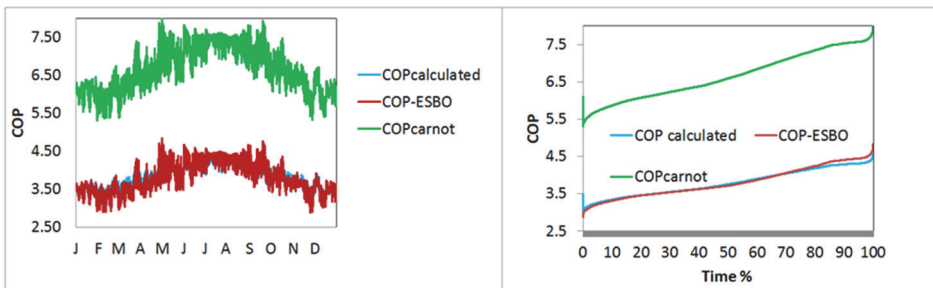
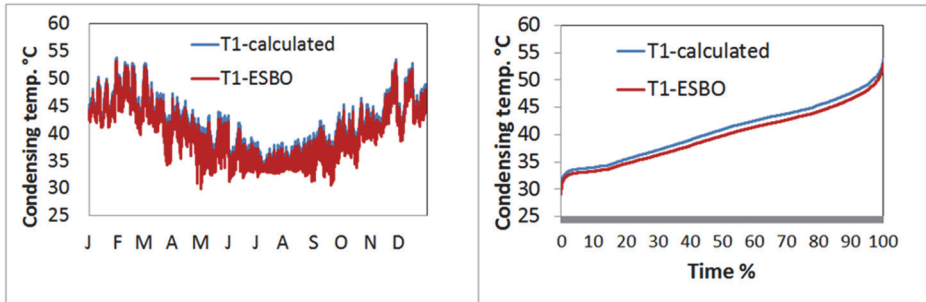


Figure 3-28 Hourly COP values (left) and the duration curve (right) calculated with simulated evaporating and condensing temperatures. 100% = 8760 hours.

Results in Figure 3-28 show that hand calculation with constant heat pump efficiency value of 0.57 gave accurate results on an annual basis. In the next

step, the condensing temperature was calculated with Eq. (36) from the flow/return temperatures, and the result was compared to the IDA-ESBO condensing temperature in Figure 3-29.



**Figure 3-29 Hourly condensing temperature (left) and the duration curve (right) calculated by Eq. (36) compared to the IDA-ESBO results. 100% = 8760 hours.**

Hand-calculated and IDA-ESBO results were very close. IDA-ESBO simulation provided an average condensing temperature of 39.8 °C and hand calculation - 40.7 °C. This slight difference was caused by the logarithmic temperature difference, which IDA calculates dynamically for every hour, but in hand calculations, constant  $\Delta t_{\log, \text{cond}} = 8$  °C from Table 2-3 was used.

From calculated hourly condensing temperatures, hourly COP values were calculated with an average constant evaporating temperature of -8 °C. Calculating the COP with the exact evaporating temperature values (from IDA-ESBO results) gave the annual SPF 0.3% lower than the simplified hand calculation with constant evaporating temperature (3.38 vs. 3.39, respectively). In the further calculations constant evaporating temperature -8 °C was assumed. Figure 3-30 describes the difference of IDA-ESBO simulated hourly COP values from the hand calculated COP, showing an annual average value of 3.80 vs. 3.69, respectively. Such a slight difference (~2.8%) in the COP values resulted in the seasonal coefficient of performance at 3.48 in the IDA-ESBO simulation and 3.39 in the hand calculation (the difference ~2.6%). This shows that the hand-made calculation with several constant values with Eq. (31) is reasonably accurate and gives almost the same values as the IDA-ESBO simulation (for hand calculation, it was necessary to use the return temperature of the simulated hourly heating system for calculating the condensing temperature).

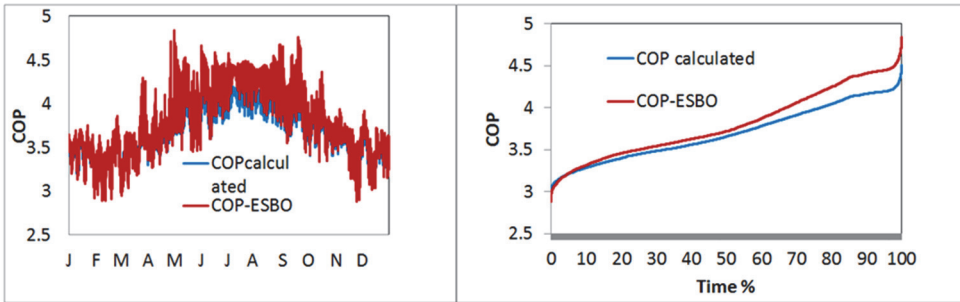


Figure 3-30 Comparison of IDA-ESBO COP values with hand calculation (left- hourly values and right - the duration curve of COP values). 100% = 8760 hours.

### 3.3.2 Calculation based on laboratory measurements

#### *Condensing temperature correlation*

Laboratory measurement data were used to describe the measured condensing temperature as a function of the flow/return temperatures of the heating system with a simple correlation equation. Results of the laboratory measurements for a wide range of return temperatures are shown in Table 3-10. Because we had a limited number of measurements, in addition, IEA Annex 28 [42] measurement results were used (Table 3-11).

Table 3-10 Laboratory measurement results ( $T_2$  – evaporating temperature °C) of the heat pump performance

	$T_1$	$T_2$	EER <sub>Carnot</sub>	EER <sub>lab,measure</sub>	$\eta$	$T_{11}$	$T_{12}$	Avg. kW	Volume flow l/s	U·A radiator
Case 1	45.06	-	5.11	2.31	0.45	29.64	49.62	8.09	0.36	0.45
Case 2	46.98	-	4.96	2.15	0.43	35.38	50.05	7.94	0.48	0.36
Case 3	48.67	-	4.82	1.97	0.41	40.15	49.98	7.79	0.7	0.31
Case 4	50.88	-	4.61	1.81	0.39	44.99	50.01	7.56	1.33	0.28

Test results show that the lower return temperature decreased the condensing temperature, resulting in higher COP<sub>Carnot</sub> (Table 3-10). According to these measurements, decrease of condensing temperature by 12.9% increased the COP by about 9%. These changes in the return temperature resulted in the pressure-enthalpy diagrams of the thermodynamic process shown in Figure 3-31.

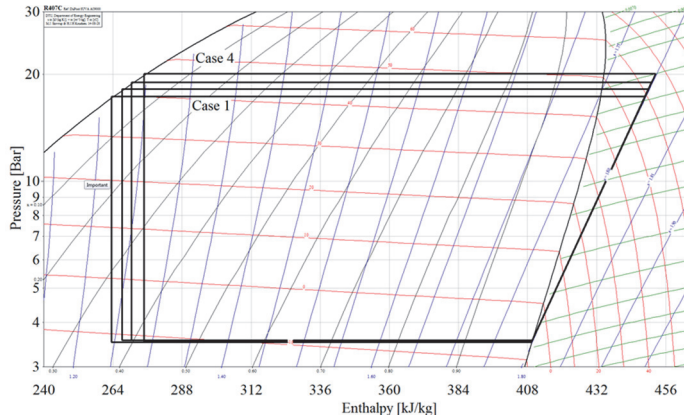


Figure 3-31 Thermodynamic process of four test cases described in Table 3-10.

Table 3-11 Measurement results from IEA Annex 28 [5] used in this study

Test no.	Heating water out °C	Heating water in °C	Brine in °C	Brine out °C	Compressor power kW	Power - total kW	Thermal power kW	COP <sub>compressor</sub>	COP <sub>total</sub>	q <sub>water</sub> m <sup>3</sup> /h	q <sub>brine</sub> m <sup>3</sup> /h
1	50.00	42.00	-5.00	-7.20	2.55	2.15	7.24	3.35	2.83	0.79	2.09
2	35.00	29.30	0.00	-3.60	2.50	2.20	10.14	4.56	4.06	1.55	2.09
3	45.00	40.00	-0.10	-3.00	2.73	2.44	9.00	3.66	3.30	1.55	2.09
4	55.00	50.60	0.00	-2.40	2.92	2.62	7.92	2.98	2.71	1.55	2.09
5	35.00	23.50	0.00	-3.80	2.38	2.14	10.52	4.42	4.89	0.79	2.09
6	35.10	30.10	-0.10	-2.90	2.53	2.23	10.26	4.05	4.57	1.77	2.57
7	55.00	51.10	0.00	-1.90	2.94	2.62	7.96	2.71	3.00	1.77	2.57
8	45.00	40.50	0.00	-2.40	2.76	2.46	9.16	3.31	3.69	1.77	2.57
9	50.00	40.10	0.00	-2.90	2.75	2.34	8.94	3.25	3.81	0.79	2.09
10	50.00	38.20	5.00	1.40	2.91	2.51	10.76	4.28	3.70	0.79	2.09

To test the condensing temperature against the measured data, the measured condensing temperatures were compared to those calculated by Eq. (36) at different  $\Delta t_{log}$  values (Table 3-12).

**Table 3-12 Condensing temperature calculation**

	T <sub>1</sub> measured	T <sub>1</sub> calc. Δt <sub>log.</sub> =1	T <sub>1</sub> calc. Δt <sub>log.</sub> =3	T <sub>1</sub> calc. Δt <sub>log.</sub> =5	T <sub>1</sub> calc. Δt <sub>log.</sub> =8
Case 1	50.88	50.04	51.17	52.91	55.76
Case 2	48.67	49.98	50.37	51.58	54.05
Case 3	46.98	50.05	50.16	50.87	52.84
Case 4	45.06	49.62	49.65	49.99	51.41

Table 3-12 shows that Eq. (36) provides an estimation and it does not enable considering the effect of return water temperature similarly to laboratory measurements.

Therefore, the correlation between the condensing and the flow/return temperature was derived from the measured data. Weightings of flow and return temperatures (x and 1-x) were used, which provided the best correlation (higher R<sup>2</sup> value) with a formula of xT<sub>11</sub>+(1-x)T<sub>12</sub>=T<sub>1</sub>. Best compliance of the condensing temperature as a function of the flow and return temperature was found for both measurements. For the IEA Annex data, this resulted in the equation: T<sub>1</sub>=0.62T<sub>12</sub>+0.34T<sub>11</sub>+4.5 with slightly higher R<sup>2</sup> value than in our measurement results T<sub>1</sub>=0.67T<sub>12</sub>+0.36T<sub>11</sub>+1.05, as shown in Figure 3-32.

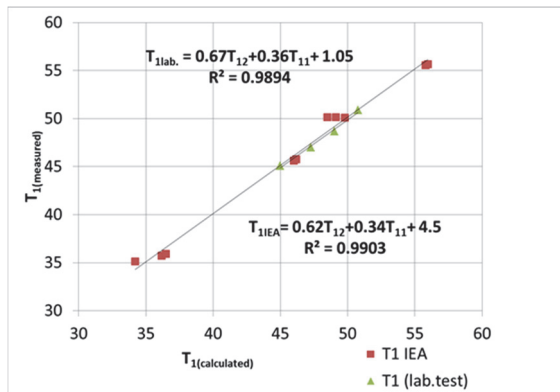


**Figure 3-32 Equations of condensing temperature correlation giving higher weighting for flow temperature.**

Data in Figure 3-32 had seven test points with a flow temperature of 50 °C, which allowed showing the dependency between the condensing temperatures and the return temperatures (Figure 3-33).

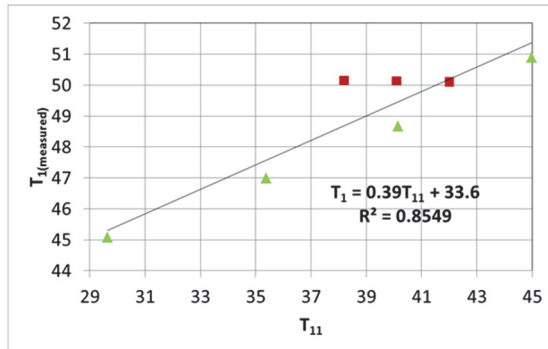


**Figure 3-33 Dependency of the condensing temperature on the return temperature at 50 °C flow temperature.**

Figure 3-33 shows that the correlation is an approximation that does not take into account all physical phenomena, however, the correlation is still reasonably high.

Derived correlations of the condensing temperature (Figure 3-32) were used to calculate the COP values. For that purpose, return temperatures of the simulated hourly heating system and the constant evaporating temperature of -8 °C were used (Figure 3-34).

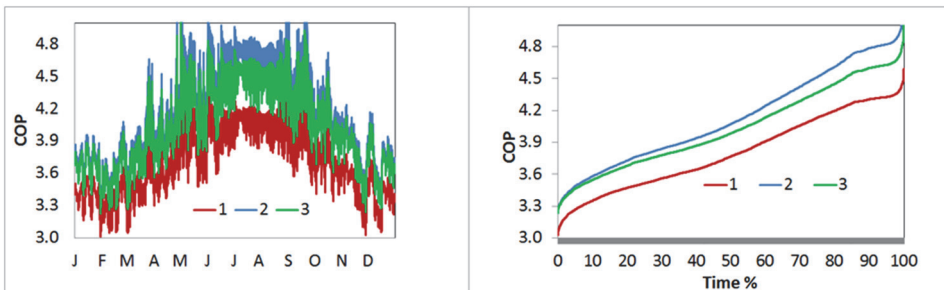


**Figure 3-34 Comparison of hourly COP (left) and the duration curve (right) of hand calculation with the condenser model (1) and derived correlation (2 – by laboratory measurements; 3 – by IEA Annex 28 measurements).**

Hourly COP values in Figure 3-34 resulted in the following SPF values (31): by the condenser model - 3.39; by laboratory measurements - 3.72 and by IEA Annex 28 measurements - 3.67.

These results show that laboratory measurements gave approximately 8-9% higher SPF value than the condenser model used in the IDA-ESBO simulation.

### ***The effect of reduced flow rates by thermostats***

Hourly simulation with the condenser model (Eq. (34)) and derived correlations (Figure 3-32) were used to test the effect of reduced flow rates by thermostats. So far, simulated return temperature was used in the calculations. At fixed flow rates (correspond to situation with exact sizing and no internal and solar gains), return temperature can be directly calculated from the flow temperature with the

assumption that heating need has linear dependency on delta T of the indoor and outdoor temperature (Figure 3-35). As input data, this calculation needs only simulated heating needs, i.e. no simulation of the radiator heating system is needed. SPF with constant water mass flow was calculated for 45/35 °C heating curve that was used in previous sections. The calculation was conducted for connection scheme No 2, where the flow temperature follows exactly the heating curve (without stratification tank effects present in connection scheme 1).

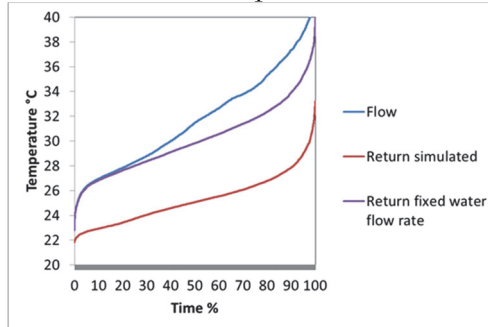


**Figure 3-35 Flow and return temperature calculations at the outdoor temperature. 100% = 8760 hours.**

Condensing temperatures were calculated by Eq. (36) and with the correlation of laboratory measurements (Figure 3-32). The use of hand calculated fixed flow return temperature (calculated with Eq. (36)) resulted in ~2 °C difference in the condensing temperature (Figure 3-36), and decreased annual SPF by ~4.5 % (SPF of 4.0 with fixed flow return temperature vs. real SPF 4.19).

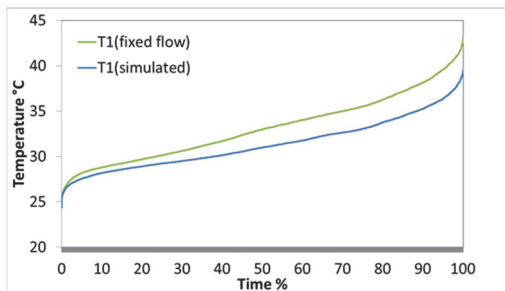


**Figure 3-36 Condensing temperature calculated by the fixed return flow rate. 100% = 8760 hours.**

***Impact of the connection scheme on the seasonal performance factor***

Four different connection schemes, which were described in section 2.2, were simulated and SPF values were computed (Table 3-13). SPF values were calculated by Eq. (31), where the compressor and the circulation pump power were computed through an hourly COP and space heating need. COPs were computed by Eq. (29) where condensing temperature correlation  $T_1=0.67T_{12}+0.36T_{11}+1.05$  was used and with the condenser model by Eq. (36).

**Table 3-13 SPF values simulated with different connection schemes**

Connection type	Laboratory	Condenser
1 separated connection with stratification	3.72	3.39
2 without bypass	4.19	3.76
3 bypass (0.1 kg/s)	3.99	3.61
3 bypass (0.05 kg/s)	4.03	3.64
3 bypass (0.02 kg/s)	4.09	3.69
3 bypass (0.005 kg/s)	4.16	3.74
4 with volume tank and bypass (0.02)	4.10	3.69

Figure 3-35 shows that the highest SPF is achieved with direct connection without bypass. The bypass reduces the SPF value, and the volume tank provides in principle a small increase without practical meaning, however the real benefits of larger water volume on the heat pump operation are out of scope of this study. The highest SPF value was achieved at the lowest return temperature, as shown in Figure 3-37.

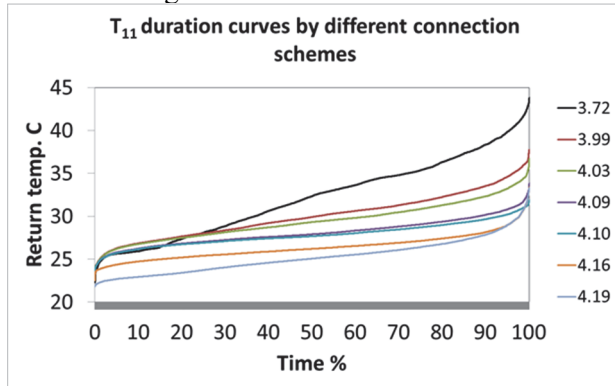


**Figure 3-37 Return temperatures with studied connection schemes described by SPF values. 100% = 8760 hours.**

## 4 DISCUSSION

### 4.1 Heating system losses and recommendation for further work

In accordance with the EPBD directive, heating losses in a well-insulated building differ from business as usual (BAU) building. The main aim of this thesis was to provide input for the revision of 15316-2-1 standard, which is one of the tasks in the preparation of second generation EPBD standards. Two papers were focused on the losses: paper I analyzed the existing standard and gave detailed results for radiator heating systems and paper IV analyzed the updated version of the standard and discussed the operative temperature correction and losses related to floor heating systems.

With regard to low energy buildings, it is questionable if all heat losses in the distribution pipe in heated rooms are recoverable, as stated in the EN 15316-2-3 standard. For that purpose, more accurate allocation was used. We defined recoverable distribution losses as heat emission emitted by the pipes until the room temperature set point was achieved. The part of the heat emission which increased room temperature over the set point was considered as non-recoverable loss. Results show that 40% of the delivered heat is uncontrolled and emitted to a room by the distribution network with the uninsulated distribution pipes. Most but not all of the distribution losses were recovered, as described in section 3.1.1. These results suggest that the methodology of distribution losses in the EN 15316-2-3 standard is out of date and needs improvement in order to be able to take into account non-recoverable distribution losses in heated rooms, as these losses may have similar magnitude compared to emission losses.

Generally, in this work distribution losses and emission losses appear together (i.e. all distribution losses were presented together with control losses) and no special effort was made to separate them. In floor heating cases, the distribution losses were not considered, i.e. the model contains no distribution pipes.

Table 4-1 combines losses in the radiator heating system based on the results of papers I and IV in order to show relative importance of the studied loss components. To calculate the total temperature variation, the P- or PI- control value was selected and all other components were summed. Similar results for floor heating are presented in Table 4-2. Comparison of lightweight and heavyweight construction and for on-off and always on cases was added to paper IV to cover all commonly used solutions. Floor heating losses are reported as total emission losses (i.e. no separation for embedded, stratification etc. were made).

**Table 4-1 Radiator system emission and distribution temperature variation**

Temperature variation, K		Tallinn (Northern-Europe)		Munich (Central-Europe)	
		Detached houses	Apartment building	Detached houses	Apartment building
Low-temperature radiator (45/35 °C)					
Control and distribution	PI	0.01	0.01	0.02	0.02
	P	0.19	0.20	0.35	0.19
Stratification	External components	0.03	0.03	0.04	0.03
	Vertical air temp.	0.06	0.05	0.06	0.05
Embedded		0.00	0.00	0.00	0.00
Operative temp. correction		0.25	0.28	0.25	0.28
Conventional radiator heating (70/55 °C)					
Control and distribution	PI	0.00	0.00	0.00	0.00
	P	0.25	0.24	0.41	0.21
Stratification	External components	0.03	0.03	0.04	0.03
	Vertical air temp.	0.06	0.05	0.06	0.05
Embedded		0.00	0.00	0.00	0.00
Operative temp. correction		0.25	0.22	0.25	0.22

**Table 4-2 Floor heating system emission temperature variation**

		Tallinn			Munich			Op.tem p. correcti on	
		Detached house							
	Constru ction method	Wall mass	PI	Alwa ys-on	on- off	PI	Always -on	on- off	
Slab on ground	Wet	Lightw.	0.78	1.25	1.67	0.84	1.5	1.69	0.06
		Heavyw.	0.72	1.32	1.55				
	Dry	Lightw.	0.88	1.42	1.31	0.96	1.78	1.43	
		Heavyw.	0.73	1.45	1.18				
Mid-floor	Wet	Lightw.	0.57	0.63	1.18	0.67	0.95	1.22	-0.07
		Heavyw. (65 UFH)	0.43	0.81	1.03				
	Dry	Lightw.	0.48	0.84	0.95	0.6	1.21	1.13	
		Heavyw.	0.3	0.94	0.84				
Apartment building									
Mid-floor	Wet	Heavy w. (65 UFH)	0.16	0.96	0.86	0.2	1.4	0.94	0.09
		Heavy w. (100 UFH)	0.12	0.93	0.77	0.14	1.37	0.95	
	Dry	Lightw.							
		Heavy w.	0.2	0.94	0.85	0.19	1.37	0.98	

According to the results, non-recoverable losses were caused mainly by control losses. Stratification losses in a room with balanced ventilation and well-insulated envelope elements can be considered very small.

A novelty value of the radiator and floor heating comparison conducted in this study was the introduced operative temperature correction that enabled fair comparison of heat emitters providing equal thermal comfort for occupants and resulted in + 0.25 K temperature variation for radiators.

Because of high number of tabulated values and especially their case and climate dependency, such tabulated approach can be seen as a dead end in future. For a more accurate approach, it would be reasonable to develop the product type models, which as open code, could be implemented in the energy simulation tools, allowing then to simulate more specific and accurate values to be used in national building codes and calculation methods. In this work, we were continuously faced with radiator model limitations in a simulation tool on the one hand and a large number of building energy need, heating system and climate combinations on the other hand.

## **4.2 Comparison of radiators and recommendations for further work**

Comprehensive studies to compare serial- and parallel connected panel radiators were conducted. This included laboratory measurements, dynamic simulations and an analytical approach. Results indicate that it is rather complicated to simulate or to make a physical test to quantify the differences of such radiators. The accuracy of the laboratory measurements was not sufficient because of the use of a proportional thermostat, which resulted in small swings in the flow rate and destroyed a resolution to show the differences between the cases. It became clear that the use of a PI-radiator thermostat would be a better choice for this type of measurement, and it would be reasonable to repeat the measurements in the future. However, our simulations showed that the radiator test room according to EN 422-2 is not sensitive to the differences studied because a room where all surfaces were cooled will compensate the positive effect of higher temperature of the front panel, resulting in higher radiation heat exchange instead of expected increased operative temperature. Therefore, it is not clear if it is possible to measure differences in such rooms even when more accurate flow rate control is applied; and it could be recommended to conduct such measurements in a room the conditions of which are more similar with real conditions, i.e., having 1-2 external walls and a window.

The radiator model used in the simulations had also limitations to study the difference between radiators with parallel and serial panel connected panels. However, the approach used was feasible but evidently it would be beneficial to work with more detailed radiator and convector models, which need more input data (e.g. number of panels, information of fins, front and rear panel etc.) than the standard model used.

Detailed simulation model could be an alternative to the CFD modeling. Previous studies have concluded that the CFD method is applicable to determine the heat output of radiators but the difference relative to experiments was up to 10% [63]. Erdogmus has concluded that the main advantage of the CFD is the control of flow properties like temperature and velocity at more than one point in the virtual test room. On the other hand, CFD solutions need experimental validation [63].

## **4.3 Effect of return temperature on heat pump performance and recommendations for further work**

Heat pump as one of the possible solutions for low temperature heating systems was analyzed analytically and by laboratory measurements in relation to achieving higher heat pump performance by lowering the return temperature. For future work, certainly the methodology needs more laboratory measurements in a wider selection of test points to make adequate implications. Although the correlation between the condensing and the flow/return temperatures was high, the investigation covers only seven test points in a

constant flow temperature of 50 °C. These seven points showed good correlation by the return temperature and the condensing temperature (Figure 3-33); however, it has too high dispersion.

Thus, more laboratory measurements are necessary to improve the condenser model so that it could consider effects of the return temperature more accurately.

## **5 CONCLUSIONS**

In this thesis the emission and distribution losses of the heating system as well as generation efficiency of a heat pump was studied for low-energy buildings. Because the existing tabulated values in the EN standards do not cover low-energy buildings, new tabulated values were derived. To enable fair comparison of the radiator and the floor heating systems, a new correction factor of the operative temperature was introduced. Efficiency aspects of the performance of radiators with parallel and serial connected panels and a radiator system with a heat pump were analyzed.

Detailed dynamic components of a heating system and the modeling covering the whole building simulation environment allowed us to quantify the distribution and emission losses for the radiator and floor heating. Based on the results reported in papers I and IV, an overall emission and distribution (in heated rooms) efficiency and loss values can be summarized for most important cases as shown in Table 5-1 (all values include the correction of the operative temperature).

**Table 5-1 Heating system emission and distribution (in heated rooms) efficiency/losses in low-energy residential buildings in Central and North European climates**

Building type and climate		System and Heating curve	Control type	Efficiency,-	Losses, %	Spatial variation of temp. K
Detached house	Tallinn	70/55 °C	P	0.94	6.95	0.60
		45/35 °C	P	0.94	6.19	0.54
		45/35 °C	PI	0.96	4.14	0.36
	Munich	70/55 °C	P	0.89	11.96	0.76
		45/35 °C	P	0.90	10.99	0.70
		45/35 °C	PI	0.95	5.63	0.37
Apartment building	Tallinn	70/55 °C	P	0.92	9.22	0.53
		45/35 °C	P	0.91	9.63	0.56
		45/35 °C	PI	0.94	6.29	0.37
	Munich	70/55 °C	P	0.90	11.40	0.52
		45/35 °C	P	0.90	10.96	0.50
		45/35 °C	PI	0.93	7.25	0.34
UFH*	Tallinn (wet-system). Lightweight	35/28 °C (MF)	on-off	0.88	13.81	1.18
		35/28 °C (MF)	PI	0.94	6.60	0.50
		35/28 °C (SG)	on-off	0.84	19.60	1.67
		35/28 °C (SG)	PI	0.92	9.08	0.84
	Tallinn (wet-system). Heavyweight	35/28 °C (MF)	on-off	0.87	15.04	0.86
		35/28 °C (MF)	PI	0.97	2.62	0.25
		35/28 °C (SG)	on-off	0.79	27.27	1.55
		35/28 °C (SG)	PI	0.89	12.55	0.72
	Munich (wet-system). Lightweight	35/28 °C (MF)	on-off	0.84	19.43	1.22
		35/28 °C (MF)	PI	0.90	10.50	0.67
		35/28 °C (SG)	on-off	0.79	27.06	1.69
		35/28 °C (SG)	PI	0.88	13.26	0.84
Munich (wet-system). Heavyweight	35/28 °C (MF)	on-off	0.82	21.72	0.97	
	35/28 °C (MF)	PI	0.96	4.06	0.20	

\**Lightweight – detached building; Heavyweight – apartment building*

The results of the thesis have been utilized in the new updated space emission losses standard prEN 15316-2:2014, including more realistic values derived in Paper I suitable for low-energy buildings. However, the standard does not enable comparison of space emission solutions on the bases of the same operative

temperature that was proposed later in Paper IV; and there are also some tabulated values which will need revision to improve the scientific quality of the standard. Based on the distribution and emission efficiency, we can conclude the following:

- No operative temperature correction is needed for floor heating, for the radiator heating, the operative temperature variation of 0.25 K is to be added.
- Emission losses occur mainly as control losses, which can be controlled with PI type thermostats.
- Non-recoverable distribution losses were not significant, but the results show that up to 40% of heat emission to the room comes from conventional heating system pipes, which are uncontrollable.
- Insulating of pipes in heated spaces proved to have no practical effect, only a small effect was observed with 70/55 °C graph.
- Distribution losses can be controlled with low temperature heating curves.
- Difference between wet and dry floor heating with a PI-controller was only 0.1 K in temperature variations.
- Losses to the ground (SG) added 0.2-0.5 K temperature variation on the top of the mid-floor value to the floor heating.
- Generally, the differences with the PI-controller were so small that the radiator and floor heating can be considered equally efficient.
- Radiator heating showed higher emission efficiency in all cases with the P-controller vs. on-off controller in floor heating at the difference of 0.5-0.9 K in equivalent temperature.

The thesis includes a comparison for the same size and type radiators with parallel and serial connected panels in the EN 442-2 test room to quantify the possible heat emission difference and energy saving of the radiator with serial connected panels. Serial radiator had 4 °C higher temperature of the front panel that resulted in slightly higher radiation share, 18 % relative to 15 % for parallel radiator in the 50 °C test. The rear panel temperature of the serial radiator was by 3 °C lower, which may have some energy saving effect in the case of poorly insulated walls. This approved the importance of the radiant temperature as a phenomenon, but in terms of energy savings there was no considerable difference between the studied radiators with parallel and serial connected panels. Parallel radiators showed slightly faster dynamic response and higher heat output, which resulted in slightly faster heating up time. By 3 % higher heat output of the parallel radiator at  $\Delta T$  50 °C increased to about 10% higher heat output at  $\Delta T$  25 °C, which gives some advantage of faster heating up time over the parallel radiator in low temperature heating systems.

In the analysis of heat pump performance with the radiator heating, the SPF of the heat pump was quantified by three different comparable models – an analytical model, the IDA-ESBO heat pump model and the correlation equation

derived from two sets of laboratory measurements. Calculations with the derived condensing temperature correlation equation stressed the effect of relatively low return temperature in a radiator heating system that resulted in 9% higher SPF. Four different domestic heat pump connection schemes resulted in a range of SPF values of 3.72 to 4.21. The highest SPF was achieved with the direct connection scheme of the heat pump, because it resulted in the lowest possible return water temperature. Additionally, the effect of reduced flow rates by radiator thermostats was computed, because the calculation with the fixed flow rate return temperature can be done as a fully hand calculation if hourly heating needs are known. Finally, the fixed flow return temperature resulted in 4.5% lower SPF value, showing the importance to use the correct return temperature corresponding to the actual flow rates in radiators.

## LIST OF REFERENCES

- [1] 2010/31/EC, “Directive 2010/31/EU of the European Parliament and of the Council on the energy performance of buildings.” European council, pp. 13–35, 2010.
- [2] P. L. Hirtl, Bettina; Bertoldi, “Energy Efficiency Status Report,” 2012.
- [3] C. a. Balaras, K. Droutsa, E. Dascalaki, and S. Kontoyiannidis, “Heating energy consumption and resulting environmental impact of European apartment buildings,” *Energy Build.*, vol. 37, no. 5, pp. 429–442, May 2005.
- [4] C. a. Balaras, K. Droutsa, a. a. Argiriou, and D. N. Asimakopoulos, “Potential for energy conservation in apartment buildings,” *Energy Build.*, vol. 31, pp. 143–154, 2000.
- [5] T. Kalamees, K. Kuusk, E. Arumägi, S. Ilomets, and M. Maivel, “The analysis of measured energy consumption in apartment buildings in Estonia,” *IEA Annex 55 (RAP-RETRO), Work. Meet.*, no. April, pp. 23–25, 2012.
- [6] M. Maivel and K. Kuusk, “Energy consumption and indoor climate analysis in detached houses,” in *Proceedings of the 2nd WSEAS International Conference on URBAN REHABILITATION AND SUSTAINABILITY (URES '09)*, 2009, no. 1, pp. 97–101.
- [7] T. Kalamees, S. Ilomets, K. Kuusk, and L. Paap, “Indoor Temperature and Humidity Conditions in Modern Estonian Apartment Buildings,” *Proc. 11th REHVA World Congr. 8th Int. Conf. Indoor Air Qual. Vent. Energy Conserv. Build.*, pp. 1–8, 2013.
- [8] J. Kurnitski, A. Saari, T. Kalamees, M. Vuolle, J. Niemelä, and T. Tark, “Cost optimal and nearly zero (nZEB) energy performance calculations for residential buildings with REHVA definition for nZEB national implementation,” *Energy Build.*, vol. 43, no. 11, pp. 3279–3288, Nov. 2011.
- [9] J. Kurnitski, K. Kuusk, T. Tark, A. Uutar, T. Kalamees, and E. Pikas, “Energy and investment intensity of integrated renovation and 2030 cost optimal savings,” *Energy Build.*, vol. 75, pp. 51–59, 2014.
- [10] K. Kuusk, T. Kalamees, and M. Maivel, “Cost effectiveness of energy performance improvements in Estonian brick apartment buildings,” *Energy Build.*, vol. 77, pp. 313–322, 2014.
- [11] ISO 13790:2008, “Energy performance of buildings — Calculation of energy use for space heating and cooling,” vol. 2006, no. 50. International Organization for Standardization, p. 162, 2008.
- [12] C. Ahern and B. Norton, “Energy savings across EU domestic building stock by optimizing hydraulic distribution in domestic space heating systems,” *Energy Build.*, Jan. 2015.

- [13] V. Monetti, E. Fabrizio, and M. Filippi, "Impact of low investment strategies for space heating control: Application of thermostatic radiators valves to an old residential building," *Energy Build.*, pp. 1–9, 2015.
- [14] EN 15316-1, "Heating systems in buildings. Method for calculation of system energy requirements and system efficiencies. Part 1: General." European Committee for Standardization, 2007.
- [15] Z. Liao and a. L. Dexter, "The potential for energy saving in heating systems through improving boiler controls," *Energy Build.*, vol. 36, no. 3, pp. 261–271, Mar. 2004.
- [16] L. Peeters, J. Van der Veken, H. Hens, L. Helsens, and W. D'haeseleer, "Control of heating systems in residential buildings: Current practice," *Energy Build.*, vol. 40, no. 8, pp. 1446–1455, Jan. 2008.
- [17] T. Cholewa, A. Siuta-Olcha, and M. a. Skwarczyński, "Experimental evaluation of three heating systems commonly used in the residential sector," *Energy Build.*, vol. 43, pp. 2140–2144, 2011.
- [18] 15316-4-1, "Heating systems in buildings. Method for calculation of system energy requirements and system efficiencies. Part 4-1: Space heating generation systems, combustion systems (boilers)." European Committee for Standardization, 2008.
- [19] EN 15316-4-2, "Heating systems in buildings. Method for calculation of system energy requirements and system efficiencies. Part 4-2: Space heating generation systems, heat pump systems." European Committee for Standardization, 2009.
- [20] E. 15316-4-3, "Heating systems in buildings. Method for calculation of system energy requirements and system efficiencies. Part 4-3: Heat generation systems, thermal solar systems." European Committee for Standardization, 2008.
- [21] EN 15316-4-4, "Heating systems in buildings. Method for calculation of system energy requirements and system efficiencies. Part 4-4: Heat generation systems, building-integrated cogeneration systems." European Committee for Standardization, 2008.
- [22] EN 15316-4-5, "Heating systems in buildings. Method for calculation of system energy requirements and system efficiencies. Part 4-5: Space heating generation systems, the performance and quality of district heating and large volume systems," *European Committee for Standardization*. 2008.
- [23] EN 15316-4-6, "Heating systems in buildings. Method for calculation of system energy requirements and system efficiencies. Part 4-6: Heat generation systems, photovoltaic systems." European Committee for Standardization, 2008.
- [24] EN 15316-4-7, "Heating systems in buildings - Method for calculation of system energy requirements and system efficiencies - Part 4-7: Space heating generation systems, biomass combustion systems." European Committee for Standardization, 2007.

- [25] B. W. Olesen and M. De Carli, "Calculation of the yearly energy performance of heating systems based on the European Building Energy Directive and related CEN standards," *Energy Build.*, vol. 43, no. 5, pp. 1040–1050, 2011.
- [26] H. Sauter, "Leistungsminderung bei Heizkörperverkleidungen," *HLH Heizung, Lüftung/Klima, Haustechnik*, vol. 36, no. 4, 1985.
- [27] A. Hesaraki and S. Holmberg, "Energy performance of low temperature heating systems in five new-built swedish dwellings: A case study using simulations and on-site measurements," *Build. Environ.*, vol. 64, pp. 85–93, 2013.
- [28] J. A. Myhren and S. Holmberg, "Flow patterns and thermal comfort in a room with panel, floor and wall heating," *Energy Build.*, vol. 40, no. 4, pp. 524–536, Jan. 2008.
- [29] M. Dovjak, M. Shukuya, and A. Krainer, "Exergy Analysis of Conventional and Low Exergy Systems for Heating and Cooling of Near Zero Energy Buildings," *Strojniški Vestn. – J. Mech. Eng.*, vol. 58, pp. 453–461, 2012.
- [30] EN ISO 7726, "Ergonomics of the thermal environment. Instruments for measuring physical quantities Tämä." International Organization for Standardization, 2001.
- [31] EN-ISO 7730, "Ergonomics of the thermal environment - Analytical determination and interpretation of thermal comfort using calculation of the PMV and PPD indices and local thermal comfort criteria." International Organization for Standardization, 2006.
- [32] EN 15316-2-1, "Heating systems in buildings. Method for calculation of system energy requirements and system efficiencies. Part 2-1: Space heating emission systems." European Committee for Standardization, 2008.
- [33] A. Hasan, J. Kurnitski, and K. Jokiranta, "A combined low temperature water heating system consisting of radiators and floor heating," *Energy Build.*, vol. 41, pp. 470–479, 2009.
- [34] "Description of Kermi GmbH serial panel radiators." [Online]. Available: [http://www.kermi.com/EN/Heiztechnik/therm-x2\\_Flachheizkoerper/Warum\\_x2/Uebersicht/index.phtml](http://www.kermi.com/EN/Heiztechnik/therm-x2_Flachheizkoerper/Warum_x2/Uebersicht/index.phtml). [Accessed: 01-Feb-2015].
- [35] K. J. Chua, S. K. Chou, and W. M. Yang, "Advances in heat pump systems: A review," *Appl. Energy*, vol. 87, no. 12, pp. 3611–3624, Dec. 2010.
- [36] A. Saari, T. Kalamees, J. Jokisalo, R. Michelsson, K. Alanne, and J. Kurnitski, "Financial viability of energy-efficiency measures in a new detached house design in Finland," *Appl. Energy*, vol. 92, pp. 76–83, 2012.

- [37] M. Scarpa, G. Emmi, and M. De Carli, "Validation of a numerical model aimed at the estimation of performance of vapor compression based heat pumps," *Energy Build.*, vol. 47, pp. 411–420, 2012.
- [38] L. Schibuola, "Heat pump seasonal performance evaluation: A proposal for a European standard," *Appl. Therm. Eng.*, vol. 20, pp. 387–398, 2000.
- [39] I. S. Ertesvåg, "Uncertainties in heat-pump coefficient of performance (COP) and exergy efficiency based on standardized testing," *Energy Build.*, vol. 43, no. 8, pp. 1937–1946, Aug. 2011.
- [40] EN 14511-2, "Air conditioners, liquid chilling packages and heat pumps with electrically driven compressors for space heating and cooling - Part 2: Test conditions." 2013.
- [41] ISO 5151:2010, "Non-ducted air conditioners and heat pumps — Testing and rating for performance," vol. 2010. International Organization for Standardization, 2010.
- [42] F. Karlsson and M. Axell, "Swedish country report for IEA HPP Annex 28," 2005.
- [43] E. 255-2, "Air conditioners, liquid chilling packages and heat pumps with electrically driven compressors - Heating mode - Part 2: Testing and requirements for marking for space heating units." European Committee for Standardization, 1997.
- [44] J. Fernández-Seara, A. Pereiro, S. Bastos, and J. A. Dopazo, "Experimental evaluation of a geothermal heat pump for space heating and domestic hot water simultaneous production," *Renew. Energy*, vol. 48, pp. 482–488, Dec. 2012.
- [45] J. Nyers and A. Nyers, "Investigation of Heat Pump Condenser Performance in Heating Process of Buildings using a Steady-State Mathematical Model," *Energy Build.*, vol. 75, pp. 523–530, Jun. 2014.
- [46] EN 15316-2-3, "Heating systems in buildings. Method for calculation of system energy requirements and system efficiencies. Part 2-3: Space heating distribution systems Täma." European Committee for Standardization, 2008.
- [47] D. V 18599-5, "Energetische Bewertung von Gebäuden - Berechnung des Nutz-, End- und Primärenergiebedarfs für Heizung, Kühlung, Lüftung, Trinkwarmwasser und Beleuchtung - Teil 5: Endenergiebedarf von Heizsystemen," vol. 12, no. D. Deutsches Institut für Normung, pp. 1–5, 2011.
- [48] RT2005, "Réglementation thermique 2005." DES BÂTIMENTS CONFORTABLES ET PERFORMANTS, 2005.
- [49] A. Bring, P. Sahlin, and M. Vuolle, "Models for Building Indoor Climate and Energy Simulation," 1999.
- [50] P. Sahlin, L. Eriksson, P. Grozman, H. Johnsson, A. Shapovalov, and M. Vuolle, "Whole-building simulation with symbolic DAE equations and general purpose solvers," *Build. Environ.*, vol. 39, pp. 949–958, 2004.

- [51] T. Kalamees, “Estonian test reference year for energy calculations.,” *Proc. Est. Acad. Sci. Eng.*, vol. 12, pp. 40–58, 2006.
- [52] ASHREA, “American Society of Heating, Refrigerating and Air-Conditioning Engineers. Inc. (ASHRAE) handbook Fundamentals 2001.” 2001.
- [53] “<https://www.riigiteataja.ee/akt/105092012004>,” 2015. .
- [54] “<https://www.riigiteataja.ee/akt/118102012001>.” .
- [55] EN 442-2:2003, “Radiators and convectors - Part 3: Evaluation of conformity.” European Committee for Standardization, 2003.
- [56] EN 215:2004, “Thermostatic radiator valves - Requirements and test methods.” European Committee for Standardization.
- [57] Equa, “User Manual IDA Indoor Climate and Energy,” 2013.
- [58] EQUA Simulation, “IDA Early Stage Building Optimization (ESBO) User guide,” 2013.
- [59] F. Karlsson, “Capacity Control of Residential Heat Pump Heating Systems,” 2007.
- [60] F. Karlsson and P. Fahlén, “Capacity-controlled ground source heat pumps in hydronic heating systems,” *Int. J. Refrig.*, vol. 30, no. 2, pp. 221–229, Mar. 2007.
- [61] G. Zhou and J. He, “Thermal performance of a radiant floor heating system with different heat storage materials and heating pipes,” *Appl. Energy*, vol. 138, pp. 648–660, Jan. 2015.
- [62] G. Salvalai, “Implementation and validation of simplified heat pump model in IDA-ICE energy simulation environment,” *Energy Build.*, vol. 49, pp. 132–141, Jun. 2012.
- [63] A. B. Erdogmus, “Simulation of the heater test room defined by EN 442 standard and virtual testing of different types of heaters.,” İzmir Institute of Technology, 2011.

## ACKNOWLEDGEMENT

This study was conducted in the Chair of Building Physics and Energy Efficiency in collaboration with the Chair of Heating and Ventilation in Tallinn University of Technology.

I would like to express my sincere gratitude to everyone who has helped and supported me throughout my studies. Above all, I want to thank my supervisors prof. Teet-Andrus Kõiv and prof. Jarek Kurnitski. Prof. Teet-Andrus Kõiv encouraged me to attend PhD courses and helped to write my first peer-reviewed papers. Prof. Jarek Kurnitski directed my studies to the next level. Thanks to Jarek I am where I am here today; his substantial support in rewriting the thesis and my latest papers is exceptional.

Also, I am extremely thankful to my colleagues in Tallinn University of Technology: prof. Targo Kalamees, prof. Hendrik Voll and our wonderful assistant Laura Kadaru for their valuable contribution to my studies.

I am sincerely grateful to all my colleagues in State Real Estate Ltd. (especially Allan Hani and Alex Roost).

I am most grateful to Mika Vuolle from Equa Simulation OY for his strong, quick and excellent support for IDA ICE simulation program; without whom I would not have been able to model so complicated heating system.

Also, I would like to thank and wish good luck for finishing PhD dissertations to all my co-PhD students: Kalle Kuusk, Martin Thalfeldt, Simo Ilomets, Üllar Alev, Raimo Simson, Alo Mikola, Endrik Arumägi, Jevgeni Fadejev, Argo Kuusik, Paul Klõšeiko and Kaspar Tennokese. I will certainly miss our common PhD parties.

I am deeply indebted to my family and my dear Katrin for their endless and invaluable love, support and patience.

This research was supported by European Social Funds Doctoral Studies and Internationalisation Programme DoRa, which is carried out by Foundation Archimedes. In addition, the research was supported by the Estonian Research Council, with Institutional Research Funding grant IUT1-15, and with a grant of the European Union, the European Social Fund, Mobilitas grant No MTT74 and SA Archimedes-s grant 3.2.0801.11-0035.

## ABSTRACT

In the past, heating system losses were of minor importance, because minimizing heat losses by insulating of external envelope resulted in a major gain. Historically, heating system losses have been scarcely studied and only a limited number of research publications concerning heating system emission and distribution losses are available. Low energy buildings have changed an overall situation with the support by the EU legislation, stressing the importance of improving the heating system efficiency. This was the main motivation why I choose the efficiency aspects of a heating system in a low energy residential building for my thesis research.

In this thesis, emission and distribution losses of a heating system as well as generation efficiency in the case of a heat pump were studied for low energy buildings.

This research is based on simulations where a detailed dynamic simulation model with heating system components was developed to quantify emission and distribution losses for a detached house and an apartment building under two climates (Northern and Central European) in heating dominated parts of Europe. One objective of the work was to provide low energy buildings and low temperature heating related input for updating of the EN 15316-2-1 standard, which is under revision. Generally, the losses of low temperature heat emitters were significantly lower than the existing ones in the standard. Besides the tabulated emission and distribution losses, we introduce a new approach where the correction factor of the operative temperature is added to enable fair comparison of radiator and floor heating systems. The use of the operative temperature set-point increased the temperature variation in the case of radiator heating by 0.2-0.3 K and for floor heating no correction was needed.

In addition, the performance of radiators with parallel and serial connected panels and a radiator system with a heat pump were studied. The thesis includes a comparison for the same size and type radiators with parallel and serial connected panels in the EN 442-2 test room to quantify a possible heat emission difference and energy saving of the radiator with serial connected panels. As a result, in terms of energy savings no considerable difference was found between the studied radiators with parallel and serial connected panels.

One way to achieve EU targets is to produce heat more efficiently. In the thesis our special interest was to study the heat pump performance in a radiator system where the temperature drop is typically higher and return water temperature is lower than that of floor heating. Unfortunately, most of existing models are simplified and they do not consider the effect of return temperature on the seasonal performance of a heat pump (SPF). We quantified the heat pump SPF by three different comparable models - analytical model, IDA-ESBO heat pump model and by a correlation equation derived from two sets of laboratory measurements. The calculation with the correlation of the derived condensing

temperature showed the effect of relatively low return temperature in a radiator heating system that resulted in 9% higher SPF.

Finally, the thesis gives an overview and recommendations for the emission and distribution losses of a heating system, their impact on thermal comfort and energy performance in low energy residential buildings.

## KOKKUVÕTE

Ajalooliselt on küttesüsteemi kadudele vähe rõhku pööratud, kuna hoone soojuskadude vähendamine soojustamise teel annab oluliselt suuremat energiasäästu. Küttesüsteemi kadusid ei ole piisavalt uuritud, vaid üksikud teaduslikud uurimustööd keskenduvad küttesüsteemi väljastamise ja jaotamise kadudele. Madala energiatarbega hooned on aga üldist olukorda oluliselt muutnud. Euroopa Liidu poolt püstitatud ambitsioonikad energiasäästu eesmärgid sunnivad aga järjest enam rõhku pöörama energiatõhusa hoone karbi kõrval ka tehnosüsteemidele ja ventilatsiooni kõrval ka küttesüsteemidele. Kogu Euroopa Liit liigub liginullenergiahoonete poole ja seniste uuringute vähesus tekitas huvi uurida vastavat ala ja kirjutada väitekirja küttesüsteemi efektiivsust mõjutavatest teguritest madala energiatarbega eluhoonetes.

Väitekirjas uuritakse madala energiatarbega hoone küttesüsteemi väljastamise ja jaotamise kadusid ja ka soojuse tootmise efektiivsust soojuspump-küttesüsteemide korral. Töö põhineb simulatsioonidel, kus detailse dünaamilise simulatsioonimudeli abil modelleeritakse väljastamise ja jaotamise kadusid eramajale ja kortermajale kahes erinevas kliimas (kaasates nii Põhja- kui ka Kesk-Euroopa). Mudeli erakordsust rõhutab küttesüsteemi komponentide detailsus, mis sisaldab ka küttesüsteemi jaotustorustikku.

Üheks oluliseks väitekirja eesmärgiks oli anda sisend CENi standardile EN 15316-2-1, mis kirjutamise hetkel on uuendusfaasis. Kehtivas standardis on peamine tähelepanu kõrgetemperatuurilistel küttesüsteemidel, kuid madalatemperatuurilistele küttesüsteemidele ja madala energiatarbega hoonetele pole pööratud piisavat tähelepanu. Üldiselt madalatemperatuuriliste soojusväljastussüsteemide kaod on madalamad kui traditsioonilistel kõrgetemperatuurilistel küttesüsteemidel.

Erinevate soovituslike jaotus- ja väljastuskadude kõrval testisime ka uut lähenemist, millega leidsime korrektsioonitegurid, et võtta arvesse operatiivne temperatuur erinevate soojusväljastussüsteemide võrdlemisel. Operatiivne, s.t inimese tunnetuslik temperatuur, võimaldab sama soojusliku mugavuse juures võrrelda põrand- ja radiaatorküttesüsteemi. Operatiivset temperatuuri kasutades tuleks radiaatorküttesüsteemi korral tõsta õhutemperatuuri 0,2–0,3 K, et saavutada põrandküttega võrdne tunnetuslik temperatuur.

Täiendavalt võrreldi paralleelse ja jadamisi küttepinnaga radiaatorite energiatõhusust ning analüüsiti soojuspumba efektiivsust radiaatorküttesüsteemi korral. Uuringus võrreldi sama suuruse ja tüübiga paralleelse ja jadamisi küttepinnaga radiaatoreid EN 422-2 testruumis, et analüüsida võimalikku soojusväljastuse erinevust ja energiasäästu jadamisi ühendatud küttepindadega radiaatoritega. Testi ja simulatsiooni tulemusel leiti, et radiaatoritel puudub oluline erinevus.

Üks võimalus tagada ELi ambitsioonikaid eesmärgi on toota soojusenergiat efektiivsemalt. Töös uuriti soojuspumba kütteperioodi keskmist soojustegurit radiaatorküttesüsteemi korral, kus võrreldes põrandaküttega on suurem tempera-

tuurilang ja tagastuva vee temperatuur on madalam võrreldes põrandküttesüsteemiga. Kahjuks enamik kasutatavaid soojuspumba mudeleid omab mitmeid lihtsustusi ning ei arvesta madalamast tagasivoolutemperatuurist saadavat kõrgemat soojuspumba soojustegurit. Võrdlesime soojuspumba aasta keskmist soojustegurit kolmel viisil: analüütiline lähenemine, IDA-ESBO standard mudeliga simulatsioon ja korrelatsioonivalemite abil tuletatud soojustegur, mis tuletati laborimõõtmistulemuste abil. Arvutused näitavad, et laborikatsete abil tuletatud korrelatsioonivalemid annavad keskmiselt 9% kõrgema aasta keskmise soojusteguri.

Lõpetuseks, väitekiri annab hea ja põhjaliku ülevaate koos soovitustega, mis võimaldavad tõsta küttesüsteemi jaotuse ja väljastamise efektiivsust ning seeläbi tõsta hoone energiatõhusust ilma järeleandmisteta soojuslikus mugavuses.

## **PAPERS PRESENTED BY THE CANDIDATE**

Maivel, Mikk; Kurnitski, Jarek (2015). Radiator and floor heating operative temperature and temperature variation corrections for EN 15316-2 heat emission standard. *Energy and Buildings*, 99, 204 - 213.

Maivel, M.; Kurnitski, J. (2015). Heating system return temperature effect on heat pump performance. *Energy and Buildings*, 94, 71 - 79.

Maivel, M.; Konzelmann, M.; Kurnitski, J. (2015). Energy performance of radiators with parallel and serial connected panels. *Energy and Buildings*, 86, 745 - 753.

Loginov, D.; Koiv, T.-A.; Maivel, M.; Kalda, K. (2015). Thermal performance of evacuated tube and flat plate solar collectors in nordic climate conditions. *International Journal of Mechanical Engineering & Technology (IJMET)*, 6(2), 81 - 91.

Simson, R.; Kurnitski, J.; Maivel, M.; Kalamees, T. (2015). Compliance with Summer Thermal Comfort Requirements in New Apartment Buildings. In: *Proceedings of REHVA Annual Conference 2015 "Advanced HVAC and Natural Gas Technologies": REHVA Annual Conference 2015 "Advanced HVAC and Natural Gas Technologies"*, Riga, Latvia, May 6-9, 2015. Riga Technical University, 64 - 69.

Maivel, M.; Kurnitski, J.; Kalamees, T. (2014). Field survey of overheating problems in Estonian apartment buildings. *Architectural Science Review*, 11

Kuusk, K.; Kalamees, T.; Maivel, M. (2014). Cost effectiveness of energy performance improvements in Estonian brick apartment buildings. *Energy and Buildings*, 77, 313 - 322.

Mikola, A.; Koiv, T.-A.; Maivel, M. (2014). Production of domestic hot water with solar thermal collectors in North-European apartment buildings. *International Journal of Mechanical Engineering & Technology (IJMET)*, 5(4), xx - xx. [ilmumas]

Maivel, M.; Kurnitski, J.; Kalamees, T. (2014). Summer Thermal Comfort in New and Old Apartment Buildings. In: *Proceedings of 8th Windsor Conference: Counting the Cost of Comfort in a Changing World: 8th Windsor Conference, International Conference held 10th - 13th April 2014, Windsor UK. (Toim.) Prof. F. Nicol; Prof S. Roaf; Dr L. Brotas; Prof Rev M. Humphreys. NCEUB 2014: Network for Comfort and Energy Use in Buildings*, 42 - 50.

Maivel, M.; Kurnitski, J. (2014). Heating System Return Temperature Effect on Heat Pump Performance. In: *11th International Energy Agency Heat Pump Conference 2014 Conference Proceedings: 11th International Energy Agency*

Heat Pump Conference Montreal, May 12-16, 2014. International Energy Agency.

Maivel, M.; Konzelmann, M.; Kurnitski, J. (2014). Energy performance of radiators with parallel and serial connected panels. REHVA journal, 51(6), 18 - 21.

Maivel, M.; Kurnitski, J. (2013). Low Temperature Radiator Heating Distribution and Emission Efficiency in Residential Buildings. Energy and Buildings, 69C, 224 - 236.

Maivel, M.; Kurnitski, J. (2013). Low Temperature Radiator Heating System Detailed Dynamic Simulation - Distribution and Emission Efficiency. CLIMA 2013, 11th REHVA World Congress and the 8th International Conference on Indoor Air Quality, Ventilation and Energy Conservation in Buildings. Prague, Czech Republic, on June 16 – 19, 2013. Elsevier.

Kalamees, T.; Ilomets, S.; Liias, R.; Raado, L.-M.; Kuusk, K.; Maivel, M.; Ründva, M.; Klõšeiko, P.; Liho, E.; Paap, L.; Mikola, A.; Seinre, E.; Lill, I.; Soekov, E.; Paadam, K.; Ojamäe, L.; Kallavus, U.; Mikli, L.; Kõiv, T.-A. (2012). Eesti eluasemefondi ehitustehniline seisukord – ajavahemikul 1990–2010 kasutusele võetud korterelamud.

Kalamees, T.; Ilomets, S.; Liias, R.; Raado, L.-M.; Kuusk, K.; Maivel, M.; Ründva, M.; Klõšeiko, P.; Liho, E.; Paap, L.; Mikola, A.; Seinre, E.; Lill, I.; Soekov, E.; Paadam, K.; Ojamäe, L.; Kallavus, U.; Mikli, L.; Kõiv, T.-A. (2012). Eesti eluasemefondi ehitustehniline seisukord - ajavahemikul 1990-2010 kasutusele võetud korterelamud: uuringu lõpparuanne. Tallinn: Tallinna Tehnikaülikooli Kirjastus

Kalamees, T.; Kuusk, K.; Arumägi, E.; Ilomets, S.; Maivel, M. (2012). The analysis of measured energy consumption in apartment buildings in Estonia. In: IEA Annex 55 (RAP-RETRO), Working meeting: Vienna, Austria. 23-25 April. 6 p.

Kõiv, T.-A.; Maivel, M.; Mikola, A.; Kuusk, K. (2011). Energy Efficiency and Indoor Climate of Apartment and Educational Buildings in Estonia. In: Recent Researches in Energy, Environment, Devices, Systems, Communications and Computers: International Conference on Energy, Environment, Devices, Systems, Communications, Computers (EEDSCC '11). (Toim.) S. Chen, Zhejiang; Nikos Mastorakis; Franklin Rivas-Echeverria; Valeri Mladenov. WSEAS, 191 - 196.

Kalamees, T.; Ilomets, S.; Arumägi, E.; Alev, Ü.; Kõiv, T.-A.; Mikola, A.; Kuusk, K.; Maivel, M. (2011). Indoor Hygrothermal Conditions In Estonian Old Multi-storey Brick Apartment Buildings. In: The 12th International Conference on Indoor Air Quality and Climate: June 5-10. Austin, Texas, USA. , 6p.

Kõiv, T.-A.; Voll, H.; Mikola, A.; Kuusk, K.; Maivel, M. (2010). Indoor Climate and Energy Consumption in Residential Buildings in Estonian Climatic Condition. WSEAS TRANSACTIONS on ENVIRONMENT and DEVELOPMENT, 6(4), 247 - 256.

Kalamees, T; Kõiv, T-A; Liias, R; Õiger, K; Kallavus, U; Mikli, L; Ilomets, S; Kuusk, K; Maivel, M; Mikola, A; Klõšeiko, P; Agasild, T; Arumägi, E; Liho, E; Ojang, T; Tuisk, T; Raado, L-M; Jõesaar, T. (2010). Eesti eluasemefondi telliskorterelamute ehitustehniline seisukord ning prognoositav eluiga. Uuringu lõpparuanne. Tallinna Tehnikaülikool

Tomson, T.; Voll, H.; Maivel, M. (2010). Solar Heat Generation in Estonia and its Peculiarities. In: Proceedings of the Eurosun2010 International Conference on Solar Heating, Cooling and Buildings: Eurosun2010 International Conference on Solar Heating, Cooling and Buildings, Graz Austria 28 September-1 October. (Toim.) W. Streicher., 10 - 18.

Tomson, T.; Maivel, M. (2010). Päikeseenergeetika ühingu perspektiiv. Elis Vollmer, Argo Normak (Toim.). TEUK kaheteistkümnenda konverentsi kogumik (45 - 48). Tartu, Maaülikool: Tartu Põllumajandusülikooli kirjastus

Tomson, T.; Voll, H.; Maivel, M. (2010). Solar Heat Generation in Estonia and its Peculiarities. In: Book of Abstracts: Eurosun2010 International Conference on Solar Heating, Cooling and Buildings. , 55 - 55.

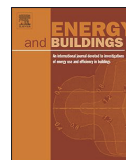
Maivel, M.; Kuusk, K. (2009). Energy consumption and indoor climate analysis in detached houses. In: Proceedings of the 2nd WSEAS International Conference on URBAN REHABILITATION AND SUSTAINABILITY (URES '09): WSEAS International Conferences, Baltimore, USA, November 7-9, 2009. WSEAS, 97 - 102.



**BIBLIOGRAPHY**

Maivel, M.; Kurnitski, J. (2014). Low Temperature Radiator Heating Distribution and Emission Efficiency in Residential Buildings. *Energy and Buildings*, 69C, 224 - 236.





# Low temperature radiator heating distribution and emission efficiency in residential buildings

Mikk Maivel\*, Jarek Kurnitski

Faculty of Civil Engineering, Department of Structural Design, Tallinn University of Technology Ehitajate tee 5, 19086, Tallinn, Estonia



## ARTICLE INFO

### Article history:

Received 6 May 2013

Received in revised form 17 October 2013

Accepted 21 October 2013

### Keywords:

Low temperature heating

Radiator heating, Distribution efficiency

Emission efficiency

Stratification efficiency

System losses

## ABSTRACT

Low and nearly zero energy buildings with decreased heating need can utilize low temperature heating systems for energy efficient heating. Distribution and emission losses for low temperature radiator heating cannot be found from European standards or scientific literature. The use of the losses of conventional systems can result in significant overestimation of heating energy use. In this paper, distribution and emission losses of low temperature and conventional radiator heating system were determined in North and Central Europe climates for low energy detached houses and apartment buildings. Detailed dynamic components of heating system in the whole building energy simulation model allowed to quantify these losses. Main findings of the study show that distribution losses can be controlled with low temperature heating curves and emission losses with PI type thermostats. For conventional systems the losses higher than 50% of heating need were calculated in the apartment building. With low temperature heating curve, PI thermostats and limited heating period distribution and emission losses were possible to keep below 1% in detached houses in both climates. In apartment buildings the minimal achievable losses were significantly higher, between 6 and 12% in North and Central European climates, respectively. Proportional thermostats add 2 to 6% to these losses. Based on results, heating curve of 45/35 °C can be recommended for detached houses and even 40/30 °C for apartment buildings. Insulating distribution and connection pipes in heated spaces proved to have no practical effect on heat losses. Compared to EN 15316-2-1:2007, the losses were significantly lower especially for low temperature heating curves. A new set of tabulated values is proposed for the revision of the standard. It was possible to explain the mechanism of losses, but still it was not possible to calculate losses from hourly energy need data with the correlation equation leading to overestimation by factor of about 10 compared to dynamic simulation.

© 2013 Elsevier B.V. All rights reserved.

## 1. Introduction

Widely used space heating systems in European buildings are radiator and floor heating or their combinations. These systems have shown performance complying with the highest indoor climate category thermal comfort specification [1] according to EN 15251:2007 [2]. In the EU, buildings account for 40% of the total primary energy use and residential buildings accounted in 2000 25.9% of final energy use [3]. Within buildings themselves, the proportion of energy allocated to space heating is 57% when averaged through [3]; 60% in UK [4] and even 62% in Estonia apartment buildings and 70% in dwellings [5,6]. Compared to existing housing stock the share of space heating energy use from total delivered energy (space heating; supply air heating; domestic hot water; cooling; fans and pumps; lighting and appliances) is 25% in nZEB detached houses and 12% in apartment buildings in northern climate [1].

General movement towards low-energy and nZEB, required by EPBD recast 2010/31/EU [7] has created new challenge for heating systems. Heating need obviously decrease, the control and system losses are stressed compared to existing buildings with higher heating energy need. According to EN 15316-1:2007 [8] heating system can be divided into four main parts: generation, storage, distribution and emission, and all these parts have losses. In this paper we focus on distribution and emission losses, generation and storage losses are not studied. A heat generation loss (i.e. boiler efficiency) has been previously extensively studied in the product development as well as in scientific studies. Some examples of these studies have found that it is possible to save energy up to 20% by improving boiler control [9] or up to 15% by changing conventional boiler to condensing boiler [10]. Generation losses are described with calculation equations and tabulated values in standards 15316-4-1:2007 [11]; 15316-4-2:2007 [12]; 15316-4-3:2007 [13]; 15316-4-4:2007 [14]; 15316-4-5:2007 [15]; 15316-4-6:2007 [16] and 15316-4-7:2007 [17].

Distribution and emission losses have not been widely studied. The reference study of 15316 [18] reports tabulated values for

\* Corresponding author. Tel.: +37256461251.

E-mail addresses: [mikk.maivel@ttu.ee](mailto:mikk.maivel@ttu.ee), [mikkmaivel@gmail.com](mailto:mikkmaivel@gmail.com) (M. Maivel).

**List of nomenclature**

nZEB	nearly zero energy building
EU	European Union
UK	United Kingdom
EPBD	Energy Performance of Buildings Directive
IDA ICE	IDA Indoor Climate and Energy
TRY	Test Reference Year
PI	proportional integral
P	proportional
Ideal	simulation case without heating system losses
Det45	detailed heating system with heating curve 45/35 °C
Det70	detailed heating system with heating curve 70/55 °C
D	distribution pipe
DC	distribution and connection pipe

distribution and emission losses of 15% for heating curves 55/45 °C and 19% for 70/55 °C in residential dwelling radiator heating system in Brussels. For low temperature heating systems we were not able to find any reference. A very old study [19] reports additional emission loss up to 5% of the heat emission of radiator in old buildings with poor insulation and less than 1% in new buildings with good insulation. The reason of very limited studies might be the complicated dynamic phenomena of distribution and emission losses. Distribution losses contribute as internal heat gains and may not be estimated by theoretical hand calculation, because of dynamic heat gain utilization process and not constant flow rates in the pipes. Emission losses depend on flow temperatures and heat output of radiator in addition to wall insulation and need also dynamic treatment. Until now, building energy simulation tools do not typically support the detailed modeling of the heating system with pipework, thermostats and radiators all with continuously changing flow rates and temperatures.

In this study we modeled the building and full heating system with special pump, pipe, valve, controller and radiator models in order to be able to run dynamic simulation of distribution and emission losses including all flow and heat transfer effects. This is arguably the most detailed radiator heating system modeling attempt ever been done in a building energy simulation tool. Conventional and low temperature radiator heating system was modeled in Estonian reference detached house and apartment building which were run with Estonian and German climate. Constant speed and constant pressure pump control was used to have realistic flow control. Most of simulations were done with PI controlled thermostatic valves, which provide de-facto ideal control and help to distinguish distribution losses. To show the effect of control losses of typical radiator thermostats, some cases were run with P controllers. As a result, we were able to quantify distribution, emission and control losses in two climates (North and Central European) for low energy houses and apartment buildings with conventional and low temperature heating curves. One objective of the study, in addition to scientific ones, was to provide input for the revision of 15316 standards, which is one task of the preparation of second generation EPBD standards, to be completed due 2015. With the data provided, the revised standard can cover low temperature heating systems, which are especially suitable for low energy and nearly zero energy buildings.

## 2. Methods

### 2.1. Classification of thermal losses of heating system

The main parts of a heating system, generation, storage, distribution and emission, all have some losses. According to

15316-2-3:2007 [20], distribution losses consist of system thermal losses and auxiliary losses (pumping energy etc.). Emission losses consist of heat loss due to non-uniform temperature distribution, heat loss due to heat emitter position and heat loss due to control indoor temperature are studied. Emission losses are described and tabulated values can be found in 15316-2-1:2007 [21].

All thermal losses are divided to recoverable and non-recoverable losses according to 15316:2007. The distribution losses caused by pipes in unheated area are calculated as non-recoverable losses and losses in heated rooms contribute as recoverable losses until the temperature set-point is not exceeded. Since the set-point is exceeded, the part of the loss becomes non-recoverable; this part can be quantified based on the comparative calculation with ideal heating and control. Emission loss caused by the heat emitter (radiator) position is the additional back-wall loss through the external wall behind the radiator (compared to the heat loss through the same external wall without radiator) and the control loss is caused by thermostatic valve type controller.

The losses are defined as additional loss to space heating energy need in %. The efficiency  $\eta$  is the reciprocal value, i.e. the energy use with losses can be calculated as  $1/\eta$ . All losses in series or parallel can be calculated as additional loss for the system in % or as the total system efficiency. If losses are in the series, the subsystem efficiencies may be calculated and the total systems efficiency is calculated by Eq. (1):

$$\eta_{\text{tot}} = \eta_{\text{emission}} \times \eta_{\text{distribution}} \times \eta_{\text{storage}} \times \eta_{\text{generation}} \quad (1)$$

where  $\eta_{\text{emission}}$  is emission efficiency;  $\eta_{\text{distribution}}$  is distribution efficiency;  $\eta_{\text{storage}}$  is storage efficiency and  $\eta_{\text{generation}}$  is heat generation efficiency, calculation rules can be found in 15316:2007 standard or sub-standards.

For example, if the heating energy need in a room is 100 kW h, emission losses 10 kW h and distribution losses 15 kW h, the  $\eta_{\text{emission}} = 100/110 = 0.909$  and  $\eta_{\text{distribution}} = 110/125 = 0.88$ . The total efficiency is  $0.909 \cdot 0.88 = 0.8$ , which can be calculated also as  $100/125 = 0.8$ . Emission efficiency, depending on parallel components, can be calculated with 15316-2-1:2007 by Eq. (2):

$$\eta_{\text{emission}} = \frac{1}{4 - (\eta_{\text{stratification}} + \eta_{\text{control}} + \eta_{\text{embedded}})} \quad (2)$$

where  $\eta_{\text{control}}$  is the part efficiency level for room temperature control;  $\eta_{\text{embedded}}$  is the part efficiency level for specific losses of the external components (embedded systems) and  $\eta_{\text{stratification}}$  is stratification efficiency it is the part efficiency level for a vertical air temperature profile (non-uniform temperature), it is calculated by Eq. (3):

$$\eta_{\text{stratification}} = \frac{\eta_{\text{str1}} + \eta_{\text{str2}}}{2} \quad (3)$$

Stratification is influenced by:

- over-temperature ( $\eta_{\text{str1}}$ ) that is neglected in this study, but analyzed in the discussion
- Specific heat loss via external components ( $\eta_{\text{str2}}$ ), (e.g. additional heat loss from back-wall of radiator), simulation model consider it.

### 2.2. Simulation model

Analyzed detached house represents a typical recently built detached house; the building has been used as a reference building in Estonian cost optimal calculations [1]. By small changes the same house was modified to describe a multi-story apartment building. External wall in one end of the building were made adiabatic, which means that the model unit represents one apartment of a long building, Figs. 1 and 2. Similarly, the external roof was change

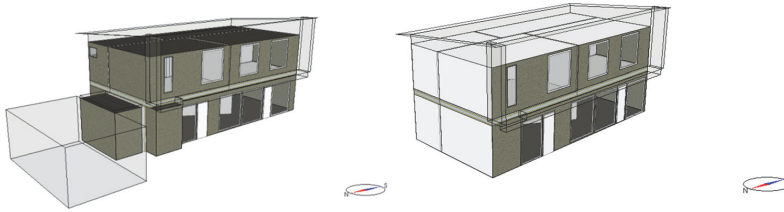


Fig. 1. Estonian reference detached house in the left, and in the right the house transferred to describe an apartment building (white envelope elements are adiabatic).

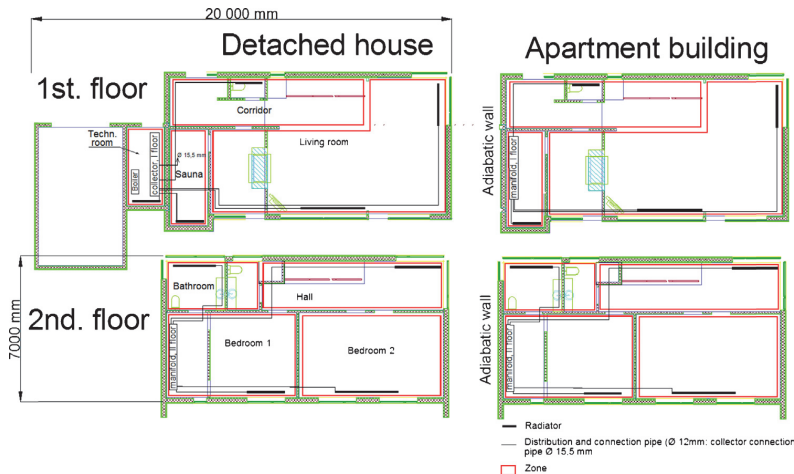


Fig. 2. Location of zones and heating system in analyzed modes.

to adiabatic, which means that the building will continue upwards. In the transformation from detached house to apartment building, the technical space and one small window on the top left in Fig. 2 were “lost”—as the apartment building is more compact. All other

geometry of a house unit remained the same in the transformation. Main technical data for both buildings are shown in Table 1.

Room set-point temperature of 21 °C has been used in all zones/rooms. Heating system supply water temperature is outdoor

Table 1  
Basic data of the building.

		Detached house	Apartment building	
$U$ -value ( $W/(m^2 K)$ )	Exterior wall	0.17 (lightweight)	0.17 (heavyweight)	
	Roof	0.14 (lightweight)	0.14 (heavyweight)	
	Ground floor	0.17	0.17	
	Windows ( $g=0.5$ )	0.8	0.8	
	Specific heat loss coefficient $H/A_{net}$ ( $W/(m^2 K)$ )	0.58	0.44	
Ventilation	Ventilation (continuous) rate $L/(s m^2)$	0.46	0.56	
	Leakage rate $q_{50} m^3/(h m^2)$	0.6	0.6	
Internal gains	Usage (max = 1)	$W/m^2$	$W/m^2$	
	Occupants	2	3	
	Lighting	8	8	
Heating power need	Equipment	2.4	3	
		$W/m^2$	$W/m^2$	
	Tallinn	Average 29.9 (15.9...49.1)	Average 22 (7.8...31.8)	
Gross heating energy need	Munich	Average 23.9 (11...39.5)	Average 15.4 (6.3...25.9)	
		$kWh/m^2$	$kWh/m^2$	
	Tallinn	55	69	
		Heat from ventilation heat recovery	59	70
	Munich	46	26	
		Heat from internal and solar heat gains	45	57
	Heat from ventilation heat recovery	61	72	
	Heat from internal and solar heat gains	31	16	
	Heat from heating system			

air temperature compensated i.e. the supply water temperature increases as the outdoor temperature decreases. Most common conventional heating curves as well as low heating curves were studied (70/55 °C (70 is a supply water temperature and 55 is return water temperature at design outdoor temperature); 45/35 °C; 40/30 °C and 35/28 °C). Simulated heating system was not balanced, all valve bodies used were in fully open position and the system was controlled with radiator thermostatic valves. In the detached house model, cooling system was not used, but in the apartment building model, ideal coolers were used because of more significant internal gains with cooling set point temperature of 25 °C. Ideal cooler and heater are standard models from IDA-ICE library and they are imaginary equipment which describe heating or cooling need without system losses. Mechanical supply and exhaust ventilation system with heat recovery (temperature ratio of 80%; supply air temperature set-point +18 °C) was used in both modes. All energy calculation input data follows the Estonian regulation of minimum requirements for energy performance [22].

**Table 1** Basic data of the building. All calculations were done with dynamic simulation software IDA-ICE 4.5 [23]. This tool is carefully validated and has advanced features for detailed building energy simulations [24]. Two test reference years were used for outdoor climate, Estonian TRY and which describes typical climate for Tallinn and applies also the rest of Estonia [25] and Munich [26]. Multi-zone models (each room is a different zone) were used as shown in Fig. 2. Internal heat gains (lighting, equipment, occupants) for zones and thermal bridges were all chosen from Estonian regulation of minimum requirements for energy performance [22] (Table 1).

Two pipe radiator heating system is used. To report heat losses from pipes we have defined connection and distribution pipes as follows. Distribution pipes are pipes which don't serve the room where they are located (i.e. distribution pipes aren't connected with room radiators, Fig. 3). Then the distribution pipe enters to the last room, it changes to the connection pipe according to this definition. Therefore, the connection pipes are defined as the pipes located in the room where the radiator is (it applies also if the room has two radiators). For analyzing insulation effect several calculations were carried out: pipes were not insulated, distribution pipes were insulated or all pipes were insulated.

The system has one circulation pump which either has constant pressure control or constant speed control. In constant speed mode, the system has a small bypass between manifolds (a pipe with diameter of 0.0001 m and length 1 m). Bypass was necessary to run simulations for spring-summer period when radiator thermostatic valves are often closed.

### 2.3. Heating system dynamic component models

#### 2.3.1. Ideal heating system

Ideal heating system was used for the reference simulations without any emission and distribution losses. It consists of ideal heaters in all rooms which have no defined physical location, but are described with convection and radiation heat output fraction. Power is calculated by the simple Eq. (4):

$$Q = C \times Q_{\max} \quad (4)$$

where  $Q_{\max}$  is maximum power of the unit (W);  $C$  is the control signal of the unit (it is controlled by PI-controller and takes input from zone air temperature). Ideal heater is controlled by PI controller, where control losses are minimal or de-facto not existing [27].

#### 2.3.2. Dynamic detailed radiator model

In the case of the standard radiator of IDA-ICE, it is connected to the external envelope element and has an additional heat loss

from the backside of the radiator, but the radiator has no mass and the flow rate is not calculated [23]. We used a detailed radiator model which has a thermal mass. Heat balance of the water side is calculated by equation:

$$P = q_m \times C_{liq}(T_{in} - T_{out}) \quad (5)$$

where  $P$  is a heat flux from the water (W);  $q_m$  is water mass flow (kg/s);  $C_{liq}$  is a specific heat of water (J/kg °C);  $T_{in}$  is a water inlet temperature to the radiator (°C);  $T_{out}$  is a water outlet temperature from the radiator (°C).

The total heat generated by the radiator is modeled by the equation:

$$P = K \times l \times dT^n \quad (6)$$

where  $K$  is a power law coefficient which depends on the width and type of the radiator (W/(m°C));  $l$  is a length of the radiator (m);  $dT$  is logarithmic temperature difference between the water and the air (°C).

The total heat balance for the radiator is written by the Eq (7):

$$P = Q_{\text{front}} + Q_{\text{conv}} + Q_{\text{wall}} \quad (7)$$

where  $Q_{\text{front}}$  is the heat transfer on the front side of the unit (long wave radiation and convection) (W);  $Q_{\text{conv}}$  is an extra convective heat load, e.g. from the back side and possible fins (W);  $Q_{\text{wall}}$  is heat transfer between the back side of the unit and the facing zone surface (W).

Heat storage which is caused by the thermal mass is calculated by the following Eq. (8):

$$m_{\text{rad}} \times C_{liq} \times \frac{dT_{\text{surf}}}{dt} = Q_{liq} - Q_{\text{air}} \quad (8)$$

where  $m_{\text{rad}}$  is a mass of water inside the radiator (kg);  $C_{liq}$  specific heat of water (J/kgK);  $dT_{\text{surf}}$  radiator surface temperature (°C);  $dt$  is a time (s);  $Q_{liq}$  is a heat flux water to surface (W);  $Q_{\text{air}}$  is a heat flux from the radiator surface to the zone/room (W).

Radiator control loop is a standard model with PI or P control in our simulations. In [26] radiator thermostat (P-controller with hysteresis) was compared with ideal P control and the differences reported have been minimal. Therefore we neglected the effect of hysteresis in our simulations. Simulated dynamic radiators were equipped with RA-N 15 valve bodies, which all were fully open (i.e. the system was not balanced, but just controlled by P or PI thermostats).

### 2.4. Pipe model

For detailed calculations a special pipe model was used (not included in standard IDA-ICE model library). The pipe model provided possibility model real system where pipes have dimensions (length and diameter and have pressure losses) and to simulate heat emissions of the pipes. All pipes were located in the room air, i.e. surface installation of pipes was considered. It is known that the surfaces installation has roughly the same heat emissions as embedded installation in protective sleeve (not insulated) as a rule of thumb. Heat emissions of pipes were calculated by Eq. (9):

$$Q_{\text{amb}} = q \times C_{liq}(t_{in} - t_{out}) \quad (9)$$

where  $Q_{\text{amb}}$  is a heat flux from the pipe (W) to the ambient;  $q$  is a massflow (kg/s);  $C_{liq}$  is a specific heat of water (J/kgK);  $t_{in}$  is a water inlet temperature (K) and  $t_{out}$  is a water outlet temperature (K). Outlet temperature depends on pipe length, pipe diameter and insulation. Heat flux from pipes can be calculated with logarithmic

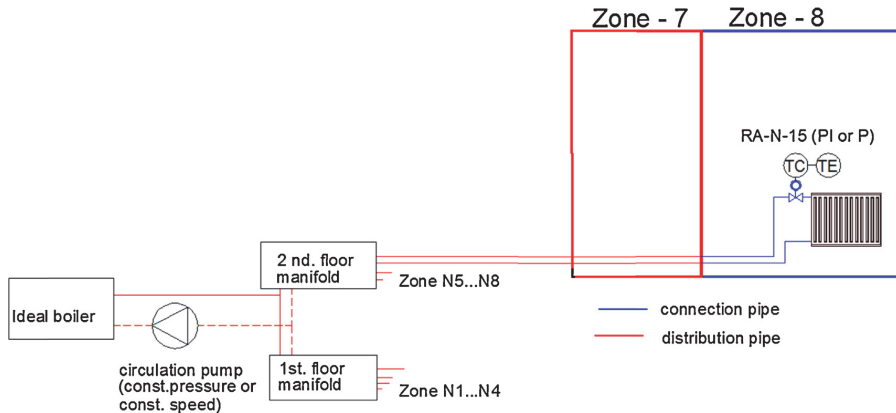


Fig. 3. Scheme of the heating system. Two last zones are shown to explain the definition of connection and distribution pipes used in heat loss reporting.

temperature difference between pipe inner temperature and ambient temperature, by Eq. (10).

$$\Delta t_{log} = \frac{Q_{amb}}{U_{wall} \times \pi \times d_{in} \times l} \tag{10}$$

where  $U_{wall}$  is the total heat transfer coefficient from fluid to ambient air ( $W/(m^2 K)$ ), for which a constant values were used, calculated by the basic heat transfer equation for circular pipes where heat transfer coefficients are expanded:

$$\frac{1}{U_{wall}} = R = \frac{1}{2 \times \pi \times \lambda} \ln \frac{d_{out}}{d_{in}} + \frac{1}{\pi d_{out} (1 \cdot 21(\Delta t/d_{p,i})^{0.25} + 4\sigma(\Delta t/2)^3 / (1 + (\epsilon_1 \times A_1/\epsilon_2 \times A_2)(1 - \epsilon_2))} \tag{11}$$

where  $\Delta t$  is temperature difference between mean air and pipe ( $^{\circ}C$ );  $\sigma = 5.67 \times 10^{-8} W/m^2 K^4$  is radiation heat transfer coefficient;  $\epsilon_1$  is pipe surface emissivity;  $\epsilon_2$  is surrounding surface emissivity;  $d_{out}$  pipe out diameter mm;  $d_{in}$  pipe inner diameter mm;  $\lambda$  thermal conductivity  $W/(m K)$ .

The calculation with pipework means that all radiators receive somewhat lower temperature than that from the boiler.

2.5. Circulation pump model

Two types of control—constant pressure and constant speed control of the pump, was used (Fig. 4). Pipe model calculate pressure drop and valves/thermostats also generate pressure drops. Because of single losses (losses which are caused of branch, valves etc.) of the pipework were neglected (have no effect on simulated heat

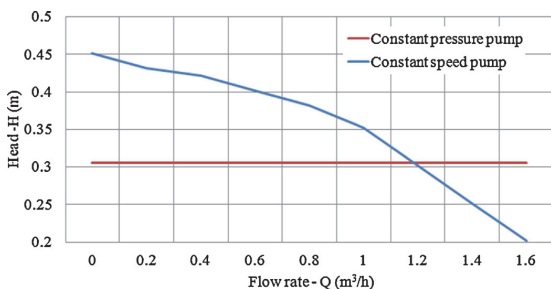


Fig. 4. Circulation pump operation curves for constant pressure and constant speed control.

emissions), 3000 Pa constant pressure head was enough for the system. Hand-made sizing calculation at design outdoor temperature showed that circulation pump pressure head of 3000 Pa was enough for the system. Constant pressure control is implemented in IDA-ICE as a standard model. To use constant speed control, the pump model with the curve shown in Fig. 4 was used.

3. Results

3.1. Heating need and the sizing of the system

Because the radiators have real dimensions in the used models and heat output depends on dimensioning, about 15% oversizing was done (i.e. radiators heat outputs were selected so that all radiators were oversized by 15% at design outdoor temperature). In first step for both buildings and climates heat loss calculations were made with design outdoor temperature and with no internal heat gains. Design outdoor temperature  $-22^{\circ}C$  was used for Tallinn and  $-15^{\circ}C$  for Munich. In typical bedrooms Type 21 radiators (2 plate radiator with one convection fin element) with height of 400 mm and width of windows provided required heat outputs with heating curve 45/35 in detached house and 40/30 in apartment building.

Heating curves were outdoor air compensated theoretical curves calculated with radiator exponent 1.28 as shown in Fig. 5. The return temperature depends also on the flow rate affecting heat carrier cooling in the system. Fig. 6 shows duration curves of flow and return temperatures from ideal boiler and in one last zone in the 2nd floor (heating curve 45/35  $^{\circ}C$ ). Flow temperature in the last radiator is significantly lower due to temperature drop in the system (total length of the pipe network was 135.8 m).

3.2. Results of one basic low temperature calculation case

To show the level of detail of simulation and the logic of main results one of the main calculation cases of detached house Det45-PI (detailed heating system with heating curve 45/35  $^{\circ}C$  with PI controller) with Estonian climate is reported in comprehensive manner in the following. Calculation time step is determined by the tool, but the hourly output is used. As simulations in IDA-ICE are made with real calculated room temperatures, effects of poor control or internal gains can be easily seen as elevated room temperatures. Radiator heat emissions fluctuate a lot during the year. While thermostatic valve is closed, heat output is close to 0 W and heat outputs close to designed values can be reached for limited

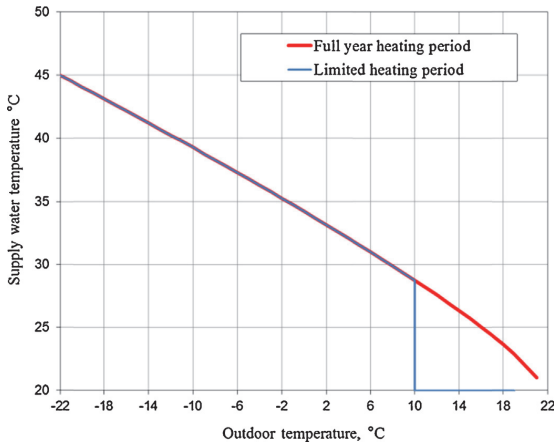


Fig. 5. Heating curves of the full year heating period and limited heating period for heating curve 45/35 °C.

periods when the valves are fully open; the heat output duration curves for all radiators are shown in Fig. 7.

Results show that about 20% of heat emissions to the room are emitted by pipes in a low-temperature heating system (Fig. 8).

It can be seen in Fig. 7 that there is almost no heating need almost half of the year, corresponding to the balance point temperature of 11 °C in detached house and 9 °C in apartment building (balance point temperature was the outdoor temperature at which all thermostatic valves were fully closed, indicating that there is no heating need). The balance point temperature was used to construct the limited heating period curve shown in Fig. 5.

### 3.3. Emission losses: control, stratification and back-wall losses

Significant heat losses can be caused by the control of the heat emission system. While energy need is calculated with ideal control (or with constant room temperature according to EN ISO 13790 [28]), the real room temperature will vary according to the control type and variations in the gains, (Fig. 9). We studied

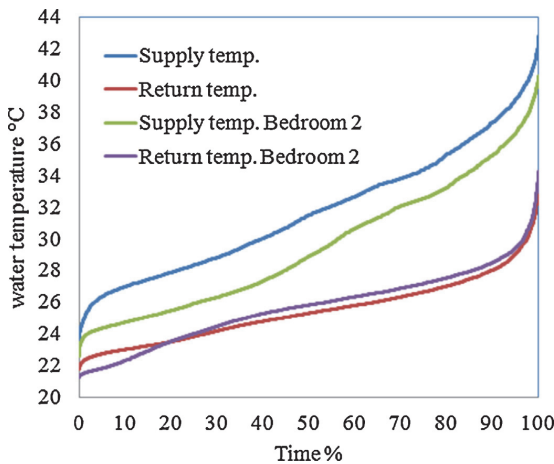


Fig. 6. Flow and return temperature duration curves in boiler and in one last zone (Bedroom 2).

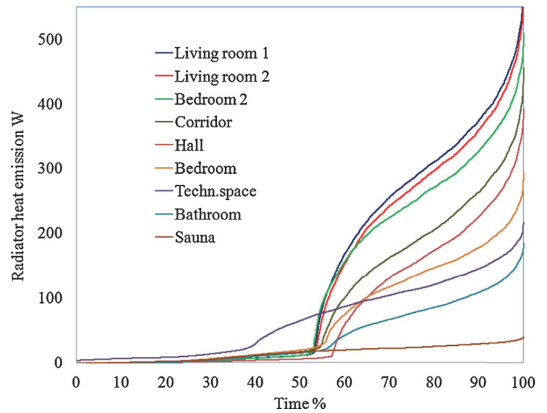


Fig. 7. D-Det45-PI radiator heat emission duration curve in all rooms.

P controller with a proportional band of 2 °C describing a typical radiator thermostat and PI controller providing de-facto ideal control. The simplest available PI controllers are battery operated thermostatic valves, i.e. they can be used as common thermostats.

Because of overheating phenomena of P controller (caused by the flow rate of 50% at temperature set-point) simulations were made to find out the P-controller set-point temperature giving equal thermal comfort compared to PI controller. The set-point of P-controller affected the boiler output. The results show that the set-point could be dropped with P-controller to keep the same room temperature as with PI controller. The set point of 20.5 °C with P-controller ensured air temperature at least 21 °C during severe winter as well as spring conditions as shown in Fig. 10. Therefore the realistic control losses are decreased from 13% with set-point of 21 °C to 3.3%, Table 2. The summary of control losses is provided in Table 2.

Summary of control losses with nP and PI controller. Another components in emission losses are caused by stratification (vertical temperature gradient and additional heat loss through the external wall behind the radiator). For the loss due to vertical temperature profile 15316-2-1:2007 tabulated value gives the efficiency of 0.95 (for heating curve 55/45 °C). However, there is evidence that these losses due non-uniform temperature may be neglected in mechanically ventilated low energy buildings, because of mixing caused by the supply airflow resulting in very small vertical temperature gradient. The vertical temperature difference of 0.7 °C in 2.5 m high room was reported in [29]. We used the data reported to calculate the average room air temperature when air

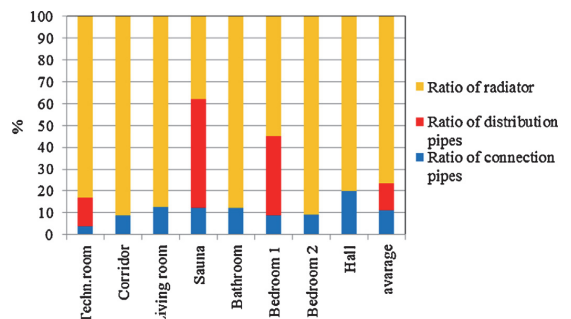


Fig. 8. Ratio of heat emissions to the zones.

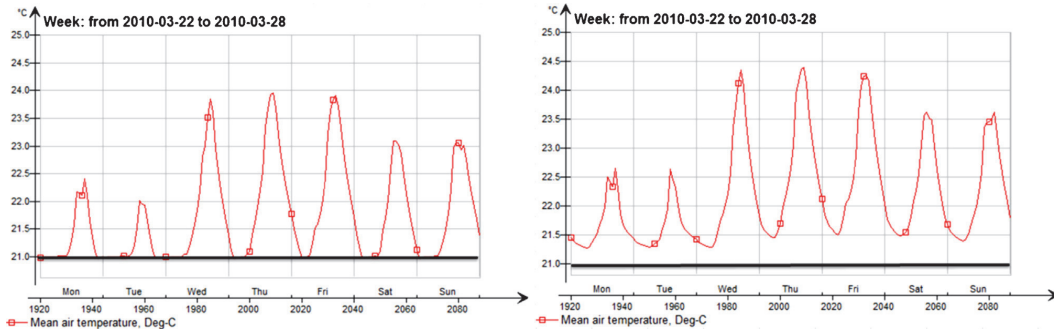


Fig. 9. Comparison of indoor air temperature by P (right) and PI (left) controller in a one week.

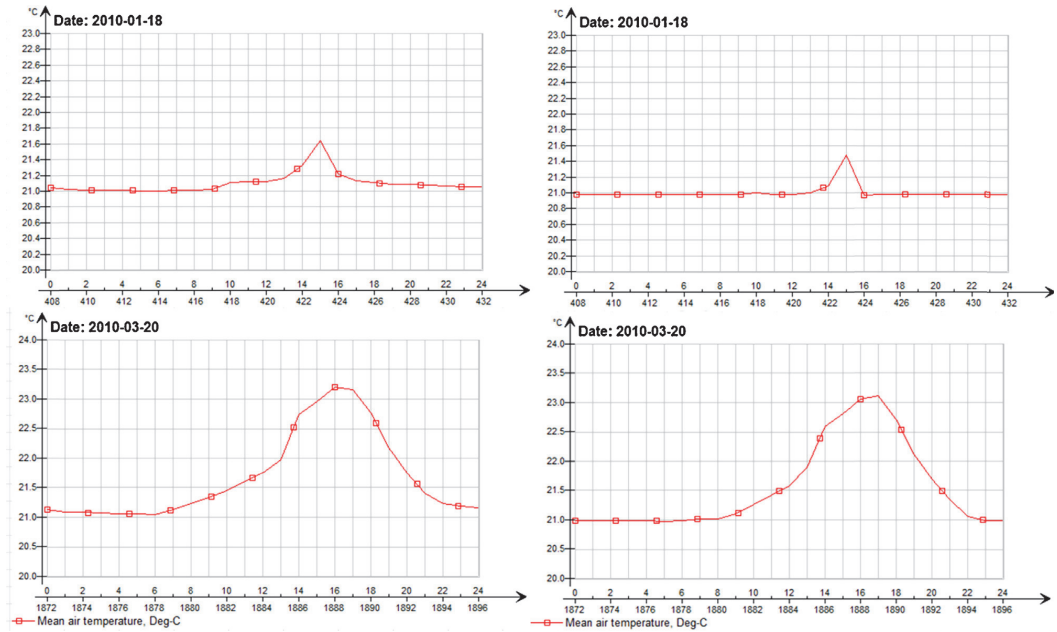


Fig. 10. Comparison of room mean air temperature by P controller (set-point of 20.5 °C (left)) and PI controller (with set point of 21 °C (right)).

temperature at 0.6 m height is 21 °C. The data shown in Fig. 11 [29] resulted in the average room air temperature of 21.05 °C that corresponds to the loss of 0.60% (efficiency of 0.994) according to our calculations.

**Table 2**  
Summary of control losses with n P and PI controller.

Mode	Climate	Simulation case	P-controller (set point 20.5 °C)		P-controller (set point 21 °C)		PI-controller (set point 21 °C)	
			Control losses (%)	Control efficiency	Control losses (%)	Control efficiency ( $\eta$ )	Control losses (%)	Control efficiency ( $\eta$ )
Apartment building	Tallinn	Det45	3.34	0.968	12.99	0.885	0.00	1.000
		Det70	3.99	0.962	18.22	0.846	0.00	1.000
	Munich	Det45	3.72	0.964	15.44	0.866	0.00	1.000
		Det70	4.40	0.958	16.10	0.861	0.00	1.000
Detached house	Tallinn	Det45	2.05	0.980	8.61	0.921	0.00	1.000
		Det70	2.81	0.973	8.70	0.920	0.00	1.000
	Munich	Det45	5.28	0.950	13.43	0.882	0.00	1.000
		Det70	6.24	0.941	13.43	0.882	0.00	1.000

Emission losses due to radiator position were calculated from heat flow density differences from the external wall element behind the radiator (radiators located in the external walls) and the element describing the rest of the external wall. Such calculation

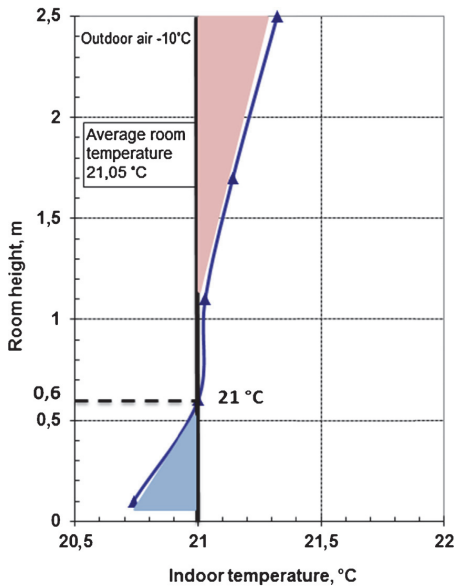


Fig. 11. Temperature gradient data reported in [29] resulting in the average room air temperature of 21.05 °C.

was possible, as IDA-ICE generates special wall element behind the radiator with the dimensions of the radiator. Temperature level (heating curve) had smaller effect on the emission loss than the radiator size, because the loss was slightly smaller with conventional heating curve, because of the smaller size of radiators. Additional emission heat losses from the back side of the radiator were between 0.2 and 0.25% with heating curves studied, which gives the emission efficiency of about 0.998.

Based on the results of control (in Table 2) and stratification efficiencies (0.994 and 0.998) total emission efficiency can be calculated with Eqs. (2) and (3). Stratification losses add 0.4% to control losses and total emission losses become 0.4% (efficiency of 0.996) with PI controller and in between 2.6 and 6.5% (efficiency 0.975–0.939) with P controller.

### 3.4. Non-recoverable distribution and emission losses

#### 3.4.1. Circulation pump control and insulation of the pipes

Three insulation levels of the distribution and connection pipes were analyzed. The cases, where only distribution pipes were insulated with insulation thickness of 40 mm are marked with letter (D) as “distribution”. Another case was with distribution pipes with insulation thickness of 40 mm and connection pipes with insulation thickness of 20 mm, marked with (DC). The cases not insulated have no letter in the case code i.e. Det-45 and Det-70 have no insulation. The results were calculated with constant pressure and constant speed circulation pump control, Table 3. The results show that the losses are somewhat reduced with insulated pipes in the case of 70/55 °C heating curve. With 45/35 °C heating curve, the insulation has no practical effect. To test the model we run some simulations also with 100 mm insulation, which provided better effect, but was still not able to cut distribution losses. Periodic operation, i.e. thermostats closed for a long time in spring and autumn, reduced the expected effect of insulation.

Effect of insulation with constant speed and constant pressure pump control on distribution and emission efficiency in Estonian

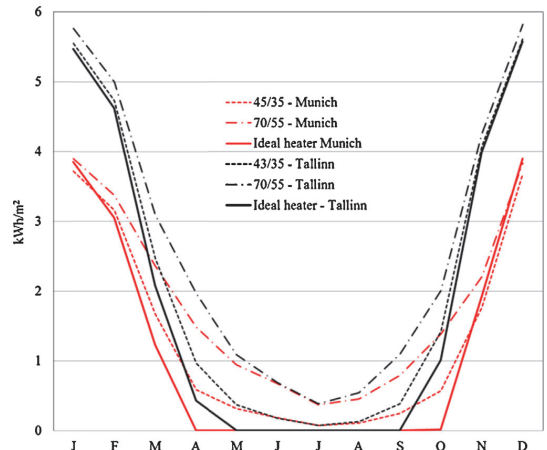


Fig. 12. Monthly delivered space heating energy in Munich and Tallinn in apartment building.

climate. All cases have PI controller. With constant speed circulation pump control, the higher losses occur specially during warmer months indicating higher heat emissions from pipes and worse utilisation of internal gains, (Table 3).

#### 3.4.2. Climate impact on the heating system efficiency

The main simulation cases were run with Tallinn and Munich climate (radiators sized accordingly) to show the effect of the climate. Results are shown in Fig. 12.

In Munich distribution and emission losses are somewhat higher than in Tallinn. The building type and the heating curve have more impact on the losses than does the climate difference. The most crucial difference is between apartment building and detached house. Monthly values of delivered space heating energy are shown in Fig. 12 for the apartment building in both climates. It can be seen that there is no heating need during the summer, but the simulations have been run since now with all year round circulation pump and boiler operation. This explains significant losses in summer caused by pipe heat emissions (radiator emissions were close to zero, because of closed thermostat valves).

#### 3.4.3. Impact of the heating period length and heating curve on system efficiency

Since now, all the simulations have been done with full year heating period. As the results in Table 4 indicate, that the shorter heating period may reduce losses, the simulations were done with shorter heating period (heating curve shown in Fig. 5). The length of limited heating period was in Tallinn 35 weeks and 32 weeks in detached house and apartment building and in Munich 32 and 28 weeks, respectively. The results show significantly reduced losses. As additional measure to reduce losses we simulated 40/30 °C heating curve. The results in Table 4 show that limited heating period decreased the losses in apartment building to 8.9% and in the detached house to 1% in Tallinn. With 40/30 °C heating curve, the losses of 6.3% in Tallinn and 12.4% in Munich were achieved in the apartment building.

Impact of heating period length on distribution and emission losses. As 40/30 °C heating curve showed significant effect in the apartment building, we simulated also a typical floor heating curve 35/28 °C for Tallinn, but the effect was minimal. Full year heating period may be relevant especially in houses as provides some possibilities to apply floor heating in wet rooms also in summer time.

**Table 3**  
Effect of insulation with constant speed and constant pressure pump control on distribution and emission efficiency in Estonian climate. All cases have PI controller.

Mode	Simulation case	Const. pressure pump		Const. speed pump	
		Distribution and emission losses (%)	Distribution and emission efficiency ( $\eta$ )	Distribution and emission losses (%)	Distribution and emission efficiency ( $\eta$ )
Apartment building	Ideal	0.00	1.000		
	Det45	12.09	0.892	14.80	0.871
	Det-45-D	11.89	0.894	14.37	0.874
	Det-45-DC	11.25	0.899	13.58	0.880
	Det-70	36.82	0.731	44.71	0.691
	Det70-D	32.72	0.753	39.66	0.716
Detached house	Det70-DC	29.19	0.774	35.21	0.740
	Ideal	0.00	1.000		
	Det45	1.63	0.984	1.98	0.981
	Det-45-D	1.63	0.984	2.20	0.978
	Det-45-DC	1.57	0.985	2.20	0.979
	Det-70	7.16	0.933	9.52	0.913
	Det70-D	6.61	0.938	8.83	0.919
	Det70-DC	6.15	0.942	8.83	0.919

**Table 4**  
Impact of heating period length on distribution and emission losses.

Mode	Climate	Simulation case	Full year heating period		Limited heating period		
			Distribution and emission losses. %	Distribution and emission efficiency. $\eta$	Distribution and emission losses. %	Distribution and emission efficiency. $\eta$	
Apartment	Tallinn	Ideal	0.00	1.000	0.00	1.000	
		Det40-PI	8.06	0.925	6.33	0.941	
		Det45-PI	14.80	0.871	8.85	0.919	
		Det70-PI	36.82	0.731	24.51	0.803	
		Ideal	0.00	1.000	0.00	1.000	
Munich	Munich	Det40-PI	15.55	0.865	12.38	0.890	
		Det45-PI	22.89	0.814	16.50	0.858	
		Det70-PI	55.75	0.642	44.75	0.691	
		Ideal	0.00	1.000	0.00	1.000	
Detached house	Tallinn	Det40-PI	1.61	0.984	0.35	0.997	
		Det45-PI	1.63	0.984	0.96	0.991	
		Det70-PI	7.16	0.933	4.35	0.958	
	Munich	Munich	Ideal	0.00	1.000	0.00	1.000
			Det40-PI	3.69	0.964	0.42	0.996
			Det45-PI	6.04	0.943	1.39	0.986
			Det70-PI	15.06	0.869	7.18	0.933

However, with used heating curves going down to 21 °C the floor heating capacity is very limited in the summer.

## 4. Discussion

### 4.1. Recoverable losses

The results reported in previous sections show the importance to control the heating system losses. System efficiencies were generally lower in warmer climates and buildings with smaller heating need and higher internal gains. In addition to non-recoverable losses, described in Section 3, recoverable system losses may be also quantified. They are part of the system thermal losses which have been recovered to decrease the energy use for heating. According to CEN standard recoverable losses are all pipe heat emission in heated rooms, but we used more accurate allocation. We defined recoverable distribution losses as heat emission emitted by the pipes until the room temperature set-point was achieved. The part of the heat emission which increased room temperature over the set-point was considered as non-recoverable loss. Results in Fig. 17 shows that as much as 40% of delivered heat is uncontrolled and emitted to room by distribution network.

### 4.2. Explanation of high losses with conventional heating curve

Results showed that distribution losses are significantly dependent on the heating curve. With the conventional 70/55 °C

curve, it was not possible to control losses; insulation of distribution and connection pipes had some effect (Table 3), but may be considered as without practical meaning. We were able to identify two reasons for high losses. First, with high temperature heating curve, average room temperature is slightly elevated, this can be seen from extract air temperature shown in Fig. 13. Secondly the

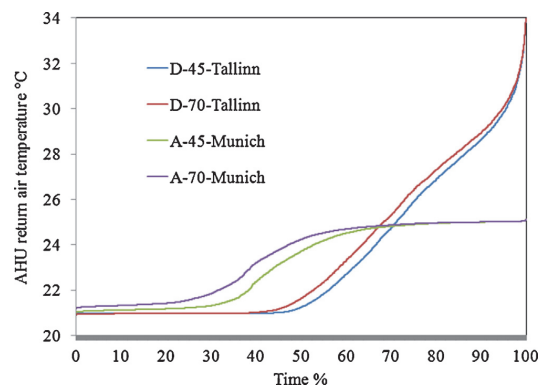


**Fig. 13.** AHU extract air temperature duration curve (A is apartment building (with cooling); D is detached building).

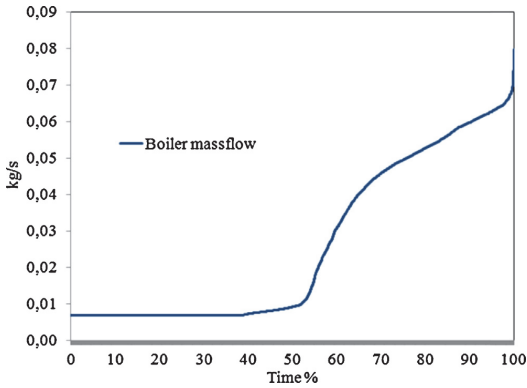


Fig. 14. Duration curve of the boiler mass-flow for case D-45-Det.

highest heat emissions compared to Ideal cases occurred during the warmer months, which can be seen from Fig. 12. This indicates in addition to the lower utilization that some flow rate through the closed valves may play some role. As we used the model of real valves, a small amount of heat carrier circulated through the closed valves in the system and caused some distribution loss. When design flow rate was 0.12 kg/s, results show very small flow rates during 50% of the time, Fig. 14. Duration curve of the flow rate also shows some challenge for the generation, which has to be able to manage with very low, say about 30% of design value, flow rates. Conventional heat pumps typically have minimal flow rates of about 2/3 of the nominal flow rate and therefore need to be operated with significant bypass flow.

4.3. Fundamentals of distribution losses

Results show that emission losses were minimal if PI control was used. To explain the distribution losses we analysed eight main cases were for apartment/detached house. Tallinn/Munich climate and 45/35 °C and 70/55 °C heating curves. We were able to find a strong positive correlation ( $R^2$  factor nearly 1) between hourly distribution losses and ratio of  $\Phi_{pipe}/\Phi_{need}$ , Fig. 15. The ratio of  $\Phi_{pipe}/\Phi_{need}$  shows the amount of heating need covered by heat emission from pipes.

The correlation equations did not give the same annual losses as a sum of simulated hourly values. The reason was in the lower part of the correlation line (even negative losses, because of dynamic effects). We shifted the starting point slightly (i.e. the constant in the equation) which did not cause significant change to  $R^2$  value, but provided the agreement between the equation and hourly values not worse than 5%. It can be seen that the correlation equations

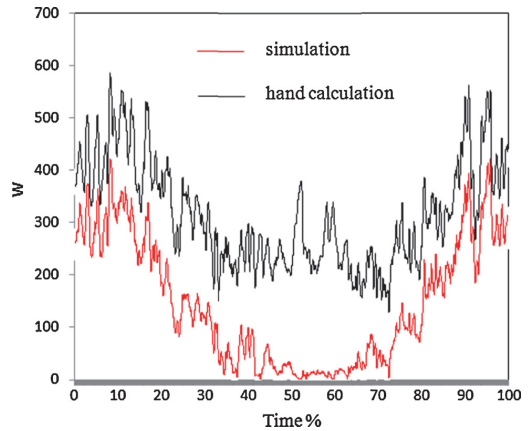


Fig. 16. Comparison of hand calculation of pipe heat emission with dynamic simulation for the case of detached house 45/35 °C in Tallinn.

are heating curve specific. The equation  $y = 170x - 40$  (where  $y$  is distribution loss (%) and  $x$  is ratio of  $\Phi_{pipe}/\Phi_{need}$ ) represents the average for 45/35 °C cases and  $y = 150x - 70$  for 70 °C/55 °C cases.

The availability of this type of equations calls for the “hand calculation” of losses. Hourly energy need can be easily calculated with any simulation or simplified hourly tool. Pipe heat emissions are possible to calculate from theoretical heating curve flow and return temperatures, however the effects of cooling and fluctuating flow rates are not easy to estimate. When neglecting these effects (i.e. calculating just with theoretical flow and return temperature) the heat emission from pipes were overestimated as shown in Fig. 16. In average the pipe heat emissions were overestimate by factor of 2.2. When these overestimated hand calculated heat emissions were used in the correlation equations derived, the distribution losses were overestimated by factor of about 11. Therefore the ratio  $\Phi_{pipe}/\Phi_{need}$  is able to provide sound explanation for the distribution loss mechanism, but neglecting the dynamics will cause the overestimation of losses by about factor 10.

4.4. Comparison of results with tabulated values of CEN standards

In Table 5 the results of low temperature heating curve 45/35 °C and conventional 70/55 °C are shown in the format used in EN 15316 both for P and PI controllers. The loss of vertical temperature profile is calculated with the room temperature set-point 21.05 relative to 21 (reported in Ch. 3.3). “External components” means radiator back-wall additional loss and embedded efficiency is 1 because of no embedded components (floor heating). Results

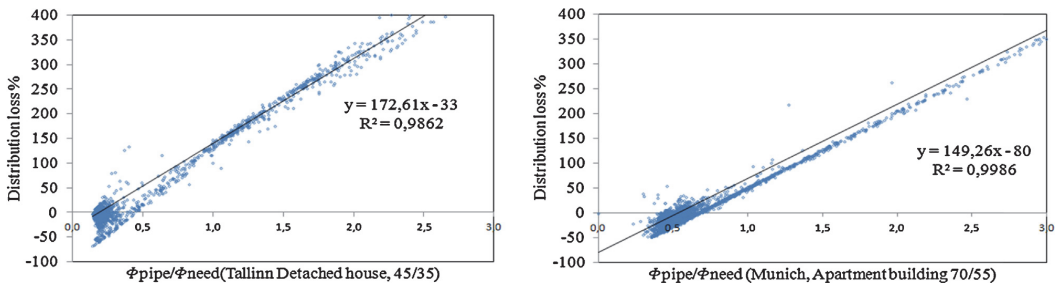


Fig. 15. Correlation between distribution loss and ratio of  $\Phi_{pipe}/\Phi_{need}$  for heating curve 45/35 °C (left) and 70/55 °C (right).

**Table 5**  
Comparison of the results (non-recoverable losses) with tabulated values of EN 15316-2-1:2007 and 15316-2-3:2007.

Detailed dynamic simulation															
Tallinn															
Detached house			Apartment building			Munich detached house			Apartment building			EN:15316 tabulated values			
P	PI		P	PI		P	PI		P	PI		P	PI		
Auxiliary efficiency															
Temperature curve															
Emission efficiency															
	0.98	45 °C/35 °C	1.00	0.97	1.00	1.00	0.95	1.00	1.00	0.96	55 °C/45 °C	0.97	0.93	0.93	0.93
Control losses (P-controller 2 K)/PI-controller															
Stratification efficiency			0.99			0.99			0.99			0.95			
		Vertical air temperature profile external components	1.00			1.00			1.00			0.95			
		1.00													
Embedded efficiency			0.90			0.98			0.88			0.89			0.81
Total efficiency	0.97		0.87	0.90	0.93	0.98	0.87	0.84	0.87	0.82	0.79	0.72	0.75	0.75	0.75
Temperature curve									70 °C/55 °C						
Emission efficiency	0.97		1.00	0.96	1.00	0.94	1.00	0.96	1.00	0.96	1.00	0.97	0.93	0.93	0.93
Control losses (P-controller 2 K)/PI-controller															
Stratification efficiency			0.99			0.99			0.99			0.93			
		Vertical air temperature profile external components	1.00			1.00			1.00			0.95			
		1.00													
Embedded efficiency			0.74			0.90			0.65			0.86			0.75
Total efficiency	0.91		0.71	0.73	0.85	0.90	0.62	0.64	0.62	0.64	0.76	0.67	0.69	0.69	0.69

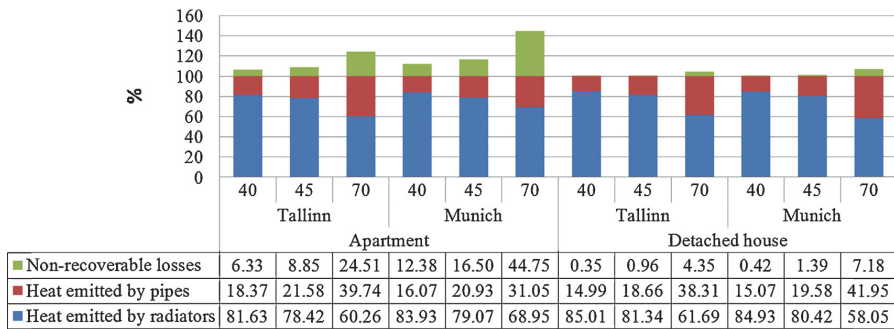


Fig. 17. Minimal achievable distribution and emission losses (non-recoverable losses. 100% = heating need) with PI thermostats and limited heating period.

in Tabel 5 show that tabulated values of EN 15316-2-1:2007 are significantly higher in all cases.

## 5. Conclusions

Detailed dynamic components of heating system in the whole building simulation model allowed us to quantify distribution and emission losses for radiator heating. Main findings of the study show that distribution losses can be controlled with low temperature heating curves and emission losses with PI type thermostats.

Emission losses in ventilated low energy buildings occur mainly as control losses. Other emission losses due to vertical temperature difference and additional heat loss through the external walls behind radiators are not more than 0.6%. Control losses caused by proportional thermostats were between 2 and 6%.

Distribution and emission losses were possible to keep below 1% in detached houses both in a cold and Central European climate if PI thermostats, low temperature heating curve and limited heating period was used. In apartment buildings the losses were significantly higher, between 6 and 12% for lowest heating curves in a cold and Central European climate, respectively, Fig. 17.

Compared to low temperature heating curves, conventional 70/55 °C curve remarkably increased the losses. Therefore, heating curve of 45/35 °C can be recommended for detached houses and even 40/30 °C for apartment buildings. In studied low energy buildings Type 21 radiators (2 plate radiator with one convection fin element) with height of 400 mm and width of windows in bedrooms provided easily required heat outputs.

Insulating distribution and connection pipes in heated spaces proved to have no practical effect on heat losses. Some effect was seen with 70/55 °C heating curve, but generally insulating the pipes can be considered ineffective—because of large heat transfer surface area, the heat emissions cannot be significantly reduced.

Compared to EN 15316-2-1:2007 and EN 15316-2-3:2007, calculated losses were significantly lower especially for low temperature heating curves. A new set of tabulated values is proposed for the revision of the standard. The values of low temperature heating curves are applicable both in Central and North European climate for nearly zero and low energy buildings.

It was possible to show that distribution losses depend on the amount of heating need covered by heat emission from pipes—the higher the ratio of heat emission from pipes to heating need the higher the losses. Correlation factor close to 1 was found, but still it was not possible to calculate losses from hourly energy need data with the correlation equation. The pipe heat emissions were over-estimated by factor of about 2 and distribution losses by factor of about 10 due to fluctuating flow rate and other dynamic effects not possible to take into account by hand calculation.

## Acknowledgment

The research was supported by the Estonian Research Council, with Institutional research funding grant IUT1–15, and with a grant of the European Union, the European Social Fund, Mobilitas grant no. MTT74.

## References

- [1] J. Kurnitski, A. Saari, T. Kalamees, M. Vuolle, J. Niemelä, T. Tark, Cost optimal and nearly zero (nZEB) energy performance calculations for residential buildings with REHVA definition for nZEB national implementation, *Energy and Buildings* 43 (11) (2011) 3279–3288.
- [2] European Standard EN. 15251, Indoor Environmental Input Parameters for Design and Assessment of Energy Performance of Buildings Addressing Indoor Air Quality, in: Thermal Environment, Lighting and Acoustics, 2007.
- [3] A. Balaras, K. Drousta, E. Dacalaki, S. Kontoyannidis, Heating energy consumption and resulting environmental impact of European apartment buildings, *Energy and Buildings* 37 (2005) 429–442.
- [4] H. Herring, R. Hardcastle, R. Phillipson, Energy use and energy efficiency in UK commercial and public buildings up to the year 2000 Energy Efficiency Series, Energy Efficiency Office, UK, 1988, ISBN 0-11-412903-7.
- [5] T. Kalamees, K. Kuusk, E. Arumägi, S. Ilomets, M. Maivel, The analysis of measured energy consumption in apartment buildings in Estonia, in: IEA Annex 55 (RAP-RETRO) Working meeting, Vienna, Austria, April 23–25, 2012, p. 6.
- [6] M. Maivel, K. Kuusk, Energy consumption and indoor climate analysis in detached houses, in: Proceedings of the 2nd WSEAS International Conference on Urban Rehabilitation and Sustainability (ures'09): wseas international conferences, Baltimore, USA, 2009 WSEAS 2009, 2009, pp. 97–102.
- [7] Directive 2010/31/EU of the European Parliament and of the Council of 19 May 2010 on the energy performance of buildings. <http://eur-lex.europa.eu/LexUriServ/LexUriServ.do?uri=OJ:L:2010:153:0013:0035:EN:PDF>
- [8] European Standard EN. 15316-1, Heating Systems in Buildings: Method for Calculation of System Energy Requirements and System Efficiencies. Part 1: General, 2007.
- [9] Z. Liao, A.L. Dexter, The potential for energy saving in heating systems through improving boiler controls, *Energy and Buildings* 36 (2004) 261–271.
- [10] L. Peeters, Van der, J. Veken, H. Hens, L. Helsen, W.D. D'haeseleer, Control of heating systems in residential buildings: current practice, *Energy and Buildings* 40 (2008) 1446–1455.
- [11] European Standard EN 15316-4-1, Heating Systems in Buildings: Method for Calculation of System Energy Requirements and System Efficiencies. Part 4-1: Space Heating Generation Systems: Combustion Systems (boilers), 2008.
- [12] European Standard EN 15316-4-2, Heating Systems in Buildings: Method for Calculation of System Energy Requirements and System Efficiencies. Part 4-2: Space Heating Generation Systems: Heat Pump systems, 2013.
- [13] European Standard EN 15316-4-3, "Heating Systems in Buildings: Method for Calculation of System Energy Requirements and System Efficiencies. Part 4-3: Space Heating Generation Systems. Solar Thermal Systems", 2007.
- [14] European Standard EN 15316-4-4, "Heating Systems in Buildings: Method for Calculation of System Energy Requirements and System Efficiencies. Part 4-4: Space Heating Generation Systems: Building Integrated Cogeneration systems", 2007.
- [15] European Standard EN 15316-4-5, "Heating Systems in Buildings: Method for Calculation of System Energy Requirements and System Efficiencies. Part 4-5: Space Heating Generation Systems: The Performance and Quality of District Heating and Large Volume Systems", 2007.
- [16] European Standard EN 15316-4-6, "Heating Systems in Buildings Method for Calculation of System Energy Requirements and System Efficiencies Part 4-7: Space heating generation systems photovoltaic systems", 2007.

- [17] European Standard EN 15316-4-7, "Heating Systems in Buildings: Method for Calculation of System Energy Requirements and System Efficiencies Part 4-7: Space Heating Generation Systems Biomass Combustion Systems", 2008.
- [18] B.W. Olesen, M. de Carli, Calculation of the yearly energy performance of heating systems based on the European Building Energy Directive and related CEN standards, *Energy and Buildings* 43 (2011) 1040–1050.
- [19] H. Sauter, *Leistungsminderung bei Heizkörperverkleidungen*, 1985, HLH Bd. 36. Nr. 4.
- [20] European Standard EN 15316-2-3, "Heating Systems in Buildings: Method for Calculation of System Energy Requirements and System Efficiencies Part 2-1: Space Heating Distribution Systems", 2007.
- [21] European Standard EN 15316-2-1, "Heating Systems in Buildings Method for Calculation of System Energy Requirements and System Efficiencies Part 2-1: Space Heating Emission Systems", 2007.
- [22] Ministry of Economic Affairs and Communication, Regulation no. 68 Minimum Requirements for Energy Performance", 2013.
- [23] A. Bring, P. Sahlin, M. Vuolle, IEA SHC Task 22—Subtask B—Models for Building Indoor Climate and Energy Simulation, 1999.
- [24] D.B. Crawley, J.W. Hand, K. Kummert, B.T. Griffith, Contrasting the capabilities of building energy performance simulation programs, *Building and Environment* 43 (2008) 661–673.
- [25] T. Kalamees, J. Kurnitski, Estonian test reference year for energy calculations, *Proceedings of the Estonian Academy of Sciences Engineering* 12 (1) (2006) 40–58.
- [26] **IDA Users Online** <http://www.equonline.com/ice4user/>
- [27] P. Sahlin, L. Eriksson, P. Grozman, H. Johansson, A. Shapovalov, M. Vuolle, Whole-building simulation with symbolic DAE equations and general purpose solvers, *Building and Environment* (2012) BAE905.
- [28] ISO, 13790 Energy Performance of Buildings Calculation of Energy Use for Space Heating and Cooling, 2008.
- [29] A. Hasan, J. Kurnitski, K. Jokiranta, A combined low temperature water heating system consisting of radiators and floor heating, *Energy and Buildings* 41 (2009) 470–479.



## PAPER II

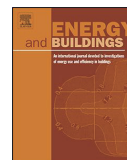
Maivel, M.; Konzelmann, M.; Kurnitski, J. (2015). Energy Performance of Radiators with Parallel and Serial Connected Panels. *Energy and Buildings*, 86, 745 - 753.





Contents lists available at ScienceDirect

## Energy and Buildings

journal homepage: [www.elsevier.com/locate/enbuild](http://www.elsevier.com/locate/enbuild)

# Energy performance of radiators with parallel and serial connected panels

Mikk Maivel<sup>a,\*</sup>, Martin Konzelmann<sup>b</sup>, Jarek Kurnitski<sup>a,c</sup><sup>a</sup> Tallinn University of Technology, Ehitajate tee 5, 19086 Tallinn, Estonia<sup>b</sup> WTP Wärmetechnische Prüfgesellschaft mbH, Oranienstrasse 161, 10969 Berlin, Germany<sup>c</sup> Aalto University, School of Engineering, Rakentajanaukio 4 A, FI-02150 Espoo, Finland

## ARTICLE INFO

## Article history:

Received 22 May 2014

Received in revised form 31 August 2014

Accepted 4 October 2014

Available online 14 October 2014

## Keywords:

Water radiator

Heat emission

Energy performance

Operative temperature

Radiant temperature

## ABSTRACT

Laboratory measurements were conducted for radiators with parallel and serial connected panels in EN 442-2 test room to quantify the possible energy saving of serial radiator. Measured results needed recalculation for the comparison, and simulations were used for annual performance assessment. Serial radiator showed 4 °C higher and 3 °C lower temperatures of the front and rear panels at 50 °C flow temperature. Parallel radiator had slightly faster dynamic response and its 3% higher heat output at  $\Delta T 50$  °C increased to about 10% at  $\Delta T 25$  °C. Measured heat emission of serial radiator was 2% lower in one and 4% higher in another test and it was not possible to quantify very small differences between radiators. Simulation showed 0.11–0.13 °C lower air temperatures of serial radiator at fixed operative temperature. In simulated EN 442-2 test room, the heat emission of radiators was exactly the same, but in the case of a residential room with less intensive radiation heat exchange, serial radiator showed 0.3% smaller heat emission and 0.7% smaller annual heating energy use. Generally, the effect of radiant temperature was possible to see from results, but in terms of energy savings there was no considerable difference between studied radiators.

© 2014 Elsevier B.V. All rights reserved.

## 1. Introduction

Emission losses of heat emitters are commonly described by EN 15316-2-1:2007 [1] where they are divided into three factors, which are losses due to non-uniform temperature distribution (stratification), losses to the outside from heating devices embedded in the structure, and losses due to imperfect control of the indoor temperature. These factors have been derived with measurements and simulation as described in [2]. The standard provides tabulated values for all of these factors as efficiency values which when can be used to calculate the total emission efficiency. In the case of radiators there are no embedded components. Stratification losses depend on over-temperature and losses via external components, i.e. location of the radiator. For a radiator with 55/45 °C flow/return temperature and normal location on external wall, the stratification efficiency is  $\eta_{\text{STR}} = 0.95$ . If we assume an ideal control, the emission losses becomes  $q_{\text{em, loss}} = (1/0.95 - 1)100 = 5.3\%$ . This value can be seen quite conservative for modern buildings as reference [3] reports additional emission loss up to 5% of the heat emission of radiator in old

buildings with poor insulation and less than 1% in new buildings with good insulation. The latter is supported with recent studies for well insulated buildings. In such buildings additional losses via external wall are as low as 0.2% [4]. In rooms with mechanical supply air there is very small temperature gradient [5] and stratification losses (due to temperature gradient and losses via external wall) remain around 0.4% [4].

Available data on emission efficiency of radiators thus allows to take into account the heating curve and insulation level of the building. To quantify the differences due to radiator configuration, more detailed methods are needed.

It is reported that radiators with serial connected panels can provide 11% energy saving [7] and this has been argued with up to 100% higher radiation heat transfer and also shorter heating up time of radiator. The objective of this study was to quantify the effect of parallel and serial connected radiator panels on emission losses and energy use with controlled laboratory measurements and dynamic simulation. The motivation was to show which differences can be measured in the laboratory and how these can be generalized to annual energy performance of conventional and low temperature radiator systems.

The limitation of the standard EN15316-2.1: 2007 is that the effect on operative temperature on heat emission is not accounted as the calculation procedure is fully based on air temperature. In

\* Corresponding author. Tel.: +372 56 461 251.

E-mail addresses: [mikk.maivel@ttu.ee](mailto:mikk.maivel@ttu.ee), [mikkmaivel@gmail.com](mailto:mikkmaivel@gmail.com) (M. Maivel).

## Nomenclature

$q$	heat transfer rate (W)
$q_{\text{tot}}$	heat emission of radiator (W)
$q_{\text{loss}}$	heat loss (W)
$T_a$	air temperature ( $^{\circ}\text{C}$ )
$T_r$	radiator front panel surface temperature ( $^{\circ}\text{C}$ )
$T_s$	cooled room surfaces temperature ( $^{\circ}\text{C}$ )
$A_r$	area of the radiator ( $\text{m}^2$ )
$A_s$	area of the non-insulated room surfaces ( $\text{m}^2$ )
$\Delta T$	over-temperature between the water and the air ( $^{\circ}\text{C}$ )
$\Delta T_{\text{In}}$	logarithmic temperature difference between the water and the air ( $^{\circ}\text{C}$ )

reality different radiators have some effect on radiant temperature and the operative temperature is the basic parameter of thermal comfort standard ISO 7730:2005 [6]. Operative temperature is calculated as an average of air and mean radiant temperature and is the temperature human being is sensing. Therefore, for the exact comparison of heat emitters energy efficiency, the measurements and simulations are needed to be conducted at the same operative temperature, that was taken into account in this study.

In this study we conducted laboratory measurements for the same size and type radiator with parallel and serial connected panels in EN 442-2:2003 [8] test room at same conditions to quantify the energy saving. Because of very small differences, we needed to analytically model the heat transfer process in EN 442-2:2003 test room in order to be able to correct operative temperature levels up to  $0.2^{\circ}\text{C}$ . This allowed the comparison at exactly the same temperature levels. Additionally we analysed the seasonal performance in dynamic simulation software which has limitations for radiator model, but allowed to model the radiator surface temperature according to the measurement results.

## 2. Methods

### 2.1. Radiator configurations

The studied radiator configurations are shown in Fig. 1. The parallel connected panels are in theory most effective in respect of the heat output, utilizing maximally the flow temperature level. In the case of serial connected panels, the hot water flows first through the front (room-side) panel and then to the back (wall side) panel. The cooled water then returns to the heating pipework. The idea of serial connection is to increase the room side surface temperature of the radiator which will increase radiation heat transfer and operative temperature.

### 2.2. Heat output and temperature measurements

Heat emission of two radiators at given room air temperature were measured in the test chamber conforming EN 442-2:2003 requirements. The radiators were 2-panel radiators physically of the same size, 0.6 m height and 1.4 m length, with parallel and serial

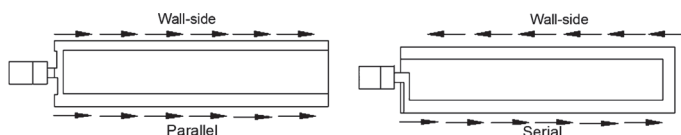


Fig. 1. Studied radiator types with parallel and serial connected panels.

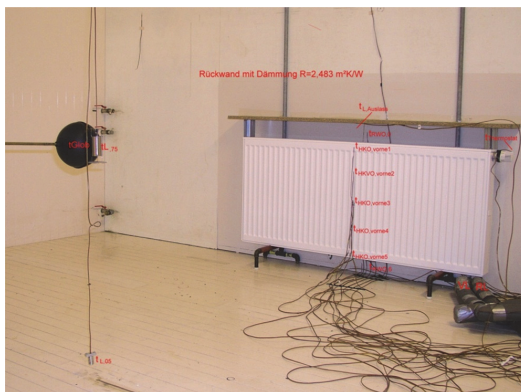


Fig. 2. Photo of the measurement arrangement.

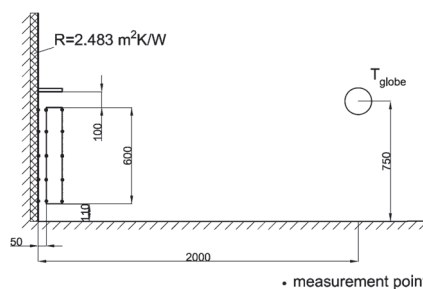


Fig. 3. Radiator and temperature measurement points locations. The room floor area is 4.0 by 4.0 m and the room height 3.0 m.

connected panels and two convection fin plates in between, both types 22-600-1400. The rated heat output of parallel was 2393 W and for serial 2332 W at over-temperature  $\Delta T 50^{\circ}\text{C}$  according to EN 442-2:2003. The air temperature and heat emission of the radiators was controlled with the same proportional thermostat, which was a typical radiator thermostat complying with EN 215:2004 [9] and operating across the proportional band of  $2^{\circ}\text{C}$  with the set point of  $20^{\circ}\text{C}$  in all tests.

In addition to the standard heat output measurement arrangements, the radiators and all surfaces were equipped with temperature measurement sensors. The effect of radiant heat transfer was estimated with measuring the 150 mm globe temperature. Figs. 2 and 3 illustrate the measurement arrangement and measurement points of the temperatures.

### 2.3. Analytical model of EN 442-2 test room heat transfer

In laboratory measurements, the room air temperature set point was  $20^{\circ}\text{C}$ , but in reality the air temperature varied by  $0.1 \dots 0.2^{\circ}\text{C}$  in different test runs. To enable the comparison at exactly the same operative temperature in the room, the correction was applied

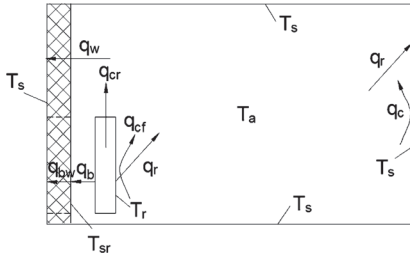


Fig. 4. Heat balance of EN 442-2 test room. Heat from cooled surfaces ( $T_s$ ) is removed with water flow.

through the analytical model of the room. In EN 442-2 test room the radiator heat emission is controlled with cooling of all room surfaces with water based circulation system. Therefore the radiator heat emission  $q_{tot}$  is controlled with surfaces temperature  $T_s$  which is the same for all room surfaces.  $q_{tot}$  was measured from water flow side.

To change the surface temperature  $T_s$  in order to recalculate all consequent heat transfer effects and other temperatures at the same operative temperature, the relation between  $q_{tot}$  and  $T_s$  needs to be described and solved:

$$q_{tot} = f(T_s) \quad (1)$$

Heat flows in the room and symbols used are shown in Fig. 4. Heat losses consist of radiation and convection and heat transmission through insulation in the wall the radiator is mounted:

$$q_{loss} = q_r + q_c + q_w + q_{bw} \quad (2)$$

where  $q_{bw}$  is the heat conduction through the area behind the radiator. Radiator heat emission is described:

$$q_{tot} = q_{front} + q_{cr} + q_b \quad (3)$$

where  $q_{front} = q_r + q_{cf}$  consist of radiation and convection from the front panel,  $q_{cr}$  is convection from convection fins and  $q_b$  is the total heat transfer from rear panel. Because the  $q_{tot}$  and surface temperatures were measured, only  $q_r$  needs to be calculated. According to steady state heat balance  $q_{tot} = q_{loss}$ .

Net radiative heat exchange can be calculated from longwave radiation Eq. [10]:

$$q_r = \sigma A_r F_{er-s} (T_r^4 - T_s^4) \quad (4)$$

where  $\sigma = 5.67 \times 10^{-8} \text{ W}/(\text{m}^2 \text{ K}^4)$  is the Stefan–Boltzmann constant and  $F_{er-s}$  is the total exchange factor:

$$F_{er-s} = \frac{1}{1/F_{r-s} + (1/\varepsilon_r - 1) + (A_r/A_s)(1/\varepsilon_s - 1)} \quad (5)$$

because the view factor  $F_{r-s} = \sum_{i=1}^5 F_i = 1$  the total exchange factor becomes:

$$F_{er-s} = \frac{1}{(1/1) + ((1/0.95) - 1) + (0.84/68)((1/0.9) - 1)} = 0.899 \quad (6)$$

As net radiation heat exchange can be calculated with Eq. (4) and  $q_{tot}$  is measured, convection  $q_c$  can be calculated from the heat balance as follows:

$$q_c + q_w + q_{bw} = q_{tot} - q_r \quad (7)$$

where heat transmission through insulation on the wall the radiator is mounted can be calculated from measured air and surface

temperatures and thermal resistance of the insulation. In the wall area behind the radiator:

$$q_{bw} = U_{bw} A_r (T_{sr} - T_s) \quad (8)$$

where the wall surface temperature  $T_{sr}$  is measured and  $U_{bw} = 1/2.483 = 0.402 \text{ W}/(\text{m}^2 \text{ K})$ . Through the rest of insulated wall:

$$q_w = U_w A_w (T_a - T_s) \quad (9)$$

where a building code default value of the surface heat resistance of  $0.13 (\text{m}^2 \text{ K})/\text{W}$  was used to calculate  $U_w = 1/(2.483 + 0.13) = 0.383 \text{ W}/(\text{m}^2 \text{ K})$ . With Eqs. (4), (8) and (9) convection heat transfer rate  $q_c$  can be calculated. From  $q_c$  the convection heat transfer coefficient  $h_c$  can be calculated:

$$q_c = h_c A_s (T_a - T_s) \quad (10)$$

$$h_c = c(T_a - T_s)^{0.25} \quad (11)$$

where  $c$  is constant.

This set of equations can be used for small adjustments of room temperature, which is needed to recalculate the results to the same operative temperature, as follows:

- change the measured  $T_{s,1}$  value to  $T_{s,2}$
- calculate new over-temperature (logarithmic temperature difference between the water and the air) for the radiator and new adjusted heat emission

$$q_{tot,2} = q_{tot,1} \frac{\Delta T_{ln,2}}{\Delta T_{ln,1}} \quad (12)$$

- calculate the new value of  $q_c$  with Eq. (7) and iterate new  $T_{a,2}$  so that the constant from Eq. (11) remains the same, i.e.  $c_2 = c_1$ .

This calculation provides new air temperature  $T_a$  and new heat emission of the radiator for given change of the surface temperature value  $T_s$ . The results apply for small changes, because the radiator surface temperatures and the wall surface temperatures behind the radiator are not corrected, i.e. secondary effects are not accounted.

From new  $T_s$  and  $T_a$  values the operative temperature can be calculated and the procedure is to be repeated until the desired operative temperature is achieved. The operative temperature was calculated with the angle factors and equations of ISO 7726:1998 [11]. For this purpose we used an angle factors between a small plane element and the surrounding surfaces used to calculate the plane radiant temperature, given in Annex C of the standard. The mean radiant temperature was calculated from the plane radiant temperatures in six directions and the projected area factors for a person in the same six directions, given in the Annex B of the standard. The operative temperature was calculated as an average of the air and the mean radiant temperature. For the comparison, the mean radiant temperature was calculated also from the measured standard globe temperature with the equation given in the standard.

#### 2.4. Case study in a dynamic simulation environment

IDA-ICE [12] simulation software with standard water radiator model was used to model the EN 442-2 test room and a typical residential room (with the same dimensions). In the case of the test room, the radiator was located on internal wall and other 3 walls, floor and ceiling were external ones with  $-22^\circ \text{C}$  outdoor temperature, Fig. 5. In the case of a residential room the radiator was located on external wall with a window and there was also another external wall (two external walls and all other surfaces were internal), Fig. 6. The residential room had exhaust ventilation

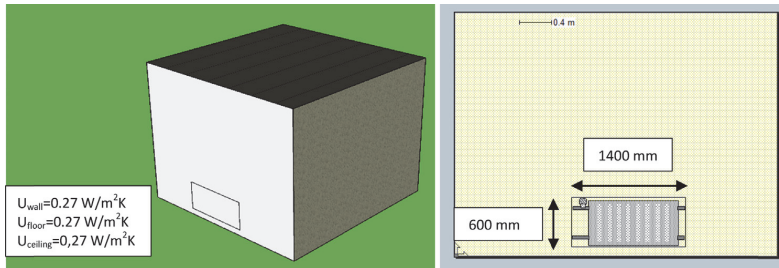


Fig. 5. Simulated EN 442-2 room and the radiator in IDA-ICE model.

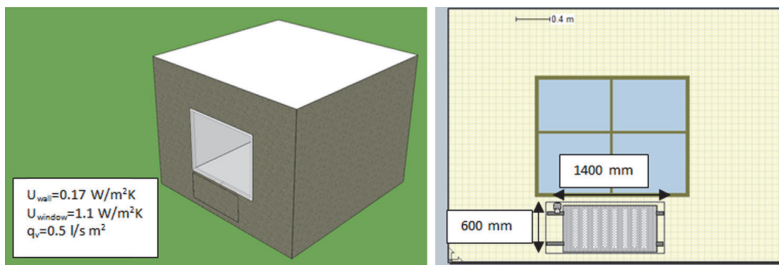


Fig. 6. Simulated residential room and the radiator in IDA-ICE model.

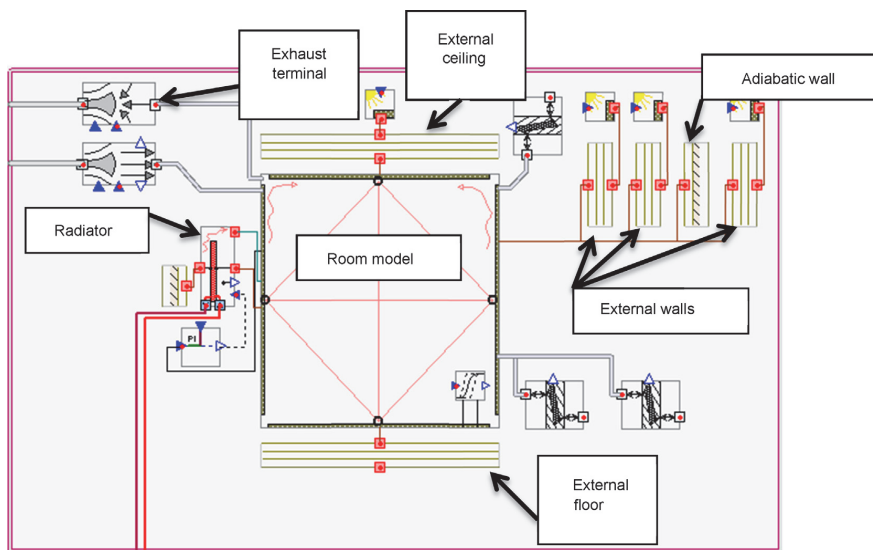


Fig. 7. Lay out of the simulation model of the test room, showing the detailed room model with radiation heat transfer calculation capability, external and internal building envelope elements, the radiator and faces connected to climate processor.

without heat recovery. The layout and components of the test room model are shown in Fig. 7.

IDA-ICE radiator model is a generic radiator model, which calculates heat transfer by convection and radiation from the front panel and the rest of heat emission is an extra convective heat transfer as described with equations below. The front panel surface temperature depends on radiator size, flow temperature and

water mass flow (the latter is typically set by return temperature in the model). Compared to measurements, the same radiator size and flow temperature were used for parallel radiator. To achieve the same front panel surface temperature as measured, slightly higher return temperature was needed to use. In the case of serial radiator we increased also the flow temperature so that the front panel temperature was identical with the measured value. The simulation

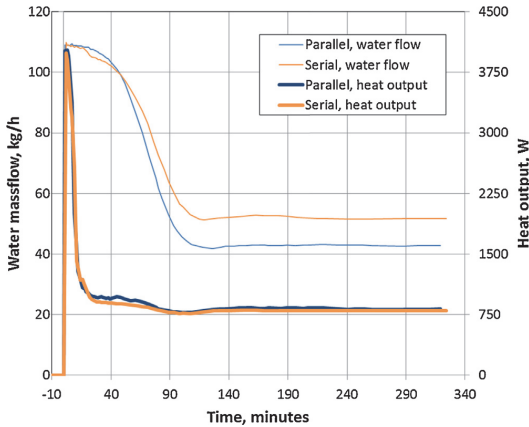


Fig. 8. Test 1 with 50 °C flow temperature: water massflows and heat outputs from water side.

was run at –22 °C outdoor temperature to compare the differences in heat outputs and all year round with Estonian TRY for annual heating energy.

In the water radiator model the leaving water temperature is calculated with the equation [13]:

$$T_{ret} = T_a + (T_{flow} - T_a) \times e^{-((T_{flow}-T_{ret})/\Delta T_{in})} \quad (13)$$

where  $T_{ret}$  is return temperature and  $T_{flow}$  flow temperature. The total heat emission is modelled with the empirical equation:

$$q_{tot} = kl\Delta T_{in}^n \quad (14)$$

where  $k$  is a powerlaw coefficient which depends on the width and type of the radiator,  $W/(mK^n)$  and  $l$  is length of the radiator. The total heat balance for the radiator is:

$$q_{tot} = q_{front} + q_{cr} + q_b \quad (15)$$

where  $q_{front}$  is the heat transfer on the front side of the unit (long wave radiation and convection). This transfer is modelled in the zone model.  $q_{cr}$  is an extra convective heat load, e.g. from the back side and possible fins.  $q_b$  is the heat transfer between the back side of the unit and the facing zone surface.

### 3. Results

#### 3.1. Laboratory measurements at 50 °C flow temperature

Two flow temperatures were used, 50 °C and 70 °C. Both measurement cycles were repeated (Test 1, Test 2) in order to control the repeatability. The thermostat with the set point as close as possible to 20 °C in all tests changed the water flow rate with respective changes in the return water temperature according to the heating need. The same thermostat was used in the measurements for both radiators tested. All test were started with heating up step change which was about 2–3 °C in the room air temperature; initial room temperature (no water flow in the radiator) was about 18 °C. At the start, the water flow was rapidly raised from zero to the nominal value of 109 kg/h which was used in all measurements.

The flow temperature of 50 °C led after the step change to stable operation, where heat output from water flow decreased from about 900 W to 800 W level, corresponding to a situation where internal heat gains are close to 15% of nominal heat output, Fig. 8. Water massflow stabilized to significantly lower level in parallel radiator. Flow and return temperatures, Fig. 9, show that parallel

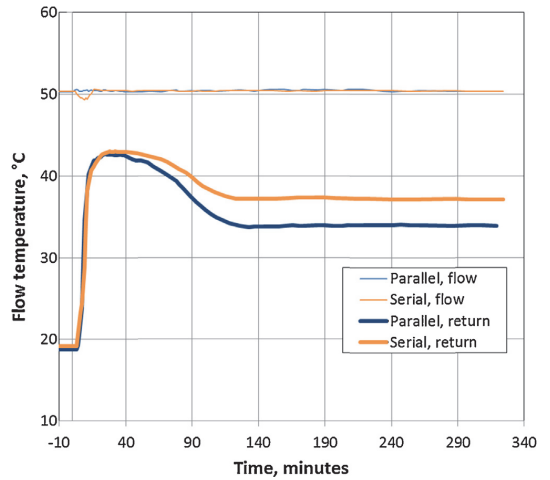


Fig. 9. Flow and return temperatures in 50 °C Test 1.

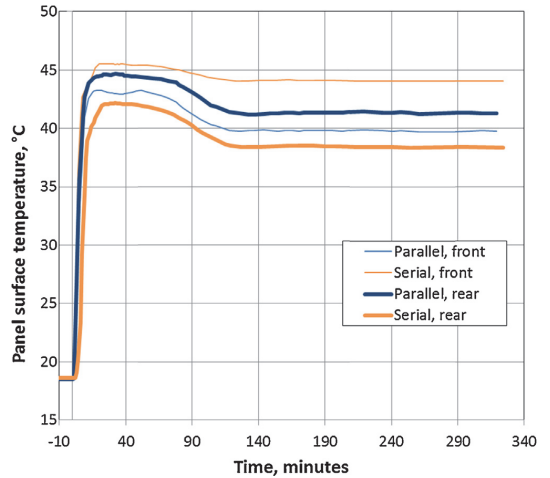


Fig. 10. Front and rear panel surface temperatures in 50 °C Test 1.

radiator operated at significantly lower return temperature on this temperature level. It was estimated that 3% higher heat output of parallel radiator at  $\Delta T$  50 °C increased to about 10% higher heat output at  $\Delta T$  25 °C.

An average front and rear panels surface temperatures (calculated as an average of 5 measurement points) show higher front panel and lower rear panel temperature in the case of serial radiator, Fig. 10. Room air and room cooled surfaces temperature results show that there were not possible to keep exactly the same temperatures in both tests (Fig. 11). Initial temperature ( $t = -10$  min in the figure) was lower in the case of parallel radiator, and the cooled surfaces temperature remained lower during the all test resulting also in the lower air temperature.

Room temperatures were analysed for stabilized period of 130 to 320 min for Test 1. For this period, an average air temperature, cooled surfaces temperature, the mean radiant temperature and operative temperature were calculated, Table 1. The operative temperature was calculated as an average of the air and the mean

**Table 1**  
Room temperatures in 50 and 70 °C tests, all values are in °C. Operative temperatures from 0.6 m height were by 0.02–0.03 °C lower than from 0.75 m height.

	Air ( $T_a$ )	Cooled surfaces ( $T_s$ )	Front panel ( $T_f$ )	Mean radiant ( $T_{rad,mean}$ )	Operative ( $T_{op,0.75\text{ m}}$ )	Operative from globe ( $T_{op,globe}$ )
Parallel 50 °C Test 1	19.98	18.38	39.79	18.79	19.39	19.62
Serial 50 °C Test 1	20.19	18.48	44.08	18.97	19.58	19.82
Parallel 50 °C Test 2	19.88	18.39	38.50	18.78	19.33	19.55
Serial 50 °C Test 2	20.07	18.47	43.15	18.95	19.51	19.74
Parallel 70 °C Test 1	19.69	17.88	40.32	18.31	19.00	19.26
Serial 70 °C Test 1	19.81	17.98	45.63	18.51	19.16	19.43

radiant temperature and was also estimated from the globe temperature as described in Section 2.3. Results show by 0.1 °C lower cooled surfaces temperature in the case of parallel radiator as well as by 0.2 °C lower air and operative temperatures. Operative temperatures estimated from the globe were about 0.2 °C higher, but the differences between the cases were the same.

Because the temperatures were not exactly the same, the cooled room surfaces temperature was adjusted as described in Section 2.3. The adjustment was done in two directions. In the case of parallel 50 °C Test 1,  $T_s$  was changed so that  $T_{op}$  changed from 19.39 to 19.58 °C. Adjusted parallel was then compared with serial having the same operative temperature of 19.58 °C, Table 2. To test the accuracy of the analytical model, serial 50 °C Test 1 was adjusted in another direction, resulting in operative temperature change from 19.58 to 19.39. Adjusted serial was then compared with parallel having the same operative temperature. The adjustment results in Table 2 show the air temperature change of 0.18 °C and cooled surfaces temperature change of 0.20 °C in both cases. Measured heat output 824.9 W of parallel changed to 815.1 W and correspondingly measured heat output 798.7 W of serial changed to 807.3 W. After the adjustment, at equal operative temperatures, the heat output of serial radiator was by 2.0 and 2.1% smaller in these two cases. This 2.0–2.1% equals to heat emission reduction of serial radiator. Analytically calculated net radiation from the front panel of radiators was 120 W and 148 W for parallel and serial, corresponding to 15% and 18% radiation share, respectively. The same procedure was used for 50 °C Test 2. This resulted in the negative reduction of –4.2 to –4.5%, i.e. parallel radiator used less energy. Without adjustments to the same operative temperature, the saving of serial was about 3% and –3% in 50 °C Test 1 and Test 2, respectively, showing the effect of adjustments by about 1%.

The difference between Test 1 and 2 were higher than the declared accuracy of the EN 442-2 test room of  $\pm 1\%$ . A measurement result show very small but continues swings in water flow rates and temperatures, which can explain the differences between Test 1 and 2 indicating that the steady state conditions were not completely achieved because of the use of proportional thermostat with limited control accuracy during the tests.

### 3.2. Laboratory measurements of dynamic performance at 70 °C flow temperature

The tests at 70 °C flow temperature corresponded to oversizing of radiators by about factor 2 (roughly 1600 W vs. 800 W). Initial room temperatures were reasonably close in tests with both radiators which enabled an exact comparison of dynamic response during the heating up step change of about 3 °C. In the case of parallel, initial room air and surface temperatures were about 0.1 °C lower, but parallel radiator reached to the same temperature as serial in 9 min. After that the air temperature curves are almost identical with slightly higher maximum value for parallel at 43 min, Fig. 12. After the heating up phase the thermostat valve was not able to keep stable temperature in both cases because of oversized radiators.

Water massflow and heat output of radiators are shown in Fig. 13. Similar to 50 °C test, parallel showed slightly higher peak power. Return temperature results, Fig. 14, show less superior performance of parallel radiator compared to 50 °C test, where return temperature of parallel radiator was significantly lower. Panel surface temperatures showed similar performance as in 50 °C test, Fig. 15.

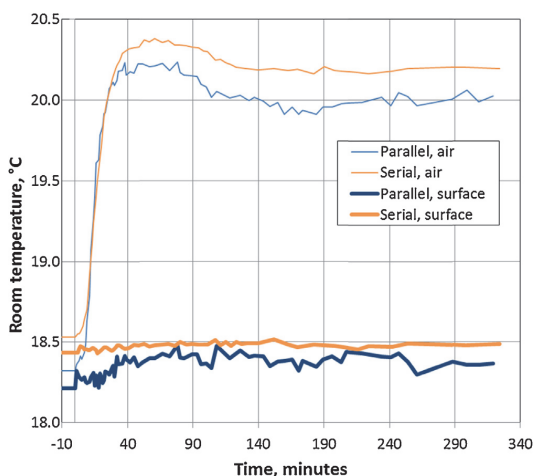


Fig. 11. Room air and cooled surfaces temperatures in 50 °C Test 1.

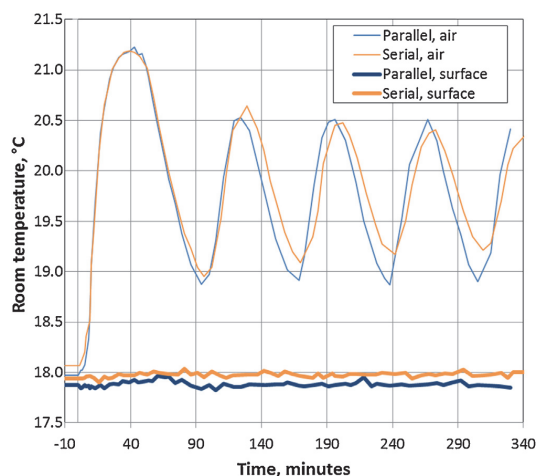
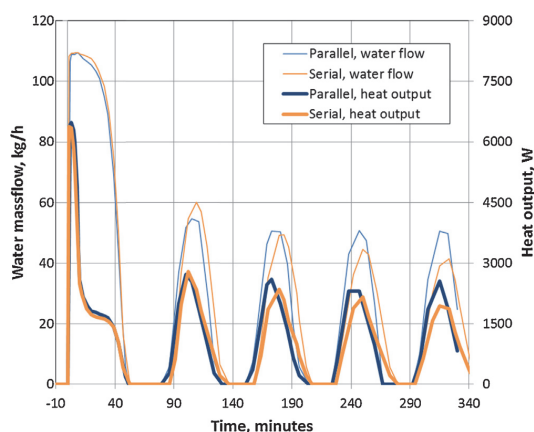
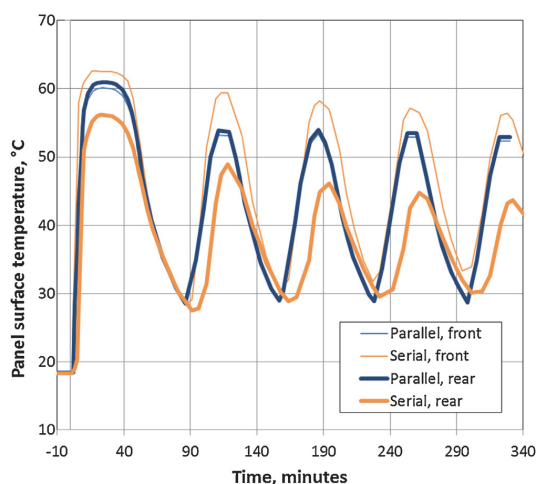
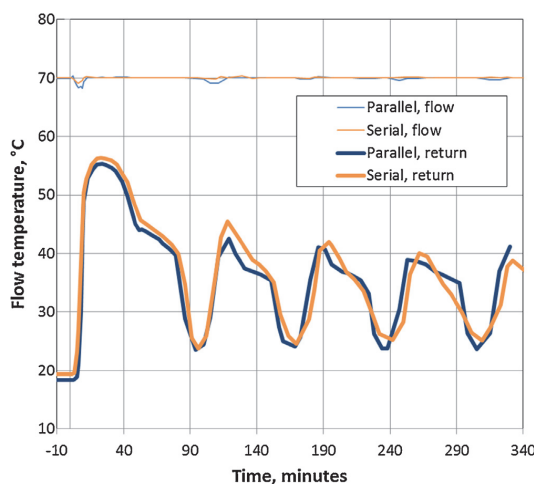


Fig. 12. Dynamic step response of the room air temperature in 70 °C Test 1.

**Table 2**

Analytically calculated adjusted values of temperatures and heat outputs of radiators.

	Test 1 ( $T_{op}$ 19.39 → 19.58)	Test 1 ( $T_{op}$ 19.58 → 19.39)	Test 2 ( $T_{op}$ 19.33 → 19.51)	Test 2 ( $T_{op}$ 19.51 → 19.33)
Air, $T_a$ , adjusted (°C)	20.16	20.00	20.05	19.90
Cooled surf., $T_s$ , adjusted (°C)	18.58	18.28	18.58	18.29
Parallel 50 °C, heat output (W)	815.1	824.9	713.1	722.4
Serial 50 °C, heat output (W)	798.7	807.3	745.0	752.7
Saving of serial (%)	2.01	2.14	−4.48	−4.20

**Fig. 13.** Water massflows and heat outputs from water side in 70 °C Test 1.**Fig. 15.** Front and rear panel surface temperatures in 70 °C Test 1.**Fig. 14.** Flow and return temperatures in 70 °C Test 1.

### 3.3. Simulation results

In the simulation of a residential room described in Section 2.4 a PI controller was used which kept the operative temperature set point of 19.5 °C with high accuracy. In the case of EN 442-2 test room the  $U$ -values were selected so that heat losses were about 800 W at outdoor temperature of  $-22$  °C. The IDA-ICE radiator model provided identical front panel surface temperature for parallel radiator when return temperature was about 6 °C higher than that in the measurements. To achieve the measured front panel temperature of serial radiator the flow temperature was increased to

**Table 3**Simulation results of EN 442-2 test room described in Section 2.3. All values at  $-22$  °C outdoor temperature.

	Parallel	Serial
Flow temperature (°C)	50.0	57.6
Return temperature (°C)	39.8	43.4
Front panel surface temperature (°C)	39.8	44.1
Rear panel surface temperature (°C)	39.8	44.1
Air temperature (°C)	20.69	20.58
Front panel $q_{front}$ (W)	178.7	227.1
Convection $q_{cr}$ (W)	624.7	576.2
Back side $q_b$ (W)	0	0
Total heat output $q_{tot}$ (W)	803.4	803.3

57.6 °C. With these settings, the front panel surface temperatures were the same as in the measurements for both radiators and the simulation resulted in the air temperatures of 20.69 °C and 20.58 °C for parallel and serial cases, respectively, as well as nearly the same heat emission of radiators, [Table 3](#).

In the case of a residential room, the input data used resulted in slightly smaller heat losses of about 630 W compared to 800 W of the laboratory tests. At outdoor temperature of  $-22$  °C, the model provided identical front panel surface temperature for parallel radiator roughly at the same flow temperature of 53 °C (vs. 50.5 °C in the measurements). To achieve the measured front panel surface temperature of serial radiator the flow temperature was increased to 58.7 °C. With these settings the rear panel surface temperatures were not correct, as can be seen from [Table 4](#). To achieve measured rear panel temperatures another simulations were run with corrected flow temperatures and the back side heat transmission from these simulations were used to correct the total heat emission of the radiator (having an effect of 0.2–0.8 W as can be seen from [Table 4](#)).

**Table 4**  
Simulation results of a residential room described in Section 2.3. All values are at  $-22\text{ }^{\circ}\text{C}$  outdoor temperature, except the annual energy use.

	Parallel	Serial
Flow temperature ( $^{\circ}\text{C}$ )	53.0	58.7
Return temperature ( $^{\circ}\text{C}$ )	38.3	43.1
Front panel surface temperature ( $^{\circ}\text{C}$ )	39.9	44.1
Rear panel surface temperature ( $^{\circ}\text{C}$ )	39.9	44.1
Air temperature ( $^{\circ}\text{C}$ )	19.61	19.48
Flow temperature for backwall correction ( $^{\circ}\text{C}$ )	57.7	53
Rear panel surfaces temperature at corrected flow temperature ( $^{\circ}\text{C}$ )	41.4	38.4
Front panel $q_{\text{front}}$ (W)	179.2	227.7
Convection $q_{\text{cr}}$ (W)	446.8	396.8
Back side $q_b$ (W)	8.6	9.2
Corrected back side $q_{b,\text{corrected}}$ (W)	8.8	8.4
Total heat output $q_{\text{tot}}$ (W)	634.6	633.7
Corrected total heat output $q_{\text{tot}}$ (W)	634.8	632.9
Annual heating energy use $\text{kWh}/(\text{m}^2 \text{ a})$	64.9	64.5

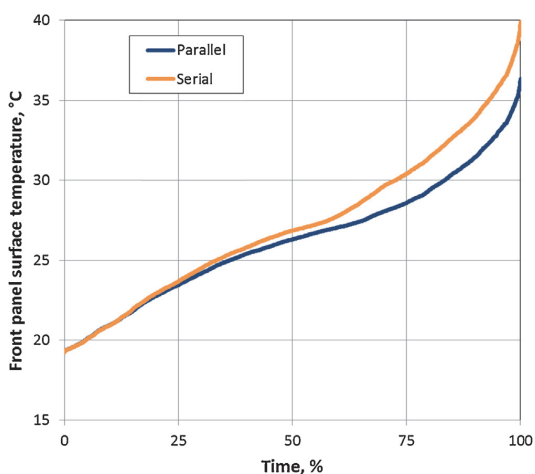


**Fig. 16.** Duration curve of the radiator front panel surface temperatures (100% = 8760 h).

Simulated heat outputs show the difference of 1.9 W corresponding to the saving of 0.3% by serial radiator. In annual energy simulation serial radiator provided heating energy saving of 0.7% and slightly higher front panel surface temperature as shown in Fig. 16. The maximum room air temperature difference appeared at  $-22\text{ }^{\circ}\text{C}$  outdoor temperature, 19.61 and 19.48  $^{\circ}\text{C}$  in the case of parallel and serial radiator, respectively.

The difference between simulated EN 442-2 test room and a residential room results (no saving vs. 0.3% saving of serial) shows the effect of cold surfaces in the room. In EN 442-2 test room the radiator faces 5 cold surfaces, and the higher surface temperature of serial radiator increased the radiant temperature (the air temperature was lower in the simulation at fixed operative temperature setpoint), but this did not provide any energy saving because of more intensive radiation heat exchange. In the case of a residential room, the radiator on external wall faces mainly internal walls and floors and the effect of higher radiator front panel and radiant temperatures resulted in quantifiable energy saving of 0.3%. These results indicate that EN 442-2 test room with cooled surfaces is radiator type neutral, i.e. radiators with higher convection or radiation share will provide similar heat emission at fixed operative temperature.

## 4. Conclusions

Laboratory measurements were conducted for the same size and type radiators with parallel and serial connected panels in EN 442-2 test room to quantify the possible heat emission difference and energy saving of the radiator with serial connected panels. With analytically modelled heat transfer in the room small temperature differences were recalculated and the comparison was conducted at exactly the same operative temperature. Additionally the performance was analysed with dynamic simulation which had limitations in the radiator model, but allowed to model the radiator surface temperature according to the measurement results.

Laboratory measurements at 50  $^{\circ}\text{C}$  flow temperature showed in the first test 3% lower and in the second test 3% higher heat emission of serial radiator. Final, recalculated results at the same operative temperature showed by 2% lower and by 4% higher heat emission of serial radiator in these test, respectively. The differences between the tests were higher than the declared accuracy of the EN 442-2 test room of  $\pm 1\%$  and were caused by very small but continuous swings in water flow rates and temperatures which may be attributed to the limited accuracy of the proportional thermostat used. Therefore, the measurement setup used did not reach the complete steady state and was not able to quantify the differences between tested radiators, however indicating that these differences were very small if they existed at all.

Simulated results for EN 442-2 test room with front panel surface temperatures of radiators identical to the measured values showed 0.11  $^{\circ}\text{C}$  lower air temperature in the case of serial radiator, but exactly the same heat emission of both radiators, because of more intensive radiation heat exchange in the case of serial radiator. Simulated results for a typical residential room showed by 0.3% smaller heat emission at design outdoor temperature and by 0.7% smaller annual heating energy use in the case of serial radiator. Therefore the radiator on external wall with higher front panel temperature as well as higher radiant temperature in the room resulted in quantifiable energy saving as the radiator mainly faced internal surfaces. This approved the importance of radiant temperature as phenomena, but in terms of energy savings there was no considerable difference between studied radiators with parallel and serial connected panels.

Serial radiator had 4  $^{\circ}\text{C}$  higher temperature of the front panel that resulted in slightly higher radiation share, 18% relative to 15% for parallel radiator in 50  $^{\circ}\text{C}$  test. The rear panel temperature of serial radiator was by 3  $^{\circ}\text{C}$  lower that may have some energy saving effect in the case of poorly insulated walls.

Parallel radiator showed slightly faster dynamic response and higher heat output which resulted slightly faster heating up time. By 3% higher heat output of parallel radiator at  $\Delta T 50\text{ }^{\circ}\text{C}$  increased to about 10% higher heat output at  $\Delta T 25\text{ }^{\circ}\text{C}$  which gives some advantage to parallel radiator in low temperature heating systems.

## Acknowledgments

The research was supported by the Estonian Research Council, with Institutional Research Funding grant IUT1-15, and with a grant of the European Union, the European Social Fund, Mobilitas grant no MTT74.

## References

- [1] EN 15316-2-1:2007, Heating Systems in Buildings Method for Calculation of System Energy Requirements and System Efficiencies Part 2-1: Space Heating Emission Systems, CEN, Brussels, 2007.
- [2] B.W. Olesen, M. de Carli, Calculation of the yearly energy performance of heating systems based on the European building energy directive and related CEN standards, Energy and Buildings 43 (2011) 1040–1050.

- [3] H. Sauter, Leistungsminderung bei Heizkörperverkleidungen, 1985, HLH-Heizung Lüftung/Klima Haustechnik, Bd. 36. Nr.4.
- [4] M. Maivel, J. Kurnitski, Low temperature radiator heating distribution and emission efficiency in residential buildings, *Energy and Buildings* 69 (2014) 224–236.
- [5] Hasan, J., Kurnitski, K., Jokiranta, A. A combined low temperature water heating system consisting of radiators and floor heating, *Energy and Buildings* 41 (2009) 470–479.
- [6] ISO 7730:2005, Ergonomics of the Thermal Environment. Analytical Determination of Thermal Comfort by Using Calculations of the PMV and PPD Indices and Local Thermal Comfort Criteria, ISO, Geneva, 2005.
- [7] Description of Kermi GmbH serial panel radiators – <http://www.kermi.com/EN/Heiztechnik/therm-x2.Flachheizkoerper/Warum.x2/Energieeinsparung/index.phtml>
- [8] EN 442-2:1996/A2:2003, Radiators and Convectors—Part 2: Test Methods and Rating, CEN, Brussels, 2003.
- [9] EN 215:2004, Thermostatic Radiator Valves—Requirements and Test Methods, CEN, Brussels, 2004.
- [10] R.D. Watson, K.S. Chapman, *Radiant Heating and Cooling Handbook*, McGraw-Hill, New York, NY, 2002.
- [11] ISO 7726:1998, Ergonomics of the Thermal Environment. Instruments for Measuring Physical Quantities, ISO, 1998.
- [12] IDA-ICE, *IDA Indoor Climate and Energy 4.6, manual* - <http://www.equa.se/deliv/ICE45eng.pdf?lic=ICE40:4812>
- [13] A. Bring, P. Sahlén, M. Vuolle, IEA SHC Task 22-Subtask B—Models for Building Indoor Climate and Energy Simulation, KTH, Stockholm, 1999.



## PAPER III

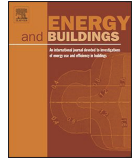
Maivel, M.; Kurnitski, J. (2015). Heating System Return Temperature Effect on Heat Pump Performance. *Energy and Buildings*, 94, 71-79.





Contents lists available at ScienceDirect

## Energy and Buildings

journal homepage: [www.elsevier.com/locate/enbuild](http://www.elsevier.com/locate/enbuild)

## Heating system return temperature effect on heat pump performance

Mikk Maivel<sup>a,\*</sup>, Jarek Kurnitski<sup>a,b</sup><sup>a</sup> Tallinn University of Technology, Tallinn, Estonia<sup>b</sup> Aalto University, School of Engineering, Espoo, Finland

## ARTICLE INFO

## Article history:

Received 6 September 2014

Received in revised form 2 January 2015

Accepted 18 February 2015

Available online 26 February 2015

## Keywords:

Heat pump

Seasonal performance factor

Radiator heating

Condenser model

Return temperature

## ABSTRACT

In this paper the heating system return temperature effect on condensing temperature and the seasonal performance factor of the heat pump was measured and quantified with analytical model, IDA-ESBO detailed simulation with heat pump model and by correlation equation derived from laboratory measurements. Results show that the calculation with derived condensing temperature correlation stressed the effect of relatively low return temperature in a radiator heating system and provided about 9% higher SPF value, compared to analytical and IDA-ESBO model. Four studied heat pump connection schemes resulted in a range of SPF values of 3.72–4.21, where the highest SPF was achieved with direct connection of heat pump and heating system, which had the lowest return water temperature. Additionally a hand calculation based on hourly heating energy needs and estimated return temperature was tested. This estimation resulted in 4.5% lower SPF value, showing the importance to use correct return temperature corresponding to actual flow rates in radiators. The results of this study indicate that calculation procedures, which do not calculate the return temperature and use simple assumptions in the condensing temperature calculation may lead to underestimation of SPF by more than 10% in the case of radiator heating.

© 2015 Elsevier B.V. All rights reserved.

## 1. Introduction

Heat pump heating systems are popular and widely used for preparing domestic hot water and space heating in all over the Europe especially in Nordic countries. According to statistics buildings account for 40% of CO<sub>2</sub> emissions in central Europe [1]. Heat pumps are being considered as one possible solution to reduce primary energy consumption and have often been proposed as a substitute for conventional systems (electric, gas boilers, oil boilers, etc.) to produce domestic hot water and space heating [2]. Especially in colder climates or in the case of higher heating needs, heat pumps have been seen financially attractive because of reasonably short payback periods [3].

As a common solutions heat pump is connected with floor heating system where temperature curve is lower than in conventional

radiator heating system. According to recent study in low-energy buildings it is also possible to use low temperature radiator heating system [4] with heating curves only by 5 °C higher compared to floor heating. Radiator system temperature drop is typically higher in sizing as well in operation compared with floor heating and it ensures lower return water temperature, having an effect on heat pump performance quantified in this study. In sizing, typical temperature drops are 15–20 °C in conventional radiator heating system, 10–15 °C in low temperature radiator heating and 5–10 °C in underfloor heating system. Most of existing heat pump models and software do not consider return water temperature effect on COP, because that would require dynamic heat output and flow rates calculation in the building that can be done with dynamic simulation tools, and simple condenser model assumption are of the used. Therefore such models not calculating the actual return temperature are more suitable for floor heating systems where temperature differences are smaller. All heat pump models make some assumptions and simplifications. Scarpa has considered that there are three main types of approaches: numerical approximation; general thermodynamic and detailed approach. Most detailed approaches achieve an accuracy of less than 10% [5]. In this paper, general thermodynamic approach was used. From literature, many models and calculation approaches of heat pump performance can be found, but most of them have made simplifications mostly in

*Abbreviations:* COP, coefficient of performance; SPF, seasonal performance factor;  $T_1$ , condensing temperature (K);  $T_2$ , evaporation temperature (K);  $T_{11}$ , return temperature (K);  $T_{12}$ , flow temperature (K);  $\eta$ , exergy efficiency;  $\phi$ , produced heating and/or cooling energy by heat pump (kWh/a);  $P$ , used electrical energy for producing heating or cooling energy (kWh/a).

\* Corresponding author at: Ehitajate tee 5, 19086 Tallinn, Estonia.

Tel.: +372 56461251.

E-mail address: [mikk.maivel@ttu.ee](mailto:mikk.maivel@ttu.ee) (M. Maivel).

<http://dx.doi.org/10.1016/j.enbuild.2015.02.048>  
0378-7788/© 2015 Elsevier B.V. All rights reserved.

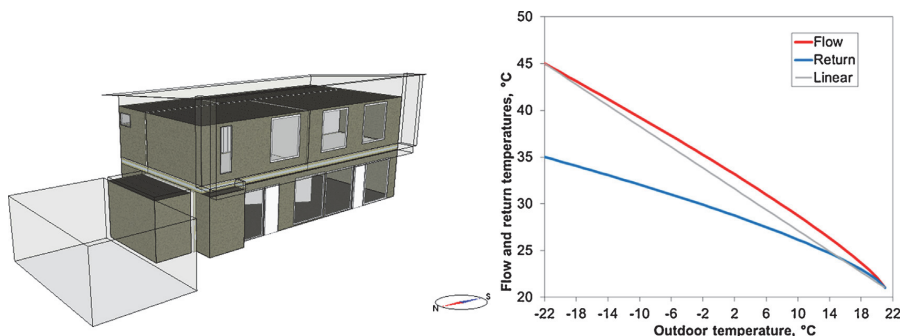


Fig. 1. Analyzed building 3D view (left) and heating curve 45/35 °C (right).

consumption side [6], i.e. it is complicated to model accurate consumption and inlet-outlet temperatures. Or alternatively, models describe steady state calculations like specified in standards [7].

Heat pump COP is influenced by working mode, i.e. space heating or preparing domestic hot water. This paper will concentrate on space heating mode therefore energy need for space heating is dynamic process; energy need for domestic hot water is influenced by usage profile. Heat pump performance testing is described in EN14511-2 [8] and ISO 5151:2010 [9]. IEA HPP (International Energy Agency Heat Pump Program) has launched Annex 28 to compare different standards [10]. Karlsson work under IEA HPP Annex 28 include heat pump tests by both EN standards and it resulted that the former standard EN 255-2 [11] gives higher COP values compared to EN 14511-2 due to mass-flows that were not defined in EN 255 and it resulted in unrealistic low inlet condensing temperatures in a few testing points. According to the EN 14511-2 heat pumps were tested at standard rating conditions temperature difference of 5 °C (for outlet temperature up to 45 °C). Karlsson's test results show like earlier studies [12] that heat pump COP is influenced by condenser inlet temperature (i.e. lowering return water temperature will increase heat pump performance). Evidently the temperature difference of 5 °C used in testing of heat pumps underestimates the performance for radiator heating systems quantified in this study. For instance Nyers have calculated by steady-state mathematical model that the condenser performance increases by 1.9 times if the inlet water temperature decreases from 50 °C to 20 °C [13].

In this paper it is shown with a whole building dynamic simulation model including radiator heating system with heat pump the condenser inlet temperature impact on heat pump SPF on annual basis. Laboratory measurements were conducted to quantify this effect against the condenser model. Applying the derived condensing temperature correlation equation in the simulations the effect of large temperature drops in a radiator heating systems and the effect of studied connection schemes was quantified.

## 2. Methods

A set of laboratory measurements was conducted to measure heat pump performance as a function of the return temperature. In modeling, two methods were used to calculate the heat pump performance as a function of heating system flow/return temperatures. In first step dynamic simulation were conducted with an existing heat pump model of IDA-ICE simulation software. In second step, an improved model based on laboratory measurements and the correlation derived was used to calculate heat pump seasonal performance ratio with actual heating system

flow/return temperatures. Four connection schemes of the heat pump were analyzed with dynamic simulations based on these methods.

### 2.1. Dynamic model of heat pump heating system

Analyzed building was typical recently built detached house, which has been chosen in earlier study for reference building in Estonian cost optimal calculations [14]. Investigated building is two-story with heated area of 178 m<sup>2</sup>. Building has three bedrooms, sauna and living room together with kitchen (Fig. 1, left). Main building elements thermal transmittance values are presented in the Table 1. Room air set-point temperature during analyze was 21 °C. Heating system supply water temperature is outdoor air temperature compensated, i.e. the supply water temperature increases as the outdoor temperature decreases. Low-temperature radiator heating system has simulated with heating curve of 45/35 °C (Fig. 1, right). There is no cooling system in the building. Mechanical supply and exhaust ventilation system with heat recovery (temperature efficiency up to 80%; exhaust temperature limit 0 °C and supply air temperature during the winter +18 °C) was used. All energy calculation input data follows the Estonian regulation of minimum requirements for energy performance [15].

Detailed overview about dynamic heating system simulation model can be found in previous paper [4]. Standard plant model were replaced to IDA ESBO plant model, which include heat pump model [16]. IDA-ESBO have more advanced plant models than that of IDA-ICE, including possibility to model different heat pumps, solar panels, wind turbines, stratification tanks, etc. In current work IDA-ESBO plant model was integrated to the IDA-ICE in the advanced level. Selected heat pump is a residential on-off type pump with variable condensing temperature with working fluid R407C. Main parameters of investigated heat pump used in mathematical model of calculating heat pump seasonal performance are shown in Table 2. In radiator heating system equipped with thermostatic valves the water flow fluctuates a lot, resulting in a temperature drop which is much higher compared steady-state standard heat pump testing value of 5 °C temperature difference

Table 1  
Thermal transmittance values for main building envelope elements.

No.	Building envelope element	U-value (W/(m <sup>2</sup> K))
1	Exterior wall	0.17
2	Roof	0.14
3	Ground floor	0.17
4	Windows (g=0.5)	0.8

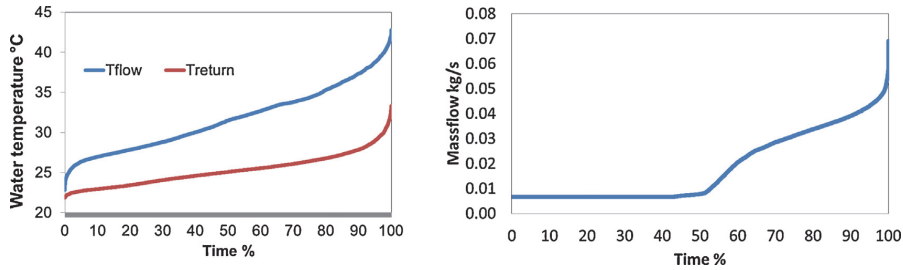


Fig. 2. Temperature drop (flow and return) duration curves in radiator heating system (left) and annual mass flow duration curve in space heating circuit (right). 100% = 8760 h.

(Fig. 2 (left)). Constant pressure circulation pump were used in all simulation cases and annual mass-flow in space heating circuit is shown in Fig. 2 (right). Mass-flow and temperature values in Fig. 2 where computed with IDA-ICE.

2.2. Connection schemes

Manufactures recommend connection scheme depending on the usage profile, consumption and working mode, etc. In this study four most used types of connection schemes were analyzed. In first step Connection No. 1 (Fig. 3) where on-off type ground source heat pump with working fluid R407C was connected to the heating system through stratification tank were modeled in IDA-ESBO simulations. This connection has three circulation pumps (between ground loop and evaporator; condenser and stratification tank and for space heating system). Stratification tank should have additional top-up heater because heat pumps often have sized to cover approximately 60% of heating power at design outdoor temperature [17], but in this study the heat pump was sized to cover 100% of building heating need at design outdoor temperature which is in Tallinn -22 °C (in simulations additional top-up heater was neglected).

Connection No. 2, 3 and 4 are also popular in domestic solutions. Connection No. 2 is a direct Connection, No. 3 has a bypass and in No. 4 is additionally a tank increasing the system water volume, which helps on-off operation of the heat pump. No 1 was both simulated with IDA-ESBO plant and calculated analytically. Connections 2, 3 and 4 were then analyzed with verified analytical formulas. Heating system hourly flow/return temperatures were simulated with IDA-ICE simulation model with detailed radiator heating system, and the effect of direct calculation from the heating curve was also tested.

2.3. Basic equations

The efficiency of heat pump can be expressed with the COP, which is the quotation between the useful heating capacity and the power input (Eq. 1). The theoretical upper limit for the COP of a heat pump operating between the condensation temperature and

evaporation temperature is expressed by the Carnot coefficient of performance. The real COP should consider the compressor power factor or exergy efficiency (Eq. 2).

$$COP_c = \frac{Q_1}{W} = \frac{T_2}{T_1 - T_2} + 1 \tag{1}$$

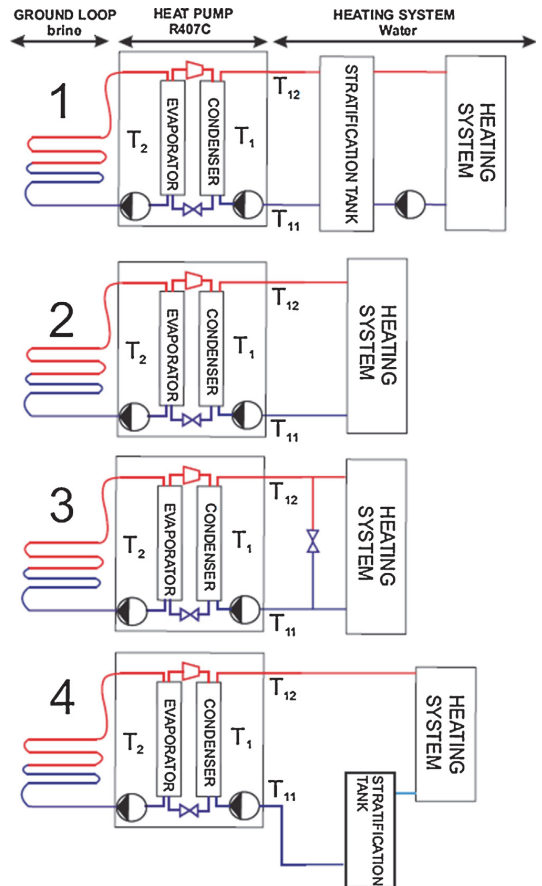


Fig. 3. Calculation schemes (E, evaporator; C, condenser; ST, stratification tank; SHS, space heating system).

Table 2  
Basic information about heat pump.

Power	5 kW
$\Delta t_{log,eva}$	8 °C
$\Delta t_{log,cond}$	8 °C
$t_{brine,in}$	0 °C
$t_{brine,out}$	-3 °C
$t_{water,in}$	30 °C
$t_{water,out}$	35 °C
$COP_{test,conditions}$	4.3

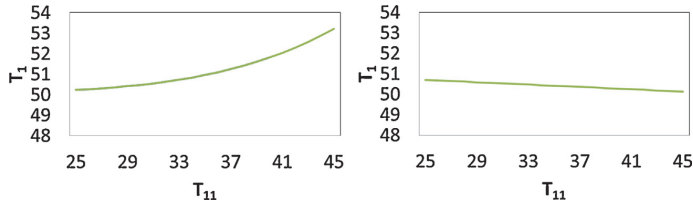


Fig. 4. Dependency between return and condensing temperature in the case of constant power of 1000 W (left) and constant mass-flow (right) of 0.012 kg/s at constant flow ( $T_{12}$ ) temperature of 50 °C.

$COP_c$  is Carnot coefficient of performance;  $Q_1$  is a useful heating capacity (W),  $W$  is a power input (W);  $T_1$  is a condensing temperature (K);  $T_2$  is an evaporating temperature (K).

$$COP_r = COP_c * \eta \quad (2)$$

$COP_r$  is heat pump coefficient of the performance;  $\eta$  is exergy efficiency, which is in a range of 0.4–0.6 for conventional domestic water/water heat pumps [18] 0.3–0.4 for air/water heat pumps and 0.15–0.3 for air/air heat pumps. [7].

Heat pump seasonal performance factor SPF was calculated with Eq. (3).

$$SPF = \frac{\phi}{P} \quad (3)$$

where  $\phi$  is produced heating and/or cooling energy by heat pump (kWh/a),  $P$  is used electrical energy for producing heating or cooling energy (kWh/a) (circulation pumps were included).

#### 2.4. IDA-ESBO simulation

In ordinary heat pump selection programs the condensing temperatures are often calculated from condenser outlet temperature (heating system flow temperature). IDA-ESBO heat pump model includes physical models of heat exchangers. Water-side heat balance is given with Eq. (4) and heat exchanger with Eq. (5). These equations allow to derive condensing temperature Eq. (6).

$$Q_{\text{evap/cond}} = m * C_p * (T_{12} - T_{11}) \quad (4)$$

$Q_{\text{evap/cond}}$  is heat flux from heat exchanger (condenser or evaporator) W;  $m$  is mass flow in space heating circuit kg/s;  $C_p$  is specific heat of water (J/kgK);  $T_{11}$  is return water temperature from space heating circuit K;  $T_{12}$  is flow water temperature to space heating circuit K.

$$Q_{\text{evap/cond}} = U * A * \frac{(T_{12} - T_{11})}{\ln(T_1 - T_{11}) / (T_1 - T_{12})} \quad (5)$$

$U$  is condenser heat transfer coefficient  $W/(m^2K)$ ;  $A$  is condenser area  $m^2$ ;  $T_1$  is condensing temperature K.

$$T_1 = T_{11} + \frac{T_{12} - T_{11}}{(1 - \text{EXP}(-U * A / m * C_p))} \quad (6)$$

Eq. (6) is illustrated in Fig. 4 showing the dependency between heating system return ( $T_{11}$ ) and condensing ( $T_1$ ) temperature at constant flow temperature of 50 °C in the case of constant power (Fig. 4 (left)) and constant mass-flow (Fig. 4 (right)).

$U * A$  characterize heat exchanger and it varies in a time step. IDA-ESBO calculates it on hourly bases with the Eq. (7).

$$U * A = \frac{Q_{\text{evap/cond}}}{\Delta t_{\text{log.cond.}}} = \frac{m * C_p * (T_{12} - T_{11})}{\Delta t_{\text{log.cond.}}} \quad (7)$$

$\Delta t_{\text{log.cond.}}$  is a condenser logarithmic temperature difference which characterize heat exchanger, usually given as a constant value from heat pump producer but IDA-ESBO heat pump model

calculates it for every time step. IDA-ESBO calculates condensing temperature compared to equation 6 in slightly different format as shown in Eq. (8).

$$\begin{aligned} T_1 &= T_{11} + \frac{T_{12} - T_{11}}{(1 - \text{EXP}(-U * A / m * C_p))} \\ &= T_{11} + \frac{T_{12} - T_{11}}{1 - \text{EXP}(-m * C_p * (T_{12} - T_{11}) / m * C_p \Delta t_{\text{log.cond.}})} \\ &= T_{11} + \frac{T_{12} - T_{11}}{1 - \text{EXP}(-T_{12} - T_{11} / \Delta t_{\text{log.cond.}})} \end{aligned} \quad (8)$$

#### 2.5. Hand calculations with measured correlation

In real heat pump working process condensing temperature is not conditionally constant, i.e. heat exchanger heat transfer is a dynamic process. A correlation was derived for condensing temperature as a function of flow and return temperature. For that purpose laboratory measurements were conducted for domestic on-off type brine to water heat pump with variable condensing at constant flow temperature and heat pump heating capacity for four different return temperatures. In addition, previous measurements of IEA Annex 28 test results were utilized to expand the measured data set.

### 3. Results

Results are presented in two main sections. The first part contains description of the model and its features such as comparison of part-load effect and stratification tank. Beside that this chapter includes seasonal coefficient of performance value calculations with IDA-ESBO plant model, dynamic simulation and SPF calculation with simplified formulas (Eq. 1–8) for connection scheme No 1.

The second part covers the derivation of variable condensing temperature correlation equation from laboratory test measurement and SPF calculation for different connection schemes (Fig. 3).

#### 3.1. IDA-ESBO heat pump simulation

This chapter aim is to give an overview of about IDA-ESBO simulation model and its results via Connection No. 1. Similar approach has been used by Salvalai who made parameter estimation of heat pump model in IDA ICE environment, but his model was a simplified one based on producers performance maps and was not the same that IDA-ESBO current model with more detailed properties [19].

#### 3.2. Stratification tank

IDA-ICE heat pump model was run via stratification tank. Tank model include tank with its dimensions and volume. Tank has heat

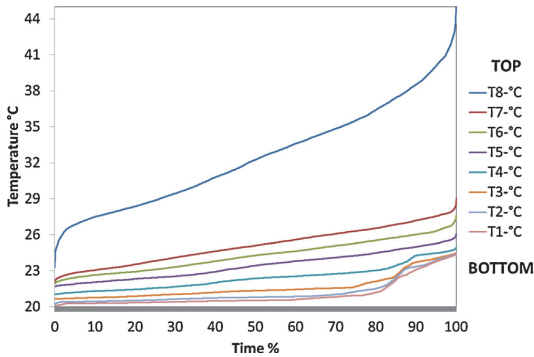


Fig. 5. Duration curve of stratification tank layer temperatures. 100% = 8760 h.

losses and the model has possibility to set the number of layers and a fill ratio. By default fill ratio is 0.2 (i.e. 20% of all water is heated to the highest set-point). Simulated tank stratification with eight layer temperatures is shown in Fig. 5.

Layer 8 is the temperature on the top of the tank and shows the flow temperature to the heating system. Tank is connected only with a space heating system, i.e. domestic hot water heating is neglected in this study.

### 3.3. Part load effect for heat pump performance

IDA-ESBO library has on-off type heat pump [15]. However, it may be operated as a capacity controlled heat pump. According to previous studies variable speed heat pump improved energy performance in the range of 10–25% [16] due to lower condensing temperatures and fewer on/off cycles with variable-speed pump compared to intermittent control. On the whole part-load helps to increase heat pump life expectancy and the ability to extend the operating range of compressor provide an opportunity to reduce the need for supplementary heat in Nordic climates, where supplementary heat is necessary. IDA-ESBO simulation results showed that variable speed control helped to achieve 13% of higher SPF than simple on-off control (SPF with on-off control was 3.07 and with variable speed 3.48 respectively). In part load working mode condenser mass-flow is lower than in on-off working mode (Fig. 6).

### 3.4. Constant refrigerant temperature heat exchanger—calculation with simplified formulas

For making hand calculations with Eqs. 1 and 2, heat pump annual performance was first calculated with IDA-ESBO simulation. Hourly exergy efficiency  $\eta$  values calculated with IDA-ICE simulation results and Eq. (2) were in the range of 0.50...0.63 with an average efficiency value of  $\eta = 0.57$ . In Fig. 7 corresponding hourly COP values of IDA-ESBO simulation; Carnot ideal process with equation 1 (evaporating and condensing temperature from

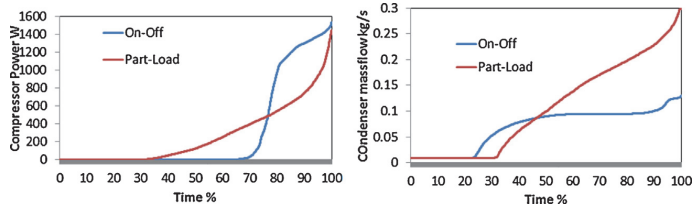


Fig. 6. Duration curve of compressor power (left) and condenser mass-flow (right) in on-off and part load working mode. 100% = 8760 h.

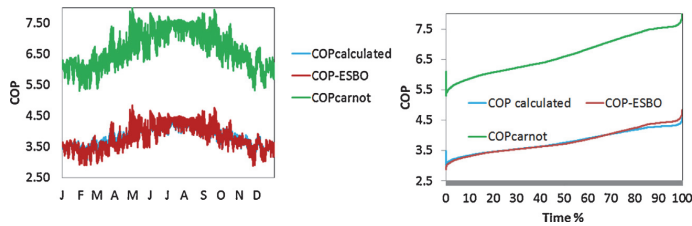


Fig. 7. Hourly COP values (left) and the duration curve (right), calculated with simulated evaporating and condensing temperatures. 100% = 8760 h.

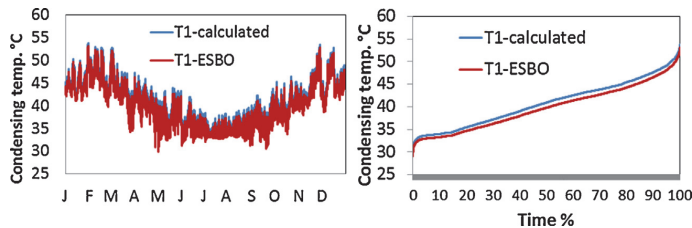


Fig. 8. Hourly condensing temperature (left) and the duration curve (right), calculated with equation 8 compared to IDA-ESBO results. 100% = 8760 h.

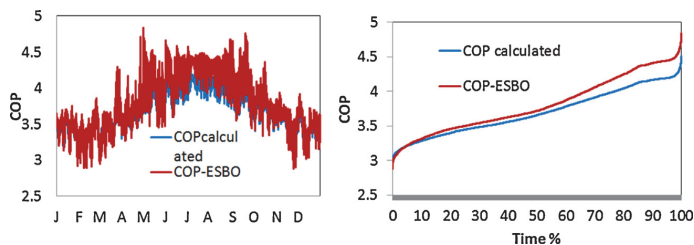


Fig. 9. Comparison of IDA-ESBO COP values with hand calculation (left-hourly values and right the duration curve of COP values). 100%=8760 h.

IDA-ICE results) and hand calculated with Eq. (2) with heat pump efficiency of 0.57 are shown.

Results in Fig. 7 show that hand calculation with constant heat pump efficiency value of 0.57 gave accurate results on annual bases. In next step, the condensing temperature was calculated with equation 8 from flow/return temperatures, and the result was compared to IDA-ESBO condensing temperature in Fig. 8.

Hand-calculated and IDA-ESBO results were very close, IDA-ESBO simulation provided average condensing temperature of 39.8 °C and hand calculation 40.7 °C. Slight difference was caused by logarithmic temperature difference, which IDA calculates dynamically for every hour, but in hand calculation constant  $\Delta t_{\log, \text{cond}} = 8$  °C from the Table 2 was used.

From calculated hourly condensing temperatures, hourly COP values were calculated with an average constant evaporating temperature of  $-8$  °C. Calculating the COP with the exact evaporating temperature values (from IDA-ESBO results) gave the annual SPF of 0.3% lower compared to simplified hand calculation with constant evaporating temperature (3.38 vs. 3.39 respectively). All further calculations include constant evaporating temperature assumption of  $-8$  °C. Fig. 9 describes the difference of IDA-ESBO simulated hourly COP values from hand calculated COP showing an annual

average value of 3.80 vs. 3.69 respectively. Such a slight difference ( $\sim 2.8\%$ ) in COP values resulted in the seasonal coefficient of performance being 3.48 in IDA-ESBO simulation and 3.39 in hand calculation (the difference  $\sim 2.6\%$ ). This shows that hand-made calculation with several constant values with equation 3 is reasonably accurate and gives almost the same values as IDA-ESBO simulation (for hand calculation, it was necessary to use simulated hourly heating system return temperature for calculating condensing temperature).

### 3.5. Calculation based on laboratory measurements

#### 3.5.1. Condensing temperature correlation

Laboratory measurements data was used to describe the measured condensing temperature as a function of heating system flow/return temperatures with simple correlation equation. Results of the laboratory measurements for a wide range of return temperatures are shown in Table 3. Because we had limited number of measurements, in addition IEA Annex 28 [10] measurement results were used (Table 4).

Test results show that the lower return temperature decreased the condensing temperature resulting in higher  $\text{COP}_{\text{carnot}}$  (Table 3).

Table 3  
Laboratory measurement results ( $T_2$  – evaporating temperature °C) of the heat pump performance.

	$T_1$	$T_2$	$\text{EER}_{\text{Carnot}}$	$\text{EER}_{\text{lab. measure}}$	$\eta$	$T_{11}$	$T_{12}$	Avg. kW	Volume flow l/s	$U^*A_{\text{radiator}}$
Case 1	45.06	−6.98	5.11	2.31	0.45	29.64	49.62	8.09	0.36	0.45
Case 2	46.98	−6.69	4.96	2.15	0.43	35.38	50.05	7.94	0.48	0.36
Case 3	48.67	−6.64	4.82	1.97	0.41	40.15	49.98	7.79	0.7	0.31
Case 4	50.88	−6.87	4.61	1.81	0.39	44.99	50.01	7.56	1.33	0.28

Table 4  
IEA Annex 28 [5] measurement results used in this study.

Heating water out °C	50	35	45	55	35	35.1	55	45	50	50
Heating water in °C	42	29.3	40	50.6	23.5	30.1	51.1	40.5	40.1	38.2
Brine in °C	−5	0	−0.1	0	0	−0.1	0	0	0	5
Brine out °C	−7.2	−3.6	−3	−2.4	−3.8	−2.9	−1.9	−2.4	−2.9	1.4
Power-compressor (kW)	2.55	2.5	2.73	2.92	2.38	2.53	2.94	2.76	2.75	2.91
Power – total (kW)	2.15	2.2	2.44	2.62	2.14	2.23	2.62	2.46	2.34	2.51
Thermal power (kW)	7.24	10.14	9	7.92	10.52	10.26	7.96	9.16	8.94	10.76
$\text{COP}_{\text{compressor}}$	3.35	4.56	3.66	2.98	4.42	4.05	2.71	3.31	3.25	4.28
$\text{COP}_{\text{total}}$	2.83	4.06	3.3	2.71	4.89	4.57	3	3.69	3.81	3.70
$q_{\text{water}}$ (m <sup>3</sup> /h)	0.79	1.55	1.55	1.55	0.79	1.77	1.77	1.77	0.79	0.79
$q_{\text{brine}}$ (m <sup>3</sup> /h)	2.09	2.09	2.09	2.09	2.09	2.57	2.57	2.57	2.09	2.09

Table 5  
Condensing temperature calculation.

	$T_1$ measured	$T_1$ calc. $\Delta t_{\log} = 1$	$T_1$ calc. $\Delta t_{\log} = 3$	$T_1$ calc. $\Delta t_{\log} = 5$	$T_1$ calc. $\Delta t_{\log} = 8$
Case 1	50.88	50.04	51.17	52.91	55.76
Case 2	48.67	49.98	50.37	51.58	54.05
Case 3	46.98	50.05	50.16	50.87	52.84
Case 4	45.06	49.62	49.65	49.99	51.41

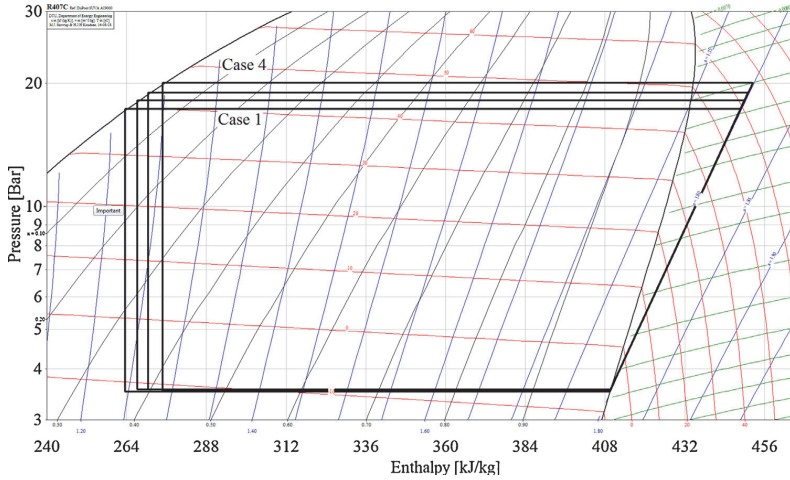


Fig. 10. Thermodynamic process of four test cases described in Table 3.

Decrease of condensing temperature by 12.9% increased the COP by about 9% according to these measurements. These changes in the return temperature resulted in thermodynamic process pressure-enthalpy diagrams shown in Fig. 10.

To test the condensing temperature Equation 8 against the measured data, measured condensing temperatures were compared to calculated ones with Eq. (8) at different  $\Delta t_{log}$  values (Table 5).

Table 5 shows that Eq. (8) provides estimation and is not able to consider return water temperature effect similarly to laboratory measurements.

Therefore, the correlation between condensing and flow/return temperature was derived from measured data. Weightings of flow and return temperatures ( $x$  and  $1-x$ ) were used providing the best correlation (higher  $R^2$ -value) with a formula of  $xT_{11} + (1-x)T_{12} = T_1$ . Best fitting of condensing temperature as a function of flow and return temperature was found for both measurements. For IEA Annex data this resulted in equation  $T_1 = 0.62 T_{12} + 0.34 T_{11} + 4.5$  with slightly higher  $R^2$ -value, than in our measurement results  $T_1 = 0.67 T_{12} + 0.36 T_{11} + 1.05$  as shown in Fig. 11.

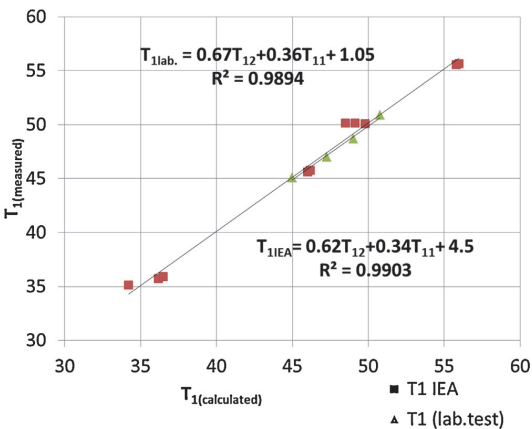


Fig. 11. Condensing temperature correlation equations giving higher weighting for flow temperature.

The data in Fig. 11 had seven test points with flow temperature of 50 °C which allowed to show the dependency between condensing temperatures and return temperatures (Fig. 12).

Fig. 12 shows that the correlation is an approximation not taking into account all physical phenomena, but the correlation is still reasonably high.

Derived correlations of condensing temperature (Fig. 11) were used to calculate COP values. For that purpose simulated hourly heating system return temperatures and constant evaporating temperature of -8 °C were used (Fig. 13).

Hourly COP values in Fig. 13 resulted in the following SPF values (Eq. 3): by condenser model 3.39; by laboratory measurements 3.72 and by IEA Annex 28 measurements 3.67.

These results show that laboratory measurement gave approximately 8–9% higher SPF value compared to condenser model used in IDA-ESBO simulation.

### 3.5.2. The effect of reduced flow rates by thermostats

Hourly simulation with the condenser model (Eq. 6) and derived correlations (Fig. 11) was used to test the effect of reduced flow rates by thermostats. So far simulated return temperature was used in calculations. In the case of fixed flow rates (correspond to situation with exact sizing and no internal and solar gains) return temperature can be directly calculated from flow temperature with

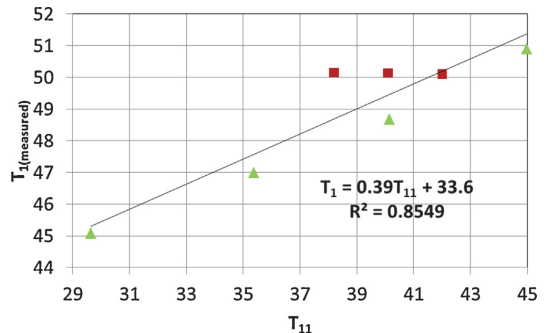


Fig. 12. Condensing temperature dependency on return temperature at 50 °C flow temperature.

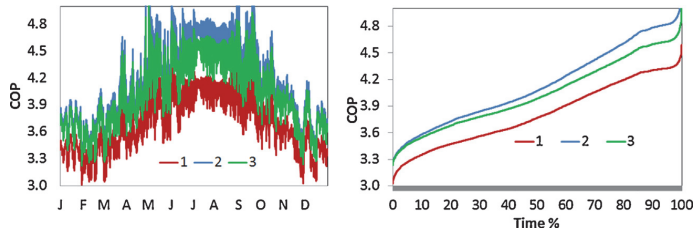


Fig. 13. Comparison of hourly COP (left) and the duration curve (right) of hand calculation with condenser model (1) and derived correlation (2 – by laboratory measurements; 3 – by IEA Annex 28 measurements).

the assumption that heating need has linear dependency with delta  $T$  of indoor and outdoor temperature (Fig. 14). This calculation needs as input data only simulated heating needs, i.e. the simulation of radiator heating system is not needed. SPF with constant water mass-flow was calculated for 45/35 °C heating curve that was used in previous chapters. Calculation was conducted for connection scheme No. 2, where flow temperature follows exactly the heating curve (without stratification tank effects present in connection scheme 1).

Condensing temperatures were calculated with Eq. (8) and with the correlation of laboratory measurements (Fig. 11). The use of hand calculated fixed flow return temperature (calculated with Eq. (8)) resulted in ~2 °C difference in condensing temperature (Fig. 15), and decreased annual SPF by ~4.5% (SPF of 4.0 with fixed flow return temperature vs. to real SPF 4.19).

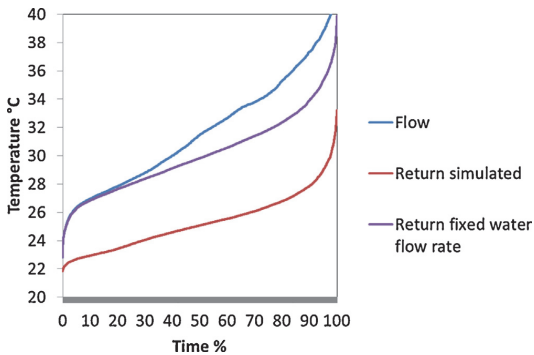


Fig. 14. Flow and return temperature calculations by outdoor temperature. 100% = 8760 h.

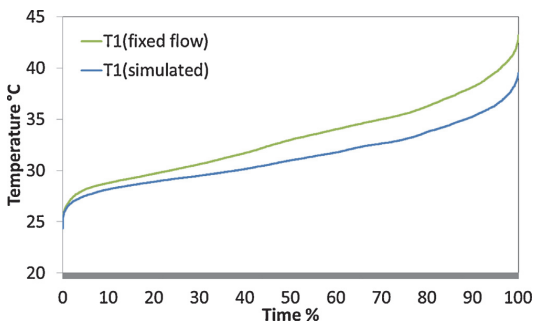


Fig. 15. Condensing temperature calculated by fixed return flow rate. 100% = 8760 h.

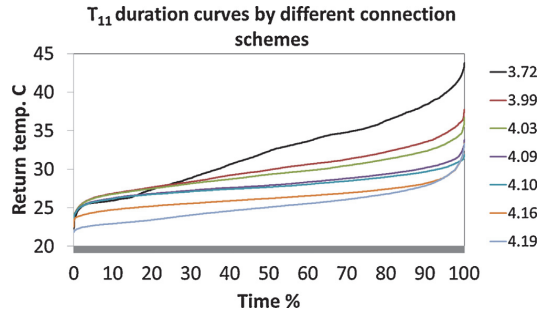


Fig. 16. Return temperatures with studied connection schemes described by SPF values. 100% = 8760 h.

Table 6

SPF values simulated with different connection schemes.

Connection type	Laboratory measurements correlation SPF	Condenser model (Eq. (8)) SPF
1 separated connection with stratification tank	3.72	3.39
2 without bypass	4.19	3.76
3 bypass (0.1 kg/s)	3.99	3.61
3 bypass (0.05 kg/s)	4.03	3.64
3 bypass (0.02 kg/s)	4.09	3.69
3 bypass (0.005 kg/s)	4.16	3.74
4 with volume tank and bypass (0.02 kg/s)	4.10	3.69

3.5.3. Connection scheme impact on seasonal performance factor

Four different connection scheme which were described in Ch.2.2 were simulated and SPF values were computed (Table 6). SPF values were calculated with Eq. (3), where compressor and circulation pump power were computed through hourly COP and space heating need. COP were computed with Eq. (1) where condensing temperature correlation  $T_1 = 0.67 T_{12} + 0.36 T_{11} + 1.05$  was used and with condenser model, Eq. (8).

Fig. 14 shows that highest SPF is achieved with direct connection without bypass. The bypass reduces SPF value, and the volume tank provides in principle a small increase without practical meaning, however the real benefits of larger water volume on heat pump operation are out of scope of this study. Highest SPF value was achieved at lowest return temperature as shown in Fig. 16.

4. Conclusion

In this paper a domestic heat pump applications with radiator heating were analyzed. The main aim was to investigate the heating system return temperature effect on the condensing temperature with consequent SPF effects. SPF of the heat pump was quantified by three different comparable models – analytical model, IDA-ESBO

heat pump model and by correlation equation derived from two set of laboratory measurements.

Results revealed that IDA-ESBO simulation together with detailed outdoor temperature controlled heating system model gave very similar seasonal performance factor compared to analytical condenser model with constant refrigerant temperature, 3.48 vs. 3.39 respectively. Two separate domestic heat pump laboratory measurements at different temperature levels were used for calculating hourly COP values with simulated heating system inlet/outlet temperatures. SPF values were calculated by derived formulas for four commonly used connection schemes in Nordic countries. Calculation with derived condensing temperature correlation stressed the effect of relatively low return temperature in a radiator heating system that resulted in 9% higher SPF value of 3.72. Four different domestic heat pump connection schemes resulted in a range of SPF values of 3.72 to 4.21. The highest SPF was achieved with direct connection scheme of heat pump, because it resulted in lowest possible return water temperature. Additionally, the effect of reduced flow rates by radiator thermostats were computed, because the calculation with fixed flow rate return temperature can be done as fully hand calculation if hourly heating needs are known. This small detail, the fixed flow return temperature resulted in 4.5% lower SPF value, showing the importance to use correct return temperature corresponding to actual flow rates in radiators.

The results of this study indicate that calculation procedures, which do not calculate the return temperature and use simple assumptions in the condensing temperature calculation may lead to underestimation of SPF by more than 10% in the case of radiator heating.

### Acknowledgements

The research was supported by the Estonian Research Council, with Institutional research funding grant IUT1-15, and with a grant of the European Union, the European Social Fund, Mobilitas grant No. MTT74.

### References

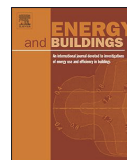
- [1] Directive 2010/31/EC of the European Parliament and of the Council of 19 May 2010 on the Energy Performance of Buildings, <http://eur-lex.europa.eu/LexUriServ/LexUriServ.do?uri=OJ:L:2010:153:0013:0035:EN:PDF>, Brussels.
- [2] K.J. Chua, S.K. Chou, W.M. Yang, Advances in heat pump systems: a review, *Appl. Energy* 87 (2010) 3611–3624.
- [3] A. Saari, T. Kalamees, J. Jokisalo, R. Michelsson, K. Alanne, J. Kurnitski, Financial viability of energy-efficiency measures in a new detached house design in Finland, *Appl. Energy* 92 (2012) 76–83.
- [4] M. Maivel, J. Kurnitski, Low temperature radiator heating distribution and emission efficiency in residential buildings, *Energy Build.* 69C (2013) 224–236.
- [5] M. Scarpa, G. Emmi, M. De Carli, Validation of a numerical model aimed at the estimation of performance of vapour compression based heat pumps, *Energy Build.* 47 (2011) 411–420.
- [6] L. Schibuola, Heat pump seasonal performance evaluation: a proposal for a European standard, *Appl. Therm. Eng.* 20 (4) (2000) 387–398.
- [7] I.S. Ertesvåg, Uncertainties in heat-pump coefficient of performance (COP) and exergy efficiency based on standardized testing, *Energy Build.* 43 (2011) 1937–1946.
- [8] EN 14511-2, Air Conditioners, Liquid Chilling Packages and Heat Pumps with Electrically Driven Compressors for Space Heating and Cooling – Part 2: Test Conditions, CEN, Brussels, 2013.
- [9] ISO 5151, International Organization for Standardization, Non-Ducted Air Conditioners and Heat Pumps – Testing and Rating for Performance, International Organization for Standardization, Geneva, 2010.
- [10] F. Karlsson, M. Axéll, P. Fahlén: Heat Pump Systems in Sweden – Country Report for IEA HPP Annex 28, Swedish country report IEA HPP Annex 28 Task 1, SP AR 2003:01 Energy Technology, <http://www.annex28.net/pdf/Annex28.N28.pdf>, Borås, Sept 2003.
- [11] EN 255-2, Air Conditioners, Liquid Chilling Packages and Heat Pumps with Electrically Driven Compressors – Heating Mode – Part 2: Testing and Requirements for Marking for Space Heating Units, CEN, Brussels, 1997.
- [12] J. Fernández-Seara, A. Pereiro, S. Bastos, J.A. Dopazo, Experimental evaluation of a geothermal heat pump for space heating and domestic hot water simultaneous production, *Renew. Energy* 48 (2012) (2012) 482–488.
- [13] J. Nyers, A. Nyers, Investigation of heat pump condenser performance in heating process of buildings using steady-state mathematical model, *Energy Build.* 75 (2014) (2014) 523–530.
- [14] J. Kurnitski, A. Saari, T. Kalamees, M. Vuolle, J. Niemelä, T. Tark, Cost optimal and nearly zero (nZEB) energy performance calculations for residential buildings with REHVA definition for nZEB national implementation, *Energy Build.* 43 (11) (2011) 3279–3288.
- [15] Ministry of Economic Affairs Communication, Regulation No. 68, Minimum Requirements for Energy Performance, 2013, <https://www.riigiteataja.ee/akt/105092012004>, (in Estonian).
- [16] IDA ESBO, User Guide, <http://www.equonline.com/esbo/IDAESBOUserguide.pdf>
- [17] F. Karlsson, Capacity Control of Residential Heat Pump Heating System, Ph.D. thesis, Building Services Engineering, Department of Energy and Environment Chalmers University of Technology, 2007.
- [18] F. Karlsson, P. Fahlén, Capacity-controlled ground source heat pumps in hydronic heating systems, *Int. J. Refrig.* 30 (2) (2007) 221–229.
- [19] G. Salvalai, Implementation and validation of simplified heat pump model in IDA-ICE energy simulation environment, *Energy Build.* 49 (2012) 132–141.



## PAPER IV

Maivel, M.; Kurnitski, J. (2015). Radiator and Floor Heating Operative Temperature and Temperature Variation Corrections for EN 15316-2 Heat Emission Standard. *Energy and Buildings*, 99, 204 - 213.





# Radiator and floor heating operative temperature and temperature variation corrections for EN 15316-2 heat emission standard



Mikk Maivel<sup>a,\*</sup>, Jarek Kurnitski<sup>a,b</sup>

<sup>a</sup> Tallinn University of Technology, Ehitajate tee 5, 19086 Tallinn, Estonia

<sup>b</sup> Aalto University, School of Engineering, Rakentajanaukio 4 A, FI-02150 Espoo, Finland

## ARTICLE INFO

### Article history:

Received 24 December 2014

Received in revised form 9 March 2015

Accepted 12 April 2015

Available online 21 April 2015

### Keywords:

Emission losses

Radiator heating system

Floor heating system

Operative temperature

## ABSTRACT

In this paper new draft standard prEN 15316:2-2014 was tested against detailed dynamic simulation and an operative temperature corrections were developed in order to enable fair comparison of heat emitters to provide equal thermal comfort for occupants. Simple one room model with different number of external envelope elements and two occupant positions were used to analyze operative temperature effects. Operative temperature corrections and comparative analyses with the tabulated values of the standard were conducted with two low energy reference building simulation models in two climates. The use of the operative temperature set-point increased the temperature variation in the case of radiator heating by 0.2–0.3 K and decreased it in the case of floor heating by 0.1 K. However, in the case of floor heating the occupant location effect provided an additional increase of 0.1 K which compensated the operative temperature effect, i.e. no correction is needed for floor heating. For the radiator heating the operative temperature variation of 0.25 K is to be added, but this increase falls well within the safety margin of about 0.35 K of existing tabulated values. The comparison of the emission efficiency of the radiator and floor heating revealed equally efficient by the PI controller.

© 2015 Elsevier B.V. All rights reserved.

## 1. Introduction

Revised version of EPBD directive [1] enhanced the role of European CEN standards and provided a mandate to update all approximately 40 EPBD standards with the aim of helping to implement EPBD directive. This study focuses to one of these standards, prEN 15316-2:2014 [2] that is in the public enquiry phase.

Overall movement towards low-energy and nearly zero-energy buildings (nZEB) has created new challenge for heating systems. EN 15316-1:2007 [3] divides heating system losses into four main parts: generation, storage, distribution and emission—all these parts have losses. In this paper we consider emission losses. The scope of prEN 15316-2:2014 is to introduce energy calculation procedure and tabulated values for additional heat losses in the heat emission system.

Previously emission losses have not been widely studied. The reference study of EN 15316:2007 [4] reports tabulated values for distribution and emission losses of 15% for temperature curves 55/45 °C and 19% for 70/55 °C in residential building radiator heating system in Brussels. For low temperature heating systems we

were not able to find any reference. Very old study [5] reports additional emission loss up to 5% of the heat emission of radiator in old buildings with poor insulation and less than 1% in new buildings with good insulation. Recent heating system simulation study showed that simulated losses in low-energy building were significantly lower compared to tabulated values of the standard [6]. Partly based on these results, a new updated prEN standard has more alternatives for considering low energy buildings.

In addition several studies have been performed for comparing different heat emission systems, especially floor and radiator heating. It has been concluded that a low-temperature heating system improves thermal comfort [7]. CFD based steady state investigations have indicated that higher PPD is achieved by floor heating, although low- and medium temperature radiator heating system reach more steady air speed and temperature level in occupied zone close to the window [8]. It has been shown that low-temperature radiant panels can help to achieve 11–27% of energy compared conventional heating systems [9]. Most of these recent studies were prepared for conventional buildings and there are lack of relevant studies for buildings with advanced building systems and well insulated envelope elements.

Thermal comfort calculation and measuring standards ISO 7726 [10] and ISO 7730 [11] are based on the use of operative temperature as a general thermal comfort temperature.

\* Corresponding author. Tel.: +372 56 461 251.

E-mail addresses: [mikk.maivel@ttu.ee](mailto:mikk.maivel@ttu.ee), [mikkmaivel@gmail.com](mailto:mikkmaivel@gmail.com) (M. Maivel).

## Nomenclature

nZEB	nearly zero energy building
CEN	The European Committee for Standardisation
EN	European Standard
CFD	computational fluid dynamics
PPD	predicted percentage dissatisfied
ISO	International Organization for Standardization
BAU	business as usual

Operative temperature is not yet implemented in prEN 15316-2:2014 methodology that calculates heating system losses from air temperature. The use of operative temperature instead of air temperature will cause a difference in the heat emission losses depending on radiant temperatures in a room. In this paper we analyzed dynamically the principal difference of air and operative temperature control and derived correction factors for radiator and floor heating allowing to consider the operative temperature effect on emission losses. To enable exact comparison of heating systems the emission losses were calculated by the dynamic simulation where thermostats were controlled according to operative or air temperature. Operative temperature control in principle results on thermal state in a room that leads to exactly the same thermal sensation by occupants, independently on used heat emission system. In the case of conventional air temperature controlled floor and radiator heating systems, the thermal sensation could be slightly different at the same air temperature set-point, because of different operative temperature.

Simple one room model with different number of external envelope elements were used to analyze operative temperature effects analytically. Because operative temperature depends on occupant location in the room, different occupant locations were used to assure the thermal comfort everywhere in the occupied zone. Operative temperature corrections and comparative analyses with the tabulated values of the standard were conducted with two low energy reference building simulation models.

## 2. Methods

### 2.1. Heating system emission losses by EN 15316-2

The methodology of the updated standard has been partly changed. Current 2007 version [2] describes two possible ways for calculation of emission losses: adopted from German regulation DIN 18599 [12] energy losses of the heat emission system and the second one adopted from French regulation RT 2005 [13]—equivalent increase in indoor temperature. Nevertheless the losses themselves are the same, but can be expressed differently. Emission losses include heat losses through the building envelope due to non-uniform temperature distribution, control inefficiencies and losses of emitters embedded in the building structure. New standard relies on the French method and all tabulated values are described by the increase of indoor temperature. With this method, equivalent temperature considering emission losses are calculated from tabulated values with the following equation:

$$\theta_{\text{int;inc}} = \theta_{\text{int;ini}} + \Delta\theta_{\text{str}} + \Delta\theta_{\text{ctr}} + \Delta\theta_{\text{emb}} + \Delta\theta_{\text{rad}} + \Delta\theta_{\text{im}} + \Delta\theta_{\text{hydr}} + \Delta\theta_{\text{roomaut}} \quad (1)$$

where  $\theta_{\text{int;ini}}$ —initial internal temperature (°C);  $\Delta\theta_{\text{str}}$ —spatial variation of temperature due to stratification (K) which resulting in an increased internal indoor temperature under the ceiling and upper parts of the room (Eq. (2));  $\Delta\theta_{\text{ctr}}$ —control variation (K) variation depending on the capacity of the control device to assure an

homogeneous and constant temperature (the standard user should choose from  $\theta_{\text{ctr1}}$  (should be used for standard calculation if no information are available) or  $\Delta\theta_{\text{ctr2}}$  (should be used for calculation with certified products);  $\Delta\theta_{\text{emb}}$ —temperature variation based on an additional heat loss of embedded emitters in the envelopes (K) (Eq. (3));  $\Delta\theta_{\text{rad}}$ —temperature variation based on radiation by type of the emission system (K);  $\Delta\theta_{\text{im}}$ —temperature variation based on intermittent operation and based on the type of the emission system (K) (Eq. (4)),  $\Delta\theta_{\text{hydr}}$ —temperature variation based on not balanced hydraulic systems (K);  $\Delta\theta_{\text{roomaut}}$ —temperature variation based on stand alone or networked operation room automatization of the system (K);  $\theta_{\text{int;inc}}$ —temperature variation based on all losses (K).

$$\Delta\theta_{\text{str}} = \frac{\Delta\theta_{\text{str;1}} + \Delta\theta_{\text{str;2}}}{2} \quad (2)$$

Stratification is influenced by over-temperature ( $\Delta\theta_{\text{str;1}}$ ) and specific heat loss via external components ( $\Delta\theta_{\text{str;2}}$ , (e.g. additional heat loss from back-wall of radiator).

$$\Delta\theta_{\text{emb}} = \frac{\Delta\theta_{\text{emb;1}} + \Delta\theta_{\text{emb;2}}}{2} \quad (3)$$

Embedded heat loss is to be formed from the data for the main influence parameters system ( $\Delta\theta_{\text{emb;1}}$ ) and specific heat losses via laying surfaces ( $\Delta\theta_{\text{emb;2}}$ ).

$$\Delta\theta_{\text{im}} = \Delta\theta_{\text{im;emt}} + \Delta\theta_{\text{im;ctr}} \quad (4)$$

where  $\Delta\theta_{\text{im;emt}}$ —temperature variation based on intermittent operation on the type of the emission system (K);  $\Delta\theta_{\text{im;ctr}}$ —temperature variation based on intermittent operation of control (K).

### 2.2. Reference buildings and heating solutions

Analyzed detached building has been previously used as a reference building in Estonian cost optimal calculations [14]. By small changes the same model was modified to describe a section of a multi-story apartment building. External wall in one end of the building were made adiabatic, which means that the model unit represents one apartment of a long building. Similarly, the external roof was change to adiabatic, which means that the building will continue upwards. In the transformation from detached house to apartment building, the technical space and one small window on the top left were “lost”—as the apartment building is more compact. All other geometry of a house unit remained the same in the transformation (Fig. 1). Main technical data for both buildings are shown in Table 1.

Room set-point temperature of 21 °C has been used in all zones/rooms. Heating was controlled with outdoor air temperature compensated heating curve (the supply water temperature increases to the maximum as the outdoor temperature decreases to the design outdoor temperature) and with individual room control with room thermostats. During the simulations two different heating curves for radiator heating were used 70/55 °C as a conventional heating system and 45/35 °C as low temperature heating system, beside that 35/28 °C was used for underfloor heating system. For the room temperature control most common room controllers were simulated, including on-off and proportional controller (P) without hysteresis, both with proportional/on-off band of 2 K, and proportional-integrated PI controller leading to almost ideal room temperature control. The models of controllers can be found from [16].

In the detached house model, cooling system was not used, but in the apartment building model, ideal coolers were used because there are higher share of internal gains. Without cooling, it is problematic to keep the room temperature in a set point level of 25 °C.

**Table 1**  
Basic data of the building.

		Detached house	Apartment building
<i>U</i> -value (W/(m <sup>2</sup> K))	Exterior wall	0.17 (lightweight)	0.17 (heavyweight)
	Roof	0.14 (lightweight)	0.14 (heavyweight)
	Ground floor	0.17	0.17
	Windows (g=0.5)	0.8	0.8
	Specific heat loss coefficient <i>H/A<sub>net</sub></i> (W/(m <sup>2</sup> K))	0.58	0.44
Ventilation	Ventilation (continuous) rate <i>L<sub>v</sub></i> (s m <sup>-2</sup> )	0.46	0.56
	Leakage rate <i>q<sub>50</sub></i> m <sup>3</sup> /(hm <sup>2</sup> )	0.6	0.6
	Usage (max = 1)	W/m <sup>2</sup>	W/m <sup>2</sup>
Internal gains	Occupants	2	3
	Lighting	8	8
	Equipment	2.4	3

Ideal cooler and heater were standard models from IDA-ICE library and they are imaginary equipment which describes heating or cooling need without system losses. Mechanical supply and exhaust ventilation system with heat recovery (temperature ratio of 80%; supply air temperature set-point +18 °C) was used in both models. All energy calculation input data followed the Estonian regulation of minimum requirements for energy performance [15].

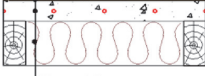
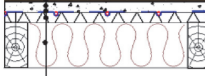
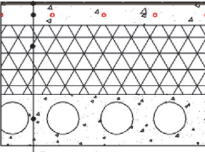
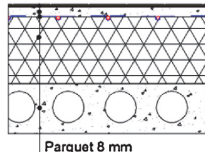
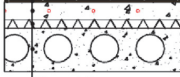
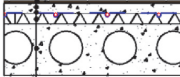
The floor construction types used for floor heating are shown in Table 2. Slab on the ground structure was the same in apartment building and detached house, but mid-floor construction type varied according to light-weight and heavy-weight structures.

In the case of floor heating it is necessary to calculate separately losses caused by the ground or mid-floor. Overall calculation

scheme is shown in Fig. 2 for calculating emission losses from mid-floor then the ground floor had an ideal situation e.g. heating system based on ideal heaters. With this scheme additional losses from the slab were eliminated that allowed to simulate only the mid-floor losses. Afterwards mid-floor losses were eliminated to calculate ground floor emission losses.

Calculations were done with dynamic simulation software IDA Indoor Climate and Energy 4.6 [16]. This tool is carefully validated and has advanced features for detailed building energy simulations [17]. Two test reference years were used for outdoor climate, Estonian TRY [18] and Munich [19]. Stratification losses were neglected in this study, because of the use of mechanical supply and exhaust ventilation. It has been previously shown that stratification is very

**Table 2**  
Simulated floor construction type for apartment building and detached house.

		Detached building		
Mid-floor	Wet system, 1st. floor			
		Parquet 8 mm Concrete 65 mm Isolation 100 mm	Parquet 8 mm Screed 25 mm Aluminium fin 0.5 mm Heavy isolation 25 mm Isolation 100 mm	
Slab on ground	Wet system, ground floor			
		Parquet 8 mm Concrete 65 mm Heavy isolation 340 mm Hollow-core slab 265 mm	Parquet 8 mm Screed 25 mm Aluminium fin 0.5 mm Heavy isolation 340 mm Hollow-core slab 265 mm	
		Apartment building		
Mid-floor	Wet system (65 mm), 1st. floor			
		Parquet 8 mm Concrete 65 mm Heavy isolation 25 mm Hollow-core slab 265 mm	Parquet 8 mm Concrete 100 mm Heavy isolation 25 mm Hollow-core slab 265 mm	Parquet 8 mm Screed 25 mm Aluminium fin 0.5 mm Heavy isolation 25 mm Hollow-core slab 265 mm

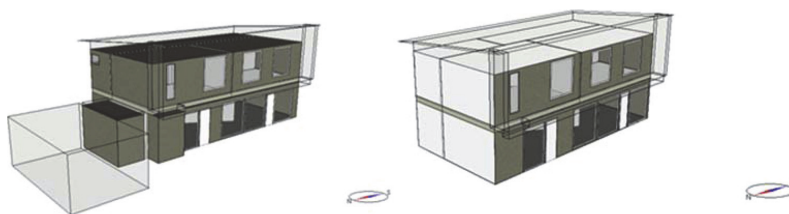


Fig. 1. Estonian reference detached house in the left, and in the right the house transferred to describe an apartment building (white envelope elements are adiabatic).



Fig. 2. Calculation scheme for calculating emission losses for mid-floor (left) and ground floor (right).

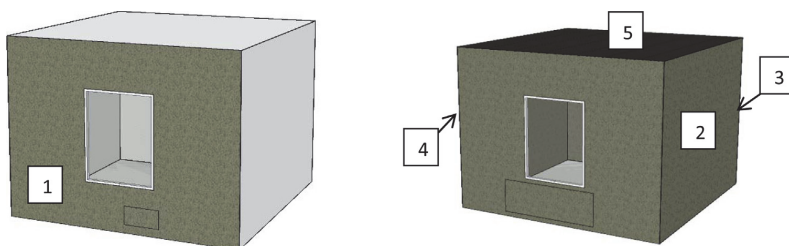


Fig. 3. Room model with one (left) and five (right) external elements (1..5 numbering of external elements).

small due to mixing caused by supply air and resulting in stratification losses of about 0.60% or 0.06 K temperature variation [6].

### 2.3. Operative temperature analysis

Analytical operative temperature analyses for one room model were conducted to analyze external envelope elements impact on operative temperature with two different occupant locations. The number of room external envelope elements varied between 1 and 5 in calculations (Fig. 3). Basic input parameters of the room model are shown in Table 3.

All calculations for different heat emission systems (conventional radiator heating 70/55 °C; low-temperature radiator heating 45/35 °C; floor heating 35/28 °C and situation where heaters were 100% convective) were made at constant indoor operative temperature (+21 °C) and constant outdoor temperature (−22 °C). Simulation itself were run for one day (24 h) period at constant outdoor temperature with the use of two week startup period with exactly the same outdoor parameters allowing to reach the

complete steady state with stabilized heating system and indoor temperatures.

To study the pure room geometry effect on operative temperature external components emission losses were eliminated both for radiator and floor heating. For that purpose  $U=0.0001$  was used for the external wall and internal (adiabatic) floor was used in the case of floor heating.

To calculate the operative temperature surface temperatures were simulated with IDA-ICE. Mean air temperature as well mean radiant temperature were calculated from surface temperature and air temperature results analytically.

The mean radiant temperature was calculated according to the procedure specified in ISO 7726:1998. For this purpose an angle factors between a small plane element and the surrounding surfaces were used to calculate the plane radiant temperature, given in Annex C of the standard. The mean radiant temperature was calculated from the plane radiant temperatures in six directions and the projected area factors for a person in the same six directions, given in the Annex B of the standard. Afterwards the mean air temperature was calculated as an average of the operative and the mean radiant temperature.

In the whole building simulation with IDA-ICE operative temperature calculation was simplified, because of limitations of the IDA-ICE room model, which calculates limited number of view factors between the zone surfaces and an infinite small cube. For each side of the cube only the view factor for the parallel surface directly in front is calculated. The sum of this first set of view factors is not 1 and thus a second corrected set is obtained by dividing with the sum of the first set [16]. This procedure led to up to 0.3 °C differences while occupant is in the center of the room according to our analytical calculations.

**Table 3**  
Basic data of room model.

	Low-energy building	BAU building
External wall ( $U$ -value) ( $W/m^2 K$ )	0.22	0.5
External wall with window ( $U$ -value) ( $W/m^2 K$ )	0.0001	0.0001
Window ( $U$ -value) ( $W/m^2 K$ )	1.1	2.9
External floor ( $U$ -value) ( $W/m^2 K$ )	0.27	0.27
Roof ( $U$ -value) ( $W/m^2 K$ )	0.28	0.5
Ventilation air rate ( $L/s m^2$ )	0.5	0.5
Supply temperature (°C)	20	20

**Table 4**  
Temperature variations with PI-control according to tabulated values of prEN 15316-2.

Temperature variation	Radiator heating 45/35 °C	Radiator heating 70/55 °C	Floor heating wet 35/28 °C (mid-floor)	Floor heating dry 35/28 °C (mid-floor)	Floor heating wet 35/28 °C (slab on ground)
$\Delta\theta_{\text{int,ini}}$	21	21	21	21	21
$\Delta\theta_{\text{str}}$	0.25	0.25	0	0	0
$\Delta\theta_{\text{ctr}}$	0.7	0.7	0.7	0.7	0.7
$\Delta\theta_{\text{emb}}$	0	0	0.4	0.25	0.4
$\Delta\theta_{\text{rad}}$	0	0	0	0	0
$\Delta\theta_{\text{in}}$	0	0	0	0	0
$\Delta\theta_{\text{hydr}}$	0	0	0	0	0
$\Delta\theta_{\text{roomaut}}$	-0.5	-0.5	-0.5	-0.5	-0.5
Total	21.45	21.45	21.6	21.45	21.6

### 3. Results and discussion

#### 3.1. Simulated vs. prEN 15316-2:2014 emission losses with air temperature control

This section compares the tabulated values of the standard with dynamic simulation results when air temperature set-points were used for thermostats.

Tabulated temperature variation components according to the prEN 15316-2:2014 (partly based on VDI standard [20] and Bauer thesis [21]) and the total temperature variation calculated with Equation 1 are shown in Table 4 for investigated buildings.

Results in Table 4 shows that in studied buildings there was no difference between apartment building and detached house, and the temperature variations for floor heating were the same for mid-floor and slab on ground. Standard doesn't distinguish climatic location and the same tabulated values should be used in all climates.

Temperature variation caused by emission losses is complicated to simulate, because of fixed set-points. Therefore emission losses in kWh were simulated and temperature variation was recalculated from the results simulated with different air temperature set-points. This allowed to derive correlations between losses and temperature variations, which depended on building type and location. These correlation equations describe linear dependence between emission loss value and set-point temperature (i.e. the losses were computed at different set-point temperatures with 0.1 °C step, 21.1, 21.2, ... 22 etc.). Two buildings in two climates resulted in four formulas: for detached building in Tallinn  $\Theta = 0.0846\eta + 0.012$ , Munich  $\Theta = 0.0616\eta + 0.023$  and for apartment building in Tallinn  $\Theta = 0.0564\eta + 0.012$  and Munich  $\Theta = 0.0436\eta + 0.023$  (where  $\Theta$  is temperature variation K and  $\eta$  is emission system loss %) (Figs. 4 and 5).

Radiator heating system emission and distribution losses were comprehensively studied in previous paper [6], therefore based on these results only the main cases were used in this study. Simulated results for floor and radiator heating systems are shown in Table 5 and Fig. 6.

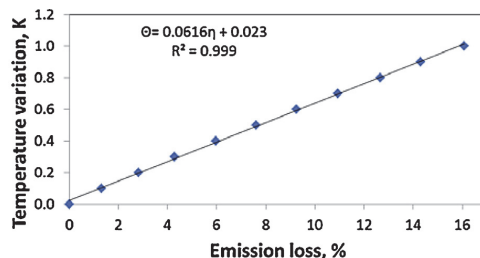
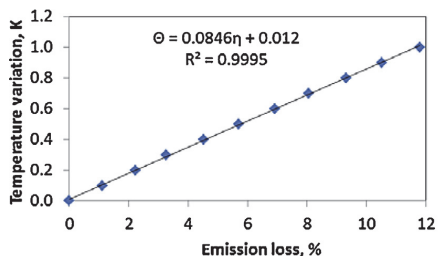


**Fig. 4.** Derived formula for calculating temperature variation from emission losses in detached house in Tallinn (left) and Munich (right).

Table 5 compares PI control as an advanced control of heating system and P control (without hysteresis and with proportional band of 2 K) for radiator heating and on-off for floor heating as conventional systems. In addition there are always on results with no control to show the effect of self-control of floor heating, being without any controller, flow always on during heating season and heating curve dropped to avoid overheating. Results show that self-control can be even more effective than P-control in a detached house. In an apartment building, due to higher share of internal gains it was not possible to set correct heating curve allowing to keep the desired indoor temperature and the losses were higher. Compared to PI, temperature variations with conventional control were substantially higher especially for floor heating and it stressed the importance to use advanced control systems to decrease energy use.

Fig. 6 shows that difference in energy use between the standard calculation and simulation was up to 8%. For radiator heating the standard recommends to use slightly higher emission losses than simulated. The overestimation is reasonable, 0.3–0.4 K in equivalent temperature that is on the safe side. In contrary for floor heating system in detached house the standard tabulated values were too low and the losses were underestimated that suggest to split the tabulated values in the standard according to the thermal mass (lightweight vs. heavyweight) of the building.

Floor heating system losses depend also on floor construction. In Table 6 the results are shown by the building mass and construction type as shown in Table 2.

Table 6 shows that beside climate also the floor type and building overall thermal mass affect emission losses. The results are in line with Zhou [22] who has indicated that using different thermal mass in floor construction have substantial effect for indoor climate quality and energy efficiency, and he has resulted that more thermal mass ensure less temperature variations.

#### 3.2. Operative temperature analyses

A single zone test room was used to analyze the effect of different heat emission systems on operative temperature. Calculations were started with one external wall and the number of external

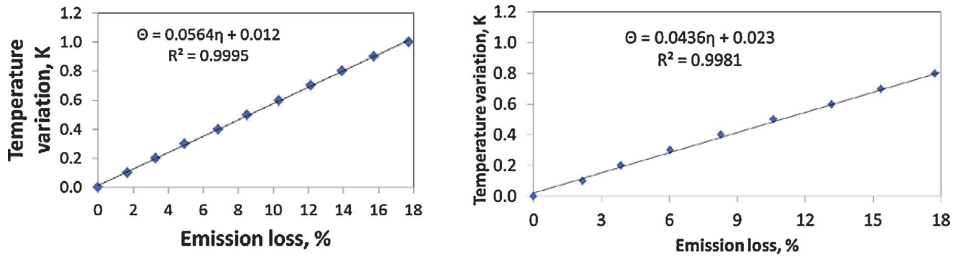


Fig. 5. Derived formula for calculating temperature variation from emission losses in apartment building in Tallinn (left) and Munich (right).

Table 5  
Simulated spatial variation of temperature (indoor air set-point temperature 21 °C).

		Heating system	PI control (K)	P (radiator)/on-off (UFH) control (K)	Always on–no control (K) (heating curve)
Detached house	Tallinn	45 °C/35 °C	0.11	0.29	
		70 °C/55 °C	0.11	0.35	
		UFH–35 °C/28 °C wet c. (mid-floor)	0.57	1.18	0.64 (30 °C/23 °C)
	Munich	UFH–35 °C/28 °C wet c. (slab on ground)	0.78	1.67	1.25 (30 °C/23 °C)
		45 °C/35 °C	0.12	0.45	
		70 °C/55 °C	0.12	0.51	
Apartment building	Tallinn	UFH–35 °C/28 °C wet c. (mid-floor)	0.67	1.22	0.95 (30 °C/23 °C)
		UFH–35 °C/28 °C wet c. (slab on ground)	0.84	1.69	1.50 (30 °C/23 °C)
		45 °C/35 °C	0.09	0.28	
	Munich	70 °C/55 °C	0.09	0.31	
		UFH–35 °C/28 °C wet c. (mid-floor)	0.16	0.86	0.96 (28 °C/22 °C)
		45 °C/35 °C	0.06	0.22	
		70 °C/55 °C	0.11	0.30	
		UFH–35 °C/28 °C wet c. (mid-floor)	0.20	0.97	1.40 (28 °C/22 °C)

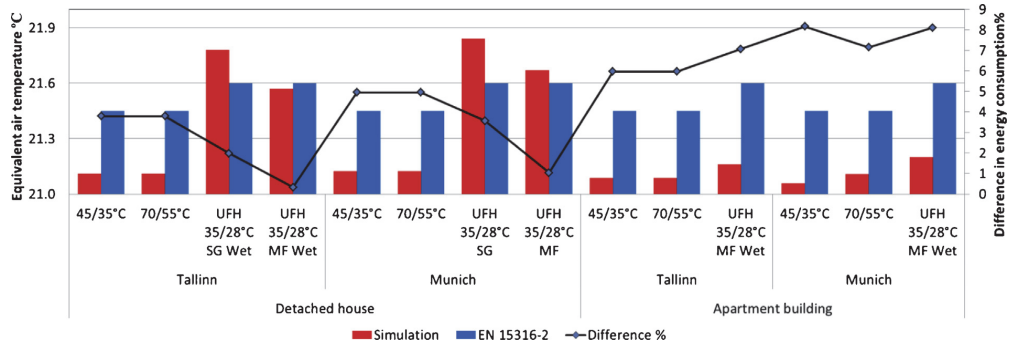


Fig. 6. Comparison of air temperature calculated with prEN 15316-2 and simulation with PI control (MF—mid-floor; SG—slab on ground).

Table 6  
Floor heating system temperature variation by emission losses.

Floor type	Construction method	Wall mass	Tallinn		Munich	
			Detached building	Apartment building	Detached building	Apartment building
Slab on ground	Wet	Lightweight	0.78		0.84	
		Heavyweight	0.72			
	Dry	Lightweight	0.88		0.96	
		Heavyweight	0.73			
Mid-floor	Wet	Lightweight	0.57		0.67	
		Heavyweight (65 mm concrete)	0.43	0.2		0.2
	Wet(100 mm)	Heavyweight (100 mm concrete)		0.12		0.14
	Dry	Lightweight	0.48		0.6	
		Heavyweight	0.3	0.2		0.19

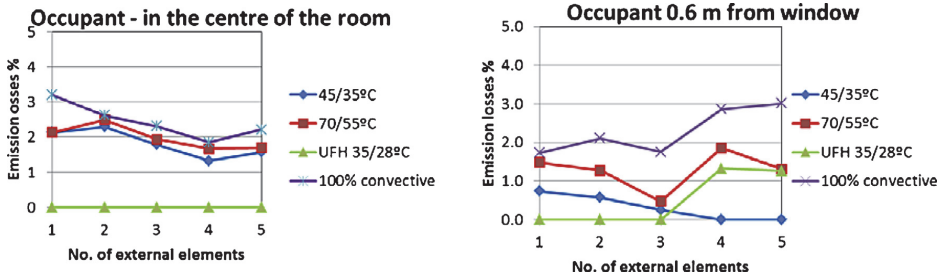


Fig. 7. Additional heating energy at  $-22^{\circ}\text{C}$  outdoor temperature relative to the case with the lowest energy with insulation level corresponding to a low-energy building.

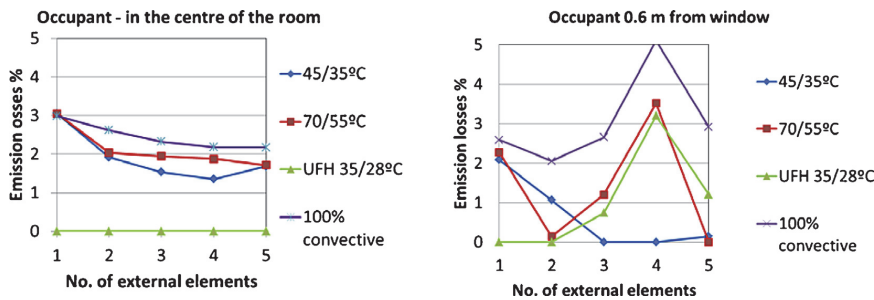


Fig. 8. Additional heating energy at  $-22^{\circ}\text{C}$  outdoor temperature relative to the case with the lowest energy with insulation level corresponding to less insulated (BAU) building.

elements was increased up to 5 following the external element numbering shown in Fig. 3. Two different occupant locations were studied—in the center of the room like in standard EN 422 [23] and 0.6m from the wall with window and radiator. The latter represents the borderline of the occupied zone, and in some cases this location can be more critical compared to the center and therefore needs to be checked in order to fulfill the operative temperature requirement within the all occupied zone. Figs. 7 and 8 summarize the results at  $-22^{\circ}\text{C}$  outdoor temperature for low-energy building and less insulated BAU building.

While occupant is in the middle of room the emission losses were not so sensitive for external construction type and the number of external walls. Best results were achieved with floor heating (heat losses of the floor were neglected because of adiabatic floor boundary condition). Moving occupant close to the radiator and external wall changed the results remarkably and emission losses were more sensitive to the number of external elements—in the case of 3–5 external element the low-temperature radiator heating system secured the lowest emission losses.

Previous simulations were made on steady state situation at constant outdoor temperature ( $-22^{\circ}\text{C}$ ). To analyze heating system

dynamics the annual simulations with PI-control were conducted, which provided smaller differences but stronger effect of the occupant position as shown in Fig. 9.

According to annual energy calculations while the occupant was in the middle of the room losses were smallest still with floor heating, but in the cases where occupant is close to the radiator the lowest losses were reached with low-temperature radiator heating system independently of the number of external elements.

Operative temperature calculation components, mean air temperature and mean radiant temperature are reported for the steady state case in Fig. 10 showing that mean air temperature raised almost linearly while the occupant is in the center of room.

To determine the correction of operative temperature which will to ensure proper indoor temperature in the whole occupied zone both occupant locations were considered. Operative temperature at 0.6 m from external wall was calculated for the case which had  $21^{\circ}\text{C}$  operative temperature with occupant in the center of room and at the center of the room for the case which had  $21^{\circ}\text{C}$  operative temperature with occupant 0.6 m from external wall (Fig. 11).

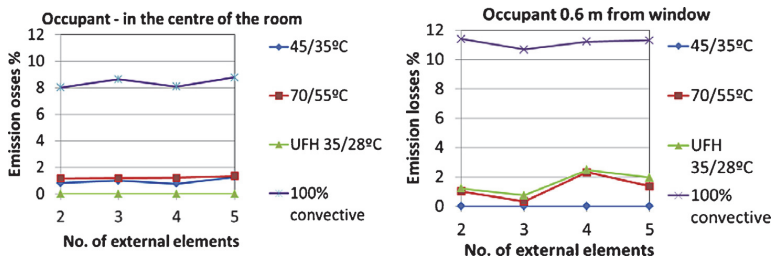


Fig. 9. Additional annual heating energy in Tallinn relative to the case with the lowest energy with insulation level corresponding to a low-energy building.

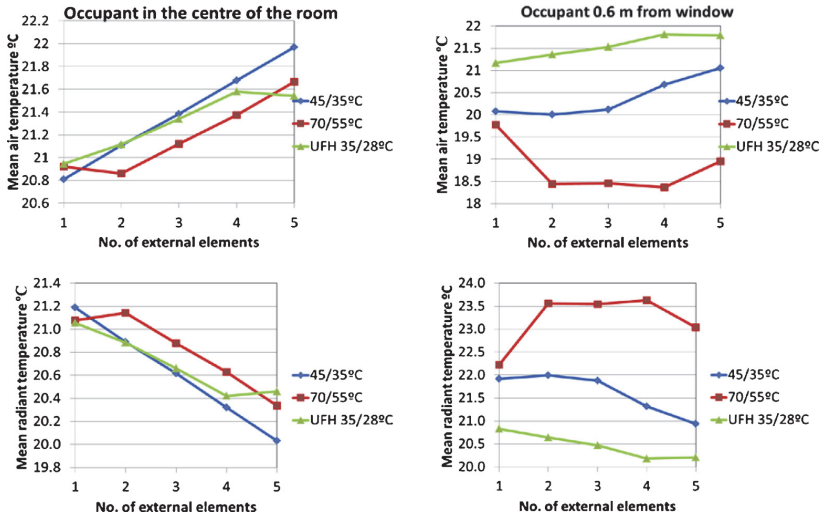


Fig. 10. Calculated mean air and radiant temperature at  $-22^{\circ}\text{C}$  outdoor temperature with insulation level corresponding to a low-energy building.

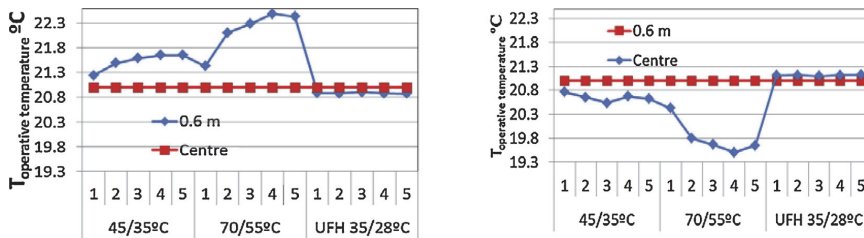


Fig. 11. Comparison of operative temperature according to different occupant location at  $-22^{\circ}\text{C}$  outdoor temperature with insulation level corresponding to a low-energy building.

Fig. 11 shows that while keeping the operative temperature  $+21^{\circ}\text{C}$  in the center of the room then the operative temperature close to radiator is up to  $1.4^{\circ}\text{C}$  higher, but in the case of floor heating the operative temperature is almost in the same level through the occupied zone, however it very slightly decreases 0.6 m from external wall. These results show that the critical occupant location for the radiator heating is the center of the room, but 0.6 m from external wall for the floor heating.

### 3.3. Heating system emission losses with operative temperature control

The temperature variation was simulated with PI-control for the cases described in Section 2 with the operative temperature control (Fig. 12). As figured out in Section 2.2 for the floor heating system the critical occupants location of 0.6 m from external wall was used in addition to the default locations in the center of the rooms.

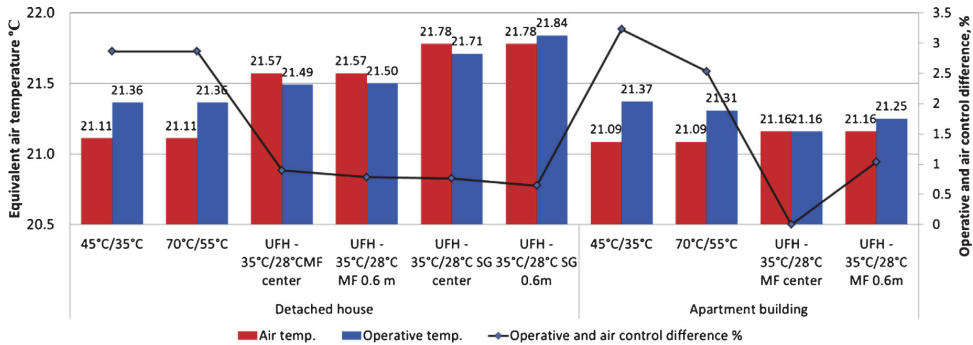


Fig. 12. Air temperature and emission losses with operative temperature setpoint of 21 and PI-control C (UFH—underfloor heating, MF—mid-floor; SG—slab on ground) in Tallinn.

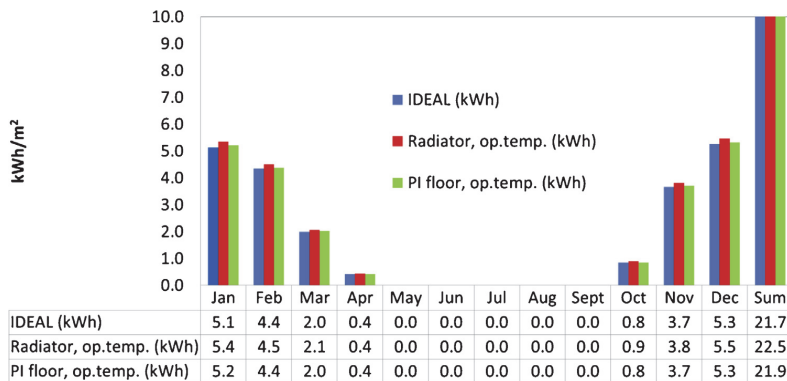


Fig. 13. Comparison of heating energy need in the case of low temperature radiator and floor heating systems with PI-control in the apartment building in Tallinn.

These results include in addition to operative temperature effect all other emission losses as described in Section 2. The operative temperature control has increased the temperature variation in the case of radiator heating, but in the case of floor heating changes are in both direction indicating multiple effects of occupant position and external walls in the real buildings. The results of 45/35 °C radiator heating and floor heating (0.6 m occupant location) are illustrated with monthly balance of heating energy need in apartment and detach building in Tallinn as shown in Figs. 12 and 13. For the ideal heater without any losses 40% radiation share was used.

Fig. 13 shows that the annual heating energy need difference between floor and radiator heating is 2.9% (radiator heating annual energy need was 3855 kWh and floor heating 3746 kWh, respectively) in the apartment building with heavy-weight structures.

Floor heating resulted in higher energy need in late spring and late autumn that is explained by slower response time on internal and solar gains.

In the detach house with light-weight structures the situation was vice versa and the low temperature radiator heating showed 3.3% smaller heating energy need compared to floor heating (annual heating energy need was 7890 kWh for radiator heating and 8155 kWh for floor heating) (Fig. 14).

4. Conclusion

On the whole new updated space emission losses standard prEN 15316-2:2014 gives more accurate values than existing version, and it is more suitable for low-energy buildings because of inclusion of low temperature heating and a combination of mechanical ventilation systems. However, the standard does not enable to compare space emission solutions on the bases of the same operative temperature and there are also some tabulated values which will need revision to improve the scientific quality of the standard.

Our simulations with two low energy residential buildings in two climates revealed that emission losses tabulated values for radiator heating were on safe side with reasonable margin, i.e. over-estimated by 3–4% in terms of annual energy use. The same did not applied for floor heating system which losses were underestimated for cases with lightweight structures and for slab on ground. Floor heating revealed to be very sensitive on control and building thermal mass. The heating energy use with the tabulated values was underestimated up to 8% which calls for revision of the tabulated values. Detailed simulations showed that the tabulated values of the floor heating should be distinguished according to the thermal mass of the building (lightweight vs. heavyweight) and the losses to the ground need to be corrected. The results did not support the

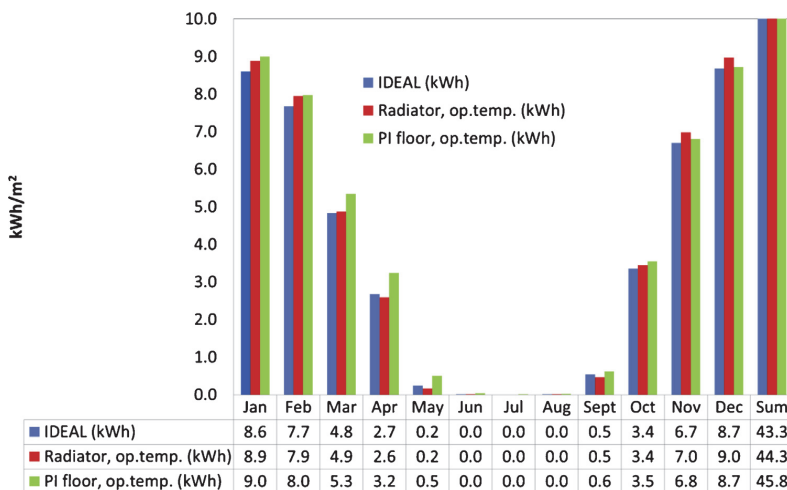


Fig. 14. in the same results as in Fig. 13 for the detached building.

approach of the standard to use the same tabulated control variation values for floor and radiator heating. In the case of PI-controller this approach worked, but in the case of P-controller temperature variation for floor heating was remarkably higher compared to the value of radiator heating.

To make different heat emitters comparable it is needed to introduce a correction factor for considering operative temperature, what occupants feel. The use of the operative temperature setpoint instead of air temperature one increased the temperature variation in the case of radiator heating by 0.2–0.3 K and decreased it in the case of floor heating by 0.1 K. However, in the case of floor heating the occupant location effect provided an additional increase of 0.1 K which compensated the operative temperature effect, i.e. no correction is needed for floor heating. For the radiator heating the operative temperature variation of 0.25 K is to be added, but this increase falls well within the safety margin of about 0.35 K of current tabulated values.

The results allow to draw the following conclusions for comparison of the emission efficiency of the radiator and floor heating systems when operative temperature effects are considered:

- radiator heating showed higher emission efficiency in all cases with P-controller vs. on-off controller in floor heating with the difference of 0.5–0.9 K in equivalent temperature;
- in the case of PI-control in heavyweight building the floor heating showed higher emission efficiency with the difference of 0.1 K in equivalent temperature;
- in the case of PI-control in lightweight building the radiator heating showed higher emission efficiency with the difference of 0.15 K in equivalent temperature;
- generally the differences with PI-controller were so small that radiator and floor heating can be considered equally efficient;
- losses to the ground (slab on ground) added 0.2–0.5 K temperature variation on the top of the mid-floor value to the floor heating;
- differences between wet and dry floor heating with PI-controller was only 0.1 K in temperature variation.

### Acknowledgments

The research was supported by the Estonian Research Council, with Institutional research funding grant IUT1-15, and with a grant of the European Union, the European Social Fund, Mobilias grant no MTT74 and SA Archimedes-s grant 3.2.0801.11-0035.

### References

- [1] Directive 2010/31/EU of the European Parliament and of the Council of 19 May 2010 on the Energy Performance of Buildings, <http://eur-lex.europa.eu/LexUriServ/LexUriServ.do?uri=OJ:L:2010:153:0013:0035:EN:PDF>, Brussels.
- [2] European Standard EN 15316-2:2014, Heating systems and water based cooling systems in buildings—method for calculation of system energy requirements and system efficiencies—Part 2: Space emission systems. (heating and cooling), CEN, Brussels, 2014.
- [3] European Standard EN 15316-1:2007, Heating systems in buildings. Method for calculation of system energy requirements and system efficiencies. Part 1: General, CEN, Brussels, 2007.
- [4] B.V. Olesen, M. de Carli, Calculation of the yearly energy performance of heating systems based on the European Building Energy Directive and related CEN standards, *Energy Build.* 43 (2011) 1040–1050.
- [5] H. Sauter, Leistungsminderung bei Heizkörperverkleidungen, in: HLH. Bd. 36. Nr. 4., 1985.
- [6] M. Maivel, J. Kurnitski, Low temperature radiator heating distribution and emission efficiency in residential buildings, *Energy Build.* 69 (2014) (2014) 313–322.
- [7] A. Hesaraki, S. Holmberg, Energy performance of low temperature heating systems in five new built Swedish dwellings. A case study using simulations and on-site measurements, *Build. Environ.* 64 (2013) 85–93.
- [8] J.A. Myhren, S. Holberg, Flow patterns and thermal comfort in a room with panel, floor and wall heating, *Energy Build.* 40 (2008) 524–536.
- [9] M. Dovjak, M. Shukuya, A. Krainer, Energy analysis of conventional and low energy systems for heating and cooling of near zero energy buildings, *Strojniški vestnik—J. Mech. Eng.* 58 (2012) 453–461.
- [10] ISO, Ergonomics of the thermal environment. Instruments for measuring physical quantities, in: ISO 7726:1998, ISO, 1998.
- [11] ISO, Ergonomics of the thermal environment—analytical determination and interpretation of thermal comfort using calculation of the PMV and PPD indices and local thermal comfort criteria, in: ISO 7730:2005, ISO, 2005.
- [12] DIN V 18599-6, Energy efficiency of buildings—Calculation of the net, final and primary energy demand for heating, cooling, ventilation, domestic hot water and lightening, DIN, Berlin, 2011.
- [13] Reglementation Thermique, Part of the French building regulation qua decret no. 2006-592 dated 24 May, in: RT2005, 2005.
- [14] J. Kurnitski, A. Saari, T. Kalamees, M. Vuolle, J. Niemelä, T. Tark, Cost optimal and nearly zero (nZEB) energy performance calculations for residential buildings with REHVA definition for nZEB national implementation, *Energy Build.* 43 (11) (2011) 3279–3288.
- [15] Ministry of Economic Affairs and Communication, Minimum requirements for energy performance, in: Regulation No 68, Ministry of Economic Affairs and Communication, 2013.
- [16] A. Bring, P. Sahlin, M. Vuolle, IEA SHC Task 22—Subtask B—Models for Building Indoor Climate and Energy Simulation, KTH, Building Sciences, Stockholm, 1999.
- [17] D.B. Crawley, J.W. Hand, K. Kummert, B.T. Griffith, Contrasting the capabilities of building energy performance simulation programs, *Build. Environ.* 43 (2008) (2008) 661–673.
- [18] T. Kalamees, J. Kurnitski, Estonian test reference year for energy calculations, in: Proceedings of the Estonian Academy of Sciences Engineering, 2006, pp. 40–58 (2006, 12. 1.).
- [19] American Society of Heating, Refrigerating and Air-Conditioning Engineers, Inc. (ASHRAE) Handbook Fundamentals 2001, American Society of Heating, Refrigerating and Air-Conditioning Engineers, Inc., 2001.
- [20] VDI 2067 Blatt 20:2000-08, Economic efficiency of building installations—energy effort of benefit transfer for water heating systems.
- [21] M. Bauer, Methoden zur Berechnung und Bewertung des Energieaufwandes für die Nutzenübergabe bei Warmwasserheizungen, University Stuttgart, Stuttgart, 1999 (PhD-Thesis).
- [22] G. Zhou, J. He, Thermal performance of a radiant floor heating system with different heat storage materials and heating pipes, *Appl. Energy* 138 (January) (2015) 648–660.
- [23] CEN, Radiators and convectors—Part 2: Test methods and rating, in: EN 442-2:1996/A2:2003, CEN, 2003.

## PAPER V

Maivel, M; Kurnitski, J (2013). Low Temperature Radiator Heating System Detailed Dynamic Simulation - Distribution and Emission Efficiency. CLIMA 2013, 11th REHVA World Congress and the 8<sup>th</sup> International Conference on Indoor Air Quality, Ventilation and Energy Conservation in Buildings. Prague, Czech Republic, on June 16 – 19, 2013. Elsevier.



# Low Temperature Radiator Heating System Detailed Dynamic Simulation - Distribution and Emission Efficiency

Mikk Maivel<sup>#1</sup>, Jarek Kurnitski<sup>#2</sup>

*#Faculty of Civil Engineering, Department of Structural Design, Tallinn University of Technology*

*Ehitajate tee 5, 19086, Tallinn, Estonia*

<sup>1</sup>mikk.maivel@ttu.ee

<sup>2</sup>jarek.kurnitski@ttu.ee

## **Abstract**

*According to the Energy Performance of Buildings directive 2010/31/EU after 31. December 2020 all new buildings must be nearly-zero-energy buildings; that require also high efficiency heating systems. In a cold climate space heating dominates in the energy balance of residential buildings stressing the importance of low system losses. In this paper low-temperature radiator heating systems and other options to reduce distribution losses are studied. We modeled radiators, distribution pipes, connection pipes in the dynamic building simulation software and conducted a fully dynamic calculation for a model detached house with 8 calculation zones. All simulations were conducted with dynamic building simulations software IDA-ICE 4.5. Input data was from the reference detached house which was chosen to the Estonian cost optimal calculations. Results show detailed recoverable and non-recoverable distribution and emission losses. From non-recoverable losses distribution and emission efficiency of the heating systems was calculated with selected system configuration and sizing options. These efficiency values allow determining tabulated efficiencies values used in energy calculation methods and building codes.*

**Keywords** – *low-temperature radiator heating system; dynamic simulation; distribution efficiency; emission efficiency; energy efficiency (key words)*

## **1. Introduction**

Widely used space heating systems in Northern climate are radiator and floor heating systems or their combinations. Air heating systems aren't common and usually do not cover the heat losses of the building i.e. it is necessary to have an additional heating system to ensure proper indoor climate conditions according to CEN standard [1].

European Commission has issued a directive of 2010/31/EU [2]. The objective of this directive is to promote the improvement of energy performance of buildings. This directive requires a calculation of the energy

performance of the building including heating, ventilation, cooling and lighting systems, based on primary energy. In a cold climate space heating dominates in the energy balance of residential buildings (according to the earlier research space heating accounts nearly 70 % of the whole yearly detached building energy consumption [3]). It demonstrates the importance of low heating system losses. Earlier investigations, which was based on the CEN standards show that heating system losses are 10 – 20 % [4]. According to CEN standard, there are three types of losses: system thermal losses; auxiliary energy consumption; recoverable system thermal losses [5]. This paper concentrates on system thermal losses which consist of distribution and emission losses. Emission losses include heat loss due to non-uniform temperature distribution (neglected because influence is small [6], but used simulation software have possibility to consider it), heat loss due to heat emitter position and heat loss due to control indoor temperature.

The model of detailed dynamic radiator heating system is used to compare low-temperature radiator heating system with conventional radiator heating system. Heat outputs from pipes and radiators are used to determine distribution and emission efficiency of the studied systems.

## **2. Building and HVAC Systems**

Analyzed building is typical recently built detached house, which has been chosen in earlier study for reference building in Estonian cost optimal calculations [7]. Investigated building is two-story with heated area of 178 m<sup>2</sup>. Building has 3 bedrooms, sauna and living room together with kitchen (Figure 1). Main building elements thermal transmittance values are presented in the Table 1. Room set-point temperature during analyze was 21 °C. Heating system supply water temperature is outdoor air temperature compensated; i.e. the supply water temperature increases as the outdoor temperature decreases. Two temperature curves 45 °C/35 °C or 70 °C/55 °C were used (Figure 2, 3). 45 °C/35 °C will describe low-temperature curve and 70 °C/55 °C conventionally used curve. There is no cooling system in the building. Mechanical supply-exhaust ventilation system with plate heat exchanger (heat recovery figure up to 80 %; supply air temperature during the winter +18 °C) was used. Constant pressure circulation pump were used in all simulation cases. All energy calculation input data follows the Estonian regulation of minimum requirements for energy performance [8].

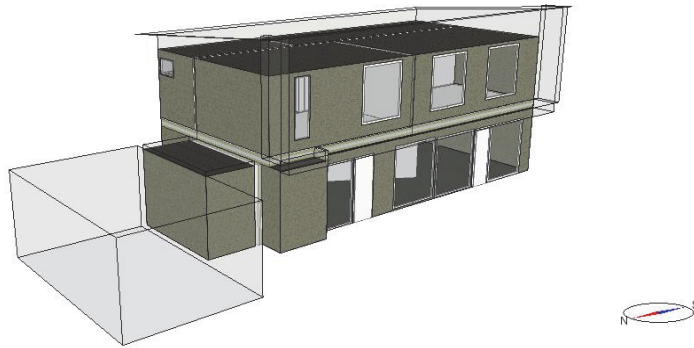


Figure 1 Analyzed building 3D view

Table 1 Thermal transmittance values for main building envelope elements

No.	Building envelope element	U-value (W/(m <sup>2</sup> K))
1	Exterior wall	0.17
2	Roof	0.14
3	Ground floor	0.17
4	Windows (g=0.5)	0.8

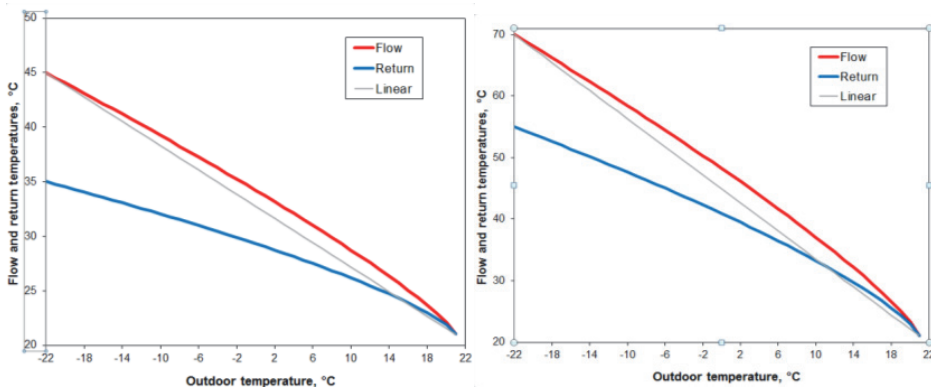


Figure 2 Studied heating curves, 45 °C/ 35 °C (left) and 70 °C/ 55 °C (right)

### 3. Method and Model Overview

All calculations were done with dynamic simulation software IDA Indoor Climate and Energy 4.5 [9]. Outdoor climate is Estonian test reference year [10]. Dynamic simulation model have 8 different zones (Figure 3), each room have on zone. Internal gains (lightening, equipment, occupants) for zones where all chosen from Estonian regulation of minimum requirements for energy performance [8]. Unheated garage was eliminated because it doesn't influence space heating demand.

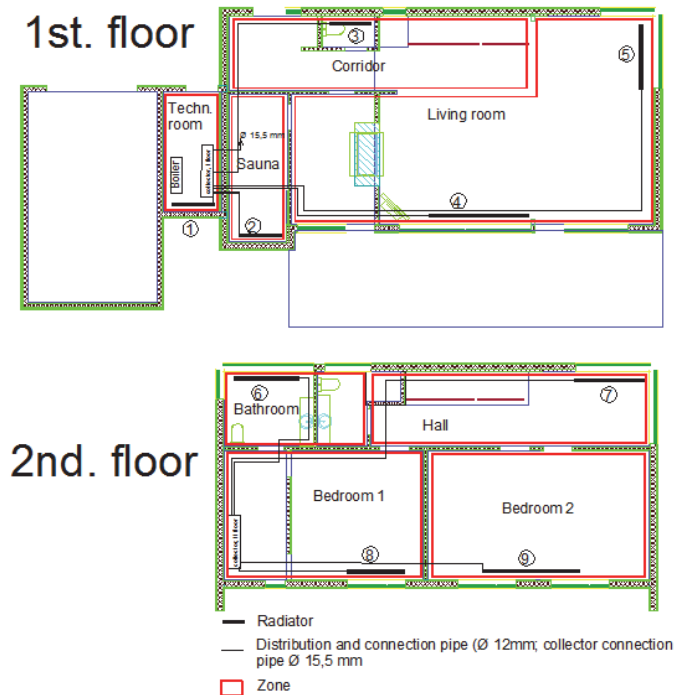


Figure 3 Analyzed building and location of zones and heating system

All rooms (except living room) have one radiator. All radiator connection pipes are alupex-type pipe 16x2.0 (inner diameter 12 mm) and distribution pipes alupex 20x2.25 (inner diameter 15.5 mm). Whole system consist two collectors and 2-pipe system connection and distribution pipes. Connection pipes are defined as the pipes located in the room where radiator is. Distribution pipes are pipes which doesn't serve the room where they are located (i.e. distribution pipes aren't connected with room heaters) (Figure 4). Depending on the calculation case, pipes were not insulated, distribution pipes were insulated or all pipes were insulated.

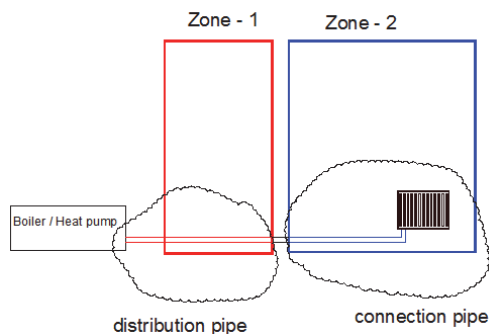


Figure 4 Definition of connection/distribution pipes used in the heat output analyses.

The heating system was modeled with pipe and dynamic radiator models (non-standard models) and the standard models were used for controllers, boiler and circulation pump. The Pipe-model is based on ASHRAE handbook heat transfer equations [11]. One important part of thermal losses can be caused by control of indoor temperature. Because the study focused on distribution and heat emitter losses, the PI (proportional-integral control) controller providing almost ideal control was used. Comparative simulation for P (proportional control) and PI (proportional-integral control) controller is shown in Figure 5. Results shows that PI controller could keep more accurately the room set-point temperature and avoid overheating which is typical for P controller. PI-controller determines directly the radiator mass flow up to the design mass flow, independently of available pressure (ideal flow control) [12].

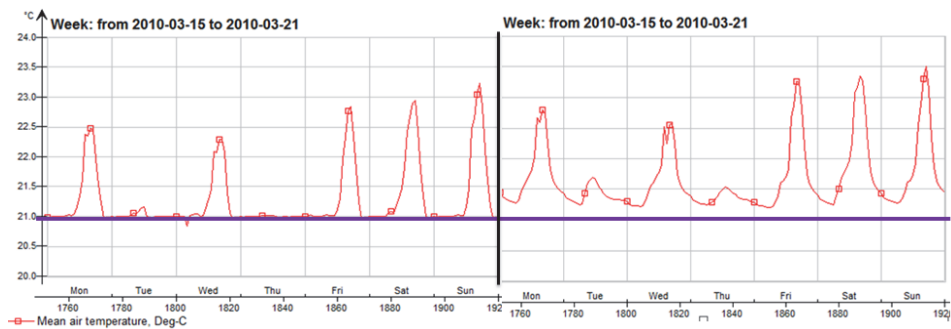


Figure 5 The effect of controller type on room temperature (PI controller on the left; P controller on the right)

The model with all pipe, controller and radiator components describes accurately the real system and includes detailed radiator model, where radiators have mass [12]. Radiators have real dimensions, location in room (connected with the chosen external wall) and dynamic model takes into account the additional heat loss from the backside of the radiator (model calculates the difference of external wall heat losses from mean air temperature and heat loss due to raised temperature by the radiator).

#### 4. Results and Discussion

The reference, ideal heating system with which all other cases were compared, was the model without pipes, without radiator mass and with eliminated additional heat loss behind the radiators to back wall. 12 cases with different insulation options, controller types and temperature curves shown in Table 2 were simulated.

Table 2 The reference (No 0) and other 12 simulation cases

No.	Radiator type	Control type	Temp. graph.	Insulation			Distribution and emission losses ( $1/\eta$ ), %	Distribution and emission efficiency, $\eta$
				D	C	A		
0	Ideal heater	PI	45 °C/ 35 °C	-	-	-	0.00	1.000
1	Detailed radiator *	PI	45 °C/ 35 °C	-	-	-	1.35	0.987
2	Detailed radiator (without pipes)	PI	45 °C/ 35 °C	-	-	-	1.56	0.985
3	Detailed radiator	PI	45 °C/ 35 °C	-	-	-	1.63	0.984
4	Detailed radiator (no mass)	PI	45 °C/ 35 °C	-	-	-	1.68	0.983
5	Detailed radiator (partly insulated)	PI	45 °C/ 35 °C	+	-	-	1.63	0.984
6	Detailed radiator (insulated)	PI	45 °C/ 35 °C	+	+	-	1.57	0.985
7	Detailed radiator	PI	70 °C/ 55 °C	-	-	-	7.21	0.933
8	Detailed radiator *	PI	70 °C/ 55 °C	-	-	-	7.06	0.934
9	Detailed radiator (partly insulated)	PI	70 °C/ 55 °C	+	-	-	6.61	0.938
10	Detailed radiator (insulated)	PI	70 °C/ 55 °C	+	+	-	6.15	0.942
11	Detailed radiator (insulated 100 mm)	PI	70 °C/ 55 °C	-	-	+	6.00	0.943
12	Detailed radiator *	P	45 °C/ 35 °C	-	-	-	10.38	0.906

\*Radiator without additional heat losses behind the radiator to the back wall, and without pipes.

D – distribution pipe (insulation 40 mm); C – connection pipe (insulation 20 mm); A – all pipes (insulation 100 mm).

In Table 2, also the main results, distribution and emission losses are shown. The losses are defined as non-recoverable additional loss to space heating energy need in %. The efficiency  $\eta$  is the reciprocal value, i.e. the losses can be calculated as  $1/\eta$ . For example,  $\eta=0.97$  equals to losses of  $1/0.97=1.031$ , i.e. 3.1%. Simulated efficiencies of conventional heating curve 70 °C/ 55°C can be compared with EN 15316-2-1:2007 tabulated values. These CEN standard tabulated efficiencies include the losses caused by vertical air temperature profile; air temperature control; specific losses of the external components (embedded systems) and distribution losses. For the case no 7 with simulated efficiency of 0.93 the standard gives 0.91. [5]

In the cases with low-temperature heating curve (No. 1-6) the losses were very small indicating that losses are mainly recoverable, because they almost fully utilized in the rooms.

Boiler output compared to delivered energy in different zones were analyzed in cases where different insulation levels were studied. Heat output results from zones show that delivered energy differences in zones were higher than it would be calculated with building based efficiency, e.g. in 70 °C/ 55°C temperature curve building delivered energy losses were approximately 5 % (Figure 6), but to compare in one zone - Sauna the difference were even up to 50 %.

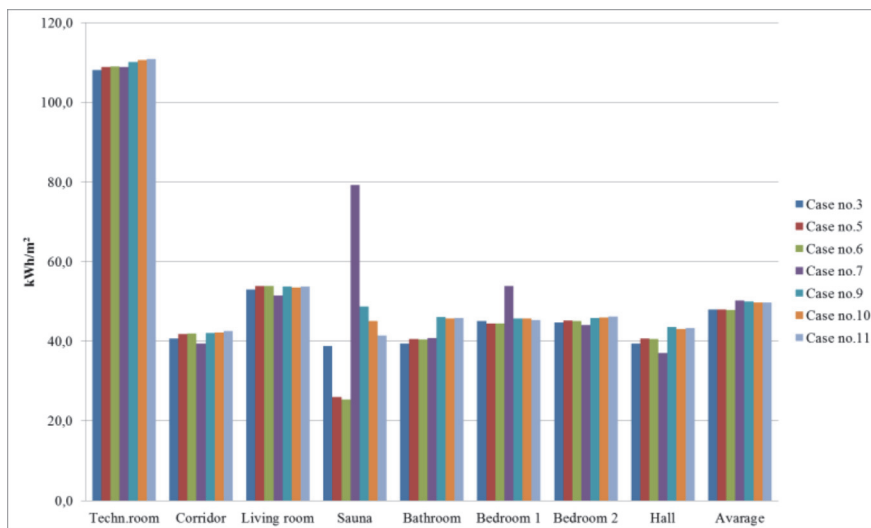


Figure 6 Delivered space heating energy to zones in simulated cases (3,5,6 temp. curve 45°C/ 35°C and 7,9,10,11 temp. curve 70°C/55°C)

Comparisons of zone mean air temperatures in different cases help to explain losses. Indoor air temperatures were compared in zone Sauna, where delivered energy use differences were extremely high due to distribution pipe

heat emissions and Bedroom 2 where differences were trivial (Figure 7, Figure 8).

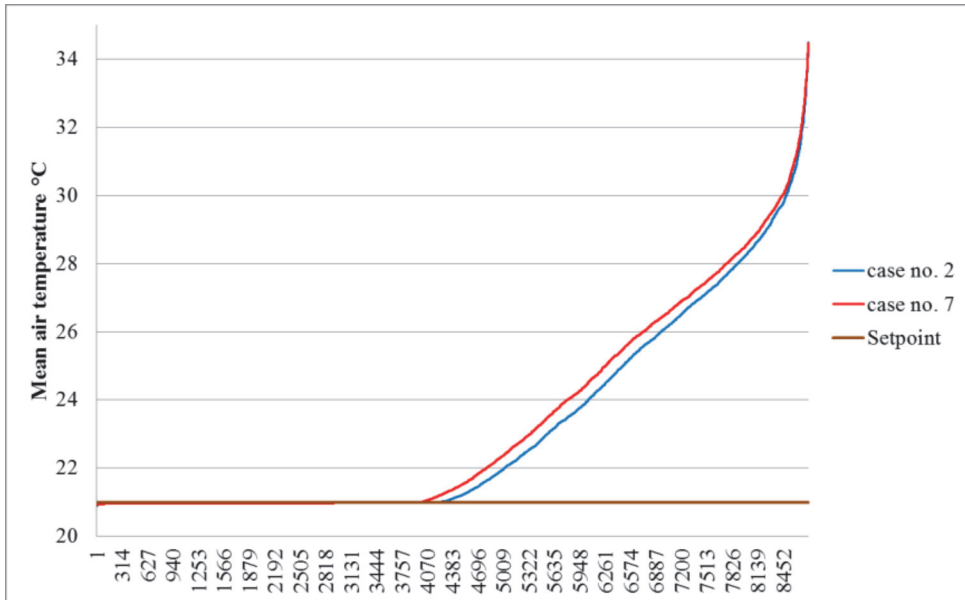


Figure 7 Sauna mean air temperature duration curve in different cases (cases with different temp. curves and different insulation levels).

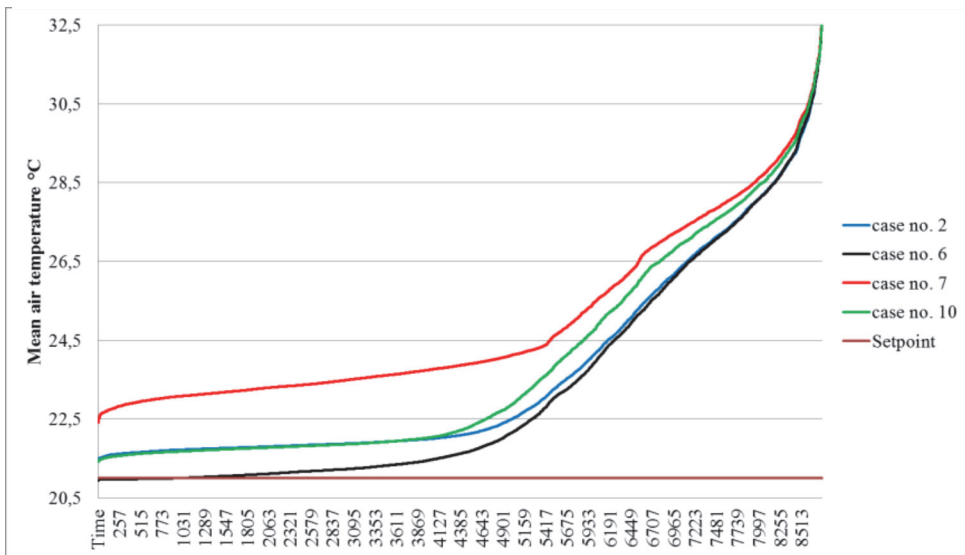


Figure 8 Mean air temperature duration curve in Bedroom 2 (cases only with different temp. curves because Bedroom 2 haven't distribution pipes i.e. case no 6 is equal to case no 2 and case no 10 is equal to case no. 7)

High differences in delivered energy in Sauna and Bedroom 2 were explained by elevated room air temperature. Because of that, in rooms next to Sauna delivered heat is lower as Sauna has high heat losses to the neighbor zones.

In Bedroom 2 mean air temperature was a little bit higher with 70 °C/ 55°C heating curve that is caused by higher share of radiation with higher temperature curve.

Beside comparing delivered energy also heat emissions to the rooms were analyzed in different simulation cases. Annual share of pipes and radiator shows that more or less recoverable heat losses were in uninsulated cases approximately 20 to 40 % (i.e. emitted heat comes to zone by pipes (depending heating curve), but by insulated cases the recoverable losses were 10 to 15 (Figure 9).

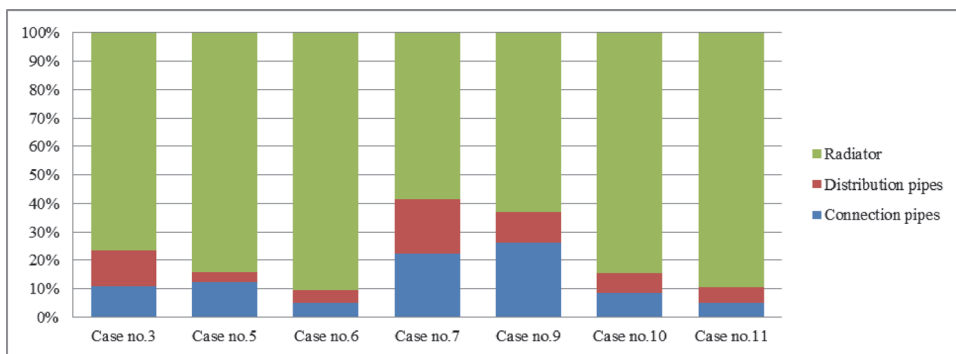


Figure 9 Distribution of heat emissions to the rooms

From the temperature curve in Figure 8 it may be expected that some differences can be caused by radiation heat transfers. Figure 10 shows that the heat emitted to room by the front panel of radiator is significantly higher with 70 °C/ 55°C heating curve.

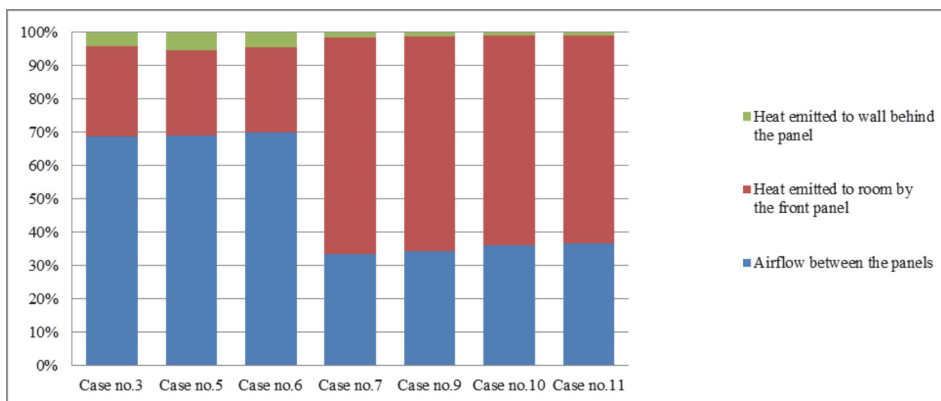


Figure 10 Distribution of radiators heat emissions

## 5. Conclusion

Emission heat losses of radiators in well insulated new detached house were extremely low with PI controller. Heat emission from radiators (with additional heat loss behind the radiator to the back wall) had efficiency of 0.99 with both temperature curves studied. Distribution efficiency with 45 °C/35 °C heating curve was also remarkably high of 0.984. 70 °C/55 °C heating curve caused much lower distribution efficiency of 0.933 caused by slightly higher mean air temperature in few rooms and lower utilization of heat losses from pipes. It may be concluded that studied low temperature radiator system (45 °C /35 °C) led to almost fully recoverable distribution losses even with not insulated distribution and connection pipes in a detached house in a cold climate. Emission losses of radiators with PI controllers were negligible in all cases because of well insulated external walls.

## 6. Acknowledgment

The research was supported by the Estonian Research Council, with Institutional research funding grant IUT1–15, and with a grant of the European Union, the European Social Fund, Mobilitas grant No MTT74.

## 7. References

- [1] EN 15251:2007. Indoor environmental input parameters for design and assessment of energy performance of buildings addressing indoor air quality, thermal environment, lighting and acoustics.
- [2] Directive 2010/31/EU of the European Parliament and of the Council of 19 May 2010 on the energy performance of buildings.
- [3] Maivel, M.; Kuusk, K. (2009). Energy consumption and indoor climate analysis in detached houses. In: Proceedings of the 2nd WSEAS International Conference on URBAN REHABILITATION AND SUSTAINABILITY (URES '09): WSEAS International Conferences, Baltimore, USA, November 7-9, 2009. WSEAS, 2009, 97 - 102.
- [4] Olesen B.W., M. de Carli (2011). Calculation of the yearly energy performance of heating systems based on the European Building Energy Directive and related CEN standards. *Energy and Buildings*, 43, 1040 - 1050.
- [5] EN 15316-2-1:2007. Heating systems in buildings - Method for calculation of system energy requirements and system efficiencies - Part 2-1: Space heating emission systems.
- [6] Hasan, A.; Kurnitski, J.; Jokiranta, K. (2009). A combined low temperature water heating system consisting of radiators and floor heating. *Energy and Buildings*, 41(2009), 470-479.
- [7] Kurnitski, J.; Saari, A.; Kalamees, T.; Vuolle, M.; Niemelä, J.; Tark, T. (2011). Cost optimal and nearly zero (nZEB) energy performance calculations for residential buildings with REHVA definition for nZEB national implementation. *Energy and Buildings*, 43(11), 3279 - 3288.
- [8] Ministry of Economic Affairs and Communication no 258 (2007) „Minimum requirements for energy performance”.
- [9] Bring, A.; Sahlin, P.; Vuolle, M. (1999) IEA SHC Task 22 - Subtask B - Models for Building Indoor Climate and Energy Simulation
- [10] Kalamees, T., Kurnitski, J. (2006). Estonian test reference year for energy calculations.–In :Proceedings of the Estonian Academy of Sciences Engineering, 2006, 12, 1, p. 40-58.
- [11] American Society of Heating, Refrigerating and Air-Conditioning Engineers, Inc. (ASHRAE) handbook Fundamentals.

[12] Sahlin, P.; Eriksson, L.; Grozman, P.; Johansson, H.; Shapovalov, A.; Vuolle, M. (2012). Whole-building simulation with symbolic DAE equations and general purpose solvers. Building and Environment, BAE905.



## PAPER VI

Maivel, M.; Kurnitski, J. (2014). Heating System Return Temperature Effect on Heat Pump Performance. In: 11th International Energy Agency Heat Pump Conference 2014 Conference Proceedings: 11<sup>th</sup> International Energy Agency Heat Pump Conference Montreal, May 12-16, 2014. International Energy Agency.



## HEATING SYSTEM RETURN TEMPERATURE EFFECT ON HEAT PUMP PERFORMANCE

*M. Maivel, early-stage researcher, J. Kurnitski, Professor  
Tallinn University of Technology  
Tallinn, Estonia*

**Abstract.** The revision of EPBD directive raises the role of increasing heating system efficiency. Due to low primary energy consumption heat pumps will be one of the key solutions for residential sector where district heating network are far. Statistical data shows that heat pumps will replace fossil fuel boilers. The aim of the study was to quantify the return temperature effect on heat pump performance. There are several studies for improving heat pump efficiency on component level, but analyzing whole annual heating system efficiency with detailed dynamical heating system model is previously not analyzed enough deeply. Simulated results with IDA-ESBO heat pump model were compared to laboratory measurements of a heat pump performance at different testing points. Based on measurements the correlation between heating system flow/return temperature and condensing temperature were derived. Results show that calculation with derived condensing temperature correlation gave about 7% higher seasonal performance factor compared to IDA-ESBO simulation model stressing the effect of relatively low return temperature in a radiator heating system.

**Key Words:** dynamic simulation, heat pump seasonal efficiency, calculating SPF

### List of nomenclature:

COP – coefficient of performance

SPF – seasonal performance factor

## 1 INTRODUCTION

Heat pump heating systems are popular and widely used for preparing domestic hot water and space heating in all over the Europe especially in Nordic countries. By common solutions heat pump is connected with floor heating system where temperature curve is lower than conventional radiator heating system. According to recent study in low-energy buildings it is also possible to use low temperature radiator heating system [1]. Radiator system temperature drop is higher compared with floor heating and it insures lower return water temperature, which have an effect on heat pump performance. Mostly existing heat pump models does not consider return water temperature and they are more suitable for floor heating systems.

Heat pump COP is influenced by working mode i.e. space heating or preparing domestic hot water. This paper will concentrate on space heating mode therefore energy need for space heating is dynamic process; energy need for domestic hot water is influenced by usage profile. Heat pump performance testing is described in EN14511-2 [2]. IEA HPP (International Energy Agency Heat Pump Program has launched Annex 28 to compare different standards [3]. Karlsson work under IEA HPP Annex 28 include heat pump tests by both standards and it resulted that the former standard EN 255-2 [4] gives higher COP values compared to EN 14511-2 duo to mass-flows that were not defined in EN 255 and it resulted in unrealistic low inlet condensing temperatures in a few testing points. According to the EN 14511-2 heat pumps were tested at standard rating conditions temperature difference

of 5 °C (for outlet temperature up to 45 °C). Karlsson’s test results show that heat pump COP is influenced by condenser inlet temperature (i.e. lowering return water temperature will increase heat pump performance).

In this paper it is shown by dynamic simulation model that condenser inlet temperature have an impact on heat pump COP. Many heat pump models are prepared to quantify the heat pump performance in working conditions, but most of such models won’t consider condenser inlet temperature and are more suitable for systems with small delta T. The effect of large temperature drops of a radiator heating systems are quantified in this paper.

## 2 METHODS

Two methods were used to calculate the heat pump performance as a function of heating system flow/return temperature. In first step dynamic simulation were conducted with IDA-ICE simulation software including a heat pump model. Afterwards, the laboratory test results of heat pump performance were used to calculate heat pump performance manually. According to measurements the correlation of the condensing temperature was derived to calculate simplified heat pump seasonal performance ratio with simulated heating system flow/return temperatures. Therefore, the derived correlation was applied for whole building/heating system simulation model results, and the heat pump was operated with real flow/return temperatures changing at each time step.

### 2.1 Dynamic Model of Heat Pump Heating System

Analyzed building is typical recently built detached house, which has been chosen in earlier study for reference building in Estonian cost optimal calculations [5]. Investigated building is two-story with heated area of 178 m<sup>2</sup>. Building has 3 bedrooms, sauna and living room together with kitchen (Figure 1, left). Main building elements thermal transmittance values are presented in the Table 1. Room set-point temperature during analyze was 21 °C. Heating system supply water temperature is outdoor air temperature compensated i.e. the supply water temperature increases as the outdoor temperature decreases. Low-temperature radiator heating system has simulated by temperature curve of 45 °C/35 °C (**Error! Reference source not found.**1, right). There is no cooling system in the building. Mechanical supply-exhaust ventilation system with plate heat exchanger (heat recovery efficiency of 80%; supply air temperature during the winter +18 °C) was used. All energy calculation input data follows the Estonian regulation of minimum requirements for energy performance [6].

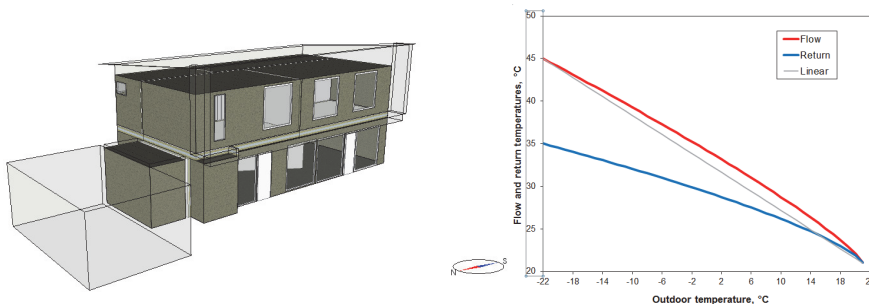


Figure 1 Analyzed building 3D view (left) and heating curve 45 °C/ 35 °C (right).

Table 1 Thermal transmittance values for main building envelope elements.

No.	Building envelope element	U-value (W/(m <sup>2</sup> K))
1	Exterior wall	0.17 W/(m <sup>2</sup> K)
2	Roof	0.14 W/(m <sup>2</sup> K)
3	Ground floor	0.17 W/(m <sup>2</sup> K)
4	Windows (g=0.5)	0.8 W/(m <sup>2</sup> K)

Detailed overview about dynamic heating system simulation model can be find in previous paper [1]. Standard plant model were replaced to IDA ESBO plant model which include heat pump calculation model [7]. Selected heat pump is common on-off type pump with variable condensing temperature. Main parameters of investigated heat pump are shown in Table 2. In radiator heating system equipped with thermostatic valves, the water mass-flow fluctuates a lot and influences a temperature drop which is for most of the time much higher compared to standard testing value of 5°C temperature difference (Figure 2 left). Constant pressure circulation pump were used in all simulation cases and annual mass-flow in space heating circuit is shown in Figure 2 (right).

**Table 2 Basic information about heat pump.**

Producer/type	IVT Greenline HTPlus
Power	5 kW
$\Delta t_{\text{log,eva.}}$	8 °C
$\Delta t_{\text{log,cond.}}$	8 °C
$t_{\text{brine.in}}$	0 °C
$t_{\text{brine.out}}$	-3 °C
$t_{\text{water.in}}$	30 °C
$t_{\text{water.out}}$	35 °C
$\text{COP}_{\text{test,conditions}}$	4.3

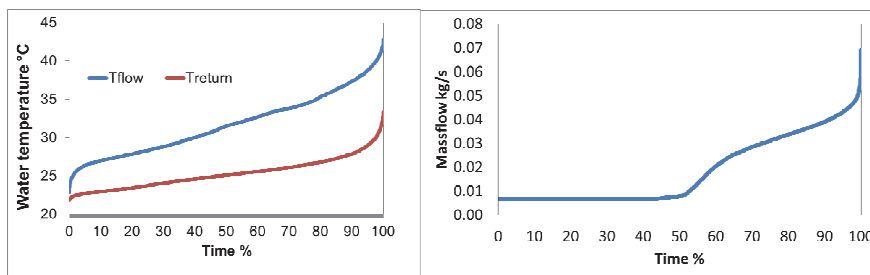


**Figure 2 Simulated flow and return temperature duration curves in radiator heating system (left) and annual mass flow duration curve in space heating circuit (right).**

## 2.2. Connection Scheme

On-off type heat pump model was connected to the heating system through stratification tank. This connection has three circulation pumps (between ground loop and evaporator; condenser and stratification tank and space heating system side pump). Stratification tank have usually additional top heater because heat pumps normally have designed to cover approximately 60% of heating power in design outdoor temperature [8] but in calculation the additional heater was neglected and selected heat pump was sized to cover building heat losses at design outdoor temperature which is in Tallinn -22 °C.

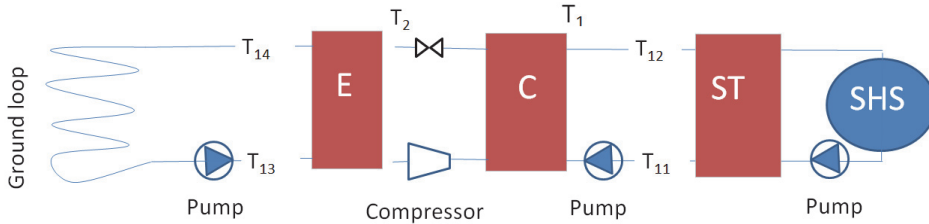


**Figure 3 Calculation scheme (E- evaporator; C- condenser; ST – stratification tank; SHS – space heating system).**

### 2.3. Basic Equations

The efficiency of heat pump can be expressed with the COP which is the quotation between the useful heating capacity and the power input (Equation 1). The theoretical upper limit for the COP of a heat pump operating between the condensation temperature and evaporation temperature is expressed by the Carnot coefficient of performance. The real COP should consider the compressor power factor or cycle efficiency (Equation 2).

$$COP_c = \frac{Q_1}{W} = \frac{T_2}{T_1 - T_2} + 1 \quad (1)$$

$COP_c$  is Carnot coefficient of performance;  $Q_1$  is a useful heating capacity (W),  $W$  is a power input (W);  $T_1$  is a condensing absolute temperature (K);  $T_2$  is an evaporating absolute temperature (K).

$$COP_r = COP_c * \eta \quad (2)$$

$COP_r$  is real heat pump coefficient of the performance;  $\eta$  is device efficiency, which is in a range of 0.4...0.6 for conventional domestic heat pumps [8]. Heat pump SPF was calculated by equation 3.

$$SPF = \frac{\phi}{P} \quad (3)$$

where  $\phi$  is produced energy by heat pump (kWh/a),  $P$  is used electrical energy for producing energy (kWh/a).

#### 2.2.1 IDA-ESBO simulation

In ordinary heat pump selection programs the condensing temperatures calculated from condenser outlet temperature (heating system flow temperature). IDA-ESBO heat pump model includes physical models of heat exchangers. Water side heat balance is given with Equation 4 and heat exchanger with Equation 5. These equations allow to derive condensing temperature equation (6).

$$Q_1 = m * C_p * (T_{12} - T_{11}) \quad (4)$$

$Q_1$  is heat flux from heat exchanger (condenser) W;  $m$  is mass flow in space heating circuit kg/s;  $C_p$  is specific heat of water (J/kgK);  $T_{11}$  is return water temperature from space heating circuit K;  $T_{12}$  is flow water temperature from space heating circuit K.

$$Q_1 = U * A * \frac{(T_{12} - T_{11})}{\ln\left(\frac{T_1 - T_{11}}{T_1 - T_{12}}\right)} \quad (5)$$

$U$  is condenser heat transfer coefficient W/ (m<sup>2</sup>K);  $A$  is condenser area m<sup>2</sup>;  $T_1$  is condensing temperature K.

$$T_1 = T_{11} + \frac{T_{12} - T_{11}}{(1 - \text{EXP}(-\frac{U * A}{m * C_p}))} \quad (6)$$

Equation 6 is illustrated in Figure 4 showing the dependency between return and condensing temperature at constant flow temperature of 50 °C and constant heat exchanger conductance of 200 W/K

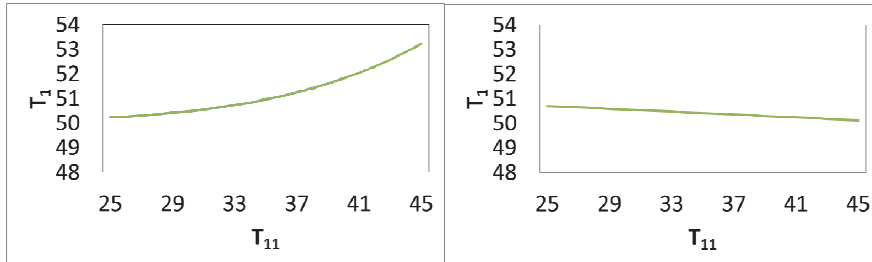


**Figure 4 Dependency between return and condensing temperature in the case of constant power of 1000 W(left) and constant mass-flow (right) of 0.012 kg/s at constant flow (T<sub>12</sub>) temperature of 50°C**

**2.2.2 Hand Calculations with Measured Correlation**

In real heat pump working process condensing temperature is not conditionally constant i.e. heat exchanger heat transfer is dynamic process. A correlation was derived for condensing temperature as a function of flow and return temperature. For that purpose the laboratory measurements were made for a domestic on-off type ground source heat pump with variable condensing at constant flow temperature and heat pump heating capacity and four different return temperatures.

**3 RESULTS**

Results are presented in two chapters. First, seasonal coefficient of performance value is calculated with IDA-ESBO. Second part covers the derivation of variable condensing temperature formula from laboratory test measurement and SPF calculation.

**3.1. Constant Refrigerant Temperature Heat Exchanger**

For making hand calculations with equation 1 and 2, heat pump annual efficiency  $\eta$  was first calculated with IDA-ESBO simulation. Hourly  $\eta$  values calculated with equation 2 were in the range of 0.50...0.63 with an average efficiency value  $\eta = 0.57$ . In figure 5 corresponding hourly COP values of IDA ESBO simulation; Carnot ideal process with equation 1 (evaporating and condensing temperature from ESBO results) and hand calculated with equation 2 with heat pump efficiency of 0.57 are shown.

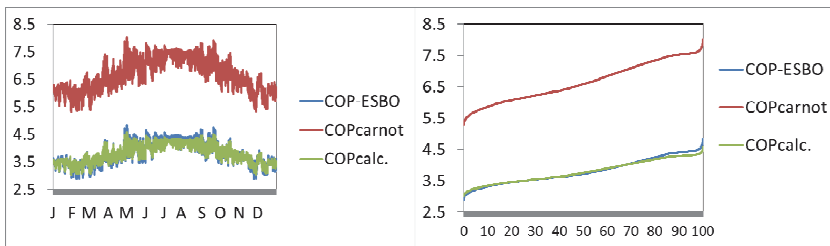


**Figure 5 Hourly COP values (left) and the duration curve (right), calculated with simulated evaporating and condensing temperatures.**

Results in Figure 5 show that hand calculation with constant heat pump efficiency value of 0.57 gave accurate results on annual bases. In next step, the condensing temperature was calculated with equation 5 from flow/return temperatures, and the result is compared to IDA-ESBO condensing temperature in Figure 6.

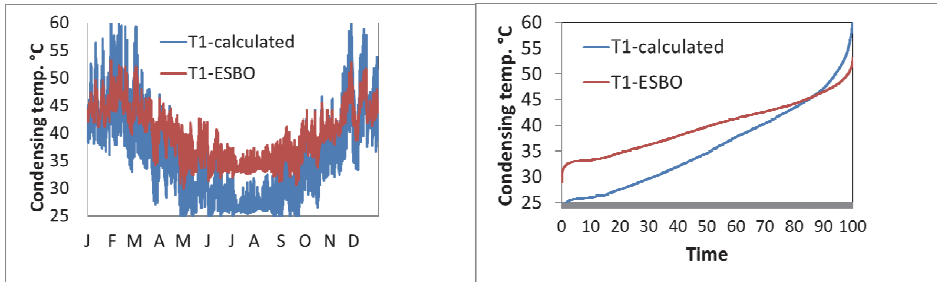


**Figure 6 Hourly based condensing temperature values by IDA simulation and by handmade calculation (left) and duration curve of condensing temperature values (right).**

Differences exist, IDA-ESBO simulation provided average condensing temperature 39.8°C and hand calculation 35.9°C. However, the differences mainly occur during summer and period with very low heating need. From calculated hourly condensing temperatures, hourly COP values were calculated with an average constant evaporation temperature of -8°C. Figure 7 describes the difference of IDA-ESBO calculated hourly COP values from hand calculated COP showing an annual average value of 3.80 vs. 4.12 respectively. Such a large difference in COP values resulted only in minor difference in the seasonal coefficient of performance being 3.48 in IDA-ESBO simulation and 3.44 in hand calculation (the difference ~1.2%). This shows that the difference of COP hourly values at low or missing heating need did not affected the results.

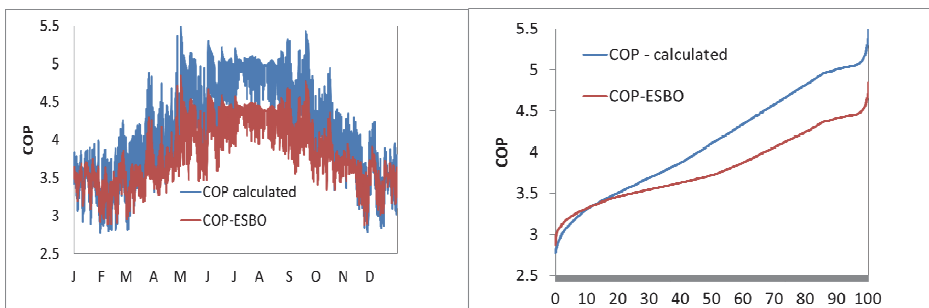


**Figure 7 Comparison of IDA-ESBO COP values with hand calculation (left- hourly values and right the duration curve of COP values).**

### 3.2. Condensing Temperature Correlation

Laboratory measurements data was used to describe the measured condensing temperature as a function of heating system flow/return temperatures with simple correlation equation. Results of the laboratory measurements with a flow temperature of about 50 °C for wide range of return temperatures are shown in Table 3.

**Table 3 Laboratory measurement results (T2 – evaporating temperature °C) of the heat pump performance.**

	T <sub>1</sub>	T <sub>2</sub>	EER <sub>Carnot</sub>	EER <sub>lab .measure</sub>	□	T <sub>11</sub>	T <sub>12</sub>	Avg. kW	Volume flow l/s	U*A <sub>radiator</sub>
Case 1	45.06	-6.98	5.11	2.31	0.45	29.64	49.62	8.09	0.36	0.45
Case 2	46.98	-6.69	4.96	2.15	0.43	35.38	50.05	7.94	0.48	0.36
Case 3	48.67	-6.64	4.82	1.97	0.41	40.15	49.98	7.79	0.7	0.31
Case 4	50.88	-6.87	4.61	1.81	0.39	44.99	50.01	7.56	1.33	0.28

Measured results show that the lower return temperature decreased the condensing temperature resulting in higher COP<sub>Carnot</sub> (Figure 8). Decrease of condensing temperature by 12.9% increased the COP by about 9%.

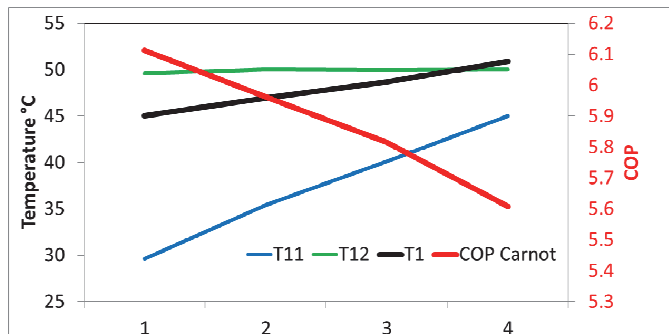


**Figure 8 Laboratory measurements showing the effect of return temperature on condensing temperature and resulting COP in four measurement points.**

Best fitting of condensing temperature as a function of flow and return temperature was found. The equation  $T_1 = 0.67T_{12} + 0.36T_{11} + 1.05$  with slightly higher impact on flow temperature, than the equation based on average of flow and return temperature, provided the best R<sup>2</sup> value as shown in Figure 9.

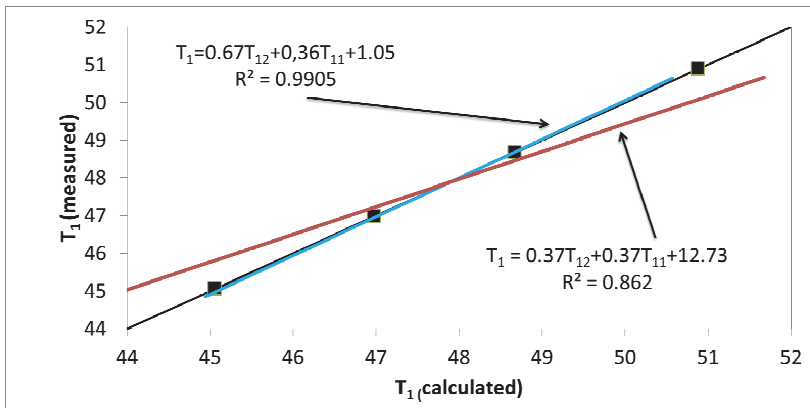


**Figure 9 Condensing temperature correlation equation.**

Hourly COP values calculated with the derived correlation (evaporating temperature was taken again as a constant of -8°C) are shown in Figure 10. Heating system hourly flow and return temperatures were taken from IDA ICE dynamic simulation. Average value of hourly

COP values was 4.12. The data calculated with the correlation in figure 10 resulted in SPF of 3.72 which was 6.9 % higher than that of hand calculation result with condenser model (SPF= 3.44).

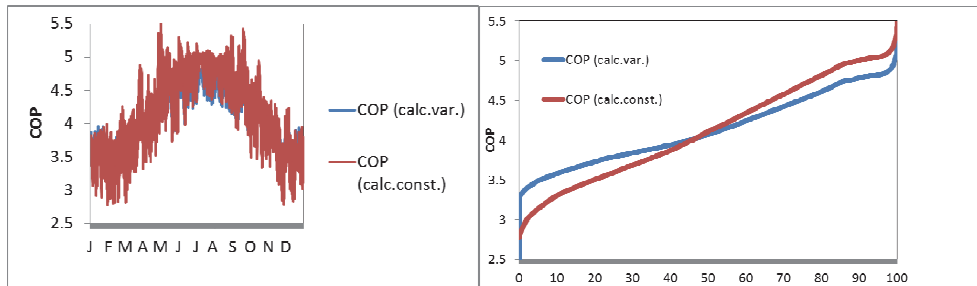


**Figure 10 Comparison hourly COP (left) and the duration curve (right) of hand calculation with condenser model and derived correlation.**

#### 4 CONCLUSION

In this paper the heating system return temperature effect on condensation temperature of the heat pump was quantified based on laboratory measurements and IDA-ESBO heat pump model. Results show that IDA-ESBO dynamic simulation together with detailed outdoor temperature controlled heating system model gave very similar SPF value than that calculated with constant refrigerant temperature condenser model, 3.48 vs. 3.44 respectively. Hourly calculation with derived condensing temperature correlation stressed the effect of relatively low return temperature in a radiator heating system and provided about 7% higher SFP value of 3.72.

#### ACKNOWLEDGEMENT

The research was supported by the Estonian Research Council, with Institutional research funding grant IUT1–15, and with a grant of the European Union, the European Social Fund, Mobilitas grant No MTT74.

#### 5 REFERENCES

- [1] Maivel, M.; Kurnitski, J. (2013). Low Temperature Radiator Heating Distribution and Emission Efficiency in Residential Buildings. *Energy and Buildings*, 69C, 224 - 236.
- [2] EN 14511-2, Air conditioners, liquid chilling packages and heat pumps with electrically driven compressors for space heating and cooling - Part 2: Test conditions. 2013, CEN, Brussels, Belgium.
- [3] Test procedure and seasonal performance calculation for residential heat pumps with combined space and domestic hot water heating - Swedish country report for IEA HPP Annex 28 SP Rapport 2004:38 Energy Technology Borås 2005
- [4] EN 255-2, Air conditioners, liquid chilling packages and heat pumps with electrically driven compressors - Heating mode - Part 2: Testing and requirements for marking for space heating units. 1997, CEN, Brussels, Belgium.
- [5] Kurnitski, J.; Saari, A.; Kalamees, T.; Vuolle, M.; Niemelä, J.; Tark, T. (2011). Cost optimal and nearly zero (nZEB) energy performance calculations for residential buildings with REHVA definition for nZEB national implementation. *Energy and Buildings*, 43(11), 3279 - 3288.
- [6] Ministry of Economic Affairs and Communication. Regulation no. 68 „Minimum requirements for energy performance”, 2013
- [7] IDA ESBO, <http://www.equaonline.com/esbo/IDAESBOUserguide.pdf>
- [8] Karlsson F. (2007). Capacity Control of Residential Heat Pump Heating System. Building Services Engineering, Department of Energy and Environment Chalmers University of Technology. Ph.D. thesis.

# CURRICULUM VITAE

## 1. Personal data

Name Mikk Maivel  
 Date and place of birth 05.09.1985, Tallinn, Estonia  
 E-mail address [mikkmaivel@gmail.com](mailto:mikkmaivel@gmail.com)

## 2. Education

Educational institution	Graduation year	Education (field of study/degree)
Tallinn University of Technology	2009	Environmental Engineering Master of Science
Tallinn Technical Secondary School	2004	Secondary education

## 3. Language competence/skills (fluent, average, basic skills)

Language	Level
Estonian	Native language
English	Intermediate level
Russian	Basic level

## 4. Special courses

Period	Educational or other organisation
17.-18.02.2010	Solar energy systems. Tallinn University of Technology
15-18.06.2010	Use of Solar Energy in Heating and Cooling of Buildings. Tallinn University of Technology
21.06.2010; 16-17.09.2010	Simulation and optimisation of indoor climate and energy use of buildings. Aalto University
13.– 16.12.2010	Post-graduate seminar on HVAC net-zero energy buildings and on site renewable energy. Aalto University

## 5. Professional employment

Period	Organisation	Position
2014-	State Real Estate Ltd.	Project manager
2012-2015	Tallinn University of Technology	Early-stage researcher
2010-2014	Fund KredEx	Project manager

## **6. Research activity, including honours and thesis supervised**

Main research activity is related to HVAC systems and indoor climate problems  
Also, building simulations are closely related to the main activity.

### **Thesis supervised:**

- Olga Petrova, MSc. Analysis of Indoor Climate and Energy Consumption in Pae Secondary School. 2013.

# ELULOOKIRJELDUS

## 1. Isikuandmed

Ees- ja perekonnanimi Mikk Maivel  
Sünniaeg ja -koht 05.09.1985, Tallinn, Eesti  
Kodakondsus eesti  
E-posti aadress [mikkmaivel@gmail.com](mailto:mikkmaivel@gmail.com)

## 2. Hariduskäik

Õppeasutus (nimetus lõpetamise ajal)	Lõpetamise aeg	Haridus (eriala/kraad)
Tallinna Tehnikaülikool	2009	Keskonnatehnika, Tehnikateaduste magister
Tallinna Tehnikagümnaasium	2004	Keskharidus

## 3. Keelteoskus (alg-, kesk- või kõrgtase)

Keel	Tase
Eesti keel	Emakeel
Inglise keel	Keskase
Vene keel	Algtase

## 4. Täiendusõpe

Õppimise aeg	Täiendusõppe korraldaja nimetus
17.-18.02.2010	Solar energy systems. Tallinna Tehnikaülikool
15-18.06.2010	Use of Solar Energy in Heating and Cooling of Buildings. Tallinna Tehnikaülikool
21.06.2010; 16-17.09.2010	Simulation and optimisation of indoor climate and energy use of buildings. Aalto Ülikool
13.– 16.12.2010	Post-graduate seminar on HVAC net-zero energy buildings and on site renewable energy. Aalto Ülikool

## 5. Teenistuskäik

Töötamise aeg	Tööandja nimetus	Ametikoht
2014-	Riigi Kinnisvara AS	projektijuht
2012-2015	Tallinna Tehnikaülikool	nooremteadur
2010-2014	SA KredEx	projektijuht

## **6. Teadustegevus, sh tunnustused ja juhendatud lõputööd**

Peamine teadustöö on seotud hoone tehnosüsteemide ja sisekliimat puudutavate teemadega. Ka hoone energiasimulatsioonid on tihedalt seotud uurimisvaldkonnaga.

Juhendatud lõputööd:

- Olga Petrova, MSc. Pae Gümnaasiumi sisekliima ja energiatarbe analüüs. 2013.

**DISSERTATIONS DEFENDED AT  
TALLINN UNIVERSITY OF TECHNOLOGY ON  
*CIVIL ENGINEERING***

1. **Heino Mölder.** Cycle of Investigations to Improve the Efficiency and Reliability of Activated Sludge Process in Sewage Treatment Plants. 1992.
2. **Stellian Grabko.** Structure and Properties of Oil-Shale Portland Cement Concrete. 1993.
3. **Kent Arvidsson.** Analysis of Interacting Systems of Shear Walls, Coupled Shear Walls and Frames in Multi-Storey Buildings. 1996.
4. **Andrus Aavik.** Methodical Basis for the Evaluation of Pavement Structural Strength in Estonian Pavement Management System (EPMS). 2003.
5. **Priit Vilba.** Unstiffened Welded Thin-Walled Metal Girder under Uniform Loading. 2003.
6. **Irene Lill.** Evaluation of Labour Management Strategies in Construction. 2004.
7. **Juhan Idnurm.** Discrete Analysis of Cable-Supported Bridges. 2004.
8. **Arvo Iital.** Monitoring of Surface Water Quality in Small Agricultural Watersheds. Methodology and Optimization of monitoring Network. 2005.
9. **Liis Sipelgas.** Application of Satellite Data for Monitoring the Marine Environment. 2006.
10. **Ott Koppel.** Infrastruktuuri arvestus vertikaalselt integreeritud raudtee-ettevõtja korral: hinnakujunduse aspekt (Eesti peamise raudtee-ettevõtja näitel). 2006.
11. **Targo Kalamees.** Hygrothermal Criteria for Design and Simulation of Buildings. 2006.
12. **Raido Puust.** Probabilistic Leak Detection in Pipe Networks Using the SCEM-UA Algorithm. 2007.
13. **Sergei Zub.** Combined Treatment of Sulfate-Rich Molasses Wastewater from Yeast Industry. Technology Optimization. 2007.
14. **Alvina Reihan.** Analysis of Long-Term River Runoff Trends and Climate Change Impact on Water Resources in Estonia. 2008.
15. **Ain Valdmann.** On the Coastal Zone Management of the City of Tallinn under Natural and Anthropogenic Pressure. 2008.
16. **Ira Didenkulova.** Long Wave Dynamics in the Coastal Zone. 2008.

17. **Alvar Toode.** DHW Consumption, Consumption Profiles and Their Influence on Dimensioning of a District Heating Network. 2008.
18. **Annely Kuu.** Biological Diversity of Agricultural Soils in Estonia. 2008.
19. **Andres Tolli.** Hiina konteinerveed läbi Eesti Venemaale ja Hiinasse tagasisaadetavate tühjade konteinerite arvu vähendamise võimalused. 2008.
20. **Heiki Onton.** Investigation of the Causes of Deterioration of Old Reinforced Concrete Constructions and Possibilities of Their Restoration. 2008.
21. **Harri Moora.** Life Cycle Assessment as a Decision Support Tool for System optimisation – the Case of Waste Management in Estonia. 2009.
22. **Andres Kask.** Lithohydrodynamic Processes in the Tallinn Bay Area. 2009.
23. **Loreta Kelpšaitė.** Changing Properties of Wind Waves and Vessel Wakes on the Eastern Coast of the Baltic Sea. 2009.
24. **Dmitry Kurennoy.** Analysis of the Properties of Fast Ferry Wakes in the Context of Coastal Management. 2009.
25. **Egon Kivi.** Structural Behavior of Cable-Stayed Suspension Bridge Structure. 2009.
26. **Madis Ratassepp.** Wave Scattering at Discontinuities in Plates and Pipes. 2010.
27. **Tiia Pedusaar.** Management of Lake Ülemiste, a Drinking Water Reservoir. 2010.
28. **Karin Pachel.** Water Resources, Sustainable Use and Integrated Management in Estonia. 2010.
29. **Andrus Räämet.** Spatio-Temporal Variability of the Baltic Sea Wave Fields. 2010.
30. **Alar Just.** Structural Fire Design of Timber Frame Assemblies Insulated by Glass Wool and Covered by Gypsum Plasterboards. 2010.
31. **Toomas Liiv.** Experimental Analysis of Boundary Layer Dynamics in Plunging Breaking Wave. 2011.
32. **Martti Kiisa.** Discrete Analysis of Single-Pylon Suspension Bridges. 2011.
33. **Ivar Annus.** Development of Accelerating Pipe Flow Starting from Rest. 2011.
34. **Emlyn D. Q. Witt.** Risk Transfer and Construction Project Delivery Efficiency – Implications for Public Private Partnerships. 2012.
35. **Oxana Kurkina.** Nonlinear Dynamics of Internal Gravity Waves in Shallow Seas. 2012.

36. **Allan Hani.** Investigation of Energy Efficiency in Buildings and HVAC Systems. 2012.
37. **Tiina Hain.** Characteristics of Portland Cements for Sulfate and Weather Resistant Concrete. 2012.
38. **Dmitri Loginov.** Autonomous Design Systems (ADS) in HVAC Field. Synergetics-Based Approach. 2012.
39. **Kati Kõrbe Kaare.** Performance Measurement for the Road Network: Conceptual Approach and Technologies for Estonia. 2013.
40. **Viktorija Voronova.** Assessment of Environmental Impacts of Landfilling and Alternatives for Management of Municipal Solid Waste. 2013.
41. **Joonas Vaabel.** Hydraulic Power Capacity of Water Supply Systems. 2013.
42. **Inga Zaitseva-Pärnaste.** Wave Climate and its Decadal Changes in the Baltic Sea Derived from Visual Observations. 2013.
43. **Bert Viikmäe.** Optimising Fairways in the Gulf of Finland Using Patterns of Surface Currents. 2014.
44. **Raili Niine.** Population Equivalence Based Discharge Criteria of Wastewater Treatment Plants in Estonia. 2014.
45. **Marika Eik.** Orientation of Short Steel Fibers in Concrete. Measuring and Modelling. 2014.
46. **Maija Viška.** Sediment Transport Patterns Along the Eastern Coasts of the Baltic Sea. 2014.
47. **Jana Põldnurk.** Integrated Economic and Environmental Impact Assessment and Optimisation of the Municipal Waste Management Model in Rural Area by Case of Harju County Municipalities in Estonia. 2014.
48. **Nicole Delpeche-Ellmann.** Circulation Patterns in the Gulf of Finland Applied to Environmental Management of Marine Protected Areas. 2014.
49. **Andrea Giudici.** Quantification of Spontaneous Current-Induced Patch Formation in the Marine Surface Layer. 2015.
50. **Tiina Nuuter.** Comparison of Housing Market Sustainability in European Countries Based on Multiple Criteria Assessment. 2015.
51. **Erkki Seinre.** Quantification of Environmental and Economic Impacts in Building Sustainability Assessment. 2015.
52. **Artem Rodin.** Propagation and Run-up of Nonlinear Solitary Surface Waves in Shallow Seas and Coastal Areas. 2015.